SYMPTOM-FREE IN ZERO-G? NOVEL TECHNIQUES FOR RAPID ASSESSMENT OF VESTIBULO-OCULAR FUNCTION AND THEIR USE IN PREDICTING PERFORMANCE FROM BASELINE METRICS

by
Kara H. Beaton

A dissertation submitted to Johns Hopkins University in conformity with the requirements for the degree of Doctor of Philosophy

Baltimore, Maryland
March 26, 2014

Abstract

Spaceflight elicits adaptive changes in neurovestibular signaling to accommodate exposure to novel gravity levels. With the prospect of longer-duration missions to Mars and beyond, NASA is currently faced with two immediate needs, which form the foundation of this dissertation: (1) portable technologies to evaluate functional decrements in sensorimotor performance that can be quickly self-administered, and (2) countermeasures that can pre-adapt astronauts prior to spaceflight, accelerate adaptation inflight, or forecast performance (e.g., adaptive capabilities or space motion sickness susceptibility) from preflight metrics alone. In this dissertation, we focus specifically on the design, development, and implementation of three innovative approaches to quantify the vestibular control of eye movements using minimal hardware, and we use these techniques to predict adaptive performance from baseline measures.

Vertical and Torsional Alignment Nulling and Vestibulo-Ocular Nulling (VON) were developed to evaluate binocular positioning misalignments and the vestibulo-ocular reflex (VOR), respectively. These tests are embedded in a hand-held device, which incorporates a tablet computer, small wireless motion sensors, and a pair of specialized eyeglasses, and employs various mobile-apps developed in-house. Through a series of experiments performed in the laboratory and in parabolic-flight, we validated these new assessment tests and explored gravity-level dependencies in vestibulo-ocular function. We found that ocular misalignments are gravity-dependent and developed a bilateral control systems model to describe this dependency. Additionally, variability in baseline torsional misalignment strongly correlates with motion-sickness susceptibility in altered gravity environments. Our VON test provides a rapid measure of dynamic gaze stability

that is more consistent than traditional measures of VOR gain. VON results vary systematically with gravity levels, providing evidence for an otolith-modulating component of the angular VOR. Finally, the strength of baseline inter-trial correlations forecast adaptive capacity in the VOR.

The portable technologies developed in this dissertation have applications beyond spaceflight operations, including bedside clinical testing, remote field-testing, or any applications limited by time constraints, resources, technical personnel, or clinical expertise. The ability to forecast performance from baseline metrics alone, without exposure to an adaptive stimulus, has important implications for the design of individualized interventions, such as rehabilitation protocols to expedite terrestrial compensation for vestibular pathologies, or preflight training and inflight countermeasures to facilitate adaptation to altered gravity environments.

Thesis advisor: Dr. Mark Shelhamer

Thesis committee: Drs. David S. Zee, Eric Young, Michael C. Schubert, Jacob Bloomberg

Primary reader: Dr. Mark Shelhamer

Secondary Reader: Dr. David S. Zee

Acknowledgements

This dissertation is the direct result of the numerous faculty advisors, professional colleagues, family members, and friends who have mentored and supported me throughout this endeavor. I am forever grateful. Specifically, I would like to thank the following individuals:

- My thesis committee Drs. Mark Shelhamer, David Zee, Eric Young, Michael Schubert, and Jacob Bloomberg, without which this body of work would not have been completed. You are true scientific pioneers, and I am honored to have had the opportunity to be your student.
- My lab mates Aaron Wong, Dale Roberts, Adrian Lasker, Amir Kheradmand, Howard Ying, and Rebecca Scholz for their invaluable technical support, engaging and insightful conversations, and life-long friendships.
- My professional colleagues and friends Drs. Scott Wood, Angus Rupert, and the late Fred Guedry for providing many opportunities for me to pursue my dreams.
- My husband Jon and family members Cary, Gayle, Jonathan, Meg, and Min for their endless love and encouragement throughout this adventure.

Dedication

To Dad and Mom,

For everything.

Table of Contents

List of Tables

List of Figures

Chapter 1

Introduction

1.1 Motivation

Spaceflight elicits adaptive changes across all physiological systems (White 1998). In particular, the altered gravity levels (g-levels) modulate otolith signaling, disrupting multiple sensorimotor subsystems simultaneously until the central nervous system (CNS) becomes properly calibrated to the current g-level (Young et al. 1986; Reschke et al. 1994). Inflight, astronauts experience altered otolith-ocular reflexes, reduced eye-hand coordination and fine motor control, changes in postural control, spatial disorientation, and perceptual illusions (Reschke et al. 1996; Clément and Reschke 2008b). Space motion sickness (SMS) remains one of the most significant and unpredictable operational challenges of spaceflight, affecting over two-thirds of all astronauts (Davis et al. 1988). Symptoms range from increased sensitivity to head motion, loss of appetite, and general lethargy to headache, nausea, and episodic vomiting. These disturbances are especially prevalent during the first several days on-orbit, when new patterns of sensory cues are developing, but in rare instances have persisted for the duration of the mission (Thornton et al. 1987a; Davis et al. 1993b). The high incidence rate associated with SMS has mandated delays in accomplishing mission-critical activities on a specified timeline: NASA

restricts crewmembers from performing extravehicular activities (EVAs, also known as "spacewalks") prior to the third day of flight to prevent SMS during an EVA, and the minimum flight duration is set to three days to ensure that astronauts are not ill immediately prior to re-entry and landing (Davis et al. 1988).

Upon Earth-return, crewmembers express clumsiness in their movements, persisting sensation aftereffects, standing and walking vertigo, nausea, difficulty concentrating, and blurred vision (Bacal et al. 2003). Furthermore, they are demonstrably unsteady, and sensorimotor tasks that are normally performed with little cognitive effort, such as standing still with eyes closed or walking heel-to-toe, are suddenly more challenging (Paloski et al. 1992; Black et al. 1995; Bloomberg et al. 1997; Reschke et al. 1998; Reschke et al. 2011). Vestibulo-ocular function is altered (Clarke et al. 1993; Dai et al. 1994). Limb and trunk movements are ataxic in nature, and there is a heavy reliance on visual cues for postural stability and control (Young et al. 1986). Dynamic visual acuity, a measure of gaze stability during head motion, is impaired when walking; in some astronauts, these deficiencies are worse than the clinical thresholds for vestibular pathology (Bloomberg and Mulavara 2003; Peters et al. 2011).

The magnitude of sensorimotor deficits and SMS susceptibility, and their corresponding time-courses of adaptation and re-adaptation, vary widely across individuals, although nominal correlations have been made with respect to flight duration, adherence to inflight exercise mandates, and previous flight experience (Wood et al. 2011). The current approach to facilitate sensorimotor adaptation on-orbit is minimal. First-time astronauts rely on anecdotal information from veteran fliers, which include recommendations as to how to move, or how not to move, following g-level transitions (Wood et al.

2011). Preflight adaptation training has had limited success, primarily due to the unavailability of appropriate ground-based flight analogs for sensorimotor function. SMS is accommodated and managed by a reduced workload and prophylactic medications during the first few days on-orbit (Davis et al. 1988; Bagian 1991; Putcha et al. 1999). A variety of anti-emetic drugs have been tested, and for many years, a combination of scopolamine and dexedrine ("scope-dex") was the remedy of choice. Although effective in preventing motion sickness if taken prior to symptom onset, the drug was associated with a variety of side effects (e.g., drowsiness and reduced psychomotor function due to the scopolamine and agitation and insomnia due to the dexedrine). It was later discovered that scope-dex was likely inhibiting adaptation, as adverse symptoms arose once the medication was ceased (Pyykko et al. 1985; Davis et al. 1993a; Shojaku et al. 1993), and therefore is no longer used inflight. Intramuscular promethazine is currently employed and has been the most successfully implemented medication thus far, but it is not yet known how this drug targets neuroreceptors to mitigate symptoms (Bagian 1991; Clément and Reschke 2008b).

Postflight rehabilitation has improved significantly over the past decade, driven primarily out of need, as mission durations have increased due to the retirement of the U.S. Space Shuttle. Astronauts returning from six-month stays on the International Space Station (ISS) now undergo highly-supervised reconditioning regimens designed to improve mobility, strength, postural control, coordination, and endurance in many physiological systems. These programs involve a two-month progression of daily rehabilitation exercises, personalized for each crewmember's specific deficiencies, and routine counsel from reconditioning specialists and flight surgeons (Wood et al. 2011).

With the prospect of even longer-duration missions to the Moon, Mars, and asteroids, appropriate sensorimotor countermeasures must be developed to maximize crew safety and mission success. These countermeasures must not only enable astronauts to live in space for prolonged periods of time during transit, but must also prepare them to re-enter a gravitational environment upon arrival at their destination. This means that crews must have the necessary proficiency, training, and technology to perform accurate self-assessments and autonomous rehabilitation. While potential solutions could include pharmacological interventions or mechanical countermeasures (such as load suits or artificial gravity), their respective side effects and large weight requirements limit their practicality (Stone 1973; Wood 1990; Reschke 1994). Remedies that require prolonged adaptation or re-adaptation procedures, or that limit workload upon a change in g-level, pose an operational hazard in emergency situations, such as if rapid egress and escape from the vehicle is necessary. Currently, *no appropriate sensorimotor countermeasures exist to offset the adverse affects of spaceflight* (Cohen 2003). These would include procedures that can pre-adapt astronauts prior to spaceflight, accelerate adaptation once inflight or upon landing at a remote destination, or forecast performance (e.g., adaptive capabilities or space motion sickness susceptibility) from preflight metrics alone.

Changes in sensorimotor function associated with spaceflight have been primarily characterized postflight because *no portable sensorimotor assessment device is readily available to quantify functional performance decrements inflight*. Furthermore, several hours or days pass before investigators have access to crewmembers at the appropriate facilities for detailed postflight assessments. Significant re-adaptation occurs during this time, thereby preventing inflight changes and post-landing recovery from being accurate-

ly captured. The majority of what we know about inflight sensorimotor adaptation stems from anecdotal crewmember reports, assumed correlations based on overt symptoms like SMS, or results from ground-based analogs. However, astronauts hesitate to report any adverse symptoms experienced inflight for fear of losing future mission opportunities, and there is great secrecy due to privacy concerns among NASA flight surgeons surrounding the release of such information (Markham and Diamond 1993). As one crewmember boldly stated:

> *Astronauts didn't want to admit to an episode of vomiting out of fear that it would eliminate them from consideration for future spacewalk missions. As a result, many astronauts were less than truthful about their symptoms. Some blatantly lied. We would hear stories of crewmembers who were seriously sick, yet the data would never appear on the flight surgeon's bar charts (Mullane 2006).*

The ability to accurately assess changes in sensorimotor function inflight would provide an objective measure of performance decrements, possibly in real-time. Furthermore, such knowledge may enable strategies to be developed that can assist crews during both the initial transition to orbit and immediately prior to landing on another planet, asteroid, or back on Earth. Ideally, such assessment technologies should incorporate simple tests that can be self-administered and provide individually-prescribed rehabilitation protocols to facilitate adaptation based on the assessment results. These topics have been principal objectives of the NASA Human Research Program in recent years, and have thus formed the foundation of our overarching *Sensorimotor Assessment and Rehabilitation Apparatus (SARA)* project, from which this dissertation work was derived.

SARA is a hand-held, wireless, tablet-based technology that incorporates a series of mobile apps developed in-house to quantify functional performance in various sensorimotor subsystems. Specifically, SARA consists of a small tablet computer (8.1 x 5.3 x 0.3in, 12.3oz), specialized eyeglasses, and wireless kinematic motion sensors, and evaluates the vestibulo-ocular, postural balance, and locomotor systems. This portable platform has applications beyond spaceflight operations, including bedside clinical testing, remote field-testing, or any enterprise limited by time constraints, resources, technical personnel, or clinical expertise. This dissertation highlights the design and development of the vestibulo-ocular assessment portion of the SARA project, and uses the associated technologies to study vestibulo-ocular performance in various laboratory-based and parabolic-flight experiments as a means of validation.

1.2 Vestibular physiology

The vestibular system guides coordinated eye movements and postural balance. Unlike the five traditional senses of sight, smell, sound, touch, and taste, the vestibular system does not give rise to distinct, conscious sensations during everyday life. Instead, vestibular signals are integrated with vision, proprioception, and somatosensation to provide internal estimates of self-motion and orientation in space (Goldberg et al. 2012c). However, acute injuries to the vestibular end organs or corresponding afferent pathways results in compelling sensations of dizziness, vertigo, imbalance, and motion sickness. In the case of spaceflight, where novel gravitational environments modulate otolith signaling, similar sensations arise; however, these are the result of maladaptive responses for a non-1g environment, not an underlying pathology.

The peripheral vestibular end organs are housed bilaterally within the bony labyrinth of the inner ear, adjacent to the cochlea, and consist of three semicircular canals (SCCs), the horizontal SCC, anterior SCC, and posterior SCC, and two otolith organs, the utricle and saccule. Together, these structures sense movement of the head in six degrees of freedom. The semicircular canals respond to angular acceleration; their inherent mechanical properties effectively integrate this incoming information, and as such, they transduce angular velocity to central structures over the physiological range of head movements (Steinhausen 1933; Fernandez and Goldberg 1971; Wilson and Melvill Jones 1979). The otolith organs measure gravito-inertial acceleration (GIA), which includes a composite representation of orientation relative to gravity (e.g., tilt) and linear acceleration (e.g., translation) (Guedry 1974; Mayne 1974). Head movements are encoded through mechanotransduction of ion channels in hair cells, which are embedded in each SCC crista ampullaris and otolithic macula. The hair cells are arranged within each end organ such that head movements in a particular direction give rise to specific patterns of primary afferent signaling. Within each SCC, all hair cells are polarized in the same direction. Hence, the three (approximately) mutually-orthogonal SCCs are excited by angular rotations in their respective planes that bring the head toward the ipsilateral side, and inhibited by angular rotations in their respective planes that bring the head toward the contralateral side. The SCCs of the left and right labyrinth are arranged in complementary, coplanar pairs: the horizontal canals form the horizontal plane, the left anterior and right posterior canals form the LARP plane, and the right anterior and left posterior canals form the RALP plane (Della Santina et al. 2005). Together, these organs transduce angular head movements in three dimensions. Hair cells in the utricle and saccule are

polarized relative to a curved central zone (the *striola*), and therefore the overall response pattern of these organs for a given linear acceleration can be complex. Nonetheless, the utricle is primarily oriented in the plane of the horizontal SCC and is predominantly excited by linear fore-aft and side-to-side accelerations. The saccule lies in the parasagittal plane, and is excited by up-down and fore-aft accelerations, although most saccular afferents have a preferred up or down direction since the saccule is the only end organ capable of sensing vertical linear motion (Fernandez and Goldberg 1976a; Carey and Della Santina 2005).

Primary vestibular afferents emanating from the end organs synapse bilaterally on brainstem vestibular nuclei, as well as ipsilaterally on the cerebellar nodulus, ventral uvula, anterior lobe, and deep interlobular fissures (Carleton and Carpenter 1984; Gerrits et al. 1989; Barmack et al. 1993; Purcell and Perachio 2001). Primary afferent projections to the nodulus are predominantly of SCC origin while primary projections to the ventral uvula are of otolith origin (Maklad and Fritzsch 2003). Secondary afferents in the vestibular nuclei project to the oculomotor nuclei (to facilitate gaze stability during head motions), cervical and spinal pathways (to stabilize head-on-trunk and coordinate posture), various cortical centers (to aid in higher-order cognitive functions, such as spatial orientation, motion perception, and path finding), and the cerebellum (to mediate adaptation) (Goldberg et al. 2012b). Cerebellar targets from these secondary afferents include the flocullus and ventral paraflocculus, in addition to the targets from primary vestibular afferents (Voogd et al. 1996). Vestibular reflexes provide both static (tonic) and dynamic (phasic) motor control.

There are two fundamental principles of vestibular physiology relevant to the experiments within this dissertation. First, primary vestibular afferents have spontaneous discharge rates, which gives rise to their bidirectional sensitivity. This enables neurons to increase firing for excitatory head movements and decrease firing for inhibitory head movements (Lowenstein and Sand 1940). As such, the loss of one labyrinth does not result in a complete inability to sense one-half of the head's movements. Second, a healthy vestibular system readily adapts to changes in internal (e.g., pathological) and external (e.g., environmental) contexts. This inherent flexibility enables vestibular patients to compensate for peripheral and central lesions and astronauts to function in non-1g environments. Various mechanisms that facilitate adaptation, and their specific roles in during spaceflight, are discussed in Section 1.4.

1.3 Vestibular control of eye movements

Vestibulo-ocular reflexes are responsible for maintaining binocular fixation and stable foveal images in the presence of acceleration stimuli acting on the head. This includes dynamic head rotations and translations, and static head tilts with respect to gravity. For the healthy individual, these reflexes are fast, reliable, and highly adaptable.

Each eye is connected to six extraocular muscles (EOMs): the lateral, medial, superior and inferior recti, and the superior and inferior obliques. Vestibulo-ocular pathways elicit contractions in the EOMs to rotate the eyes vertically, horizontally, and torsionally. The exact direction of rotation for a given muscle contraction depends on the position of the eye in the orbit at the time of the contraction. The actions of the extraocular muscles during straight-ahead gaze are outlined in Table 1.1 (Leigh and Zee 2006a).

The primary muscle action refers to the axis about which the eyes predominantly rotate, while the secondary and tertiary muscle actions refer to the axes about which there are smaller rotations. Movements that rotate both eyes by the same amount and in the same direction are called *versions* or *conjugate movements*. Movements that rotate the eyes in opposite directions (or in the same direction but by different amounts) are called *vergence* or *disjunctive movements*.

Table 1.1 Actions of the extra-ocular muscles during straight-ahead gaze.

muscle	primary action	secondary action	tertiary action
medial rectus	adduction	—	—
lateral rectus	abduction	—	—
superior rectus	elevation	intorsion	adduction
inferior rectus	depression	extorsion	adduction
superior oblique	intorsion	depression	abduction
inferior oblique	extorsion	elevation	abduction

In general, the EOMs work in reciprocal pairs: medial rectus–lateral rectus, superior rectus–inferior rectus, superior oblique–inferior oblique. Furthermore, these EOM pairs align with the horizontal, LARP, and RALP semicircular canal pairs: the horizontal SCCs are coplanar with the bilateral medial and lateral recti, the LARP SCCs are coplanar with the left superior and inferior recti and right superior and inferior obliques, and the RALP SCCs are coplanar with the right superior and inferior recti and left superior and inferior obliques. This relationship likely explains the lateral insertions of the oblique EOMs to the ocular orbits (Carey and Della Santina 2005). As such, stimulation of the SCCs elicits eye movements in the plane of that canal. Eye movements in response to otolith stimulation are more complicated due to the fact that the otolith maculae are curved structures, whose hair cells are polarized non-uniformly. However, general conclusions can be made from animal experiments that measured eye movements during

utricular and saccular stimulation pre- and post-lesion: utricular stimulation primarily activates horizontal and torsional eye movements, and saccular stimulation primarily activates vertical eye movements (Suzuki et al. 1969; Fluur 1970; Fluur and Mellstrom 1970b; Fluur and Mellstrom 1970a; Fernandez and Goldberg 1976a; Uchino et al. 1996; Isu et al. 2000; Newlands et al. 2003; Goto et al. 2004).

There are two additional principles of oculomotor control especially relevant to Chapter 3 of this dissertation, where we examine changes in vertical and torsional ocular positioning alignment during exposure to novel g-levels under near-viewing conditions. First, while horizontal and vertical eye positions are subject to voluntary control, ocular torsion is not[1]. Ocular-counterroll, the ocular torsion response to changes in head orientation relative to gravity, is a latent, vestigial reflex that is controlled by gravity (Kompanejetz 1925). Second, during roll head tilt, compensatory OCR (the phylogenetically "old" reflex) and binocular vergence (the "new" reflex) are competing behaviors. Stereopsis is better served when OCR is minimal, and so OCR is suppressed to reduce vertical disparity during head tilts (Misslisch et al. 2001). This is especially true for near targets.

1.3.1 Quantifying vestibulo-ocular reflexes

Vestibulo-ocular reflexes are traditionally evaluated through simultaneous measures of eye and head movements. Although numerous techniques have been developed to measure eye movements, the two most prevalent approaches are the magnetic scleral search coil technique and video-oculography (VOG). The magnetic search coil

[1] There is some evidence that voluntary torsion can be trained in some individuals (Balliett and Nakayama 1978). However, such voluntary cyclorotations require significant practice over many days, as they are not naturally-occurring phenomena. Such a trained ability does, however, demonstrate the large plasticity within the oculomotor system.

technique is generally regarded as the most reliable, versatile, and widely used method for evaluating eye movements (Robinson 1963; Leigh and Zee 2006b). It is highly sensitive and can capture binocular three-dimensional movements at samples rates of at least 1000Hz. The primary disadvantages, however, are that subjects must wear a scleral annulus on the eye and topical anesthetic drops are required, although most people tolerate this well and the risk of corneal abrasion is low (approximately 1/500). Additionally, the large frame housing the magnetic field restricts the subject to a fixed central position, and so eye recordings during more natural movements, such as locomotion, are not possible with this technique. A more portable, wireless version has been developed, but is not yet fully operational (Roberts et al. 2008).

In VOG, small cameras are fixed relative to the head to record the orientation of the eyes in space. Image processing algorithms track movements of the pupil to derive horizontal and vertical eye position and rotational deviations in iris landmarks to quantify ocular torsion. Significant technological advances over the last decade have led to less bulky headgear and increased video resolution. But VOG is limited by fragile and expensive equipment and large computational requirements. Binocular recording and torsion tracking capabilities are not always available. Furthermore, great care must be taken to ensure that the camera does not slip relative to the head, which would lead to artificial deviations in eye position, and as such, many head-mounted systems must be tightly secured to the head, making them uncomfortable to wear.

The advantage of recording eye movements is that they provide a direct, objective measure of motor output. However, their associated lack of portability and high computational expense limit their practicality for spaceflight operations. Moreover, it has been

shown that there are differences in pure motor outputs and functional measures of gaze stability (Grunfeld et al. 2000; Beaton et al. 2014). This is explored in detail in Chapter 5. From an operational perspective, quantifying metrics that characterize functional performance is critical. For example, while an astronaut who experiences decreased VOR gain during spaceflight may be of scientific interest, if this gain reduction does not interfere with his ability to safely and effectively perform mission objectives, then rehabilitating this reflex should not be a high operational priority. On the other hand, if another astronaut experiences a similar reduction in VOR gain but is unable to perform his responsibilities, then rehabilitation exercises must be a high operationally priority for him. Having the appropriate assessment technology available inflight to quickly measure changes in sensorimotor *performance* fulfills a risk management gap well recognized in the human spaceflight community (NASA 2009). There is a similar need in the clinical community where, for example, patients demonstrate clear decrements in standard electronystagmography testing, yet do not complain of dizziness or gaze instability and vice versa (Grunfeld et al. 2000; Hall et al. 2010). These types of functional measures will provide an important complement to traditional physiologic measures. Thus, the foundation of this dissertation is to develop more functionally-based techniques to evaluate vestibulo-ocular performance. We focus on binocular positioning alignments and the vestibulo-ocular reflex, both of which lead to gaze instability if improperly calibrated.

1.3.2 Clear vision requires proper binocular positioning alignment

The evolution of bilateral frontal vision has provided humans with considerable advantages: increased field of view, the ability to see in depth, and redundancy in the case of injury or disease. However, with these benefits comes the additional requirement

of maintaining adequate binocular positioning alignment so that visual images falling onto each retina can be fused into a single, *stereoscopic* (three-dimensional) percept. If binocular fusion cannot be achieved, *diplopia* (double vision) or *suppression* (the ignoring of information from one eye) transpires. Aside from the apparent visual discrepancies, diplopia and suppression are further exacerbated by eye strain, headache, and fatigue (Hoffman and Brookler 1978). Clinically, binocular misalignments arise most commonly in patients with strabismus, vestibular hypofunction, and cerebellar disease due to muscle palsies and lesions. Spaceflight research has demonstrated that healthy individuals also experience binocular positioning misalignments in the presence of novel acceleration stimuli (Kornilova et al. 1983; Diamond and Markham 1991; Young and Sinha 1998), presumably due to miscalibrated central compensatory mechanisms that normally account for inherent otolith asymmetries on 1g Earth (Yegorov and Samarin 1970; von Baumgarten and Thümler 1979).

Binocular fusion can be subdivided into motor and sensory components (von Tschermak-Seysenegg 1942; Kertesz 1981; Hara et al. 1998). The motor component arises in the form of compensatory eye movements. The sensory component is a central phenomenon (Nelson 1975) that facilitates fusion even in the presence of small motor misalignments. Thus, perfect motor alignment (i.e., images that fall onto precisely identical locations on the retinae) is not necessarily a requisite for clear vision. For a target projected onto a specific point on one retina, there exists a small circular region on the other retina onto which the corresponding target can fall that will still render fusion. This is known as *Panum's fusional area* (Panum 1858), which defines the magnitude of the sensory component.

The total fusion capacity, as well as the relative contributions of the motor and sensory components, depends on the image's size, retinal location, complexity (number of salient features), and distance from the eye. The direction about which fusion must be attained (horizontal, vertical, or torsional ("cyclofusional")) is also an important factor, as vertical fusion and cyclofusion are more heavily constrained by their slow speeds and restricted amplitudes than horizontal fusion (Kertesz and Sullivan 1978; Perlmutter and Kertesz 1978; Leigh and Zee 2006d). The accuracy of the horizontal fusion system is what allows us to see clearly in depth. This dissertation focuses on vertical and torsional ocular misalignments, as these are the eye movements that are the least subject to voluntary control and are the most heavily influenced by changes in static otolith signaling.

Images that are larger and more complex are more readily fused than images that are smaller and contain fewer salient features (Fender and Julesz 1967; Kertesz and Sullivan 1978; Kertesz 1981; Allison et al. 2000; Cornell et al. 2003). Furthermore, images projected more peripherally onto the retina elicit larger fusion capacities than the same images projected onto the fovea because Panum's areas increase in size as retinal locations become more peripheral (Burian 1939; Winkelman 1951; Ogle 1964). Hence, the inclusion of peripheral retinal regions during fusion stimulation can itself drive fusion. These principles have important implications for the design of our perceptual oculomotor misalignment tasks, described further in Chapter 3.

The relative contributions of the motor and sensory components vary across individuals, but in general, the motor component always predominates for vertical fusion. For foveal targets, the total capacity for vertical fusion is on the order of 2°, with the motor component contributing approximately 70-85% (Yamamoto and Arai 1975; Houtman

et al. 1977; Perlmutter and Kertesz 1978; Sharma and Abdul-Rahim 1992; Hara et al. 1998). For larger stimulus images, the relative proportions of motor and sensory components are preserved, even though the total amount of fusion increases (Kertesz 1981). When viewing foveal targets close to the eye, the motor component of vertical fusion is increased; the sensory component is relatively constant for near and far viewing (Hara et al. 1998).

Because Panum's fusional areas increase in size in the periphery, up to 8° of sensory cyclofusion can be observed (Crone and Everhard-Hard 1975; Guyton 1988). Cyclofusion motor components have been measured to be up to 6-8°, but only with large stimuli (Crone and Everhard-Hard 1975; Kertesz and Sullivan 1978). Thus, it is possible to observe up to 15° of cyclofusion, if the images incorporate a large field-of-view (Guyton 1988).

There are various techniques for measuring ocular positioning misalignments. Binocular eye positions can be recorded directly using the magnetic scleral search coil or VOG techniques, as described above. Alternatively, various subjective techniques are routinely used by clinical ophthalmologists. One such technique is the Lancaster red-green test (Lancaster 1939). In this test, the patient sits in front of a large grid, wears a red filter over the right eye and a green filter over the left eye, and holds a green Foster Torch (specialized flashlight that projects a green linear streak). The examiner uses a red Foster Torch to project a red linear streak onto the grid, and the subject is tasked with aligning his green line with the examiner's red line. Based on the position and direction of the examiner's line relative to the grid, and the corresponding patient's response, three-dimensional (horizontal, vertical, and torsional) binocular misalignments at various

directions of gaze can be assessed. The red and green filters enable dichoptic presentation of the red and green lines (i.e., the right eye only sees the red line and the left eye only sees the green line) and testing is performed under low levels of background light to minimize visual cues that would otherwise drive fusion. In Chapter 3, we develop a similar technique for evaluating binocular positioning misalignments, but we incorporate a fully-portable platform and quantify the misalignments through more objective means.

1.3.3 The vestibulo-ocular reflex facilitates gaze stability during head motion

Maintaining clear and stable vision requires that rotations of the eyes compensate for motions of the head. This ability is especially important during locomotion and is accomplished through the vestibulo-ocular reflex (VOR). The linear vestibulo-ocular reflex (lVOR) is driven by the otolith organs, and the angular vestibulo-ocular reflex (aVOR) is driven by the semicircular canals. Together, they facilitate gaze stability during linear and angular head movements.

In a healthy individual, when the head translates, the lVOR moves the eyes in the opposite direction by the appropriate amount such that gaze remains fixed-in-space. Side-to-side and up-and-down head translations rotate the eyes horizontally and vertically, respectively, and fore-aft translations move the eyes in vergence. When the head turns in yaw and pitch, the aVOR rotates the eyes by an equal amount in the opposite direction. Dynamic roll-plane movements elicit torsional eye movements through the aVOR, although only by approximately one-half of the amplitude of the head movement; the precise amount is influenced by how the axis of the roll rotation is oriented with respect to the gravity vector (Peterka 1992; Bartl et al. 2005). Static head tilts in the roll

plane elicit ocular-counterroll (OCR), a vestigial, otolith-driven response that torts the eyes in the opposite direction of the head tilt, but only by approximately 10% of its magnitude (Collewijn et al. 1985). Dynamic head tilts relative to gravity, namely in the pitch and roll planes, activate both the aVOR and the lVOR. This is significant for spaceflight operations, as the ocular response to pitch and roll head motion has been shown to be smaller in space than on Earth; this is presumably due to the missing otolith-modulating component of the VOR (Berthoz et al. 1986; Viéville et al. 1986). This idea is further expounded upon in Chapter 5.

The latency of the VOR (i.e., the time from the initiation of the head movement to the start of the compensatory eye response) is on the order of 7-15ms in humans, and as such, the VOR is the fastest sensorimotor reflex in the body (Collewijn and Smeets 2000). In comparison, the latency of visually-mediate eye movements is 75-100ms (Gellman et al. 1990). The VOR's fast response is due to a direct three-neuron pathway between the vestibular ganglion and oculomotor nuclei: primary afferents leaving the end organs synapse on secondary afferents in the vestibular nuclei, which project to the various oculomotor nuclei to synapse on oculomotor motor neurons (Adrian 1943; Szentagothai 1950). Parallel polysynaptic projections further facilitate compensatory eye movements, including an indirect neural integrator pathway that generates the eye position signal necessary to hold the eye in its final position following the end of the head movement (Robinson 1975). All VOR pathways provide bilateral, excitatory and inhibitory contributions.

Within the range of natural head movements (0.5-5Hz), the VOR can be approximated as a linear control system (Robinson 1975). Thus, it is typically characterized

through the parameters of gain and phase. VOR gain is defined as the ratio of the amplitude of eye rotation to the amplitude of head rotation. For sinusoidal stimuli, this is usually calculated from the ratio of peak slow phase eye velocity to peak head velocity. The sign of either the eye or head movement is typically inverted so that the gain value is positive. The phase of the VOR refers to the temporal difference between the head and eye movements and is measured in degrees (referenced to a sinusoid of a given frequency). Conventionally, a zero-phase-shift is defined as the eye and head reaching their peak velocity (or peak position) at the same time. A perfectly compensatory VOR has a gain of 1.0 and phase of 0°, meaning that the corresponding eye movement for a given head movement is such that a stationary visual scene will not move on the retina when the head moves. Deviations from these values result in *oscillopsia*, the illusory motion of the visual scene with head movements. For example, if the VOR gain is too large, images will appear to move in the direction of the head movement, and if the gain is too small, images will appear to move in the opposite direction of the head movement. If the VOR phase is non-zero, timing latencies will also result in a perception of gaze instability. A VOR gain of 0.0 means that the eyes are moving by the same amount in space and in the same direction as the head; this is referred to as VOR cancellation and is typically seen during combined eye-head tracking (Waterston and Barnes 1992).

Functionally, VOR gain and phase do not need to be exactly 1.0 and 0°, respectively, for adequate performance. It is likely that higher-order visual and cognitive processes, though mediated through slower neural reflexes, augment the VOR during everyday movements. For example, the brain knows that objects such as buildings or furniture are stationary, and thus unlikely to be moving, even if small amounts of retinal slip are

present during head motion. As such, the additional neural fine-tuning efforts of the VOR to ensure precise compensatory control may be unnecessary. This idea is supported by the notion that VOR gain is reduced in the dark and that the system itself is enhanced through visual following mechanisms (Collewijn et al. 1983; Fetter et al. 1995; Das et al. 2000; Han et al. 2005).

The VOR can be influenced by active versus passive movements, target distance, gaze direction, cognitive function, and age. VOR gain measured during active head rotations is typically larger and more compensatory than VOR gain measured under passive stimuli (Collewijn et al. 1983; Jell et al. 1988). Part of this increase may be due to additional cervical reflexes that augment the VOR during active movements, when the head is rotated about a fixed trunk, which are not activated during passive whole-body rotations (Hikosaka and Maeda 1973; Tomlinson et al. 1980). Predictive mechanisms and higher-level cognitive control may also contribute (Cullen 2004). It has been proposed that while active and passive head movements are similarly processed by the vestibular labyrinth, they are differentially processed at the level of the vestibular nuclei, thereby leading to the differences observed in active and passive gain values (Cullen and Roy 2004).

During yaw and pitch head movements, the eyes are displaced in front of the axis of rotation. Hence, the VOR must compensate for both the rotational head movement and the translational component associated with the distance between the orbits and the axis of rotation. For far targets, this additional translational component is negligible, but this is not the case for near targets. As such, the apparent gain of the VOR for yaw and pitch head movements increases inversely with target proximity (Viirre et al. 1986; Paige et al. 1998). Translation of the eyes during roll minimally alters image stabilization re-

quirements (only blur in the periphery and a small vertical skew (Migliaccio et al. 2006)), and so the gain of the VOR during roll head movements is not increased for near targets; in fact, there is evidence that the gain is actually decreased to minimize vertical misalignments that necessarily arise between the two eyes during head tilts (Bergamin and Straumann 2001; Misslisch et al. 2001; Migliaccio et al. 2006).

The lVOR depends on gaze direction, as the correct compensatory response (in terms of amplitude, direction, and disconjugacy) is dictated by the position of the eyes in the orbits (Paige and Tomko 1991b). For example, if a subject translates forward with the eyes looking up at a fixed target, then the correct compensatory response is an upward vertical movement. However, if the subject translates forward with the eyes instead looking at a fixed target to the right, then the correct compensatory movement is a rightward horizontal movement.

The VOR, like many sensorimotor reflexes, can be modulated by cognitive processes. During rotational testing in the dark, VOR gain can be increased or decreased depending on whether the subject imagines a target fixed-in-space or fixed relative to the head (VOR cancellation task); the former generates gains close to 1.0, while the later generates gains of approximately 0.1 (Barr et al. 1976; Melvill Jones et al. 1984; Moller et al. 1990b; Johnston and Sharpe 1994). If subjects are distracted with mental tasks or daydreams, the gain of the VOR is reduced by 25-50% (Barr et al. 1976; Moller et al. 1990a; Matta and Enticott 2004). Thus, mental alertness is important when evaluating the VOR.

Reductions in VOR gain and increases in phase-lead are observed in elderly individuals, presumably due to age-related loss of neurons within the vestibular system

(Paige 1992; Baloh et al. 2001). Furthermore, children have higher VOR gain values (Sakaguchi et al. 1997).

A fundamental attribute of the VOR is its considerable ability to adapt to novel conditions, including pathologies (e.g., peripheral and central lesions) and external environmental factors (e.g., eyeglasses and head-mounted optical devices). Gonshor and Melvill Jones provided some of the earliest examples of the high level of plasticity within the VOR when they exposed individuals to horizontal reversing prisms for prolonged periods of time (2 – 27 days) (Gonshor and Melvill Jones 1976). Reversing prisms cause the visual scene to appear to rotate in the same direction as the head during yaw movements, and the resultant retinal slip during head motion provides the error signal to the brain to adjust the VOR. During these experiments, all subjects experienced dramatic reductions in VOR gain, consistent with the notion that the eyes needed to move less for a given head movement to facilitate gaze stability while wearing these prisms. Subjects who wore the prisms for one month also experienced large phase lags, reflecting an attempt to reverse the direction of the VOR as needed for gaze stabilization with reversed viewing. Upon removal of the prisms, VOR gain and phase returned rapidly to pre-adaptation values. Motion sickness was prevalent throughout the experiment due to the visual-vestibular conflict. Although the stimulus was highly artificial, these experiments were pivotal in demonstrating the large adaptive capacity of the VOR. More realistic examples are seen when individuals first don a new pair of eyeglasses. Spectacle lenses have a rotational magnification, and so individuals who wear such corrections much adjust the gain of the VOR (i.e., increase VOR gain for hyperopia, decrease VOR gain for myopia) to account for this magnification (Cannon et al. 1985).

Adaptation to large, novel stimuli (e.g., x2 magnifying lenses or following unilateral vestibular lesions) is best achieved when the adaptation demand is presented in smaller incremental amounts, as opposed to all at once (Schubert et al. 2008); this may be related to the *credit assignment problem*, which would presume that the error signal generated during conventional adaptation (full stimulus at once) is too large and is therefore more likely to be interpreted as an external environmental error that should be ignored (Kluzik et al. 2008). Adaptation is also frequency-specific, meaning that the largest changes in VOR gain (following an adaption paradigm) are observed during head movements near the adaptation stimulus frequency (Lisberger et al. 1983). Furthermore, adaptation is orientation-specific; there is relatively little evidence of transfer of pitch adaptation to yaw and vice versa (Bello et al. 1991). Finally, the VOR is subject to habituation, namely a reduction in the gain and the time constant, following repetitive stimuli (Baloh et al. 1982; Ahn et al. 2000). Thus, the careful design and application of the adaptive training paradigms is an important issue, which we address in Chapter 5.

Experiments that study VOR adaptation are significant because they enable us to examine the conditions that best, and least, take advantage of the inherent plasticity in the system. This is especially important when designing rehabilitation protocols, both for astronauts following g-level transitions and for patients following vestibular hypofunction. For example, the frequency and direction specificity of the VOR imply that exposure to a wide variety of training conditions is required for functional improvements. Building a rehabilitation protocol based on incremental rather than all-at-once training will simultaneously increase subject comfort during the adaptive process, which may en-

hance compliance. Thus, the careful design and application of adaptation and training paradigms is an important issue, which we address in Chapter 2.

1.4 Vestibular adaptation to spaceflight

Examining adaptive processes renders insight regarding brain connectivity and motor learning techniques. Such knowledge is important for the development of countermeasures to the debilitating aspects of spaceflight, as the underlying neural circuitry may be paired with specific behavioral responses that can be manipulated through rehabilitation protocols to facilitate adaptation. Spaceflight provides a unique environment to study vestibular adaptation since the varying g-levels elicit changes in otolith primary afferent signaling: baseline firing rates increase in hyper-g (e.g., during launch and landing) and decrease in hypo-g (e.g., during Earth orbit). The end organs evolved phylogenetically under the Earth's gravitational pull, and as such, vestibular processes are acclimated to this pervasive 1g force (von Baumgarten and Thümler 1979). Thus, upon entering a novel gravitational field, otolith reflexes are initially maladaptive, until the central nervous system (CNS) becomes properly calibrated for the current g-level (Graybiel et al. 1977). Following Earth-return, crewmembers once again encounter challenges until the CNS recalibrates for Earth's gravity. While the neurovestibular challenges faced by astronauts mimic various terrestrial pathologies (e.g., spinocerebellar ataxia and vestibular hypofunction), they do in fact represent *healthy* processes behaving normally under *abnormal* circumstances (i.e., novel gravitational forces).

Active movement is essential in promoting adaptation (Wood et al. 2011). Movements induce error signals, which communicate to the CNS that behavior must be

modified. In this dissertation, *adaptation* is defined as the systematic adjustment of (miscalibrated) motor responses over multiple trials to achieve sufficient *functional* performance. Various neurophysiological mechanisms facilitate adaptation. In the simplest case, adaptation is specific to a single, trained response. For example, an individual wearing a newly prescribed pair of eyeglasses will need to recalibrate his VOR to maintain retinal stability during head movements. Repeated exposure to the new magnification power induces retinal slip, which is the corresponding error signal that induces adaptive changes in the VOR.

In many instances, subsequent exposure to the same adaptive stimulus is facilitated by *savings*, namely adaptation that takes place more quickly and fully because of the ability to recall past experience (even following complete washout). In the eyeglasses example, if the individual dons their spectacles for a second time, after a period of time in which they were not worn, adaptation will occur faster. It is currently unknown whether or not veteran fliers adapt faster during their second mission since there is relatively little data concerning sensorimotor performance, and even less regarding adaptive processes, inflight. We do know, however, that there is minimal evidence that motion sickness symptoms are improved on repeat flights. Two comprehensive motion sickness studies examined the more than two hundred space shuttle astronauts who flew between 1981 and 2000. Although there were some nominal differences in symptom occurrence between career and non-career astronauts, commanders and pilots versus mission specialists, males versus females, and first-time versus repeat fliers, none were statistically significant (Davis et al. 1988; Locke 2003). Furthermore, those who were susceptible on their first mission were also susceptible on later missions; while a slight improvement in

symptoms was seen in 35% of these astronauts during their second mission, 9% experienced symptoms that were actually more severe (Davis et al. 1988). If we presume that motion sickness susceptibility is indicative of a maladapted system, then we can infer that most astronauts do not appear to adapt faster to the weightless environment on repeat flights. This is interesting, given the fact that on Earth, many adaptive processes are subject to savings (Seidler 2007; Krakauer 2009). But perhaps this is because the spaceflight environment is so extreme compared to anything experienced on Earth, and so the brain never fully consolidates the motor programs learned inflight to be recalled at a later time.

1.4.1 The otolith tilt-translation ambiguity and otolith tilt-translation reinterpretation hypothesis

There is an inherent ambiguity in acceleration due to gravity (tilt) and acceleration due to inertial motion (translation), as postulated by Einstein in his Equivalence Principle (Einstein 1908). This tilt-translation ambiguity is demonstrated in the intrinsic inability of otolith afferents to accurately distinguish linear accelerations (Loe et al. 1973; Fernandez and Goldberg 1976a; Anderson et al. 1978; Si et al. 1997). In other words, the same GIA sensed by the otolith organs can be generated by either a head tilt to one side or a lateral translation toward the other side. This is significant because the desired compensatory responses to these two stimuli are quite different. In regards to eye movements, the appropriate response to counteract head tilt is OCR, and the appropriate response for head translation is horizontal eye movements (Baarsma and Collewijn 1975; Bronstein and Gresty 1988; Crawford and Vilis 1991; Schwarz and Miles 1991; Cohen et al. 2001). It is therefore a requirement of the CNS to accurately discriminate tilt from translation in order to elicit the appropriate compensatory responses. Past literature has

theorized two neural strategies to resolve the tilt-translation ambiguity: (1) frequency segregation, in which low frequency motion is interpreted as tilt and high frequency motion as translation (Mayne 1974; Paige and Tomko 1991a; Teleford et al. 1997; Seidman et al. 1998), and (2) multisensory integration, in which the brain uses information from other sensory sources, such as the semicircular canals or vision, to distinguish the two types of motion (Guedry 1974; Young 1974; Angelaki et al. 1999; Merfeld et al. 1999). While traditionally posed as competing hypotheses, recent evidence suggests that these theories are not mutually exclusive and that both are likely employed (Wood 2002; Merfeld et al. 2005).

If we believe that (some aspect of) the ambiguity in otolith-signaling is distinguished by frequency, as substantial evidence supports, then there necessarily exists a crossover frequency in which tilt responses become interpreted as translations, and near this frequency, the ambiguity of otolith afferent information is greatest (Wood 2002; Wood et al. 2007). What is particularly interesting about this crossover range is that it coincides with the frequency of motions known to elicit motion sickness (Denise et al. 1996). Given that sensory conflict is one of the primary theories behind motion sickness (Reason and Brand 1975; Oman 1982), it has been postulated that motion sickness may peak in the frequency range where tilt and translational motions are most ambiguous (Wood 2002).

Spaceflight provides a unique environment to test the tilt-translation ambiguity. Parker and colleagues examined the eye movements and motion perceptions of astronauts during various exposures to tilt and translational stimuli pre- and postflight (Parker et al. 1985). They found that postflight, roll tilts were perceived as lateral translations and that

horizontal eye movements were more robust during roll stimuli. These findings were simultaneously confirmed in an independent study by Young and colleagues (Young et al. 1984). The results led to the otolith tilt-translation reinterpretation (OTTR) hypothesis, which suggests that during spaceflight, the otoliths do not respond to static tilt due to the absence of sensed gravity, and therefore the interpretation of otolith signals as tilt is meaningless. Thus, during adaptation to weightlessness, the brain reinterprets all otolith output to be derived from translational motion. Upon Earth return, the OTTR hypothesis predicts that rightward roll tilts will be interpreted as leftward translations and upward pitch tilts will be interpreted as forward translations. This would lead to incorrect compensatory eye movements, which may explain the blurred vision and oscillopsia (illusory motion of the visual scene with head movements) experienced by crewmembers immediately upon Earth-return (Bacal et al. 2003). Various preflight training protocols have been proposed to pre-adapt astronauts to recalibrate the relationships between otolith and visual signals in a manner that would be appropriate for weightlessness (Parker et al. 1985; Harm and Parker 1994). Due to the small sample population of astronauts tested in the initial studies, and inconsistencies found in later data, various revisions to this model have been proposed (Merfeld 2003; Parker 2003).

1.4.2 Context-specific adaptation and adaptive generalization may facilitate preflight adaptation

One of the challenges of spaceflight sensorimotor adaptation is that the exact movements that facilitate adaptation, and thus enable inflight homeostasis, are the same ones that initially generate miscalibrated compensatory reflexes and symptoms of motion sickness. Motion in the pitch and roll planes are especially relevant to sensorimotor func-

tion during spaceflight, as the otoliths best respond to accelerations in these direction. Many astronauts have reported hypersensitivity to pitching movements on-orbit and following re-entry (Thornton et al. 1987b; Oman et al. 1990; Black et al. 1999). Therefore, the idea that crews can be pre-adapted prior to flight is appealing, as this may enable astronauts to forego some of the adverse consequences of inflight adaptation. Context-specific adaptation and adaptive generalization are two forms of adaptation that may facilitate such acclimation preflight.

There are many spaceflight operations in which initial errors have detrimental consequences, such as landing a spacecraft or attempting to walk following prolonged exposure to microgravity. Thus, the ability to perform a task correctly on the first try, without experiencing an initial error first, can be vital. Previous experiments have demonstrated that *context-specific adaptation* (CSA) may be a useful adaptive strategy, that can potentially be entrained preflight, to help crewmembers withstand such initial performance errors (Shelhamer et al. 1992; Martin et al. 1996; Kramer et al. 1998; Yakushin et al. 2000; Shelhamer et al. 2002).

CSA is the ability to simultaneously maintain different adapted states, each of which are associated with a particular context cue, and then switch between adapted states immediately upon a change in context (Shelhamer and Zee 2003). The hallmark of CSA is that the initial response following a context change is correct for that new context; this is distinct from dual-state (or error-state) adaptation, in which an error must first be sensed before a change in context is detected (Flook and McGonigle 1977; Welch et al. 1993). Thus, in CSA, multiple adaptation states are retained concurrently, without the need to relearn each time the context is present, and so CSA prevents repetitive cycles of

learning, unlearning, and relearning. The best context cues are those that are relevant to the process being adapted (e.g., two different vertical eye positions as the context cues for two different vertical saccade adaptation gain values) and that contain a salient motor component (i.e., are not purely sensory) (Shelhamer and Clendaniel 2002b; Krakauer 2009). Furthermore, preliminary evidence suggests that the inclusion of a secondary context cue can augment the primary context cue, further enhancing the ability to recall the sensorimotor program appropriate for the given context (Shelhamer and Beaton 2012).

For example, Shelhamer and colleagues performed a series of experiments in which two different adapted states of horizontal saccade gain (gain-up and gain-down) were paired with two different horizontal eye positions (gaze right and gaze left) (Shelhamer and Clendaniel 2002a). Saccade gain-up adaptation was entrained with the eyes gazing right and saccade gain-down adaptation was entrained with the eyes gazing left. Following this adaptation period, it was found that a change in the context cue alone (i.e., gazing right versus left) elicited saccades of the appropriately paired magnitudes. Follow-on experiments demonstrated that both target color, namely red paired with one primary context state and green paired with the other, and limb vibration, on paired with one primary context state and off paired with the other, were effective secondary context cues (Shelhamer and Beaton 2009, unpublished raw data).

From this, one can envision how CSA might enable astronauts to internalize both spaceflight-appropriate and Earth-return-appropriate (or novel-g-appropriate) sensorimotor responses simultaneously by pairing the correct responses (adapted states) to the different g-levels (context cues). This training could be done preflight in the alternating 0g and 1.8g phases of parabolic flight, for example. Shelhamer and colleagues demonstrated

such a concept by showing that two different values of saccade gain could be associated with the two different g-levels of parabolic flight (Shelhamer et al. 2002).

One limitation of CSA is that it requires preliminary training in each of the different context environments. Because it is unrealistic to train for every variation on a given task, adaptive interventions that promote general skill learning are ideal. The ability to transfer learning that has not been explicitly trained from one condition to another, or from one task to another, is known as *adaptive generalization* (Schmidt 1975). This is best described as the "learning to learn" phenomenon, in which subjects who are trained in a variety of discrimination tasks are better suited for solving new examples of this type of problem (Harlow 1949).

Adaptive generalization is most successful when the new task is closely related to previously-trained ones (Welch et al. 1993; Abeele and Bock 2001; Mulavara et al. 2009). Furthermore, repeated exposure to dissimilar motor tasks also promotes transfer if variations in sensory input are incorporated into the learning of the original task, conceivably because varied training promotes a global improvement in associative learning (Roller et al. 2001; Seidler 2004). For example, Bloomberg and colleagues performed an experiment in which two groups of healthy subjects were trained in postural balance (group 1) or treadmill walking (group 2) while wearing either three different pairs of visual distortion lenses, a single pair of visual distortion lenses, or sham lenses (Mulavara et al. 2009). Post-tests involved maneuvering through an obstacle course while wearing a novel pair of lenses, never worn by any of the subjects during their adaptation training. The best post-test performers were those individuals who trained on the treadmill (group 2) while wearing multiple pairs of lenses. The authors proposed that the locomotor com-

ponent of the treadmill training was a salient feature that facilitated generalized adaptability to the post-test obstacle course. Additionally, the variable lens training during adaptation better prepared these subjects to manage the unique visual conditions in the post-test.

It is important to note that CSA and adaptive generalization are not mutually exclusive training mechanisms. In some circumstances, it may be ideal to pair specific responses to specific contexts, as the strongest performance is always expressed under test conditions that most closely resemble the original training environment. On the other hand, variable task training has significant potential in situations where the precise environmental context, or correct response, is unknown; training under multiple conditions and then demonstrating high performance under novel circumstances can give crewmembers confidence that their preflight training will effectively transfer to the spaceflight environment.

Chapter 2

Experimental design and methods

2.1 Introduction

The prevailing objective of this dissertation was to develop novel assessment techniques to evaluate various aspects of vestibulo-ocular function and to use these methodologies to explore the underlying neurophysiology. Because we desired simple approaches that employed portable equipment and aimed to quantify functional performance parameters, as opposed to clinical physiologic metrics, we developed perceptual vestibulo-ocular assessment tests that did not involve measuring eye movements directly. Eye movement recordings were used in several of the experiments, however, to validate our new techniques and to compare perceptual responses to pure motor measures. By testing these technologies in the alternating g-levels of parabolic flight, we were able to explore how vestibulo-ocular function modulates with static otolith stimulation.

This dissertation work is divided into three sets of experiments. In the first set, Vertical and Torsional Alignment Nulling (VAN and TAN) were developed to quantify binocular positioning misalignments (Chapter 3). These tests were validated in the laboratory using prisms to induce known visual disparities and tested in parabolic flight to explore gravity-dependencies and forecast motion sickness susceptibility. A model was developed to describe the process by which binocular misalignments are centrally compen-

sated during exposure to novel g-levels (Chapter 4). In the second set of experiments, Vestibulo-Ocular Nulling (VON) was developed to quantify gaze stability during head motion (Chapter 5). VON results were compared to traditional VOR gain during adaptation to telescoping lenses in the laboratory, which allowed us to explore differences in perceived retinal slip and motor gain responses. VON was tested in parabolic flight, and the results demonstrated that the angular VOR is modulated by otolith signaling. In the final experiment, various computational techniques were employed to characterize adaptive capabilities from baseline performance metrics in the VOR system (Chapter 6). A strong connection between baseline inter-trial correlations and adaptation is found. The concluding chapter brings the three sets of experiments together to describe how a portable sensorimotor assessment platform could benefit both the operational and basic science communities (Chapter 7). Follow-on experiments to expand on the vestibulo-ocular technologies developed in this dissertation and further test the underlying physiology are described.

This chapter describes the general experimental procedures and data analysis techniques common among the three sets of experiments that comprise this dissertation. Methodologies specific to only one experiment are contained within the chapter dedicated to that experiment.

2.2 Definition of terms

The following definitions and acronyms are used throughout this dissertation:

CNS	central nervous system
SCC	semicircular canal

VOR	vestibulo-ocular reflex
aVOR	angular vestibulo-ocular reflex
lVOR	linear vestibulo-ocular reflex
OCR	ocular-counterroll
EOM	extraocular muscle
NO	naso-occipital
IA	interaural
VT	vertical
CW	clockwise
CCW	counter-clockwise
SARA	Sensorimotor Assessment and Rehabilitation Apparatus; a hand-held, portable technology developed for NASA to evaluate sensorimotor performance in astronauts during and following spaceflight
VAN	Vertical Alignment Nulling; a technique for quantifying vertical binocular positioning misalignments without measuring eye position
TAN	Torsional Alignment Nulling; a technique for quantifying torsional binocular positioning misalignments without measuring eye position
VON	Vestibulo-Ocular Nulling; a technique for quantifying perceived retinal slip without measuring eye movements
DVA	dynamic visual acuity; a measure of one's ability to read various optotypes (e.g., letters) while moving the head
HMD	head-mounted display; device worn on the head that contains two small display screens viewed by each eye

oscillopsia	apparent, illusory motion of the environment during head movements
PD	prism diopter; unit of prismatic deviation; a 1PD prism deflects a beam of light one centimeter onto an orthogonal plane located one meter away from the prism
VOG	video-oculography; eye movement measurement technique that employs small, head-mounted, infrared video cameras and motion sensors
UC	unilateral centrifugation; rotational test that quantifies left versus right utricular function independently
6DOF	six-degrees-of-freedom; used in reference to a kinematic motion sensor capable of recording 3-axis angular rate and 3-axis linear acceleration
CSA	context-specific adaptation; the ability to maintain different adapted states, each paired with a particular context cue, and switch between adapted states immediately upon a change in context
SMS	space motion sickness; one of the most serious physiological concerns associated with spaceflight as it has affected over two-thirds of the astronaut population; symptoms include general malaise, headache, fatigue, lethargy, loss of appetite, nausea, and episodic vomiting
GIA	gravito-inertial acceleration; vector sum of all linear accelerations acting on the body due to both tilt with respect to gravity and translation; precisely what the otolith organs measure
g-level	gravity level; magnitude of the GIA; equal to $9.81 m/s^2$ (denoted by "1g") for a stationary object on the surface of the Earth

g-vector — gravity vector; three-dimensional vector defining the both the magnitude and direction of the GIA; equal to 9.81m/s^2 directed at the center of the Earth for a stationary object on the surface of the Earth

hyper-g — hyper-gravity; g-level greater than 1g

hypo-g — hypo-gravity; g-level less than 1g.

The following terms are used to describe the experimental procedures:

task — objective measure in the current experiment

trial — single instance of the task; trials were grouped into blocks, separated by short breaks

block — group of trials run consecutively without breaks

session — all of the test blocks for a given task collected during a single experiment; different experimental sessions were executed on separate days to prevent test subject fatigue, the exception being for the VAN and TAN parabolic-flight experiments, which occurred on the same day during the same flight

probe — intermediate assessment of performance during an adaptation experiment; executed between adaptation blocks.

Throughout this dissertation, we frequently refer to the free-fall condition associated with orbital spaceflight and the top half of the parabolic flight trajectory. This condition is routinely labeled "zero-gravity," "microgravity," or "weightlessness" due to the lack-of-gravity sensation felt by astronauts or passengers inside the vehicles. However, for both orbital spaceflight and parabolic flight, these terms are technically incorrect, as orbital spacecraft and parabolic flight aircraft are subject to (nearly) the same pull of

gravity inflight as someone standing still on the surface of the Earth; the difference is that the net *acceleration* on these vehicles (and hence the occupants inside) is zero. Thus, because the passengers are falling at the same rate as their vehicle, and no reaction force is imposed on them by the vehicle itself, a *perception* of weightlessness ensues. Nonetheless, in keeping with the conventional phraseology accepted in the literature, we will use the term *g-level* to describe the *net acceleration* (i.e., *perceived* g-level) experienced by the astronaut or parabolic flight passenger. Furthermore, we will refer to the free-fall condition of parabolic flight as "0g" because it is the prevailing term used by the NASA Reduced Gravity Office to denote the 0g sensation felt by the passengers inside the cabin (i.e., 0 times the GIA on the surface of the Earth). Analogously, we will refer to the hyper-acceleration pullout phase of the parabolic trajectory, in which a larger-than-9.81m/s^2 acceleration is imposed to regain sufficient altitude in preparation for the next parabolic maneuver, as "1.8g" (i.e., 1.8 times the GIA on the surface of the Earth).

The coordinate reference frame used in this dissertation to describe the direction of head movements follows a right-hand rule, in which the positive X axis is directed out of the nose, the positive Y axis is directed to the left, and the positive Z axis is directed out of the top of the head. Fore-aft translation is along the NO (X) axis, left-right translation is along the IA (Y) axis, and up-down translation is along the VT (Z) axis. Head roll to the right, head pitch down, and head yaw to the left are all positive angular movements.

2.3 Test subjects

Healthy individuals with no known vestibular, oculomotor, or neurological deficits volunteered as test subjects for the experiments in this dissertation. All provided

written, informed consent to a protocol pre-approved by the Johns Hopkins Medicine Institutional Review Board (JHMIRB). Subjects who participated in parabolic flight-testing also provided written, informed consent to a protocol pre-approved by the NASA Johnson Space Center Committee for the Protection of Human Subjects (NASA JSC CPHS); these individuals were recruited through the NASA JSC Human Test Subject Facility (HTSF), and were required to pass a modified Air Force Class III flight-physical examination. We further screened our parabolic-flight subjects for individuals who were (1) naïve to the parabolic-flight environment (i.e., had never previously flown in parabolic flight), and (2) highly insusceptible to motion sickness on Earth. Previous studies have shown diminished sensorimotor responses with repeated exposure to the altered g-levels associated with parabolic flight, likely due to context specific adaptation or rapid re-adaptation (Lackner and Graybiel 1982; Shelhamer et al. 2002). Since our tests were designed to capture the adaptive process, it was essential that we select subjects whose adaptive processes could be traced from the beginning. Some experienced fliers, however, were used as initial pilot subjects and as controls. We did not allow our flight subjects to take any anti-motion sickness medications (including the scopolamine offered preflight by NASA flight surgeons), as they are known to inhibit some of the sensorimotor responses we were measuring (Pyykko et al. 1985; Davis et al. 1993a; Shojaku et al. 1993). Furthermore, some of our experiments employed repeated, active head movements, which are known to be especially provocative in altered gravity environments (Lackner and Graybiel 1986). Thus, it was in our best interest to select individuals with a high tolerance for provocative motion environments on Earth.

In total, twenty-six subjects were tested across three different sets of experiments. The characteristics of each test subject are outlined in Table 2.1 at the end of this chapter. Subjects ranged in age from 20–59yr. An attempt was made to test the same individuals in multiple experiments, so that conclusions could be drawn across experiments. Data from five of these test subjects were excluded from some aspects of the final results due to (1) severe motion sickness in the parabolic flight environment (and therefore a lack of sufficient data), and (2) excessive blinking during experiments involving eye movement recordings. In the VAN and TAN parabolic-flight experiments, subjects V, W, and X experienced chronic motion sickness very early in their respective flights, and were unable to perform the VAN and TAN testing inflight; their baseline 1g data was included, however, as it was collected prior to takeoff and before the onset of any symptoms. In the VON parabolic-flight experiment, subject Q also experienced motion sickness symptoms during his parabolic flight, and was unable to complete a sufficient number of trials inflight. In the VOR correlation experiment, subject C blinked in over 30% of her baseline trials, and was therefore excluded from the experiment, as elimination of that many trials compromised the validity of her spectral analysis results.

2.4 Test environments

All experiments described in this dissertation were conducted in the Vestibular and Eye Movement Laboratory at the Johns Hopkins University School of Medicine, or during parabolic flights, which operated out of Ellington Field, Houston, TX. The vestibulo-ocular assessment tests were performed in a dark room within the laboratory or under a shroud during parabolic flight. The only visible cues during VAN and TAN test-

ing were the stimuli targets to be nulled (i.e., two lines), which prevented sensory fusion mechanisms from attenuating ocular misalignments. VOR adaptation was performed in the light to maximize adaptation, but VOR gain testing was performed in complete darkness with a remembered target to avoid washout during adaptation. VON testing was performed with a single moving target, which was not a de-adapting stimulus, as described further in Chapter 5.

2.4.1 Parabolic-flight testing

Parabolic flight provides a unique environment to experience repeated cycles of hyper-g (1.8g) and hypo-g (0g). It is, in fact, the only way to experience sustained free-fall on Earth in a controlled setting. Details regarding the aircraft dynamics and flight controls are described in a paper by Karmali and Shelhamer (2008). Briefly, the aircraft flies a parabolic trajectory that provides alternating levels of 0g and 1.8g, as perceived by the passengers inside. Each 0g and 1.8g phase lasts approximately 25s and 40s, respectively, and transitions between cycles are brief (< 1s). A typical flight encompasses forty 0g parabolas, although some flights incorporate Martian parabolas (0.38g) and/or Lunar parabolas (0.17g); Martian and Lunar parabolas are also separated by 1.8g pullout maneuvers. Although the aircraft gains and loses 10,000ft in altitude and rotates through 90° in pitch during every parabola, precise control of thrust and lift by the pilot ensures that the g-vector felt by the passengers is predominantly directed vertically through the floor of the aircraft; lateral (side-to-side) and longitudinal (fore-aft) forces are minimal, and rarely perceived by the naïve flier (Figures 2.1 and 2.2). Hence, during parabolic flight, the occupants remain in the same location and orientation within the aircraft.

Our experiments were performed in both the 0g and 1.8g phases of parabolic flight (and Martian-g and Lunar-g, if available). Subjects were trained on the different nulling tasks several days before their flight, and baseline 1g data was collected on the morning of their flight prior to takeoff. Postflight testing was typically not performed, as access to the aircraft was limited after landing in preparation for the subsequent flight.

During flight, subjects were loosely strapped to the floor of the aircraft (enough to "hover" approximately 1-2in and thus be in true "free-float" during the 0g phases of flight, but not so much that they were at risk of injury during the 1.8g pullout). Subjects repeated the nulling tasks as many times as possible throughout the 0g and 1.8g phases of the parabolas to perform as many trials as possible. The nulling programs integrate wireless motion sensors to record synchronous six-degrees-of-freedom (6DOF) aircraft dynamics, which enabled subjects' inflight data to be separated by g-level during offline data processing postflight.

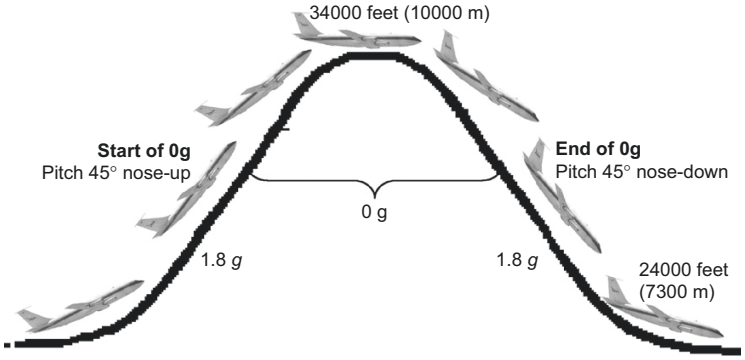

Figure 2.1 Parabolic-flight profile. The aircraft starts by accelerating to gain velocity before pulling up to convert horizontal velocity into vertical velocity. During the pull-up the g-level increases. When a sufficient upward velocity is achieved, the pilots "push-over" and reduce thrust so that the aircraft and occupants fall together. At the end of the parabola the pilots pull up and the g-level increases again. The cycle is then repeated. From Figure 1 of *Karmali, F and Shelhamer, M (2008). The dynamics of parabolic flight: Flight characteristics and passenger percepts. Acta Astronautica 63, 594-602*. with permission from Elsevier (license number 3323381238215)

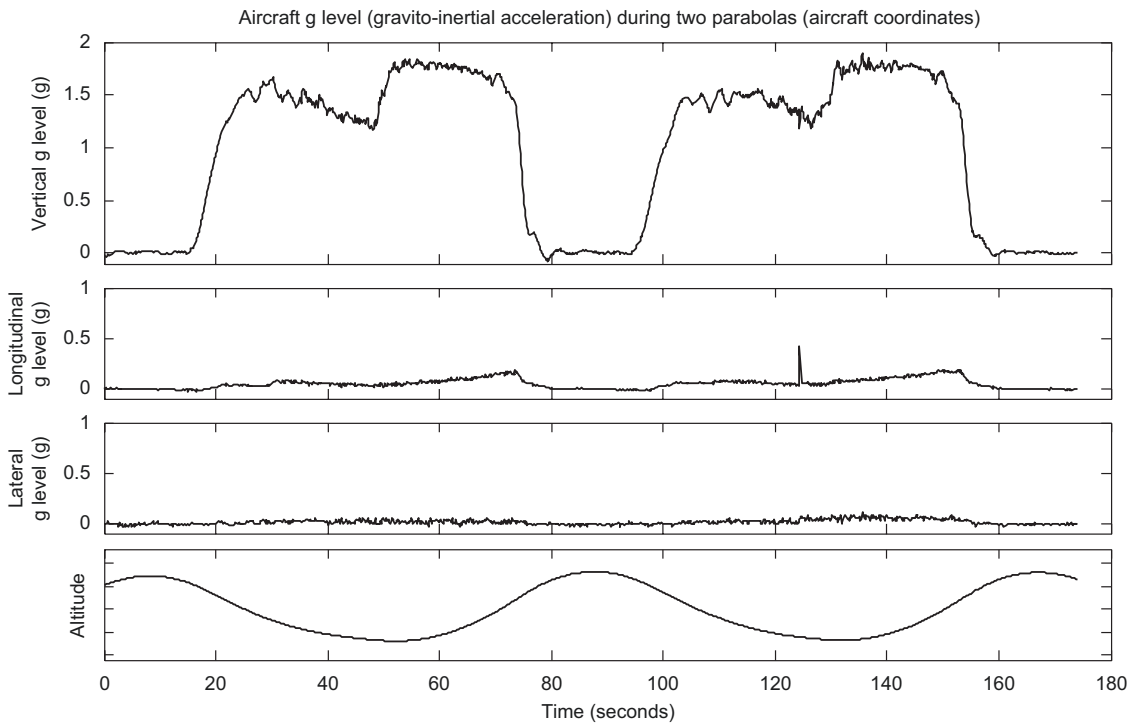

Figure 2.2 Parabolic-flight aircraft g-level. Actual g-levels on the NASA "Weightless Wonder" C-9B during parabolic flight, along the vertical (z), longitudinal (x), and lateral (y) axes of the aircraft. The altitude is an approximation (derived from accelerometer recordings) for demonstration only and not based on altimeter data. Changes in net gravito-inertial acceleration (GIA) occur overwhelmingly along the aircraft vertical axis, even when the aircraft vertical is not aligned with Earth's gravity. There is a small aft-ward increase in longitudinal *g* level near the end of the 1.8*g* phase, which is the longitudinal component of gravity as the aircraft pitches up. The pilots could eliminate it by reducing thrust and allowing the aircraft to decelerate, but this would reduce airspeed and thus the time in 0*g* (Figure based on data gathered by the authors). From Figure 6 of *Karmali, F and Shelhamer, M (2008). The dynamics of parabolic flight: Flight characteristics and passenger percepts. Acta Astronautica 63, 594-602*. with permission from Elsevier (license number 3323381238215).

2.5 VOR adaptation experiments

2.5.1 VOR adaptation stimulus

The two VOR adaptation experiments in this dissertation (Chapters 5 and 6) employed active, yaw-plane head movements while viewing through telescopic lenses to induce VOR gain adaptation. The purpose of these experiments was to validate Vestibulo-Ocular Nulling (VON), a new measure of gaze stability (Chapter 5), and to com-

pare baseline performance to adaptive capabilities in the VOR (Chapter 6). VOR gain was computed before, during, and after the adaptation paradigm using video-oculography (VOG). Although pitch-plane head movements are more traditionally relevant to space-flight research due to their otolith-modulating component, yaw-plane adaptation was employed due to higher-fidelity horizontal eye tracking capabilities of the VOG system.

Head-mounted optical devices, such as telescopic (magnifying and minifying) lenses, Dove prisms, and reversing prisms, have long been utilized to disrupt the normal relationship between visuomotor and proprioceptive-motor responses for the purpose of studying how these systems adapt to novel task demands (Gauthier and Robinson 1975; Gonshor and Melvill Jones 1976; Miles and Eighmy 1980; Istl-Lenz 1985; Roller et al. 2001). Wearing such spectacles causes images to slip on the retina when the head moves, thereby signaling the brain to adjust the gain (and sometimes also the phase) of the VOR to compensate for the new visual requirements. Upon removal these optical devices, the VOR goes through a re-adaption process to return to a baseline gain of 1.0 and zero phase. Telescopic lenses not only change the size of visual images, but also the speed with which they travel across the retina during head movements. The magnification power dictates the amplitude and direction of adaptation necessary to acquire retinal image stability (Demer and Amjadi 1993). For example, when a healthy individual with VOR gain equal to 1.0 initially dons x2 magnifying lenses, images move twice as fast across the retina during head motion. Hence the eyes must move twice as fast for a given head movement, thereby requiring a VOR gain of 2.0 for perfect compensation.

The VOR adaptation experiments in this dissertation employed x0.5 minifying lenses, and as such, perfect compensation would require the eye velocity to be reduced by

one-half to eliminate retinal slip during head motion. Specifically, the adaptation protocols consisted of 20min of active, yaw-plane, sinusoidal head rotations (i.e., repeatedly nodding "no") while wearing the lenses. Subjects were paced with a metronome at 90 beats-per-minute (90bpm, one half-cycle per beat, 0.75Hz sinusoidal motion) and rotated through approximately 40° on each cycle. During the head movements, subjects focused on a stationary point target 1.5m away and were encouraged to simultaneously engage their peripheral field-of-view to maximize adaptation (Demer et al. 1989). Adaptation was performed in four 5min blocks, between which VOR gain and VON motion-gain were probed and subjects were allowed to rest for several minutes (in complete darkness to prevent washout).

The active, continuous nature of the head movements was intended to challenge the vestibulo-ocular system to promote gain-adaptation as quickly and effectively as possible. Such gaze stability exercises (GSE) are routinely given to vestibular hypofunction patients to facilitate compensation following unilateral or bilateral loss (Shumway-Cook and Horak 1990; Herdman 2000). Adaptation in our experiments was further expedited by our choice to employ minifying, rather than magnifying, lenses. One limitation of employing active head movements was that they did not allow precise control of the adaptation stimulus on a cycle-by-cycle basis, and therefore there was no way to verify that each subject experienced the exact same stimulus. However, subjects practiced making the 40° head movements in time with the metronome before the experiments began, during which they received feedback from the investigator. This ensured subjects settled into a comfortable, methodical rhythm that could be maintained throughout the adapta-

tion paradigm. Furthermore, investigators monitored the subject continuously throughout the adaptation and corrected head excursion and speed as needed.

2.5.2 VOR gain calculations

VOR gain was derived from simultaneous recordings of monocular (right eye), two-dimensional (horizontal and vertical) eye position and three-dimensional (roll, pitch, and yaw) angular head velocity (EyeSeeCam VOG, Munich Germany). Data was captured at 220Hz and processed offline using the algorithms described below. The VOR gain probes between adaptation blocks employed the same active, yaw-plane, sinusoidal head movements (Lisberger et al. 1983), but tests were performed in complete darkness while subjects remembered a fixed, imaginary target at 1.5m to prevent adaptation washout. For the baseline head-impulses (Chapter 6), subjects fixated on a stationary point-target at 1.5m in an otherwise dark room and moved their heads swiftly to the left and right of center (~30° amplitude, 300°/s peak velocity, 5000°/s^2 peak acceleration) in time with a metronome set at 60bpm (one head-impulse per beat).

VOR gain has been traditionally defined as the ratio of peak eye velocity to peak head velocity. However, differentiation of the sinusoidal eye position data obtained during the adaptation probes resulted in noisy eye velocity traces, rendering peak detection subject to filtering artifacts, and so VOR gain for the adaptation probes was instead defined as the ratio of peak-to-peak eye position to peak-to-peak head position. Extracting peak eye velocities from the differentiated head-impulse eye data, however, was easily achieved due to the high velocity and acceleration profiles associated with the head-impulses, and so VOR gain for the head impulses was defined as the ratio of peak eye velocity to peak head velocity.

A behavioral calibration sequence was implemented at the beginning of each VOR gain test, in which subjects viewed targets projected 8.5° up, down, left, and right of straight-ahead gaze. Eye-position-in-space was computed so that blinks and fast-phases could be automatically detected, based on a velocity (sign-change) threshold. Blinks were removed. The head velocity sensor was fixed to the eye camera, which was positioned just above the right eye, but the sensor was rotated relative to the subject's head (eye) reference frame; the direction and amount of this rotation depended on how the camera needed to be oriented so that the subject's eye was centered in the camera's field-of-view. As such, when the subject moved his head in pure pitch or pure yaw, the head velocity sensor contained non-zero data in all three axes. The VOG system did not incorporate a 3-axis linear accelerometer, and so rotating the head velocity data from the sensor reference frame into the head reference frame and integrating it (in three-dimensions) to obtain angular head position was not feasible. Therefore, the following solution was implemented: Because head movements were always restricted to a single body axis (pitch or yaw) and these movements primarily stimulated one axis of the velocity sensor (i.e., the sensor was approximately rotated in the same plane as the head), principal component analysis (PCA) was applied to each of the two-dimensional eye and three-dimensional head data to generate 1D vectors of eye and head data that best represented the single-axis movements (Figure 2.3).

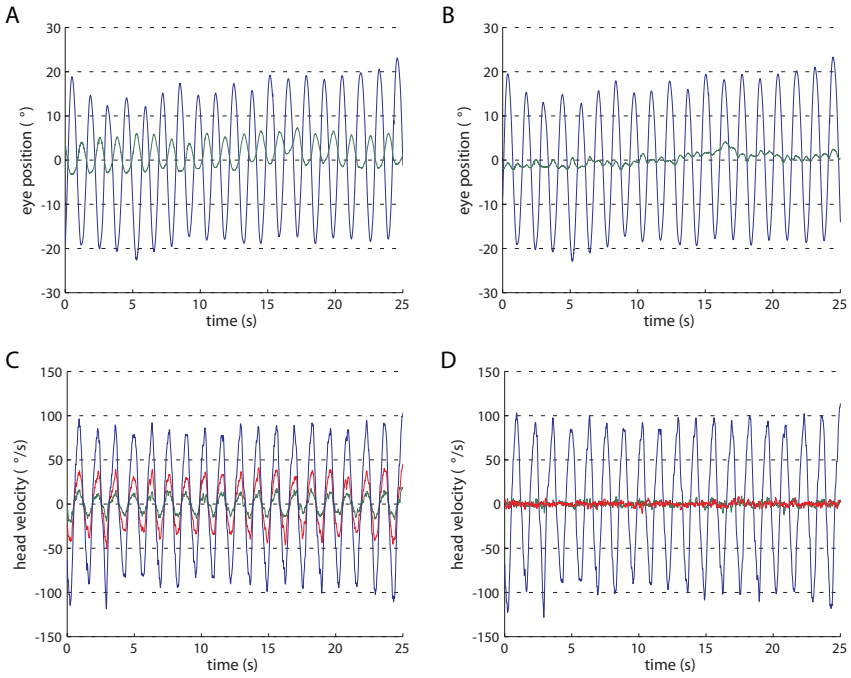

Figure 2.3 Application of PCA to raw eye position and head velocity data. Data taken from one VOR gain probe from one representative subject. (A) Raw eye data. (B) Eye data transformed by PCA. (C) Raw head data. (D) Head data transformed by PCA. Principal components of eye and head data are colored blue in (B) and (D).

PCA is a powerful mathematical tool to reduce complex, high-dimensional (and often redundant) data into a more tractable, lower-dimensional form without losing significant information. In PCA, *n*-dimensional data is projected onto *p* orthogonal basis vectors, or principal components ($p <= n$). Principal components are determined by accounting for as much variability as possible in the original dataset: the first principal component is in the normalized direction vector that maximizes the variance in the original data, the second principal component is in the normalized direction vector that maximizes the variance among all directions perpendicular to the first principal component, the third principal component is the normalized direction vector that *next* maximizes the variance among all directions perpendicular to the first two principal components, and so on (Moore 1981). The first principal component of the eye and head data represents the single, primary direction of eye and head movement, and was equivalent to the subject's

perception of the yaw plane. As such, only the data associated with the first principal component was kept (blue traces of Figure 2.3 B and D), which we refer to as the one-dimensional eye position and one-dimensional head velocity magnitude data. The data corresponding to the remaining principal components (second principal component for the eye data and second and third principal components for the head data) were discarded as out-of-plane motion and noise. All subsequent VOR gain computations were performed on these one-dimensional magnitude vectors.

Fast phases and saccades within the one-dimensional eye position data were automatically detected, and manually verified, based on velocity threshold (sign change in the position trace), and removed using a linear regression estimate over the 25ms before and after the fast phase. Since all VOR testing was done in complete darkness with an imagined target, the subject's perception of straight-ahead gaze often drifted; therefore, any linear trends were also removed from the de-saccaded data. The one-dimensional head velocity data was integrated to obtain head position. Peaks in the eye and head position traces were automatically detected (and manually verified) using a velocity threshold. Half-cycles containing blinks were eliminated, and VOR gain values were calculated for the remaining peak-to-peak pairs and then averaged.

Table 2.1 Subject demographics and experiment participation (PF: parabolic flight, p#: total number of parabolas flown previously, *: data excluded).

					Chapter 3		Chapter 5		Chapter 6
subject	age	sex	affiliation	prior PF experience p# (year agency)	VAN/TAN prism	VAN/TAN PF	VON vs. VOR	VON PF	VOR adaptation vs. β
A	29	M	JHU	—	—	—	×	—	×
B	27	M	JHU	—	—	—	×	—	×
C	21	F	JHU	—	×	—	×	—	×*
D	25	M	JHU	—	—	—	×	—	×
E	35	M	JHU	—	—	—	×	—	×
F	24	F	JHU	—	—	—	×	—	×
G	38	F	JHU	—	—	—	×	—	×
H	31	F	JHU	—	×	—	×	—	×
I	20	M	JHU	—	×	—	×	—	×
J	52	M	JHU	—	—	—	×	—	×
K	27	M	JHU	—	—	—	×	—	×
L	27	M	JHU	—	—	—	×	—	×*
M	45	M	JHU	1400 (2011 NASA)	×	×	—	×	—
N	26	F	JHU	—	×	—	—	—	—
O	29	M	NASA	0	—	—	—	×	—
P	49	M	NASA	0	—	—	—	×	—
Q	51	M	NASA	0	—	—	—	×*	—
R	53	M	NASA	6400 (2009 NASA)	—	—	—	×	—
S	27	F	NASA	0	—	×	—	—	—
T	23	M	NASA	0	—	×	—	—	—
U	27	F	NASA	0	—	×	—	—	—
V	28	F	NASA	0	—	×*	—	—	—
W	26	F	NASA	0	—	×*	—	—	—
X	24	F	NASA	0	—	×*	—	—	—
Y	36	M	NASA	0	—	×	—	—	—
Z	59	M	NASA	250 (2007 ESA)	—	×	—	—	—

Chapter 3

Vertical and Torsional Alignment Nulling quantify binocular misalignments and forecast motion sickness susceptibility

3.1 Introduction

3.1.1 Overview

The vestibular system evolved for two specific functions: to guide eye movements during self-motion, and to identify the terrestrial vertical so that upright posture and locomotion could be maintained, even in the absence of visual cues (von Baumgarten and Thümler 1979; Spoor et al. 1994; Goldberg et al. 2012c). Since its development took place within the Earth's gravitational field, proper vestibular function, especially of the otolith organs, depends on this constant 1g force. Therefore, one should expect performance decrements in vestibular processes upon exposure to novel gravitational conditions (White 1998; Bacal et al. 2003; Williams 2003; Blaber et al. 2010). Such conditions include not only extreme environments such as orbital spaceflight or the surface of the Moon, but also those associated with modern-day air, land, and sea transportation, as the inner ear was not designed to identify strong inertial accelerations because they did not play a fundamental role in evolutionary development. Hence, humans routinely experience sensorimotor disturbances, visual and sensory illusions, and motion sickness when subject to prolonged, unconventional motion paradigms.

The purpose of this first set of experiments is to explore one favorable hypothesis underlying the vestibular perturbations experienced during altered g-exposure. This *vestibular asymmetry central compensation* model outlines a potential neurophysiological mechanism by which vestibular deficits and motion sickness susceptibility arise during spaceflight. As such, this chapter will examine: (1) the innate asymmetry between the left and right vestibular apparatuses and why this feature is problematic in unfamiliar gravitational environments, (2) how this asymmetry can be measured non-invasively, and (3) how parabolic-flight testing can provide evidence for how such an asymmetry is resolved. In the process, a new approach for quantifying ocular misalignments without measuring eye movements directly is developed, a correlation between baseline performance and parabolic-flight motion sickness susceptibility is found, and differences in utricular versus saccular central compensation are proposed.

3.1.2 The CNS compensates for otolith asymmetries

In 1979, von Baumgarten and Thümler proposed a hypothetical model for vestibular adaptation in altered gravitational states that specifically addressed the following two questions: (1) What neurophysiological mechanisms facilitate vestibular adaptation to weightlessness and re-adaptation upon Earth-return? (2) Why is the threshold for motion sickness susceptibility so variable across individuals? (von Baumgarten and Thümler 1979). Their model is based on the theory that there exist inherent asymmetries between the left and right vestibular end organs and corresponding afferent pathways, and that these asymmetries are centrally compensated through additional neural impulses stemming from the brainstem reticular formation or the cerebellum (von Bechterew 1909; Yegorov and Samarin 1970; Schaefer and Meyer 1974). It is entirely conceivable that

nature does not (and cannot) produce precisely identical otoconial maculae on both sides of the head, and as such, small anatomical asymmetries likely exist in at least some individuals (Yegorov and Samarin 1970; von Baumgarten and Thümler 1979). Likewise, asymmetries in hair cell sensitivity, distribution, or numbers, or in the neural relationships between first order afferents and their receptors may also occur (Bracchi et al. 1975; Markham and Diamond 1993). During early development, central processes regulate these asymmetries, thereby mitigating functional vestibular deficits, such as vertigo, nystagmus, and imbalance.

In their model, von Baumgarten and Thümler posit two compensating centers (one on the left and one on the right) and an orientation center that compares the left and right afferent information to generate an overall central vestibular percept (Diamond and Markham 1998; Clarke et al. 1999; Kondrachuk 2003). As an example, they describe a healthy individual with a left otolith mass of 100μg and right otolith mass of 50μg (Figure 3.1)[2]. Under the normal 1g pull of gravity, the right compensation center generates additional neural impulses to counterbalance the two-fold difference in end organ masses, thereby leading to a balanced, and hence "un-sensed," orientation center. Therefore, this individual does not experience any spontaneous vestibular reflexes (e.g., nystagmus) or anomalous vestibular sensations (e.g., vertigo) in 1g. If this person suddenly enters a 0g environment, primary afferent signaling on the left and right is reduced to zero, as each otolith now measures zero GIA. However, the compensating centers continue to rectify a presumed anatomical asymmetry, and hence an unbalanced, and now "sensed," orientation center arises. This leads to vestibular disturbances, until the compensating centers

[2] In reality, a difference of only several μg is necessary to produce the following effect, due to the extreme sensitivity of the otolithic system (Gundry 1978); such a large asymmetry is solely employed for ease of illustration.

adapt for the new (zero) GIA; von Baumgarten and Thümler propose that balance re-occurs once the left compensation center learns to supply the same amount of neural signaling as the right compensation center. If this individual then returns to Earth, the newly acquired, 0g-tuned compensation is inappropriate for 1g, and hence symptoms occur once again, until re-adaptation brings the central compensation back to baseline 1g levels.

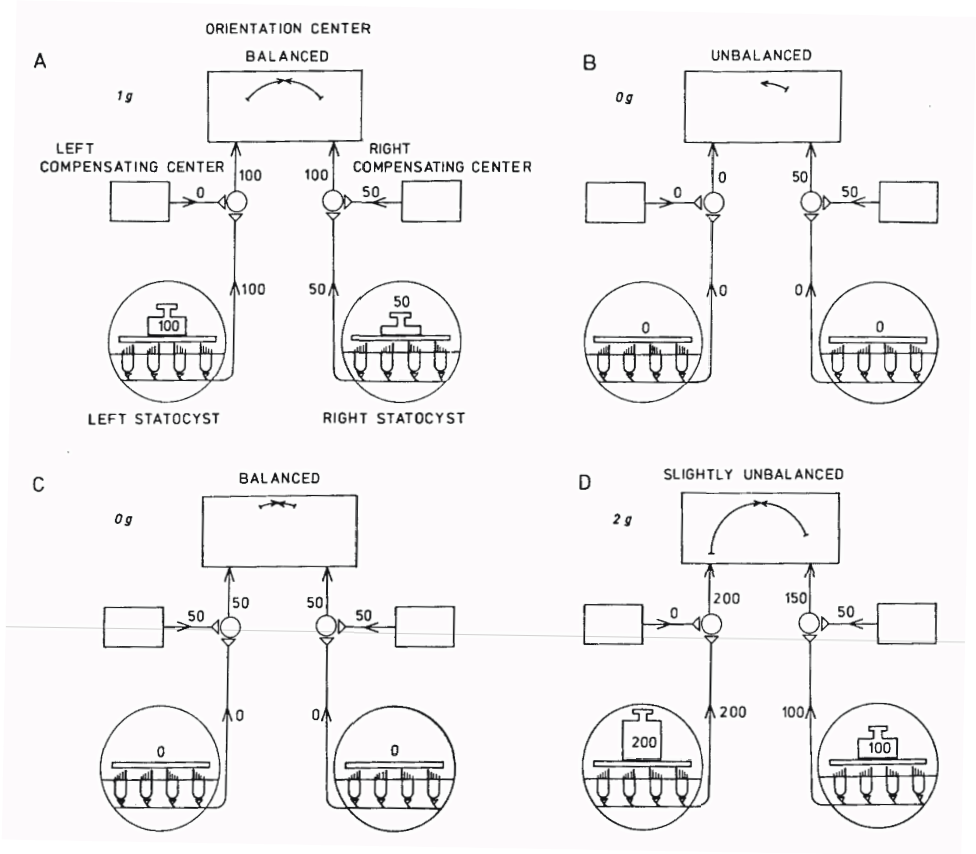

Figure 3.1 Model of vestibular habituation to hypo- and hyper-g in the case of a bilateral otolith asymmetry. (A) On the ground, (B) in weightlessness before habituation, (C) in weightlessness after habituation, and (D) in hyper-gravity states. From Figure 1 of *von Baumgarten, RJ and Thümler, R (1979). A model for vestibular function in altered gravitational states. Life sciences and space research 17, 161-170.* with permission from Elsevier (license number 3323641449406).

The mechanism by which neural signaling compensates for otolith asymmetries (i.e., additive neural compensation on the deficient side) proposed by von Baumgarten and Thümler predicts a reversal in the direction of imbalance when transitioning from 1g

to hypo-g versus from 1g to hyper-g[3]. For instance, suppose that one of the vestibular responses experienced during g-level transitions by the individual described above is nystagmus. Upon transition from 1g into 0g, the left and right primary otolith afferents are silenced due to the zero GIA, but the neural impulses that balance the end organ mass asymmetry continue to be sent to the right compensation center. This additional firing on the right establishes a left unilateral hypofunction scenario, which would elicit right-beating (slow phases to the left) nystagmus. If this individual instead transitions from 1g into 2g, there would be a relative reduction in stimulation from the right side (by 25%, in the example above), analogous to a right unilateral hypofunction, and a left-beating nystagmus would be generated.

Under the von Baumgarten and Thümler model, individuals with larger bilateral asymmetries would require greater adjustments to their central compensatory processes following exposure to novel g-levels. Consequently, these people may experience functional deficits, such as vertigo, nystagmus, or motion sickness, of a more extreme nature or that persist longer in these new environments. Hence, this model can explain why all astronauts undergo a period of adaptation at the beginning of their missions (i.e., it is physiologically improbable that individuals have perfectly symmetrical otolith systems), and why some astronauts experience symptoms of a more detrimental nature than others (i.e., presumably those who have larger left-right otolith asymmetries). Importantly, this model does not conflict with the widely accepted sensory conflict theory for the etiology of motion sickness. The sensory conflict theory, briefly, delineates motion sickness as the end result of a neural mismatch among vestibular, visual, and proprioceptive infor-

[3] Note that a simple multiplicative model (e.g., gain change) would not enable adequate compensation in 0g, when no signals are coming from either side.

mation or their stored relationships (Reason and Brand 1975; Oman 1982). The von Baumgarten and Thümler model simply provides a specific mechanism by which conflicting otolith information may be transmitted to higher cortical centers, thereby establishing a sensory mismatch that could lead to motion sickness.

3.1.3 Otolith asymmetries manifest as binocular positioning misalignments

From the discussion above, one can envision how the ability to quantify otolith asymmetries may lead to predictions of vestibular performance, including motion sickness susceptibility, during exposure to novel g-levels. In fact, numerous studies have correlated otoconial mass asymmetries in fish with swimming patterns observed during centrifugation, parabolic flight, and spaceflight (von Baumgarten et al. 1972; Wetzig 1983; Ijiri 1995; Scherer et al. 1997; Anken et al. 1998; Hilbig et al. 2002; Helling et al. 2003). Lateral preponderances were found in fish that displayed disturbed swimming motions, lethargic behaviors, and emesis.

Although there are no clinical tests to explicitly measure such anatomical asymmetries in humans, asymmetries in behavioral responses (namely, in eye movements) can be examined as evidence of their existence. Among other processes, the otolith organs control vertical and torsional eye movements, and as such, innate otolith asymmetries will manifest as vertical and torsional ocular positioning misalignments. Measures of binocular torsion have been the primary eye movement of choice when considering otolith asymmetries (Lackner et al. 1987; Wetzig et al. 1990; Diamond and Markham 1991; Cheung et al. 1992; Diamond and Markham 1992a; Diamond and Markham 1992b; Markham and Diamond 1992; Markham and Diamond 1993; Wuyts et al. 2003); this may be because static torsion is primarily a reflexive, vestigial eye movement that, unlike ver-

tical eye movements, is not subject to voluntary control (Collewijn et al. 1988; Misslisch et al. 2001). It is important to recognize that the purpose of measuring these ocular misalignments is not necessarily to look for functional visual deficits (e.g., diplopia), although these will certainly occur with large otolith asymmetries. Instead, small positioning misalignments should be considered in light of an underlying otolith asymmetry, which carries important implications for motion sickness susceptibility and other vestibular performance deficiencies in novel gravitational fields. Therefore, one should not simply dismiss as unimportant those ocular misalignments that appear small in magnitude, as they may be representative of a more fundamental property of that individual's vestibular system.

Ocular positioning misalignments can be suppressed by binocular vision, as the visual system is remarkably capable of fusing disparate visual scenes (up to 2° vertically and 15° torsionally (Ogle and Prangen 1953; Crone and Everhard-Hard 1975; Houtman et al. 1977; Guyton 1988)). Hence, ocular misalignments should be characterized in either complete darkness or in the presence of monocular visual stimuli only. Furthermore, ocular misalignments due to otolith asymmetries are not easily observed in a 1g environment, as they are likely masked by central compensation. Therefore, one should not expect to necessarily measure larger ocular misalignments during baseline 1g testing in individuals who are presumed to have larger otolith asymmetries. In fact, one study was unable to elicit ocular torsion misalignments during static 5° and 10° roll tilt on Earth in subjects who had demonstrated significant torsional misalignments during the 0g and 1.8g phases of parabolic flight (Markham and Diamond 1992); such small tilts are likely subject to central compensation because they are routinely experienced in everyday life.

(It should also be noted that these investigators did not eliminate binocular visual cues during either their 1g ground or parabolic-flight tests, which would further diminish the ability to observe ocular misalignments due to an underlying otolith asymmetry.) So, in summary, uncovering an inherent otolith asymmetry through observations of ocular positioning misalignments requires (1) exposing the individual to novel accelerations or gravitational forces, the best contenders being those motion stimuli that cannot be related to other terrestrial experiences, and (2) eliminating extraneous visual cues that might act in a suppressive manner.

One viable technique for revealing otolith asymmetries on Earth is through unilateral centrifugation (UC), as the large, unconventional centrifugal forces associated with this test are unlikely to be centrally compensated. Corresponding ocular measurements are typically performed in complete darkness using infrared VOG. UC is a clinical procedure for diagnosing unilateral utricular deficits in vestibular patients, as it evaluates the left and right utricles independently (Wetzig et al. 1990; Clarke and Engelhorn 1998; Wuyts et al. 2003). During UC, the subject is seated upright and rotated about an Earth-vertical axis at a high velocity (400°/s). Once canal signals have subsided, the subject is then translated along the IA axis approximately 4cm from the axis of rotation. This positions the ipsilateral utricle "on-axis," while exposing the contralateral utricle to a centrifugal acceleration of approximately 0.4g at 400°/s. In healthy individuals, this results in OCR and a perceptual roll-tilt of approximately 20° toward the ipsilateral side, which can be quantified with eye movement recording devices and psychometric tests, respectively. The subject can then be translated in the opposite direction such that the ipsilateral utricle now becomes the contralateral utricle; the corresponding OCR or perceptual tilt can be

measured and compared to the other side. The IA translation can be performed dynamically (sinusoidal motion) to acquire continuous, repeated-measures data from both sides. In the case of a utricular asymmetry, the magnitude of the OCR differs during leftward versus rightward utricular stimulation; for example, if left utricular stimulation is associated with larger OCR, one might proposed that this side is associated with a larger anatomical mass.

In theory, UC could be employed preflight to look for potential asymmetries in astronauts. One might surmise that those with larger OCR asymmetries brought out by the centrifugation may have more difficulty with entry into orbit and following Earth-return. However, the associated bulky equipment, time-consuming procedures, and uncomfortable nature of centrifugation limit the practicality of such a test during crewmembers' busy preflight schedules. Furthermore, and possibly more importantly, there is a lack of appropriate countermeasures that can be employed should a large asymmetry be found in the first place. For these reasons, UC has yet to be applied in a predictive manner preflight.

3.1.4 Altered g-levels elicit binocular misalignments and provide evidence for central compensation

Measuring ocular misalignments during spaceflight would provide a direct method for quantifying otolith asymmetries, and correlating these results with motion sickness susceptibility would provide a scale for functional performance decrements for otolith asymmetries of a given size. Diamond and Markham measured ocular torsion in three astronauts, one during the 1994 30-day Euromir mission and two during the 1995 180-day Euromir mission (Diamond and Markham 1998). Monocular torsion was recorded

inflight in the 30-day astronaut, and binocular torsion was recorded inflight in the two 180-day astronauts. Throughout the duration of the missions, spontaneous eye torsion was significantly offset from that in preflight 1g tests in all three astronauts. Furthermore, the 180-day astronauts showed a marked torsional misalignment inflight. Postflight, the 180-day astronauts also showed increased OCR, which gradually returned toward (but did not achieve) preflight values over the 13 days of postflight testing. The authors concluded that the sudden change in otolith signaling due to the altering g-levels decouples the inherently fragile connections between oculomotor torter motoneurons, thereby leading to the asymmetrical responses seen inflight and postflight.

As there have been limited capabilities for measuring eye movements during spaceflight missions themselves, one could infer otolith asymmetries through postflight data: the presumed adoption of a 0g-tuned central compensatory mechanism following several days in orbit would result in a maladapted compensation (and hence ocular misalignments) upon Earth-return. Kornilova et al. reported a strong correlation between spaceflight motion sickness susceptibility and postflight OCR asymmetry in 36 Russian cosmonauts (Kornilova et al. 1983). In this study, eleven out of twelve long-duration crewmembers (missions between 30 and 211 days) who experienced SMS inflight also exhibited asymmetries in OCR postflight. In another study, Vogel and Kass measured OCR elicited by leftward and rightward roll tilts up to 90° in four Spacelab-1 crewmembers pre- and postflight (Vogel and Kass 1986). The astronaut who was the most prone to SMS expressed the largest asymmetry in OCR gain preflight, while the astronaut who was the least prone to SMS showed nearly symmetrical OCR gain preflight and quickly returned to these baseline levels postflight. Young and Sinha reported that all Spacelab

SLS-2 astronauts generated symmetric OCR during leftward and rightward roll tilts pre-flight, but asymmetric responses postflight (Young and Sinha 1998). Although they did not correlate these results with motion sickness susceptibility, their findings indicate that central compensation had been re-programmed during exposure to 0g.

Parabolic-flight testing provides a more affordable and readily accessible platform for measuring binocular misalignments in both hypo-g and hyper-g environments. Diamond and Markham performed a series of experiments in astronauts that correlated asymmetries in binocular torsion during the altered g-levels of parabolic flight with SMS experience (Diamond et al. 1990; Diamond and Markham 1991; Diamond and Markham 1992b). Torsional asymmetry was measured in thirteen crewmembers during the 0g and 1.8g phases of parabolic flight, approximately 2–5 years following their most recent spaceflight (Diamond and Markham 1991; Diamond and Markham 1992b). Prior to the parabolic-flight testing, each astronaut completed a detailed SMS questionnaire regarding motion sickness experience during past spaceflight missions; investigators were blind to these results until after the torsional asymmetry data had been analyzed. Torsional asymmetry, defined as the difference in the right and left mean torsion amplitudes, was then measured during the 0g and 1.8g phases of parabolic flight. A mean difference in torsional asymmetry between the 0g and 1.8g phases was computed for each astronaut. The astronauts were rank-ordered, based on their respective mean difference in torsional asymmetry between the 0g and 1.8g phases, and it was found that those with the largest ranks (largest difference in torsional asymmetry between the 0g and 1.8g phases of parabolic flight) were the ones who experienced the most severe SMS during their missions. The authors surmised that these more susceptible astronauts had larger inherent otolith

asymmetries (whose effects were well compensated in 1g, but unmasked in altered g-levels), which is what led to their SMS during their respective spaceflights. The authors thus proposed the measurement of binocular torsion in parabolic flight as a predictive test of SMS. Such procedures remain, however, to be measured in crewmembers preflight.

In another study, Diamond et al. examined instability in ocular torsion during parabolic flight in two astronauts (one who had experienced SMS and one who had not, during their respective spaceflights) and eight healthy controls (Diamond et al. 1990). Torsional instability was quantified from fluctuations in disconjugate torsional eye positions. The ten subjects were divided into two groups, comprised of the five individuals with the highest instability scores and the five individuals with the lowest instability scores. The astronaut who had experienced SMS was in the high instability group, while the astronaut who had not experienced SMS was in the low instability group. Although the mean amplitude of ocular torsion was no different between two groups in the 0g and 1.8g phases of flight, the torsional variability between these two groups was significantly different. The authors proposed that the spontaneous torsional motions seen in the high-variability group were evidence of an unstable otolith system. None of these test results were significantly different in 1g, which supports the notion that central compensation facilitates stable, symmetric responses. Furthermore, and of considerable interest to the parabolic-flight experiment described later in this chapter, the astronaut who did not experience SMS during his spaceflight had a very large index of torsional instability during 1g baseline testing and experienced significant motion sickness during his parabolic flight. This astronaut also reported that he was extremely susceptible to motion sickness on Earth, including during previous parabolic flights. The correlation between baseline torsional

instability and a propensity for motion sickness during parabolic flight was not confirmed in the other subjects, although these other individuals had significantly reduced baseline 1g torsional instability scores (by more than a factor of 3) and it was not revealed which, if any, of the other individuals did or did not experienced motion sickness during their parabolic-flight testing. The fact that the one astronaut who did not experience SMS is highly susceptible to Earth motion sickness, including parabolic-flight exposure, provides evidence that the link between motion sickness on Earth versus motion sickness in space is complex. Other studies have hinted at this lack-of-straightforwardness as well (Thornton et al. 1987b; Lackner and Dizio 2006).

Lackner et.al. compared parabolic-flight motion sickness susceptibility with 1g preflight OCR elicited by leftward and rightward body tilts of 25° and 50° in 71 individuals (Lackner et al. 1987). During the 1g tilt testing, an asymmetry index, defined by the ratio of OCR during the leftward versus rightward tilts, was computed for each subject. Parabolic-flight motion sickness susceptibility was scored using the Graybiel, Wood, Miller, and Cramer diagnostic criteria (Graybiel et al. 1968). The primary result from this study was that subjects with larger asymmetries in OCR during the 1g leftward versus rightward body tilts were significantly more susceptible to motion sickness in parabolic flight. Note that these results are in contrast to the Markham and Diamond study mentioned earlier that did not find significant OCR asymmetries during small 5° and 10° tilts (Markham and Diamond 1992); the most likely reason for this difference is that while Markham and Diamond's 5° and 10° tilts are common during everyday tasks, Lackner et al.'s 25° and 50° are not, and therefore more likely to be uncompensated in 1g.

Few studies have examined otolith asymmetries in light of vertical ocular misalignments. We presume that this is due to the fact that vertical eye movements are subject to voluntary control, and that fusion readily eliminates any such misalignments under normal viewing conditions. Hence, experiments must be carefully designed to exclude extraneous visual cues, which preclude many of the studies described above (see also Section 3.5.1). But because otolith signaling drives both torsional and vertical eye movements, we presume that properly designed experiments may also be useful in studying otolith asymmetries. Vertical eye movements are advantageous because they are relatively easy to measure, especially in comparison to ocular torsion. In one such study, Karmali et al. observed gravity-dependent changes in vertical misalignments during horizontal eccentric viewing in parabolic flight (Karmali et al. 2006). In this experiment, five subjects expressed differences in vertical misalignment between the 0g and 1.8g phases of parabolic flight ($\bar{x}$ = 1.37°, s = 0.89°) when horizontal gaze was directed 25° eccentrically. Similar to the ocular torsion results found in other studies, these authors posit that these vertical misalignments were also due to inherent otolith asymmetries whose central compensatory mechanisms were calibrated for 1g.

3.2 Objectives

The fundamental concept behind the vestibular asymmetry central compensation model is that the inherent plasticity within the CNS facilitates adequate compensation for a variety of maladapted states, such as those stemming from anatomical or physiological asymmetries, but this compensation must be learned. Hence, upon a change of g-level, inherent otolith asymmetries, manifest through ocular positioning misalignments, are

unmasked. While these ocular misalignments may not be large enough to elicit visual performance decrements, their link with motion sickness susceptibility renders them important to quantify for spaceflight operations and research. Therefore, the experiments in this chapter were designed to:

1. Develop technology to measure vertical and torsional binocular misalignments using portable equipment and simple tests.
2. Validate the technology in the laboratory by employing prisms to induce known visual disparities and in a spaceflight operationally-relevant environment (i.e., parabolic flight).
3. Use the parabolic-flight results to further examine the role of altered g-levels on binocular positioning asymmetries that may be related to an underlying otolith asymmetry.
4. Correlate the parabolic-flight results with motion sickness experience, focusing especially on baseline data as potential preflight predictors of motion sickness susceptibility.
5. Update the von Baumgarten and Thümler central compensation model with any new findings from the parabolic-flight testing, especially in regards to vertical misalignment data, which has been much less characterized in altered g-levels to-date.

The final objective is the principle aim of Chapter 4.

3.3 Materials and methods

3.3.1 VAN and TAN design

Vertical Alignment Nulling (VAN) and Torsional Alignment Nulling (TAN) were developed to measure vertical and torsional ocular positioning misalignments, respectively, using portable, hand-held equipment and simple tests that could be quickly self-administered. By eliminating the need to measure eye movements, we eliminate the delicate equipment and computationally expensive algorithms typically associated with binocular eye movement recording. The VAN and TAN hardware consists of a small (8.1 x 5.3 x 0.3in, 12.3oz) active-matrix organic light-emitting diode (AMOLED) tablet computer (Toshiba Excite, Android OS) and a pair of red-blue eyeglasses (the left lens houses a red filter, and the right lens houses a blue filter). Wireless motion sensors can also be incorporated (synchronized into the VAN and TAN program via Bluetooth) to record various types of kinematic movement; for example, a head-mounted sensor can track relative head-to-tablet movement during testing, and a reference sensor secured to the floor of the aircraft can capture changes in g-level.

In VAN and TAN, the subject wears the red-blue eyeglasses and views one red and one blue line on the tablet screen; this arrangement provides different visual information to each eye. During the tests, one line remains fixed on the tablet screen, while the other line (designated the "moving line") can be repositioned vertically during VAN or rotated during TAN. This is accomplished by either dragging the moving line, or using the *up/rotate counter-clockwise* and *down/rotate clockwise* buttons located near the bottom of the tablet screen. Both techniques have equal resolutions (1 pixel vertically, 0.1° rotationally). Dragging the moving line is typically faster, but the buttons provide

tactile feedback for each incremental step, which better facilitates fine-tuning of responses in subjects with large binocular fusion capacities.

At the beginning of each test, the tablet is fixed relative to the subject's head: it is either held out in front, or mounted on a desk or wall. When the app is started, the VAN and TAN home screen appears (Figure 3.2). The subject selects which task will be performed (V for VAN or T for TAN) and which eye will be associated with the moving line (RE for right eye or LE for left eye) from the radio buttons in the upper left-hand corner of the screen. If external motion sensors are being used, they are activated next by selecting their respective radio buttons. When the *open file* button is pressed, two new files (a *small file* and a *large file*) are created for storing the test results. During testing, the tablet's timestamp, current line positions, trial number, and kinematic data from the tablet's onboard accelerometer and any external wireless motion sensors are exported to the data files in real-time. Data from the tablet's three-axis linear accelerometer can detect if the tablet screen, and hence the red and blue lines, was tilted relative to the local g-vector during the test, or if the orientation of the tablet changes during the test (e.g., due to arm fatigue if the subject is holding the tablet). The *small file* records a row of data each time the line is incrementally moved, while the *large file* records a row of data every 10ms. The *large file* is especially useful when external motion sensors are being used to keep track of motion, such as when recording g-level. The *small file* is typically sufficient when the subject is in a stationary environment. The file names are automatically generated based on the current date and timestamp of the tablet (to prevent accidental overwriting), the task (VAN or TAN), and the moving line (right or left). The subject presses the *new trial* button to begin the test block.

AMOLED technology allows only the designated pixels on the tablet to be illuminated. Once the *new trial* button is pressed, only the red and blue lines and color-matched trial counter are visible. All other visual cues, including the test settings along the top of the screen and button labels, become invisible, although the functions and vibrotactile feedback for the buttons that reposition the moving line, reset the next trial, and close the current file remain active. All testing is performed in complete darkness, either in a dark room or under a shroud. These features are critical for ensuring that peripheral visual cues, such as a tablet screen "border" (as seen on traditional LCD screens due to the screen backlight), do not mask the misalignments (Burian 1939; Ogle and Prangen 1953; Kertesz and Jones 1970; Crone and Everhard-Hard 1975; Kertesz 1981; Guyton 1988).

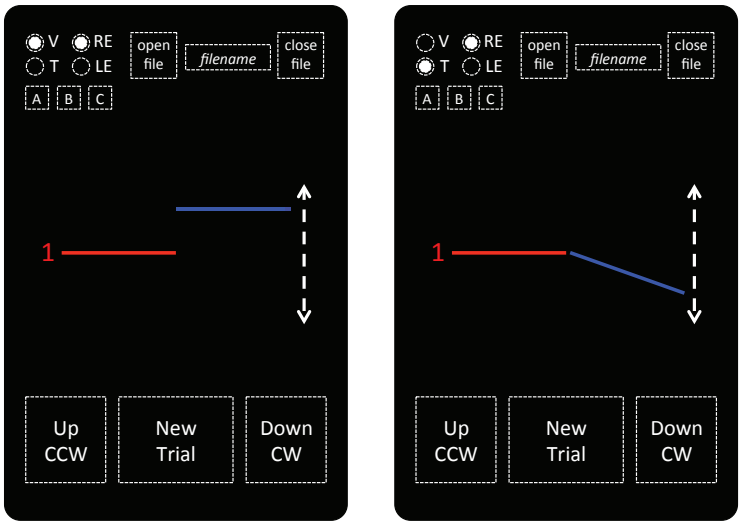

Figure 3.2 VAN (Left) and TAN (Right) home screens. The subject selects which test will be performed (V or T) and which eye will be associated with the moving line (RE or LE) using the radio buttons in the upper left hand corner of the screen. Wireless motion sensors (A, B, and C) are activated, as needed. At the beginning of each test block a new file is opened (open file), which displays the filename. At the start of each trial, the vertical position (in VAN) or rotation angle (in TAN) of the moving line is altered, which subjects adjust until a single, continuous red-blue line is perceived; this is accomplished by dragging the line using an invisible slider button (indicated by the dashed white double-arrow) or repeatedly hitting the up/down/rotate CW/rotate CCW touch buttons on the bottom of the screen (areas outlined by the dashed-white boxes). During the actual testing, the white text is invisible and subjects use tactile feedback to interface with the app.

When the *new trial* button is pressed at the beginning of each trial, the red and blue lines are initially vertically offset from one another during VAN or rotated relative to one another during TAN. The subject is tasked with aligning the two lines until a single continuous straight line is perceived. The amount of initial offset is randomized between 2° and 4° for VAN and 2° and 5° for TAN; the goal is for the program to select values that require the subject to reposition the moving line, but not by so much that unnecessary time is wasted fine-tuning each trial. If there exists a range of values for which a continuous line can be perceived, meaning that the subject can perceptually fuse a physical offset, the subject is instructed to find the middle of that range. The key instruction for both VAN and TAN is that the moving line should be set *relative* to the fixed line. So for example, even if the fixed line appears tilted with respect to the subject's perception of the Earth's horizon during TAN, the subject must still rotate the moving line until it is in-line with the fixed line, not in-line with the perceived horizontal. Furthermore, if during TAN the lines appear vertically offset from one another, subjects are instructed to make the lines parallel to one another. Depending on the subject's horizontal vergence angle, the two lines may appear either overlaid or horizontally separated (see Section 3.5.2 for further details). The final amount by which the lines are offset from one another vertically or rotated relative to one another provides a measure of perceptual vertical and torsional ocular misalignment, respectively.

Once the trial is completed, the subject presses the *new trial* button (in the same central location on the tablet, but now invisible) to generate the next trial. A trial counter located just lateral to the fixed line allows subjects to keep track of how many trials they

have completed; this counter is also useful in noting which trials should be eliminated during post-processing due to an accidental button press, for example. Once the desired number of trials has been completed, the subject closes the file using the *close file* button in the upper right-hand corner of the screen. Pressing the *close file* button illuminates the home screen once again, so that the test conditions can be configured for the next test block.

If the subject has perfect vertical and torsional binocular alignment, then at the end of each trail, the lines will be perfectly aligned (Figure 3.3). If the subject has a vertical misalignment such that the right eye is elevated above the left eye, for example, then he will set the right line above the left line. If the subject has a torsional misalignment such that the right eye is extorted relative to the left eye, then he will orient the right line clockwise relative to the left line. The following conventions are used for the misalignment data in the exported data file:

- VAN primary output: y_{pos} = position of left (red) line – position of right (blue) line in pixels (i.e., $y_{pos} > 0$ indicates that the left line is above the right line and $y_{pos} < 0$ indicates that the left line is below the right line). This value can be converted from pixels to degrees post-test, based on the pixel pitch (which is 191 pixels/in for our AMOLED tablet) and subject-to-screen distance:

$$\angle = \frac{180°}{\pi} \tan^{-1}\left(\frac{{}^{y_{pos}}/_{191}}{subject - to - screen\ distance\ in\ inches}\right) \qquad (1)$$

- TAN primary output: y_{ang} = number of degrees that the right (blue) line is rotated clockwise ($y_{ang} > 0$) or counterclockwise ($y_{ang} < 0$) relative to the left (red) line.

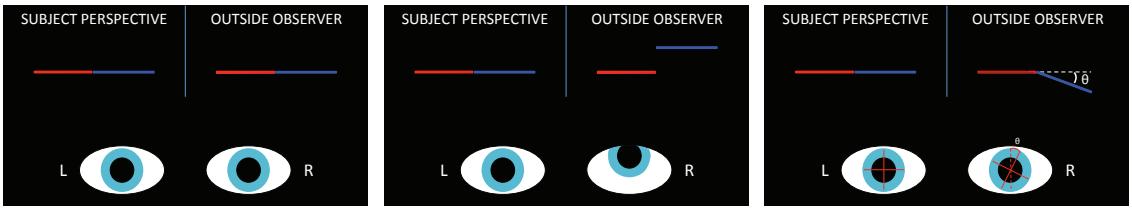

Figure 3.3 Examples of ocular misalignments inferred by VAN and TAN results. Subjects reposition the moving line until they perceive a single continuous line, thereby positioning each line on the center of each retina. Binocular misalignment is inferred from the relative positioning of the lines at the end of each trial. (Left) If the subject has perfect binocular alignment, then the lines will be perfectly aligned at the end of the trial. (Center) If the subject sets the right line above the left line during VAN, we infer that the right eye is elevated above the left eye. (Right) If the subject orients the right line CW relative to the left line in TAN, we infer that the right eye extorted relative to the left eye.

3.3.2 Prism validation experiments

VAN and TAN laboratory validation experiments were performed in five healthy subjects (Table 2.1) to demonstrate that VAN and TAN could accurately account for visual disparities induced by various prisms of known prismatic power during straight-ahead gaze. Four of these five subjects were naïve to the objectives of the experiments and the details regarding how the prisms altered the visual images. Throughout the experiments, the prisms were placed in front of the right eye, thereby inducing systematic visual shifts in the right line (Bagolini 1976). We hypothesized that in order for subjects to perceive a single continuous line, they would need to adjust the right line by an amount equal in magnitude but opposite in direction to the visual disparity induced by the prisms.

For each VAN and TAN prism, three tests were performed: (1) *conventional*, (2) *always above*, and (3) *always below*. In the *conventional* tests, the initial position (VAN)/orientation (TAN) of the moving line was randomized to be either above/counterclockwise or below/clockwise the theoretical final position/orientation. During these tests, if subjects experienced a range of values for which a single continuous line could be perceived, they were instructed to find the middle of this range. The *con-*

ventional tests are what are typically performed for VAN and TAN. In the *always above* tests, the initial position/orientation of the moving line was always above/counterclockwise the theoretical final position; during these tests, subjects were only allowed to reposition the moving line in one direction (down/clockwise) and were instructed to stop as soon as they could fuse the two lines into a single continuous line. In the *always below* tests, the initial position/orientation of the moving line was always below/clockwise the theoretical final position/orientation; during these tests, subjects were only allowed to move the line up/counterclockwise, and were instructed to stop as soon as they could fuse the two lines into a single continuous line. The purpose of the *always above* and *always below* tests was to explore each subject's capacity for sensory fusion. Previous literature has indicated that healthy individuals can fuse up to 2° vertically and 15° torsionally (Ogle and Prangen 1953; Crone and Everhard-Hard 1975; Houtman et al. 1977; Guyton 1988), and we were interested in how VAN and TAN results compared to these standards.

To maintain a consistent subject-to-screen distance (crucial for VAN) and to ensure that the head wasn't rotated relative to the tablet screen (which may have made the TAN test more difficult if the fixed line appeared tilted with respect to the horizon), subjects were seated upright in a chair with the head secured via a custom-molded dental biteboard and the tablet mounted 18in directly in front of them. Testing of VAN and TAN were performed on separate days to prevent fatigue. VAN and TAN control tests were performed without any prisms in both the standard upright position and while lying supine; we refer to these as the 0 and 0S tests. The supine test was intended to explore

whether a change in the direction of the gravity vector, and hence a different pattern of otolith stimulation, induced systematic changes in VAN and TAN perceptual responses.

The VAN validation experiment employed triangular ophthalmic prisms (3M Press-On Optics, The Fresnel Prism and Lens Co.), which bend incident light rays toward the base of the prism. Thus, placing one of these prisms base-up in front of the eye generates images that appear to have moved down by an amount proportional to the angle of deflection of the prism. A prism diopter (PD, or Δ) is the arbitrary standard of prismatic power: a prism that deflects a beam of light by 1cm per 1m is defined as a 1PD prism. Mathematically, this is equivalent to:

$$1\Delta = 100 * \tan(deflection\ angle)$$

In the VAN validation experiment, 1, 2, 3, 6, and 10PD prisms were placed base-up in front of the right eye, which resulted in downward vertical shifts of the right line by 0.57°, 1.15°, 1.72°, 3.43°, and 5.71°, respectively. Therefore, in order for subjects to perceive the right line as in-line with the left line, they needed to move the right line up by 0.57° – 5.7°. The initial conditions for the *new trial* button were reprogrammed so that the right line was initially offset either above or below the current prism's deflection angle plus a random amount between 2° and 4°. So for example, the initial conditions for the 10PD test, in which the prism deflects the image by 5.71°, were set so that the initial position of the right line was between 5.71°+2° = 7.71° and 5.71°+4° = 9.71° above the left line, or between 7.71° and 9.71° below the left line. This was done so that subjects were required to reposition the moving line by an amount proportional to the deviation angle of the prism. Asking subjects to adjust the line from initial positions that were both too high and too low was important for ensuring that the final y_{pos} results were not biased

in the direction of the initial condition; this was also especially important for subjects who had larger vertical fusion capacities, where finding the "center" of this fusion range may have been more difficult.

In the TAN validation, a 15mm Dove prism (Edmund Optics, Inc.) was placed in front of the right eye to induce a visual rotation of the right line. As added insurance in controlling for any angular offset between this Dove prism and the tablet, which would have resulted in inaccurate y_{ang} results, a second (unrotated) Dove prism was place in front of the left eye and stabilized against the right Dove prism. Dove prisms are traditionally known for their inversion property: when viewing down the longitudinal axis of the prism, images appear upside-down. But their inherent design is also such that when they are rotated about the longitudinal axis, the transmitted image is rotated by twice as much. In the TAN validation, the right Dove prism was rotated counterclockwise by 1°, 2.5°, and 5°, thereby inducing counterclockwise visual rotations of the right line by 2°, 5°, and 10°. Thus, in order for subjects to perceive the right line as in-line with the left line, they needed to rotate the right line clockwise by 2°, 5°, and 10°. Again, the initial conditions for the *new trial* button were reprogrammed so that the right line was initially rotated either clockwise or counterclockwise by the current visual rotation angle induced by the prism plus a random amount between 2° and 4°. So for example, the initial conditions for the 10° stimulus condition was set so that the initial orientation of the right line was between 10°+2° = 12° and 10°+4° = 14° clockwise, or between 10° and 14° counterclockwise. During these tests, the prisms were placed on a machinist micro-adjustable angle block (Anytime Tools Precision Measuring, Inc.) to ensure the small rotation angles were accurate. Because there were no prisms employed during the supine test, two

control tests were necessary: one with no Dove prisms (0_{np}) and one with both Dove prisms (0).

Subjects were trained on VAN and TAN for approximately 10min prior to testing to become comfortable with performing the tests. Prismatic power and *conventional*/*always above*/*always below* tests were counterbalanced across subjects. There were a total of 21 VAN blocks ([0S, 0, 1, 2, 3, 6, 10PD] × [*conventional*, *always above*, *always below*]) and 18 TAN blocks ([$0S_{np}$, 0_{np}, 0, 2, 5, 10°] × [*conventional*, *always above*, *always below*]). Fifteen trials were completed for each block. Breaks with full-field vision were taken between blocks to minimize any adaptive effects of the prisms (Maxwell and Schor 2006).

3.3.3 Parabolic-flight experiments

VAN and TAN were tested in the altering g-levels of parabolic flight to validate the technology in an operational environment, and to investigate the role of otolith stimuli in determining ocular misalignments. Nine subjects, including seven naïve fliers and two experienced fliers (Table 2.1), each flew one forty-parabola flight, which consisted of five Martian parabolas (0.38g), five Lunar parabolas (0.17g), and thirty 0g parabolas (all alternating with 1.8g pullout maneuvers). Importantly, subjects were not allowed to take the anti-motion sickness medication (subcutaneous scopolamine), as it has been shown to suppress vestibular responses (Pyykko et al. 1985; Shojaku et al. 1993).

Based on laboratory VAN and TAN testing, past flight experience, and literature surrounding ocular misalignments in altered g-levels, the following predictions were made preflight (von Baumgarten and Thümler 1979; Diamond and Markham 1991; Diamond and Markham 1992b):

1. Subjects would experience larger vertical and torsional ocular misalignments in the 0g and 1.8g phases of parabolic flight than during baseline 1g testing due to presumed otolith asymmetries.
2. The degree of misalignment would be larger in 0g than in 1.8g, due to the lack of background stimulation in 0g (Weber-Fechner law, (Hoagland 1930)).
3. The direction of misalignment would be reversed in 0g versus 1.8g.
4. Subjects with past parabolic-flight experience would show smaller (if any) ocular misalignments in altered g-level (Lackner and Graybiel 1982; Shelhamer et al. 2002).
5. If any subjects experience motion sickness, they would also show larger differences in torsional misalignments between their 0g and 1.8g TAN responses, and possibly more variable responses during baseline 1g testing.

During the parabolic-flight tests, the tablet was secured to the side wall of the aircraft. The subject sat on the floor facing the tablet at a distance of 15in, which was chosen based on the location of straps used to loosely secure the subject to the floor of the aircraft during the flight testing. The subject and tablet were enclosed in a black shroud to prevent any peripheral visual cues from masking potential ocular misalignments. A small battery-operated fan was placed inside the shroud to mitigate excess heat. Two wireless 6DOF motion sensors (Shimmer Inc.), one fixed to the subject's forehead via an elastic strap and one anchored to the floor of the aircraft, measured relative head motion and aircraft g-level. Two subjects were tested simultaneously inflight (Figure 3.4).

Figure 3.4 Two subjects performing VAN and TAN in parabolic flight. Subjects are inside the black shrouds to eliminate external visual cues that would otherwise mask the ocular misalignments.

Subjects were trained on the VAN and TAN tasks several weeks prior to their actual parabolic flight, and training was refreshed the morning of their respective flights just prior to baseline data collection. Baseline 1g data consisted of 20 trials of VAN and 20 trials of TAN, which were collected onboard the aircraft under the shroud approximately one hour prior to takeoff.

The nominal VAN and TAN test plan is shown in Table 3.1. During each flight, the aircraft flew four blocks of ten consecutive parabolas with brief 1g breaks in between each block. During the test parabolas (parabolas 1–20 and 31–40), subjects were instructed to perform as many successive VAN or TAN trials as possible; trials were separated by g-level during postflight data analysis. During the adaptation parabolas (parabolas 21–30), subjects were removed from the shroud and straps so that they could experience the parabolas with full-field vision and whole-body movement in response to the changing g-levels. The purpose of this adaptation period was to fully expose subjects to the parabolic-flight environment to induce adaptation. Testing was typically paused during the 1g breaks between parabola blocks to allow subjects to rest outside of the shroud. If at any point subjects began to experience any motion sickness symptoms, including hot or cold sweats, stomach awareness, dizziness, nausea or vomiting, testing was stopped

immediately and subjects were instructed to close their eyes and rest while operators removed the shroud.

Table 3.1 VAN and TAN parabolic-flight test plan.

parabola #	g-level	task
1-5	0.38g, 1.8g	VAN
6-10	0.17g, 1.8g	TAN
11-15	0g, 1.8g	VAN
16-20	0g, 1.8g	TAN
21-30	0g, 1.8g	ADAPT
31-35	0g, 1.8g	VAN
36-40	0g, 1.8g	TAN

3.4 Results

3.4.1 VAN and TAN quantify visual disparities induced by prisms

Results from the VAN and TAN *conventional* tests are displayed in Figures 3.5 and 3.6, respectively. In each of these figures, the raw data is displayed on the left and the raw data minus the upright control condition (0) is displayed on the right. The red line marks the stimulus condition, namely how much misalignment subjects were expected to perceive based solely on prismatic power. All subjects expressed small, non-zero vertical and torsional misalignments during the upright control tests (no prisms); when these values were subtracted from the prism results, each subject's response curve aligned closely with the red stimulus line.

In Figure 3.5, the vertical misalignment data is negative. By y_{pos} convention, negative vertical misalignments mean that the right line is positioned above the left line at the end of the trial. This is exactly what we expect from healthy individuals in response

to a right line visually displaced below the left line: to null such a visual disparity, the right line must be moved up for the subject to perceive a single continuous straight line. Thus, to an outside observer, the right line will be positioned above the left line at the end of the trial. Analogously, in Figure 3.6, the torsional misalignment data is positive. By y_{ang} convention, positive torsional misalignments mean that the right line is rotated clockwise with respect to the left line at the end of the trial. Again, this is what we would expect from healthy individuals in response to a right line visually rotated counterclockwise to the left line.

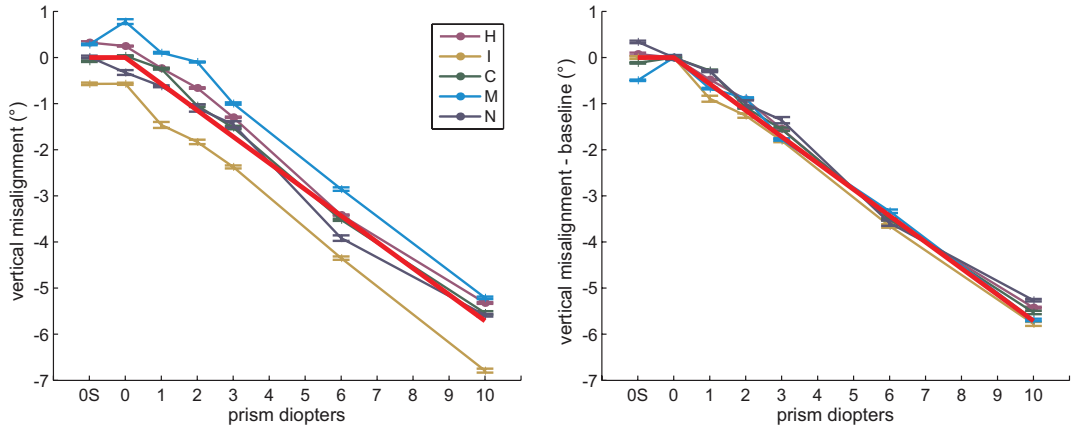

Figure 3.5 VAN *conventional* prism results from five subjects viewing through vertically displacing prisms in front of the right eye. 0 represents the control test with no prisms. 0S was performed in the supine position (without prisms); all other tests were performed upright. The red line represents the visual offset stimulus induced by the prisms. Error bars represent 1SE. By convention, negative vertical misalignments indicate that the right line was positioned above the left line. All subjects showed a small vertical misalignment during the upright control test (0), which is subtracted out in the graph on the right.

In general, VAN and TAN *conventional* results were highly consistent both within the individual subjects (small error bars within each test block) and across the five subjects (small scatter among the subject means for each test block). The fact that the TAN misalignment data is 1° larger than the stimulus prediction (red line) for the 10° test block may have been due to a slightly imprecise orientation of the Dove prism; although care

was taken in precisely rotating the prism by the desired amount, the 11° center (as opposed to 10°) can be explained simply if the prism was unintentionally rotated by an additional 0.5° (recall that Dove prisms rotate the visual scene by twice the angle with which they themselves are rotated). The fact that the spread among the mean TAN scores for the five subjects during this block is consistent with the other test blocks lends this to be the most probable cause of the small discrepancy.

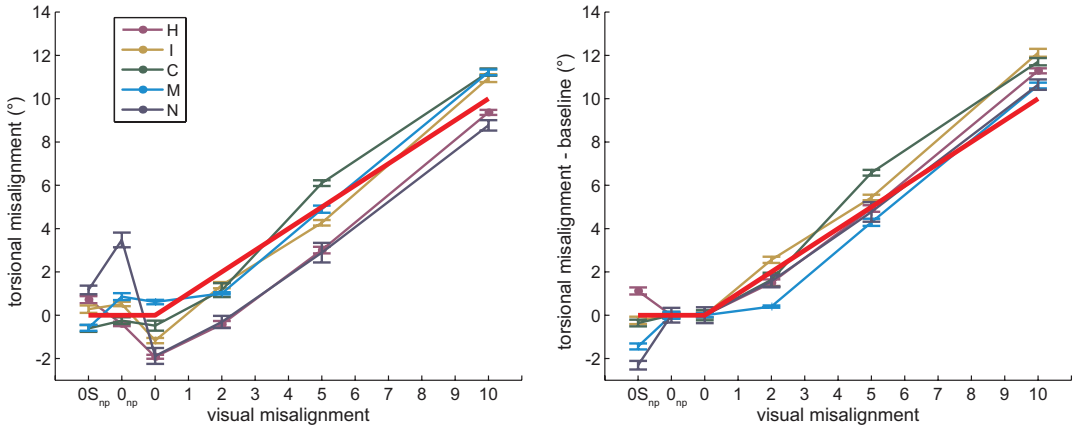

Figure 3.6 TAN *conventional* prism results from five subjects viewing through Dove prisms in front of the right eye. 0_{np} (no prisms) and 0 represent control tests. $0S_{np}$ was performed in the supine position (without prisms); all other tests were performed upright. The red line represents the visual offset stimulus induced by the prisms. Error bars represent 1SE. By convention, positive torsional misalignments indicate the right line rotated CW relative to left line. All subjects showed a small torsional misalignment during the upright control test (0), which is subtracted out in the graph on the right.

Results from the VAN *always above* and *always below* tests are shown for two subjects in Figure 3.7. On these graphs, the top of the colored boundary is the mean of the *always above* results, where the initial moving line positions were always too high and subjects were only allowed to shift the moving line down until a single continuous line could be fused. The bottom of the colored boundary is the mean of the *always below* results, where the initial moving line positions were always too low and subjects were only allowed to shift the moving line up until a single continuous line could be fused.

The shaded colored region in between represents the presumed amount of vertical sensory fusion. The red line marks the stimulus conditions and the black line is the results from the *conventional* tests. The graph on the left is from one subject (subject H), who was also representative of three other subjects (subjects C, M and N), who had small sensory fusion capacities, while the graph on the left is from the one subject (subject I) who had a much larger sensory fusion capacity.

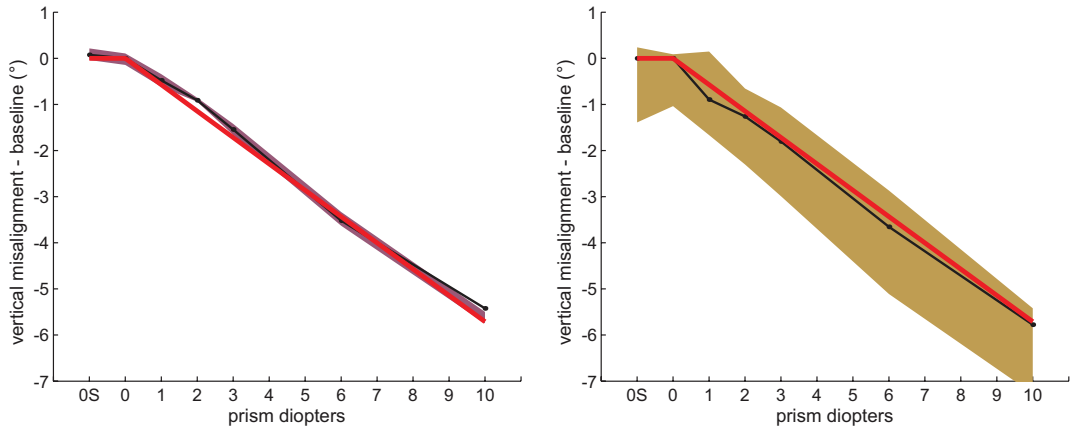

Figure 3.7 VAN *always above* and *always below* prism results for two subjects (left: subject H, right: subject I). The top of the colored boundary is the mean of the *always above* results, the bottom of the colored boundary is the mean of the *always below* results, and the shaded region in between represents the amount of vertical sensory fusion. The subject on the left displays a small sensory fusion capacity, while the subject on the right displays a large sensory fusion capacity. The red line marks the stimulus conditions and the black line is the results from the *conventional* tests.

Results from the TAN *always above* and *always below* tests are shown for one representative subject in Figure 3.8. On this graph, the top of the colored boundary is the mean of the *always above* results, where the initial moving line positions were always rotated too far in the counterclockwise direction and subjects were only allowed to rotate the moving line clockwise until a single continuous line could be fused. The bottom of the colored boundary is the mean of the *always below* results, where the initial moving line positions were always rotated too far in the clockwise direction and subjects were

only allowed to rotate the moving line counterclockwise until a single continuous line could be fused. The shaded colored region in between represents the presumed amount of torsional sensory fusion. The red line marks the stimulus conditions and the black line is the results from the *conventional* tests. All five subjects showed approximately the same amount of torsional sensory fusion capacity.

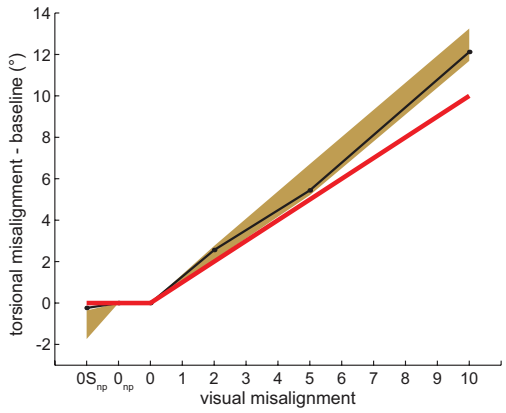

Figure 3.8 TAN *always above* and *always below* prism results for one representative subject. The top of the colored boundary is the mean of the *always above* results, the bottom of the colored boundary is the mean of the *always below* results, and the shaded region in between represents the amount of torsional sensory fusion. The red line marks the stimulus conditions and the black line is the results from the *conventional* tests.

Table 3.2 Average time of completion (in seconds) per VAN trial during *conventional* tests.

Subject	0S	0	1	2	3	6	10
H	6.42	6.72	8.33	7.15	9.95	10.57	10.23
C	2.07	4.98	3.21	4.61	5.31	8.50	4.90
I	9.42	9.81	10.18	11.78	7.12	15.90	9.96
M	3.68	8.48	4.03	4.98	5.52	5.53	8.52
N	3.73	8.12	4.81	8.89	5.17	11.30	9.07

Table 3.3 Average time of completion (in seconds) per TAN trial during *conventional* tests.

Subject	$0S_{np}$	0_{np}	0	2	5	10
H	11.17	6.57	8.96	9.64	8.34	12.05
C	4.30	6.00	3.59	2.62	3.91	4.90
I	7.47	6.93	4.86	5.15	4.16	6.80
M	3.78	4.27	4.32	3.95	4.72	6.70
N	7.20	5.40	14.40	5.10	6.97	7.39

During testing, subjects were asked to be as accurate as possible, regardless of how long it took to perform each trial. Nonetheless, subjects performed VAN and TAN quickly, on the order of a few seconds per trial. Tables 2 and 3 outline the average time in seconds to complete one trial for the various *conventional* prism tests. The subject who took the longest time to complete the VAN trails (subject I) was the individual with the largest vertical sensory fusion capacity, as indicated in Figure 3.7; this was because it took longer to locate the center of the fusion range for the *conventional* test.

3.4.2 Variability in baseline torsional misalignment correlates with motion sickness susceptibility

During the VAN and TAN parabolic-flight testing, three out of the nine test subjects (subjects V, W, and X) experienced severe motion sickness, including nausea and vomiting, within the first several parabolas of their respective parabolic flights. As such, they were unable to perform the VAN and TAN tests during the actual parabolas. We examined all nine subjects' baseline 1g data to look for differences in ocular misalignments between the three individuals who experienced motion sickness inflight and the six who did not (Figure 3.9). There was no difference in the mean vertical or torsional ocular misalignments between these two groups (two-sample t-test, VAN: $p = 0.45$ and $r^2 = 0.29$, TAN: $p = 0.22$ and $r^2 = 0.45$). This is in agreement with the notion that these reflexes are subject to 1g-tuned compensation, and are therefore not likely to predict vestibular dysfunction in non-1g environments. There was also no difference in the variability of the vertical ocular misalignments between these two groups (two-sample t-test, $p = 0.19$ and $r^2 = 0.48$). There was, however, a strong difference in the variability of the torsional ocular misalignments (two-sample t-test, $p < 0.001$ and $r^2 = 0.92$).

This finding is in agreement with the Diamond et al. (1990) study that correlated instability of ocular torsion during the 0g phases parabolic flight with spaceflight motion sickness (see Section 3.1.4). One result of this study, dismissed by the authors as an unknown anomaly, was that the one astronaut who experienced motion sickness during his parabolic flight (and happens to be highly prone to motion sickness on Earth) had an extremely large amount of ocular torsion instability during baseline 1g testing. The authors do not provide any direct explanation for why torsional instability may lead to increased propensity for motion sickness.

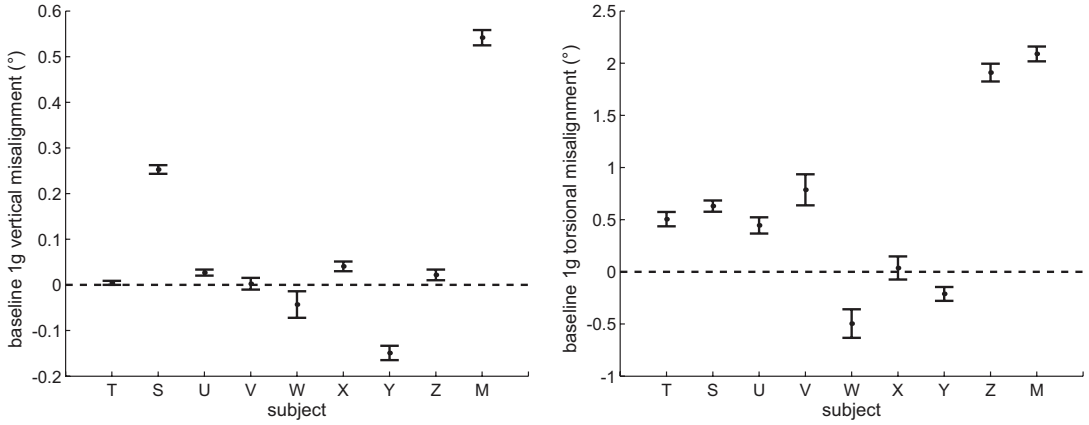

Figure 3.9 VAN (Left) and TAN (Right) parabolic-flight baseline 1g results. Error bars are 1SE. Subjects V, W, and X experienced severe motion sickness, including nausea and vomiting, very early in their respective parabolic flights.

It is interesting that this correlation result is only observed using the torsion data and not the vertical data. We presume that this is because static torsional eye positioning represents a vestigial reflex, much less subject to voluntary control than vertical eye movements. Therefore, while subjects may be able to better control the consistency in their VAN responses, they may be less able to do so for TAN. Notice that the variability in baseline VAN tests were significantly less (by an order of magnitude) than the varia-

bility in baseline TAN tests for all nine subjects (observed by comparing the size of the error bars in Figure 3.9; note the difference in scale for the y-axis).

3.4.3 Binocular misalignments increase in novel g-levels

VAN and TAN data were collected according to the test plan outlined in Table 3.1 on the six subjects who did not experience motion sickness during their respective flights. VAN data were collected during the Martian-g parabolas (parabolas #1-5), TAN data were collected during the Lunar-g parabolas (parabolas #6-10), and two sets of VAN and TAN data (Early: parabolas #10-20 and Late: parabolas #30-40) were collected during the 0g parabolas. Subjects were asked to perform the VAN and TAN trials continuously during the five-parabola test blocks, and tablet accelerometer data was used postflight to group the individual trials according to g-level. Within the five-parabola test blocks, subjects performed approximately 15-25 trials during the hypo-g phases and approximately 25-40 trials during the hyper-g phases.

The mean VAN and TAN results are displayed in Figures 3.10 and 3.11, respectively, for each subject. Subject U's tablet was not functioning properly during the Martian-g parabolas, and so we were unable to obtain VAN data on her during these parabolas. Subject J did not participate in either the Martian-g or Lunar-g parabolas because he was attending to one of the subjects who was motion sick. Subject T did not participate in the Late 0g data collection due to excessive heating (likely due to being enclosed in the shroud) and stomach awareness (although he did not report any symptoms of nausea).

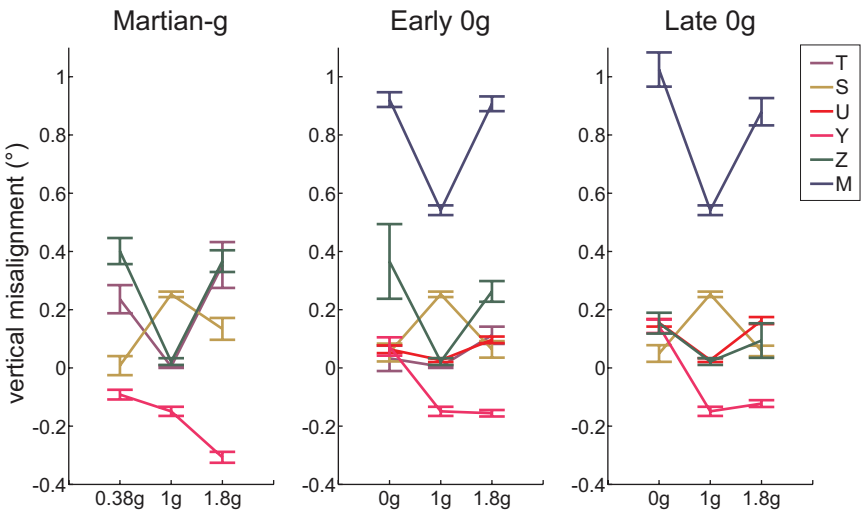

Figure 3.10 VAN parabolic-flight results for the six subjects who did not experience motion sickness during their respective flights. (Left) Martian-g data collected during parabolas #1-5. (Center) Early 0g data collected during parabolas #10-15 (the first five 0g parabolas). (Right) Late 0g data collected during parabolas #30-35. Error bars are 1SE. Subjects U and J did not participate in the Martian-g data collection and subject T did not participate in the Late 0g data collection.

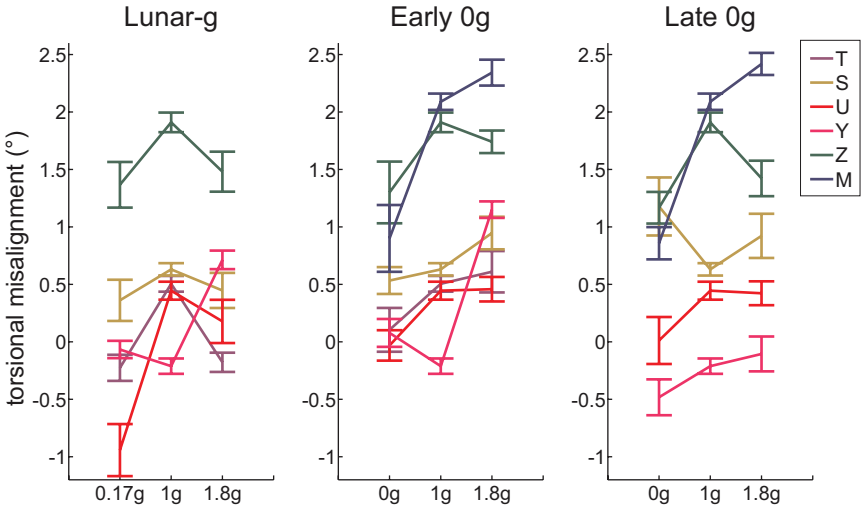

Figure 3.11 TAN parabolic-flight results for the six subjects who did not experience motion sickness during their respective flights. (Left) Lunar-g data collected during parabolas #6-10. (Center) Early 0g data collected during parabolas #16-20 (the second five 0g parabolas). (Right) Late 0g data was collected during parabolas #36-40. Error bars are 1SE. Subject J did not participate in the Martian-g data collection and subject T did not participate in the Late 0g data collection.

There are several general conclusions that can be drawn from these results. First, both the vertical and torsional ocular misalignments in Martian-g, Lunar-g, 0g, and 1.8g

were significantly different from the misalignments in 1g for all subjects. Most subjects expressed ocular misalignments that were larger in the novel g-levels than in 1g, although a few subjects showed decreased ocular misalignments in some of the novel g-levels. However, the primary metric of interest was whether or not there was a *change* in the ocular misalignments under novel gravity conditions, as this could be representative of an underlying otolith asymmetry. Note that what appears on these graphs as "decreases" in ocular misalignment (smaller numerical values) should really be thought of as changes in the directional orientation of one eye relative to the other. For example, recall that we infer a positive baseline TAN value to mean that the right eye is extorted with respect to the left eye in 1g. Thus a smaller positive TAN value in a novel g-level means that the right eye is now intorted more than it was during baseline testing. As none of the subjects experience motion sickness, or any other overt vestibular performance decrements, in the normal 1g (stationary) environment, we presume that whatever ocular misalignment they have during baseline 1g testing is precisely what their individual vestibular systems deem "balanced" or "nominal." Furthermore, as these baseline ocular misalignments are too small to elicit functional visual deficits, there is little incentive for the CNS to adjust these responses (e.g., expend more neural "effort" to generate misalignments even closer to 0 in 1g). Thus, the important parameter in these results is the *difference* between the ocular misalignments observed under novel g-levels and those observed in 1g.

Second, both VAN and TAN results were fairly comparable between the Early 0g and Late 0g testing, despite subjects experiencing a ten-parabola adaptation period in the middle of these two test sessions. This means that (1) subjects were consistent in their

reporting from the start of their first 0g parabola to the end of their thirtieth 0g parabola (in terms of both their mean responses and variability within the individual trials), and (2) relatively little adaptation occurred over the course of the flight. If adaptation had occurred, we would expect the ocular misalignments to return towards the preflight 1g levels in the hypo-g and hyper-g phases of flight. However, this was not the case for most subjects, the possible exceptions being subject Z in VAN and subject Y in TAN.

As we are primarily interested in changes in ocular misalignments between 1g and novel g-levels, we can graph these differences directly. We focus on the Early 0g data, as this condition represents the first exposure to the most extreme g-level (and we also obtained results from all six subjects during these parabolas). Figures 3.12 and 3.13 display the Early 0g VAN and TAN raw data on the left and the raw data minus the baseline 1g data on the right. These figures further highlight the statistically significant differences between the 1g and non-1g VAN and TAN responses, which agree with the von Baumgarten and Thümler model: a small, inherent otolith asymmetry that is centrally compensated in 1g will manifest as ocular positioning misalignments in non-1g environments. The TAN results are also in agreement with the von Baumgarten and Thümler model, which proposes that the direction of misalignment from 1g to hypo-g is the opposite of the direction of misalignment from 1g to hyper-g; this is seen in all subjects except for subject Y (although this individual did show this trend in his Late 0g TAN results). The VAN results, however, do not meet this condition: the change in vertical misalignment from 1g to hypo-g is in the same direction as the change in vertical misalignment from 1g to hyper-g for all subjects. The details surrounding these VAN results are discussed briefly in the next section, and are the focus of the subsequent chapter.

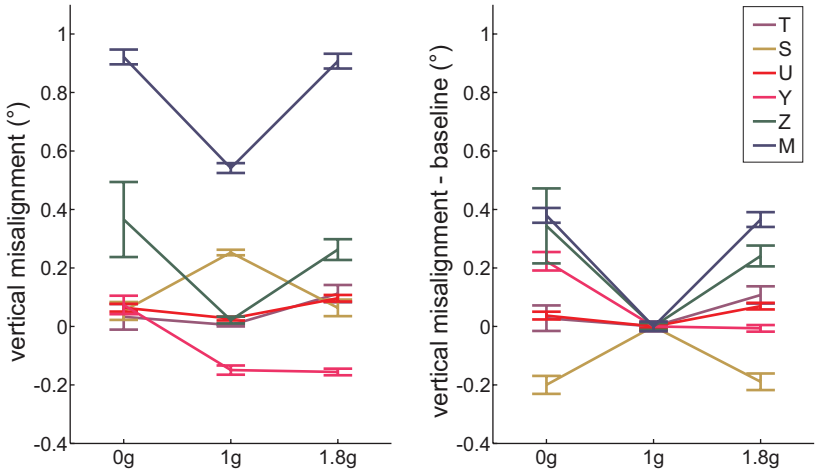

Figure 3.12 VAN Early 0g raw data (Left) and raw minus 1g baseline data (Right).

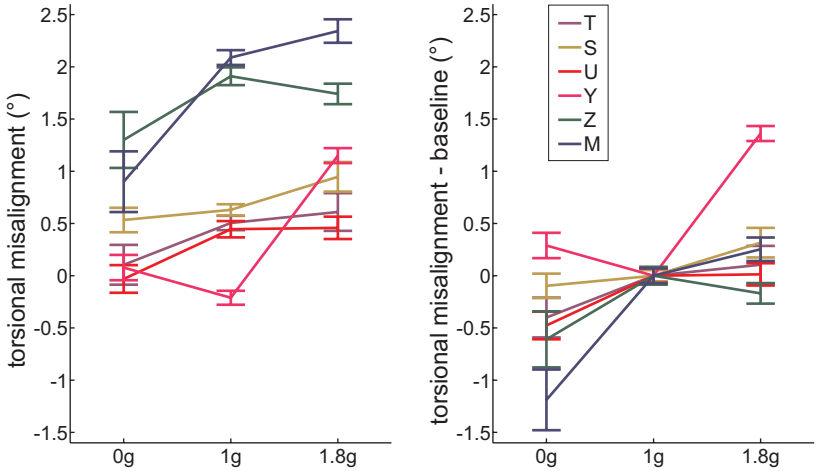

Figure 3.13 TAN Early 0g raw data (Left) and raw minus 1g baseline data (Right).

Von Baumgarten and Thümler also propose that the degree of imbalance (in our case, ocular misalignment) should be greater in 0g than in 2g because the differential sensitivity is increased when the background stimulus decreases (i.e., due to the Weber-Fechner law (Hoagland 1930)). Four of the TAN results (subjects T, U, Z, and M) and one of the VAN results (subject Y) suggest this might be the case. However, it should be noted that the parabolic-flight hyper-g level is 1.8g (and for many parabolas, the actual flight data revealed hyper g-levels closer to 1.6-1.7g), so the difference in g-level be-

tween 1g and hypo-g (0g) and 1g and hyper-g (1.6-1.8g) is not equivalent, and thus the comparison between 1g and hypo-g versus 1g and hyper-g may not be as strong.

3.5 Discussion

The development of a hand-held apparatus for evaluating ocular misalignments has provided a simple technology to evaluate binocular control in a variety of environments. The rapid assessment and self-administration capabilities, along with the minimal hardware, make VAN and TAN the ideal tests for evaluating ocular misalignments in the parabolic-flight environment. We presume these tests would be equally viable in other operational settings where minimal resources (e.g., time, equipment, or personnel) are available, such as remote field testing or bedside clinical assessment. Furthermore, the corresponding results from these experiments, along with the literature described at the beginning of this chapter, demonstrate the value of binocular assessment: the apparent independent control of the two eyes cannot be detected using the simpler and more common monocular tests (Markham et al. 2000).

In general, VAN and TAN software and hardware performed well in both the laboratory and parabolic-flight environments. The programs were stable and performed reliably from one test to another. It is important to note that testing in complete darkness was imperative to achieve accurate and consistent results, and also made the prism validation testing feasible for the subjects. The CNS's robust ability to fuse disparate images was a crucial factor in the final design of the VAN and TAN technology and this fact established the requirement of testing in environments void of extraneous visual stimuli.

3.5.1 Prism experiments reveal test requirements

Earlier versions of VAN and TAN incorporated a more conventional LCD tablet, whose glossy, reflective screen and LCD backlight provided additional undesired visual cues. Furthermore, subjects were not originally enclosed in a dark room or under a shroud during testing. At the time, preliminary tests generated reasonable results, including the expected changes in vertical misalignment during head-tilt tests (Figure 3.14) and gravity-dependent vertical and torsional misalignments in some subjects during parabolic-flight testing (Figure 3.15). Although the VAN head-tilt data was smaller than we might expect from other studies (Maxwell and Schor 1996), it was in the correct compensatory direction and fairly linear as a function of tilt angle. We could not predict (or verify postflight) how large the binocular misalignments should be in the parabolic-flight environment, as the numerical values would depend on each individual's inherent asymmetry, which could not be explicitly measured. But we anticipated that there would be a difference in the misalignment data in the altered g-levels, which we observed for most subjects. Because the only difference between the 0g, 1g, and 1.8g test conditions was the g-level itself, we presumed that these changes in the vertical and torsional misalignments were due to the g-level directly.

However, when we began the formal prism validation experiments, all subjects experienced large, vertical drifts of the right line (viewed through the prism) during VAN testing, and were therefore unable to complete these tests. The direction of the drift depended on the orientation of the prism: when the prism was oriented base up, the right line drifted down, and when the prism was oriented base down, the right line drifted up. Although blinking would "reset" the initial starting position of this drift, it did not elimi-

nate the drift itself. Subsequent research and discussions with clinical ophthalmologists revealed that disparate visual cues from the border of the tablet screen and other objects in the periphery, brought out explicitly by the monocular prism arrangement, were driving vertical fusion and effectively overriding even the centrally-fused (due to proper alignment) red and blue lines (Guyton 1988; Howard et al. 1997; Leigh and Zee 2006d). In fact, several studies have shown that peripheral fusion can actually disrupt central fusion (Burian 1939; Winkelman 1951). The relatively slow speed of vertical vergence was manifesting as visual drifts of the right line as the CNS attempted to merge the disparate peripheral images (Houtman et al. 1981). This effect rendered the original VAN task undoable whenever prisms were placed in front of one eye. The TAN prism tests were not subject to this phenomenon, presumably because the brain does not generate large torsional reflexes. Once the LCD tablet was replaced with an AMOLED tablet and subjects were tested in complete darkness, the apparent vertical drifts were eliminated and the VAN prism tests were easily completed.

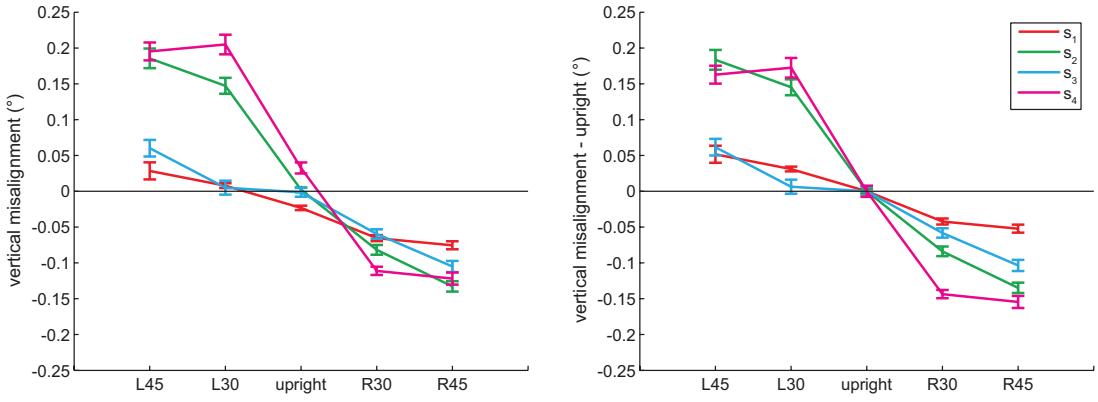

Figure 3.14 VAN results from four subjects during rightward and leftward head tilts of 30° and 45° using an earlier version of the hardware (LCD tablet) and testing under ambient light conditions. (Left) Raw vertical misalignment data. (Right) Vertical misalignment data centered around each subject's upright baseline. Roll tilts elicit vertical misalignments such that the ipsilateral eye is depressed (Carey and Della Santina 2005). Twenty trials were completed for each block. Error bars are 1SE.

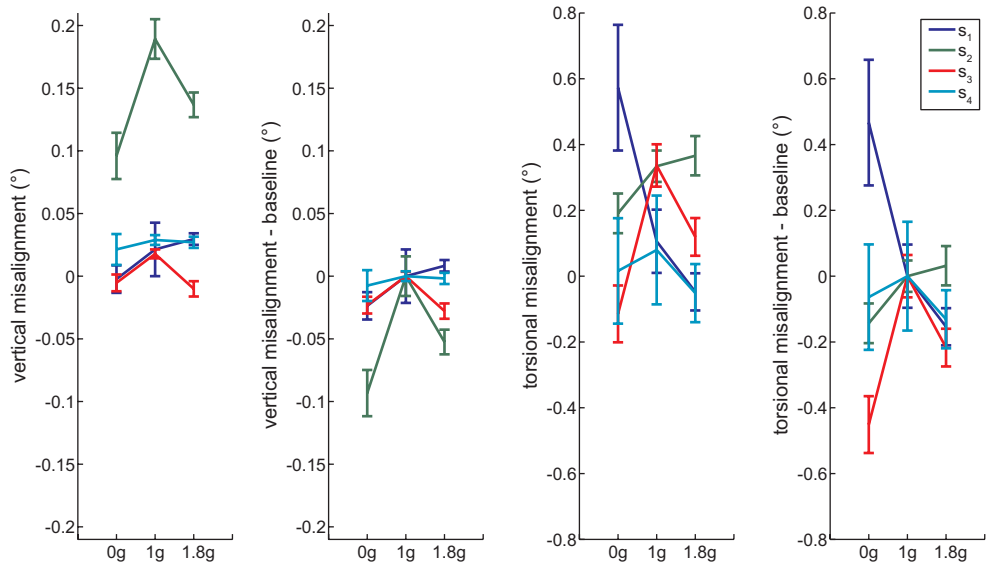

Figure 3.15 VAN and TAN parabolic-flight results in four subjects using previous hardware (LCD tablet) and testing under bright light conditions. For each subject, ~10–25 trials were completed per non-1g g-level and 20 trials were completed for baseline 1g data. Some subjects showed statistically significant g-level dependencies on their misalignment data.

Although we obtained statistically significant results with the LCD tablet in environments subject to ambient light, the ancillary visual cues were likely masking some proportion of the actual misalignments that may have been observed had the experiments been performed in complete darkness. We believe that the effects of gravity (i.e., the change in the direction of the g-vector during the terrestrial head-tilt tests and the change in its magnitude during the parabolic-flight testing) were strong enough to override the competing visual demands (i.e., sensorimotor fusion) during these earlier experiments, but the balance between these two phenomenon led to reduced amplitudes of the misalignment data. The lessons learned during the prism validations prompted the switch in the hardware and lighting conditions. Parabolic-flight testing was performed again (in new test subjects), and these results revealed binocular misalignments larger than the original results by an order of magnitude; this is easily recognized when comparing the results in Figure 3.15 to those in Figures 3.12 and 3.13.

It should be noted that many of the experiments described at the beginning of this chapter did not consider the effects of extraneous visual cues (both central and peripheral) on binocular fusion capabilities. For example, in the Diamond, Markham, and Lackner studies, binocular eye positions were captured using a 35mm film camera (for subsequent data analysis), in which subjects were simply instructed to stare at the center of the lens. Although the lens occluded part of the central field of view, peripheral cues were still available. This might have led to diminished results, and is a valid reason why some of these investigators' baseline tests (including head tilts) did not show any substantial binocular misalignments.

3.5.2 Limitations of current design

The primary limitation of VAN and TAN is that, in their current form, horizontal vergence cannot be controlled. Monocular red and blue stimuli are required so that vertical and torsional fusion do not mask the corresponding misalignments during VAN and TAN testing. Visual cues to binocularly "lock" torsional alignment during VAN or vertical alignment during TAN are not needed because subjects are instructed to make the red and blue lines parallel, if a single continuous line cannot be perceived. For example, if during TAN testing the stationary line appears slightly elevated above the moving line, the subject ignores this apparent vertical displacement and proceeds to rotate the moving line until it is parallel to the stationary line. If during VAN testing the stationary line appears slightly rotated, the subject adjusts the moving line until the middle of the two lines are vertically aligned.

The horizontal vergence angle describes how near or far the subject perceives the red and blue lines to be. We know that vertical eye movements, and probably to a lesser

degree torsional eye movements, are modulated by depth perception. For example, when the eyes are horizontally converged, the ability for vertical fusion is slightly increased (by as much as 0.5° (Hara et al. 1998)). While an uncontrolled horizontal vergence angle may not affect VAN *conventional* tests, in which subjects are instructed to find the middle of the range in which vertical fusion can be achieved, it can make this test more challenging. For instance, subjects who generate small convergence angles (far viewing) will perceive the red and blue lines as farther apart. This can make properly aligning the lines more difficult, and probably more time consuming, as subjects have to "look back and forth" between the two lines to check the alignment. In contrast, subjects with large convergence angles (near viewing) will perceive the red and blue lines as overlaid, which makes the alignment easier and faster. Follow-up conversations with subject H, who had the second longest VAN times and longest TAN times of the five subjects tested (Tables 2 and 3), indicated that it did indeed take her longer to perform the VAN and TAN tests because she perceived the lines as horizontally separated from one another.

An uncontrolled horizontal vergence angle will affect the *always above* and *always below* VAN tests; in light of the Hara et al. study, we presume that subjects who converge more will be able to perceptually fuse a wider range of vertical positioning misalignments. In fact, this is likely the case for subject I, whose *always above* and *always below* data is highlighted on the right in Figure 3.7; follow-up conversations with this individual indicated that he perceived the red and blue lines to be completely overlaid, which agrees with the near-viewing hypothesis and therefore larger fusional capacity.

Hence, the disadvantage of not being able to precisely control horizontal vergence is that we may see deviations in responses across subjects, or possibly within the same

subject if a consistent vergence angle isn't maintained within a given test block or session, simply because they are perceiving the lines to be closer or farther away. However, based on anecdotal reports from subjects and pilot data implementing repeated trials across multiple days, we do not believe that horizontal vergence changes much within a given subject. The only exception to this may be during testing in altered g-levels, as two parabolic-flight subjects reported that the lines appeared to move closer together in one g-level and then farther apart in another. This certainly raises an interesting point, and should be tested in future experiments, perhaps by measuring the horizontal vergence directly using a separate Horizontal Alignment Nulling (HAN) test, for example.

Unfortunately, the only way to control horizontal vergence is to provide a binocular visual stimulus to "lock" the horizontal gaze angle. However, providing such a stimulus in the current design would also fix the vertical and torsional alignment, which is therefore not an option. Clever implementation of polarizing filters over the red and blue lines (and on the red-blue eyeglasses), arranged at specific angles relative to one another with an uncovered section in the center of the tablet to facilitate a binocular fixation target, would allow for binocular (to lock horizontal vergence) and monocular (for the alignment tests) stimuli to be presented simultaneously. However, the polarizing filters must be arranged differently for the VAN and TAN tests, thereby doubling the hardware, and additional equipment is required to mount the polarizing filters such that touch-screen capabilities can be maintained. Together, these issues reduce the overall portability of VAN and TAN, thereby rendering the setup more cumbersome and less practical for operational environments. The more viable alternative would be to implement a third

alignment test (e.g., Horizontal Alignment Nulling) to quantify how far apart the red and blue lines appear, and then use this data to calibrate the VAN and TAN results.

3.5.3 Future ground validation experiments

The VAN and TAN prism experiments provided a simple means to validate the VAN and TAN technology, in terms of both the accuracy of the test and its operational performance (ease of use, stability, etc.). They performed well on all accounts.

There are several simple ground experiments that should be performed to further characterize the precise nature of what VAN and TAN are measuring. For example, we know that binocular fusion is comprised of both motor and sensory components (Guyton 1988; Hara et al. 1998). We presume that VAN and TAN primarily measure the sensory component, as they are perceptual tests. But there is likely a motor component as well, as evidenced from the similarity in our parabolic-flight results to those of other investigators who measured the eye movements (motor component) inflight directly. One way to test this would be to repeat the prism validations while simultaneously recording the eye movements. The eye movements would delineate the motor component, and the difference between these results and the VAN and TAN results would constitute the sensory component. The key in this test is not necessarily to record the eye movements while the moving lines are being repositioned (although this may render a different set of interesting data), but to capture the binocular positions once the VAN and TAN trials have been completed.

Another test that has yet to be formally performed is the repeatability test. We presume that there may be slight variations in ocular misalignments from day-to-day, in accordance with other oculomotor processes that vary as a function of fatigue, cognition,

etc. (Bahill and Stark 1975; Matta and Enticott 2004). It would be important to demonstrate whether or not VAN and TAN capture these same effects. Because of the CNS's vertical and torsional fusion capabilities, VAN and TAN may be relatively unaffected by the small day-to-day changes typically observed in pure motor data. However, if day-to-day (or session-to-session) variations are observed, the VAN and TAN results should be correlated with eye movement recordings to ensure that the nature of the VAN and TAN tests themselves is not the cause. Furthermore, there is evidence that fusion disparities can be adapted with repeated exposure to the same stimuli (Maxwell and Schor 1996; Maxwell and Schor 1999). Although we did not see this during our early and late parabolic-flight tests, we have not looked at how these responses might be adapted over the course of multiple flights, or on the ground with repeated exposure to prisms, for example.

3.5.4 Parabolic-flight experiments affirm operational readiness and reveal the nature of g-level dependencies

Parabolic flights facilitated VAN and TAN testing in an operationally-relevant environment, similar to what astronauts might experience if these tests were performed during spaceflight: novel g-levels, limited timetables, high electronic noise from surrounding experiments, and test subjects naïve to the details of the science. The hardware performed well, and the subjects were able to complete the tasks as easily inflight as during preflight training. The primary operational challenge was maintaining a consistent subject-to-screen distance in the three-dimensional 0g environment, which was especially critical for the VAN testing (equation (1)). Although subjects were lightly strapped to the floor of the aircraft and the shroud further restricted vertical movement, fore-aft mo-

tion was not as easily controlled. Subjects lost track of how far they were from the tablet, and so operators were responsible for continuously monitoring and maintaining the head-to-screen distance. The addition of a lanyard around the subject's neck and secured to the back of the tablet, which when held taught designates the appropriate distance, would be a simple solution for future flights. Furthermore, a portable shroud would be less cumbersome operationally and would provide operators with better hands-on access to the subjects, especially during the 0g portions of the parabola. The shroud could be designed so that once the tablet is mounted inside, the subject-to-screen distance is automatically set.

The flights also provided a platform to study potential otolith asymmetries and connections with motion sickness susceptibility. Even though three subjects experienced adverse symptoms that prevented them from completing VAN and TAN tests inflight, their baseline data alone was useful in that a strong correlation between variability in pre-flight torsional misalignments and motion sickness experience was found. Since this result has only been confirmed in three individuals to-date, we cannot draw any definitive conclusions yet. However, our results are suggestive that this correlation might hold true for at least some individuals. Thus, we may be able to hypothesize that *if* another individual shows a relatively large variability in baseline torsional misalignment, then, based on what other similar subjects have demonstrated, he or she *may* have more difficulty with motion sickness in the parabolic-flight environment. This is an interesting outcome that agrees with results from previous investigators and can be interpreted through underlying neurophysiology. Further experiments to test this correlation in a larger sample size would certainly be beneficial, as this result may have important implications for predict-

ing SMS susceptibility in first-time astronauts. Experimentally, it would be relatively simple to ask naïve parabolic-flight subjects (who do not take the anti-motion sickness medications) to perform TAN during preflight tests only, and then correlate these results with inflight motion sickness experiences. However, the operational feasibility (namely obtaining the necessary approvals for preflight data collection) may be an arduous endeavor.

For the six subjects who did not experience motion sickness symptoms, g-level dependent vertical and torsional misalignments were observed. The torsional misalignments were consistent with the von Baumgarten and Thümler model and results from previous investigators. This was the first time systematic gravity-dependent vertical misalignments were also observed. Importantly, these results were repeatable early and late in the flights, even with a ten-parabola adaptation period in between. Hence, we believe that these results represent some underlying neurophysiological mechanism that is modulated by gravity. Since none of these subjects experienced motion sickness symptoms, we could not correlate their inflight results with motion sickness susceptibility, as was done by previous investigators. Similarly, since the three individuals who experienced motion sickness were unable to complete any testing during the parabolas themselves, we did not have any inflight data to correlate with their susceptibility. However, we can conjecture, based on the results from other investigators, that if our three susceptible subjects had been able to perform TAN inflight, they would express larger torsional misalignments than our six subjects who did not experience any symptoms.

It is interesting to compare the differences in the misalignment data across g-levels for the six parabolic-flight subjects to the differences in the misalignment data ob-

served during upright versus supine tests for the five prism validation subjects. First of all, it should be noted that only one subject was tested in both experiments (which were separated by more than one month), and so definitive conclusions cannot be made at this time. Nonetheless, it is intriguing that the relative difference between the VAN 1g and non-1g results is similar to (of the same order of magnitude) the relative difference between the VAN upright and supine results; the same holds for the corresponding TAN results. If we attribute the increased misalignments observed during parabolic flight to an uncompensated otolith asymmetry and presume that our parabolic-flight subjects would have generated similar supine data, then incorporating the upright versus supine results into the central compensation theory suggests that the compensation is not simply g-level-tuned (i.e., dependent on the magnitude of the current gravity level), but it is g-vector-tuned (i.e., dependent on the direction of gravity through the Z-axis of the body). In other words, the compensation may be paired not to a particular g-level, but to a specific direction in which that g-level is experienced. As we have evolved to interact with our environment in the upright orientation, it makes sense that compensatory mechanisms are preferentially tuned for this posture. Furthermore, this argument agrees with the 1g tilt-tests performed by previous investigators who found that binocular misalignments increased during large tilts to the right and left (Lackner et al. 1987). Of course parabolic flight and supine tests must be performed in the same subjects before this corollary can be established. But it would be advantageous to add 1g preflight (and possibly1.8g in-flight) supine tests to future parabolic-flight protocols.

One striking feature of our TAN parabolic-flight results was that the direction of the misalignment when transitioning from 1g to 0g versus from 1g to 1.8g was the same

across all six subjects: relative to the left eye, the right eye was intorted in 0g and extorted in 1.8g. We investigated this further by examining the results from previous studies, but we did not find anything conclusive. For example, Vogel and Kass' four crewmembers all showed higher OCR gains during leftward tilts preflight and during rightward tilts postflight (Vogel and Kass 1986). Diamond and colleagues, however, found the opposite result in seven non-astronaut subjects: larger OCR was observed during rightward tilts than leftward tilts, and the depressed eye torted more than the elevated eye (Diamond et al. 1979). Lackner and colleagues claimed that their parabolic-flight subjects who did not experience inflight motion sickness symptoms generated larger amounts of OCR during rightward body tilts than leftward ones, and interpreted this as a greater "efficiency" of the left otoliths in generating OCR in individuals who are less prone to motion sickness during exposure to altered g-levels (Lackner et al. 1987). Therefore, given these mixed results (and the associated small sample sizes), we believe that the fact that our subjects tended to generate ocular misalignments in the same direction was merely coincidental.

Previous parabolic-flight experiments have indicated that some individuals adapt rapidly to the parabolic-flight environment, and that these adaptations can be observed within a single flight (Lackner and Graybiel 1982; Shelhamer et al. 2002). Therefore, we originally anticipated that some of our subjects might demonstrate adaptive responses during their flight. This hypothesis was tested through early and late VAN and TAN tests, which looked specifically for trends toward preflight 1g levels as the flight progressed. However, adaptation was not observed.

In hindsight, we should have originally predicted that adaptation would *not* be observed. Error-based learning is the primary driver of adaptive processes, but in reality, we did not expose our subjects to enough "errors" to warrant substantial adaptation during their respective flights. Throughout the majority of the parabolas, subjects were stationary under the shroud, focused on the VAN and TAN tests, and not exposed to any of the strong visual cues telling them that their surrounding environment was different (e.g., people floating by upside down). Furthermore, substantial evidence from both clinical and spaceflight research indicates that active movements are necessary to elicit adaptation (Nooij et al. 2011; Wood et al. 2011), which subjects did not perform. Even during the dedicated ten-parabola adaptation period, most subjects chose to remain relatively still, with the exception of gently floating up and down by a few inches during the g-level transitions. Subjects were fairly intentional about not making extraneous head movements out of fear of experiencing adverse motion sickness symptoms, especially because they had not taken the anti-motion sickness medications offered to the other fliers (some of whom were ill close by).

It is worth noting that many of the previous parabolic-flight experiments in which adaptation across a single flight was observed implemented protocols that themselves drove adaptation (e.g., pitch VOR adaptation experiments). However, the nature of the VAN and TAN tests is such that no error is ever presented to the brain because the lines are viewed monocularly, and subjects are given control over any perceived visual misalignments and tasked with eliminating them. Because VAN and TAN do not involve head movements or visual stimuli to drive adaptation, true adaptation of VAN and TAN responses will only occur when the CNS realizes, through other processes, that otolith-

driven reflexes are miscalibrated. This will then modify how subjects must adjust the relative positioning of the red and blue lines to perceive a single continuous line, but this process will likely occur unbeknownst to the subjects: they will still perceive their completed trials as single, continuous lines, just as they did in the unadapted state.

Along these same lines, one might expect subjects with prior parabolic-flight experience to show smaller ocular misalignments than naïve fliers because previous exposure to the novel g-levels might be recalled through context-specific adaptation or through rapid re-adaptation due to savings. However, this was not observed in the two experienced test subjects (subjects M and Z). This may be because it had been several years since these two individuals had flown (2007 and 2011). Hence, if gravity-dependent context cues had not been learned during previous flights, sufficient savings might not have been retained to warrant faster re-adaptation than what was experienced by the naïve subjects. Furthermore, although subject Z had only flown previously, his experience was limited to the European Space Agency (ESA) platform, whose parabolic-flight profile is much milder than NASA's: only 31 total parabolas are flown per flight, and parabolas are separated by 1g breaks of one minute between each parabola, four minutes between every set of five parabolas, and eight minutes at the halfway point. Additionally, subjects M and Z happened to be the oldest of the nine fliers (by several decades), and so it is possible that age-related decrements in vestibular adaptive capabilities led to adaptive responses that more closely resemble those of the younger naïve subjects (Paige 1992).

Finally, the von Baumgarten and Thümler model predicts that the direction of misalignment observed when transitioning from 1g to hypo-g will be the opposite of the

direction of misalignment when transitioning from 1g to hyper-g. Our TAN data exhibited this property, in agreement with results of previous investigators. However, our VAN data did not demonstrate this trend, as the change in vertical misalignment from 1g to 0g was in the same direction as the change in vertical misalignment from 1g to 1.8g for all subjects. One potential limitation of the von Baumgarten and Thümler model is that it assumes that all otolith processes will be compensated by the same central mechanism. While this may be a reasonable initial assumption, it has not been explicitly tested until now; the only experiments that attempted to describe central compensation have been through measures of binocular torsion, which we know to be primarily driven by the utricles (Suzuki et al. 1969; Fluur and Mellstrom 1970b; Uchino et al. 1996). Therefore, it is possible that non-torsional otolith processes, or more generally processes that are primarily saccular-driven, may be compensated differently. The utricle and saccule are tuned for distinct functions (Riley and Moorman 2000; Clarke et al. 2003; Newlands et al. 2003), and so it is reasonable that asymmetries in these end organs they may be compensated through slightly different means. We consider this possibility more fully in the next chapter, where we develop a model, based on a more general version of the von Baumgarten and Thümler one, whose parameters can be adjusted to account for both the VAN and TAN results observed in our parabolic-flight experiments.

Chapter 4

Gravity-dependent ocular misalignments and central compensation can be described through a bilateral control systems model

4.1 Introduction

4.1.1 Overview

The VAN and TAN parabolic-flight results described in the previous chapter can be summarized as follows: Both VAN and TAN tests displayed increased ocular misalignments in altered g-levels, but the direction of the misalignment in hypo-g versus hyper-g reversed for TAN and remained the same for VAN. These results characterize the behavior of the otolith-ocular system, but they do not explain how neurophysiological pathways might be organized to produce such results. Understanding the underlying neural circuitry associated with otolith-ocular reflexes may enable us to pair changes in specific elements of the neural pathways with changes in behavior. This has important implications for developing various interventions, such as the design of countermeasures for astronauts to facilitate adaptation to novel g-levels, or the design of rehabilitation protocols for vestibular patients to facilitate terrestrial compensation for various pathologies. Hence, the primary objective of this chapter is to develop a model that can explain the ocular misalignments observed in the altered g-levels of parabolic flight and to connect it with the appropriate neuroanatomical structures.

Von Baumgarten and Thümler (1979) proposed a simple conceptual model for how otolith reflexes, including ocular misalignments, might respond following a change in g-level and how these reflexes can adapt to the new gravitational environment. This has been discussed extensively in Chapter 3.1. Applying their model to our VAN and TAN parabolic-flight results yields a plausible explanation for our TAN results, but not for our VAN results. Therefore, in this chapter, we develop a new model that can account for both data sets, using the von Baumgarten and Thümler model as the foundation and incorporating additional parameters that account for our experimental results and align with our current understanding of the underlying neurophysiology. We begin by considering the von Baumgarten and Thümler model in a more generic form, and then show that adding a nonlinear gravity-dependent parameter to the central compensation facilitates the desired directional changes observed in our VAN and TAN parabolic-flight results. We highlight the presumed neurophysiological circuitry that can account for such a model. Finally, we conclude by proposing simple future experiments that can be conducted to determine our model's free parameters.

4.1.2 Previous models predict initial imbalance in opposite directions for hypo-g versus hyper-g

The von Baumgarten and Thümler model that allows a balanced orientation center in the presence of an inherent otolith asymmetry (Figure 3.1) can be drawn more generically, as depicted in Figure 4.1. Here, g is the current g-level, k is the otolith asymmetry parameter describing the anatomical or physiological asymmetry between the left and right otolith systems ($0 < k < 1$), LCC and RCC represent the left and right compensation centers, respectively, and a and c are the amounts of additive neural compensation

required for a balanced perception of orientation ($a, c \geq 0$). The orientation center compares the signals stemming from the left and right sides to generate the perception of balance. We assume that whichever side provides compensation, that compensation is positive; mathematically, a negative compensation from one side should be interpreted as a positive compensation of the same magnitude from the other side.

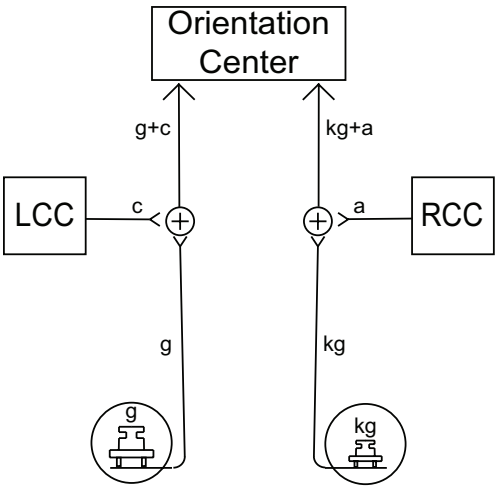

Figure 4.1 Generalized version of the von Baumgartenand Thümler (1979) model for central compensation of an anatomical otolith asymmetry. g is the current g-level, k is the otolith asymmetry parameter ($0 < k < 1$), LCC and RCC are the left and right compensation centers, respectively, and a and c are the amounts of additive neural compensation required for balance between the left and right sides ($a, c \geq 0$).

Under the 1g balanced condition, von Baumgarten and Thümler assume that the compensation center on the side of the weaker afferent signal (in this case, the right side) supplies additional neural impulses and that the compensation center on the opposite side provides no additional neural impulses. In other words, in the balanced 1g condition, $a > 0$, $c = 0$, and the otolith signal from the left is equivalent to the otolith signal from the right:

$$g + 0 = kg + a \implies 1 = k + a \Leftrightarrow k = 1 - a.$$

(In the event that the asymmetry parameter k is instead on the left side, then $a = 0$, $c > 0$, and $k = 1 - c$.)

Let $I(g)$ be the amount of imbalance between the left and right sides upon an *immediate* change in g-level (i.e., prior to any adaptation), defined as the signal from the right minus the signal from the left. Then

$$I(g) = (kg + a) - (g + 0) = \big((1 - a)g + a\big) - g = a(1 - g). \qquad (2)$$

If $I(g) = 0$, then the left and right sides are balanced (i.e., when $g = 1$ at baseline). If $I(g) > 0$, then the signal on the right is stronger than the signal on the left, and if $I(g) < 0$, then the signal on the left is stronger than the signal on the right. We denote $I(g) > 0$ by the symbol ↶, and $I(g) < 0$ condition by the symbol ↷, analogous with the directional arrows used in the von Baumgarten and Thümler model (Figure 3.1). By graphing equation (2), it is easily seen how the direction of imbalance is dictated by g-level: When an individual is suddenly placed in a novel hypo-g environment, then the direction of imbalance is positive (i.e., ↶), whereas when this individual is suddenly placed in a novel hyper-g environment, then the direction of imbalance is negative (i.e., ↷) (Figure 4.2).

Under this model, if an individual is suddenly exposed to a novel g-level, say $g = G$, and then allowed to adapt to this g-level, the following scenario arises. Immediately upon the change in g-level,

$$I(g = G) = (kG + a) - (G + 0) = (1 - a)G + a - G = a(1 - G).$$

Adaptation is achieved when

$$(kG + a) - (G + c) = (1 - a)G + a - G - c = a(1 - G) - c = 0$$

$$\Longrightarrow c = a(1 - G).$$

So, for example, if the novel g-level is $G = 0g$, then balance can be achieved when $c = a$. If the novel g-level is $G = 2g$, then balance can be achieved when $c = -a$. This

makes the LCC compensation negative, which we interpret as a positive compensation of a by the RCC. In other words, at $G = 2g$, the imbalance is in the $\curvearrowright$ direction, and adaptation would occur only by additional input from the RCC.

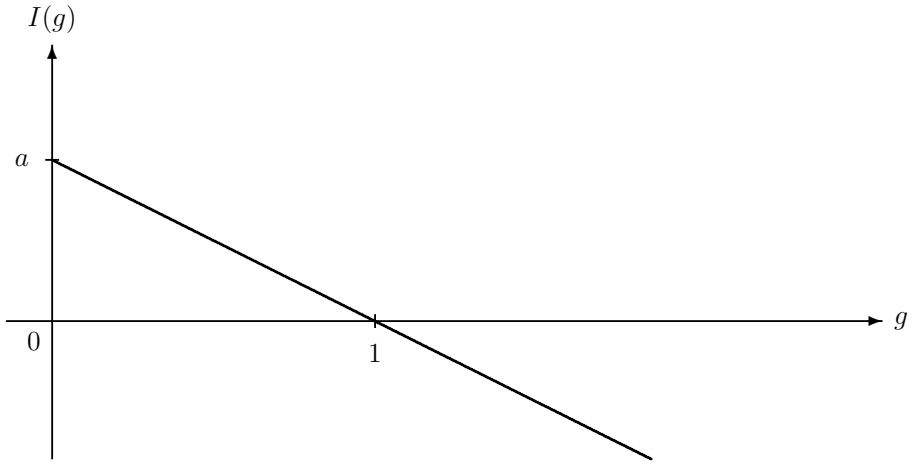

Figure 4.2 Imbalance as a function of g-level for the von Baumgarten and Thümler model. The direction of imbalance experienced upon an initial change in g-level depends on whether the new g-level is hypo-g or hyper-g.

The von Baumgarten and Thümler model does not distinguish among different otolith-driven responses; it assumes that utricular and saccular processes, for example, are governed by the same central compensatory mechanism. However, given the fact that the utricle and saccule are separate end organs, each of which may be subject to different amounts of asymmetry, and that each end organ is tuned for distinct functional roles, such as their directional control of eye movements (Fluur 1970), and additional roles of the saccule in vestibulocollic and vestibulospinal processes (Wilson et al. 1977; Colebatch et al. 1994; Mhoon et al. 1997; Sato et al. 1997; Newlands et al. 2003), it is reasonable to presume that they might be subject to different forms of compensation. Our parabolic-flight data, in fact, supports this notion. The von Baumgarten and Thümler model described in Figure 4.1 is appropriate for the TAN parabolic-flight results (Figure 3.13), as

the direction of imbalance reverses in the 0g versus 1.8g phases of parabolic flight. However, it is not appropriate for the VAN parabolic flight results, where the direction of imbalance is the same in the 0g and 1.8g phases (Figure 3.12). Therefore, we now develop an alternate model, which can explain both the TAN and VAN parabolic-flight results simultaneously. This model may also provide insight into the different compensatory control mechanisms underlying utricular and saccular processes.

4.2 Materials and methods

Our goal was to design a model whose outputs from the RCC and LCC facilitate central compensation for an innate left-right asymmetry in multiple g-levels. We designate these outputs as $R(g)$ and $L(g)$, respectively. Generalizing the idea of von Baumgarten and Thümler, we assume that the compensation is additive. (Note that a purely multiplicative compensation would not allow for the possibility of compensation in 0g.) This model should account for both utricular (the primary driver of ocular torsion (Suzuki et al. 1969; Fluur and Mellstrom 1970b; Uchino et al. 1996)) and saccular (the primary driver of vertical eye movements (Fluur and Mellstrom 1970a; Isu et al. 2000; Goto et al. 2004)) responses, in accordance with the TAN and VAN parabolic-flight results. Mathematically, the only computational requirements for the model are that:

1. Balance between the left and right sides is maintained in (baseline) 1g.
2. Imbalance between the left and right sides occurs immediately upon a change in g-level.
3. The direction of imbalance for both hypo-g and hyper-g occurs in accordance with the VAN and TAN parabolic-flight data (Figures 3.12 and 3.13).

However, from a neurophysiological perspective, the model should also meet the following criteria:

1. The general form of compensation should be maintained between utricular-driven processes and saccular-driven processes, as the utricle and saccule are both otolith organs responsible for transducing linear acceleration. However, because the end organs are tuned for different functions (e.g., torsional versus vertical eye movements, the fact that the saccule also plays a prominent role in postural control, etc.), the individual parameters within $R(g)$ and $L(g)$ necessary for utricular versus saccular compensation may differ to account for saccular-ocular versus utricular-ocular responses.
2. The general forms of $R(g)$ and $L(g)$ should be the same, in accordance with the overall symmetry between the left and right hemispheres. However, the precise values of the parameters within $R(g)$ and $L(g)$ will depend on the particular asymmetry between the right and left sides.
3. The mathematical components of $R(g)$ and $L(g)$ should be simple in nature and representative of known neurophysiological transformations (Silver 2010; Hildebrandt et al. 2011).
4. Model parameters should be robust across a reasonable set of g-levels, which can be confirmed through sensitivity analyses.
5. The model should incorporate known neurophysiological connections. For example, it has been established that there is a 3:1 preponderance in ipsilateral-to-contralateral primary afferent signaling in the utricle (Fernandez and Goldberg 1976a).

4.3 Results

4.3.1 Incorporating a nonlinear gravity component into central compensation facilitates the parabolic-flight results

Figure 4.3 outlines the proposed model that facilitates compensation for an inherent otolith asymmetry in multiple g-levels (g-level ≥ 0) and can be used to explain both the VAN and TAN parabolic-flight results. Much of this model is analogous to the one proposed by von Baumgarten and Thümler: left and right otolith organs with an inherent asymmetry between them, compensation centers on the left and right, and an orientation center that compares the outputs from the left and right sides. The proposed model also incorporates crossover terms r_L and r_R to describe the unequal innervation to ipsilateral and contralateral central structures (defined previously for the utricle (Fernandez and Goldberg 1976a) and presumed to also exist for the saccule) and central compensation functions $L(g)$ and $R(g)$ that are gravity-dependent (for reasons described below).

The otolith asymmetry parameter k $(0 < k < 1)$ describes the anatomical or physiological asymmetry between the left and right otolith systems. In healthy individuals, it is presumed that the magnitude of this asymmetry is relatively small, and hence it is likely that k is very close to 1. However, the model allows k to vary between 0 and 1, and as such, it is appropriate for individuals with unusually large asymmetries, including those with unilateral vestibular pathologies.

Throughout this discussion, we define the asymmetry such that the right otolith sends a slightly weaker primary afferent signal than the left otolith (e.g., due to a mass asymmetry in which the right otolith is smaller than the left otolith). As in the von

Baumgarten and Thümler model, 1g compensation is achieved through additional neural impulses from the right compensation center only (i.e., $R(g) > 0$ and $L(g) = 0$) to enable a balanced perception of orientation. Should the asymmetry instead be that the left otolith sends the weaker afferent signal, all that is needed is to reverse the diagram in Figure 4.3, and the following computations remain the same.

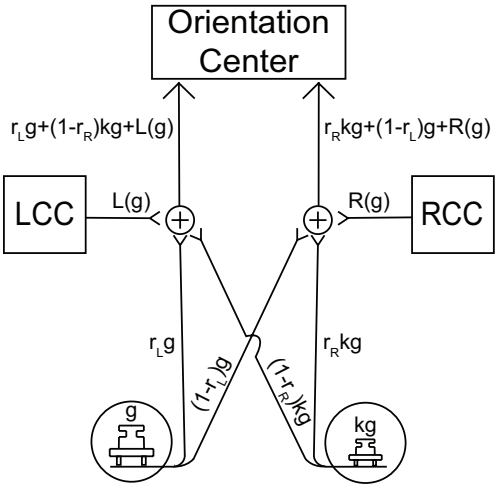

Figure 4.3 Proposed model for compensation of an inherent otolith asymmetry. For illustration purposes, we define the asymmetry such that the right otolith sends a slightly weaker neural signal than the left otolith (due to an anatomical or physiological asymmetry). g is the current g-level, k is the asymmetry parameter, r_L and r_R are the preponderance parameters, and $L(g)$ and $R(g)$ are gravity-dependent functions that facilitate compensation to novel g-levels.

The preponderance parameters r_L and r_R ($0 \leq r_L, r_R \leq 1$) describe the innervation between the end organ and target neurons on both the ipsilateral and contralateral sides. Values of 1 indicate that the end organ sends 100% of its projections to the ipsilateral side. While r_L and r_R are likely to be similar in magnitude, the model allows for unequal magnitudes, as slight differences may be present due to innate asymmetries between the left and right sides. Fernandez and Goldberg measured r_L and r_R to be 0.75 in the utricle, through recordings of superior vestibular nerve primary afferents in the squirrel monkey in response to static left and right roll tilts (Fernandez and Goldberg 1976a). To the best of our knowledge, no ipsilateral-to-contralateral preponderance ratio has been

quantified for saccular afferents to date, but it is presumed here to exist. (This model does allow for preponderance parameters of 1, which represent no crossover to the contralateral side.)

The central compensation functions $L(g)$ and $R(g)$ facilitate a balanced orientation center. Upon exposure to a novel g-level, parameters within these functions are modified so that adaptation to the new gravitational environment can be achieved. While the von Baumgarten and Thümler model treats $L(g)$ and $R(g)$ as constants, the additional gravity-dependent component in our model provides flexibility so that the direction of imbalance can change in hypo-g versus hyper-g. This flexibility facilitates both the torsional and vertical misalignment data observed in the parabolic-flight results, and is described in further detail below.

The orientation center compares the difference in the signals originating on the left and right sides to generate a perception of balance. We assume that the compensation center on the side of the weaker afferent signal supplies additional neural impulses and that the compensation center on the opposite side provides no additional neural impulses in the 1g balanced condition. As such,

$$R(g = 1) > 0 \Leftrightarrow R(1) > 0$$

and

$$L(g = 1) = 0 \Leftrightarrow L(1) = 0.$$

In order for the orientation center to receive a balanced signal in 1g,

$$r_R kg + (1 - r_L)g + R(g) = r_L g + (1 - r_R)kg$$

$$\Longrightarrow r_R k + (1 - r_L) + R(1) = r_L + (1 - r_R)k.$$

Therefore,

$$R(1) = 2r_L - 2r_R k + k - 1 \quad (3)$$

The imbalance function $I(g)$ is defined as

$$I(g) = [r_R kg + (1 - r_L)g + R(g)] - [r_L g + (1 - r_R)kg]$$

$$I(g) = g(2r_R k - 2r_L - k + 1) + R(g). \quad (4)$$

As for the imbalance function in equation (2), the left and right sides are balanced when $I(g) = 0$, ↶ if $I(g) > 0$, and ↷ if $I(g) < 0$. So, for any g, assuming balance at $g = 1$,

$$I(g) = g\big(-R(1)\big) + R(g) = R(g) - gR(1).$$

Thus, for ↶ imbalance

$$R(g) - gR(1) > 0 \iff gR(1) < R(g),$$

and for ↷ imbalance

$$R(g) - gR(1) < 0 \iff gR(1) > R(g).$$

Note that

$$I(1) = R(1) - 1R(1) = 0,$$

which is the balanced 1g condition.

From these imbalance equations, we can now see that the particular form of $R(g)$ will dictate which g-levels generate imbalance in a given direction (i.e., ↶ or ↷). There are a variety of $R(g)$ functions that may reproduce the VAN and TAN parabolic-flight data, and one reasonable example is discussed in the following section. One interesting result of this model is the fact that both the amount and the direction of imbalance are independent of the preponderance terms r_L and r_R, once $R(g)$ is known. There are no restrictions on $R(g)$, other than what is required to achieve balance in 1g, namely equation (3).

Importantly, this model supports the well-known "re-adaptation" phenomenon, in which re-adaptation to 1g (following adaptation to some non-1g environment) generates responses (e.g., imbalance) in the opposite direction (Young et al. 1984; Parker et al. 1985; Correia 1998). Assume that an individual has a balanced orientation at $g = 1$; hence, $I(1) = 0$. Suppose this individual is now exposed to a novel g-level $g = G \neq 1$ and that this g-level generates ↶ imbalance; hence, $I(G) > 0$. Adaptation drives the LCC to generate additional neural signaling such that the compensation function $L(g) > 0$. As such, the new amount of imbalance between the left and right sides is

$$I^*(g) = [r_R kg + (1 - r_L)g + R(g)] - [r_L g + (1 - r_R)kg + L(g)] = I(g) - L(g).$$

When adaptation is complete and balance has been restored at $g = G \neq 1$, then $I^*(G) = 0$. If this individual now returns to $1g$, then

$$I^*(1) = I(1) - L(1) = 0 - L(1) = -L(1) < 0.$$

So, returning to $1g$ following adaptation to some novel g-level $g = G \neq 1$ generates imbalance in the direction opposite to that which was experienced at g-level $g = G \neq 1$.

4.3.2 Specifying the central compensation functions

There are a variety of functions $R(g)$ and $L(g)$ that can facilitate central compensation in multiple g-levels that fit the observed experimental data. One reasonable set of functions, both mathematically and neurophysiologically, is

$$R(g) = a + bg^{\varepsilon}$$

and

$$L(g) = c + dg^{\mu},$$

where a, b, c, d, ε, and μ are free parameters. We presume that under balanced 1g conditions $a, b > 0$ and $c = d = 0$. (In the event that the asymmetry parameter k is on the

left side, then a = b = 0 and $c, d > 0$) (Figure 4.4). We define $\varepsilon, \mu > 0$ (although they do not need to be integers), as described further below.

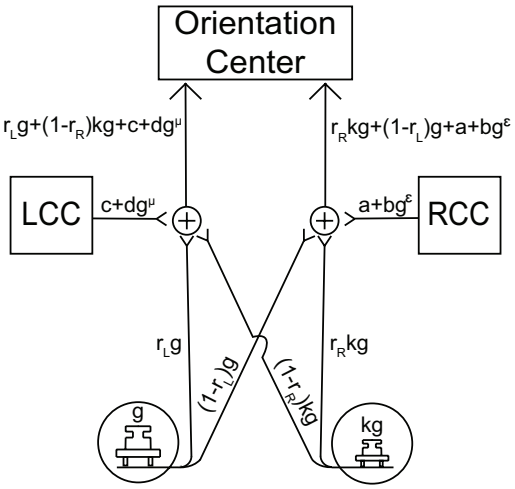

Figure 4.4 Proposed $L(g)$ and $R(g)$ functions for the model described in Figure 4.3

Assuming only the RCC provides compensation in 1g,

$$a + bg^{\varepsilon} > 0$$

and

$$c = d = 0 \text{ (any } \mu > 0).$$

In order for the orientation center to receive a balanced signal in 1g,

$$r_R kg + (1 - r_L)g + a + bg^{\varepsilon} = r_L g + (1 - r_R)kg$$

$$\Longrightarrow r_R k + 1 - r_L + a + b = r_L + (1 - r_R)k$$

Therefore,

$$a + b = 2r_L - 2r_R k + k - 1 \qquad (5)$$

The imbalance function $I(g)$ can be defined as

$$I(g) = [r_R kg + (1 - r_L)g + a + bg^{\varepsilon}] - [r_L g + (1 - r_R)kg]$$

$$= g(2r_R k - 2r_L - k + 1) + a + bg^{\varepsilon}.$$

Incorporating equation (5),

$$I(g) = a + bg^{\varepsilon} - g(a+b) \qquad (6)$$

Again, the left and right sides are balanced when $I(g) = 0$, ↶ if $I(g) > 0$, and ↷ if $I(g) < 0$.

For ↶ imbalance

$$a + bg^{\varepsilon} - g(a+b) > 0 \iff \frac{g(a+b) - a}{b} < g^{\varepsilon} \qquad (7)$$

and for ↷ imbalance

$$a + bg^{\varepsilon} - g(a+b) < 0 \iff \frac{g(a+b) - a}{b} > g^{\varepsilon}$$

Note that

$$I(1) = a + b - (a+b) = 0,$$

which is the balanced 1g condition.

For the VAN parabolic-flight data in Figure 3.12, we are interested in model parameters that enable the direction of imbalance to be the same in 0g and in 1.8g. We can consider only the ↶ imbalance condition described in equation (7). Mathematically, there are 3 cases in which equation (7) can be satisfied subject to this constraint:

Case 1: $g(a+b) - a \leq 0 \iff g \leq \frac{a}{a+b}$

Thus, whenever this condition is met, regardless of the value of ε, we have ↶ imbalance. Note that as $a, b > 0$, $\frac{a}{a+b} < 1$.

Cases 2 and 3: $g(a+b) - a > 0$

Case 2: $\frac{a}{a+b} < g < 1$

$$\frac{g(a+b)-a}{b} < g^{\varepsilon} \Leftrightarrow \frac{\ln\left(\frac{g(a+b)-a}{b}\right)}{\ln(g)} > \varepsilon \qquad (8)$$

Case 3: $g > 1$

$$\frac{g(a+b)-a}{b} < g^{\varepsilon} \Leftrightarrow \frac{\ln\left(\frac{g(a+b)-a}{b}\right)}{\ln(g)} < \varepsilon \qquad (9)$$

Let

$$F(g) = \frac{\ln\left(\frac{g(a+b)-a}{b}\right)}{\ln(g)}$$

with $\frac{a}{a+b} < g$, and $a, b > 0$. We can graph $F(g)$ and $I(g)$ to examine the g-levels in which ↶ is achieved. There are two scenarios, depending on the magnitude of ε relative to the magnitudes of a and b. When $\varepsilon > 1 + a/b$, we obtain the results in Figure 4.5. When $1 < \varepsilon < 1 + a/b$, we obtain the results in Figure 4.6. The primary difference between these two scenarios is that in the first, the direction of imbalance is the same for $g < F^{-1}(\varepsilon)$ and $g > 1$ (i.e., values of a, b, and ε can be selected such that the direction of imbalance is the same for 0g and 1.8g), while in the second, the direction of imbalance is the reverse $g < 1$ and $g > F^{-1}(\varepsilon)$ (i.e., values of a, b, and ε can be selected such that the direction of imbalance is the reverse for 0g and 1.8g).

Figures 4.5 and 4.6 can be understood as follows. In Case 1, regardless of the value of ε, we have ↶ imbalance when $0 \leq g \leq \frac{a}{a+b}$. This is seen in the graphs of $I(g)$ in both Figures 4.5 and 4.6. Consider now Case 2 where the values of g are in the range $\frac{a}{a+b} < g < 1$ when $\varepsilon > 1 + a/b$, as illustrated in Figure 4.5, or when $1 < \varepsilon < 1 + a/b$, as illustrated in Figure 4.6. We have ↶ imbalance precisely for the values of g when $F(g)$ lies above the horizontal line marked at ε in the graph of $F(g)$ in each figure. In

Figure 4.5, this occurs when $\frac{a}{a+b} < g < g_\varepsilon$ where $F(g_\varepsilon) = \varepsilon$, that is, when $\frac{a}{a+b} < g < F^{-1}(\varepsilon)$, as seen in the graph of $I(g)$. In Figure 4.6, this occurs when $\frac{a}{a+b} < g < 1$, as reflected in the graph of $I(g)$.

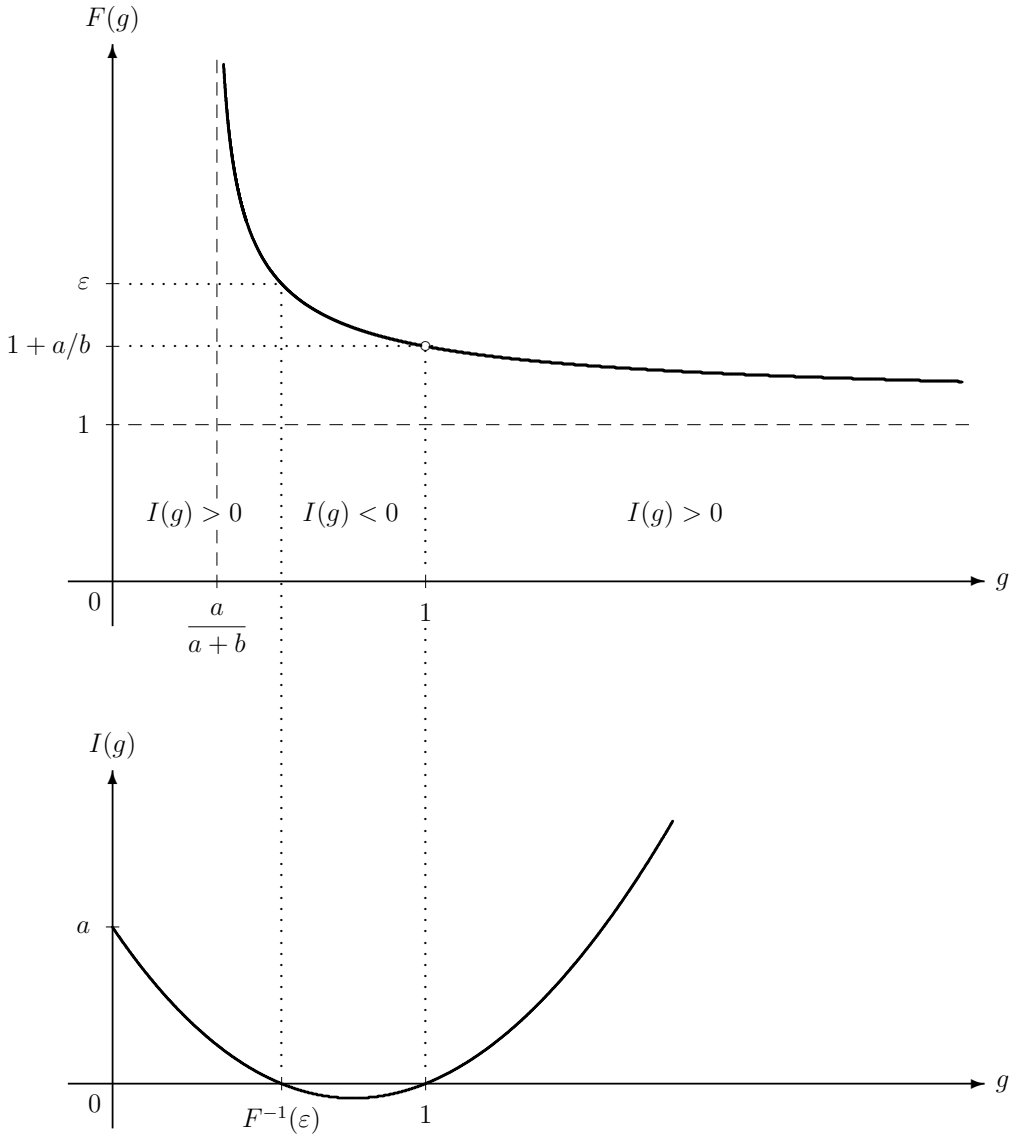

Figure 4.5 $I(g)$ for $\varepsilon > 1 + a/b$. Under this condition, the direction of imbalance is the same for $g < F^{-1}(\varepsilon)$ and $g > 1$.

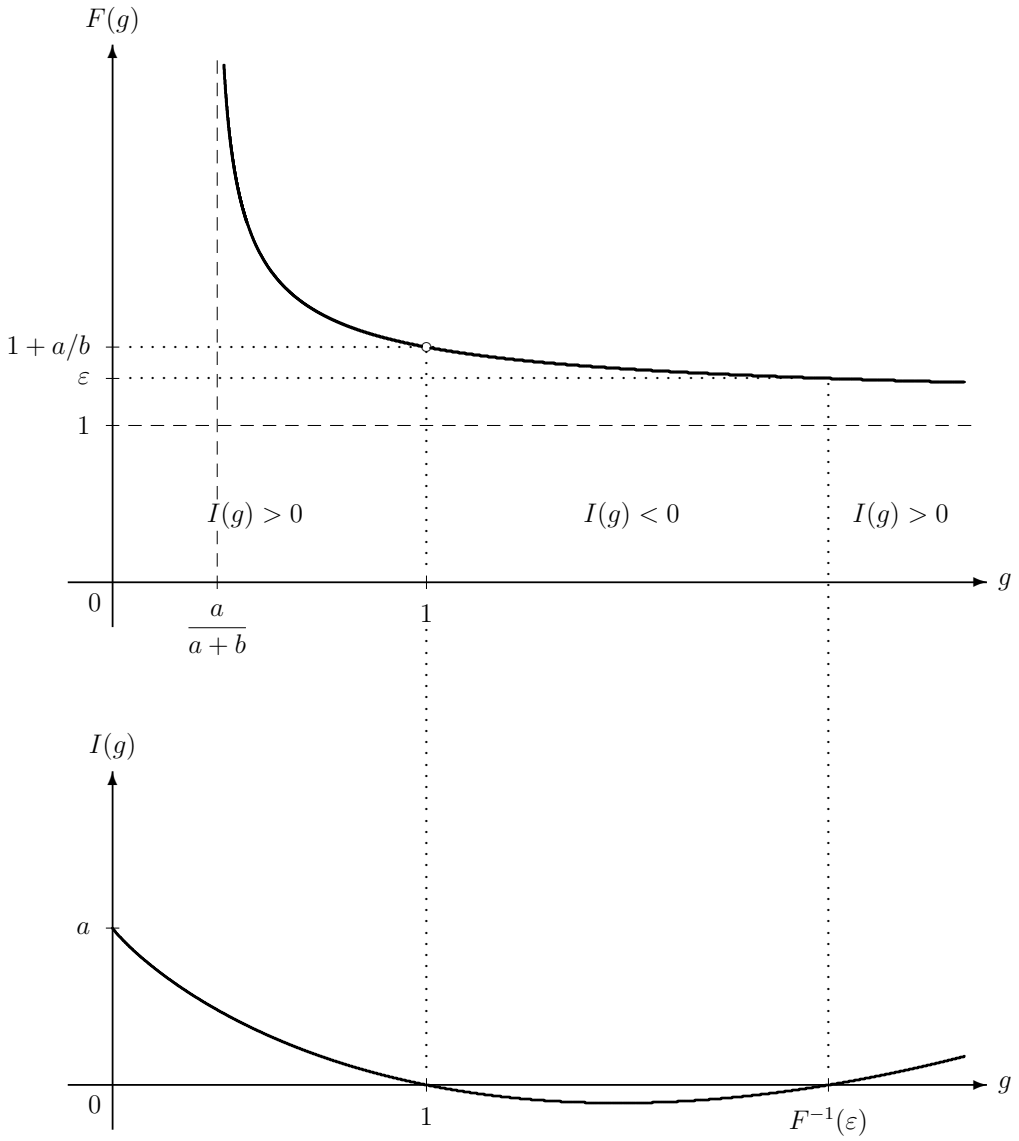

Figure 4.6 $I(g)$ for $1 < \varepsilon < 1 + a/b$. Under this condition, the direction of imbalance is the same for $g < 1$ and $g > F^{-1}(\varepsilon)$.

Now examine Case 3 where the values of g are in the range $1 < g$. In either Figure 4.5 or 4.6, we have $\curvearrowleft$ imbalance precisely for the values of g when $F(g)$ lies below the horizontal line marked at ε in the graph of $F(g)$. In Figure 4.5, if $\varepsilon > 1 + a/b$, this occurs for all $1 < g$, as seen in the graph of $I(g)$. In contrast, in Figure 4.6, if $1 < \varepsilon < 1 + a/b$, this occurs when $g_\varepsilon < g$ where $F(g_\varepsilon) = \varepsilon$, that is when $F^{-1}(\varepsilon) < g$,

as seen in the graph of $I(g)$. We remark that if $0 < \varepsilon \leq 1$, $F(g)$ would always lie above the horizontal line marked at ε, indicating that we have $\curvearrowleft$ imbalance precisely when $0 \leq g < 1$. This shows that a value of ε with $0 < \varepsilon \leq 1$ is not possible if in fact $\curvearrowleft$ imbalance occurs for some $g > 1$. In both Figures 4.5 and 4.6, we have balance when $g = 1$, even though $F(1)$ is undefined. It should be noted that small changes in the parameters a, b, and ε induce small changes in the imbalance function $I(g)$. Specifically, using partial derivatives, if a is changed by Δa, then $I(g)$ is changed by $(1 - g)\Delta a$; if b is changed by Δb, then $I(g)$ is changed by $(g^{\varepsilon} - g)\Delta b$; and if ε is changed by $\Delta\varepsilon$, then $I(g)$ is changed by $b\ln(g)g^{\varepsilon}\Delta\varepsilon$. This indicates that the model is robust.

In summary, what we learn from these figures is that the direction of imbalance for a given g-level is dictated precisely by the relative magnitudes of the a, b, and ε model parameters. Furthermore, if we know the values of a, b, and ε, we can derive exactly which g-levels should generate each of the two directions of imbalance ($\curvearrowleft$ versus $\curvearrowright$). In regards to our VAN and TAN parabolic-flight results, we can thus infer some potential numerical values for these model parameters, by which our flight data might arise. For example, if we fix the values of a and b for both the utricular-ocular and saccular-ocular compensation, we can select two values of ε, one for utricular-ocular compensation and one for saccular-ocular compensation, such that the direction of imbalance changes between 0g and 1.8 in the utricular-ocular model (in accordance with our TAN parabolic-flight results) but is preserved between 0g and 1.8 in the saccular-ocular model (in accordance with our VAN parabolic-flight results). Alternatively, we can vary a and b and maintain a common ε, or vary all three model parameters for each otolith-ocular system.

4.3.3 Neurophysiological correlates of the proposed model

Figure 4.7 depicts the presumed neurophysiological pathways within which the proposed model exists. For simplicity, we consider primary otolith-ocular pathways only, namely that ocular torsion is driven primarily by the utricles and that vertical positioning is driven primarily by the saccules, which is highly supported through intracellular recordings and lesion experiments in which the superior or inferior divisions of the vestibular nerve were sectioned (Suzuki et al. 1969; Fluur 1970; Fluur and Mellstrom 1970b; Fluur and Mellstrom 1970a; Uchino et al. 1996; Isu et al. 2000; Goto et al. 2004).

In Figure 4.7A, the torsional eye movement pathway begins with the left and right utricles sensing the current GIA. Afferents innervating the medial portion of the utricle project ipsilaterally, while afferents innervating the lateral portion project contralaterally; this ratio has been measured to be 3:1 (Fernandez and Goldberg 1976a). These primary afferents project to the vestibular nuclei (VN), which send ipsilateral secondary projections to the oculomotor (III) and trochlear nuclei (IV). Tertiary afferents project ipsilaterally from III to inferior oblique (IO) oculomotor neurons and contralaterally from IV to superior oblique (SO) oculomotor neurons. The projections for this otolith-ocular three-neuron arc are all excitatory. Excitation of IO oculomotor neurons results primarily in extorsion, while excitation of SO oculomotor neurons results primarily in intorsion.

In Figure 4.7B, the vertical eye movement pathway begins with the left and right saccules sensing the current GIA. Primary afferents project ipsilaterally and contralaterally to the VN, which send ipsilateral collaterals to III. Tertiary afferents project ipsilaterally from III to inferior rectus (IR) oculomotor neurons and to superior rectus (SR) oculomotor neurons. The projections for this otolith-ocular three-neuron arc are all excitato-

ry. Excitation of IR oculomotor neurons results primarily in depression, while excitation of SR oculomotor neurons results primarily in elevation.

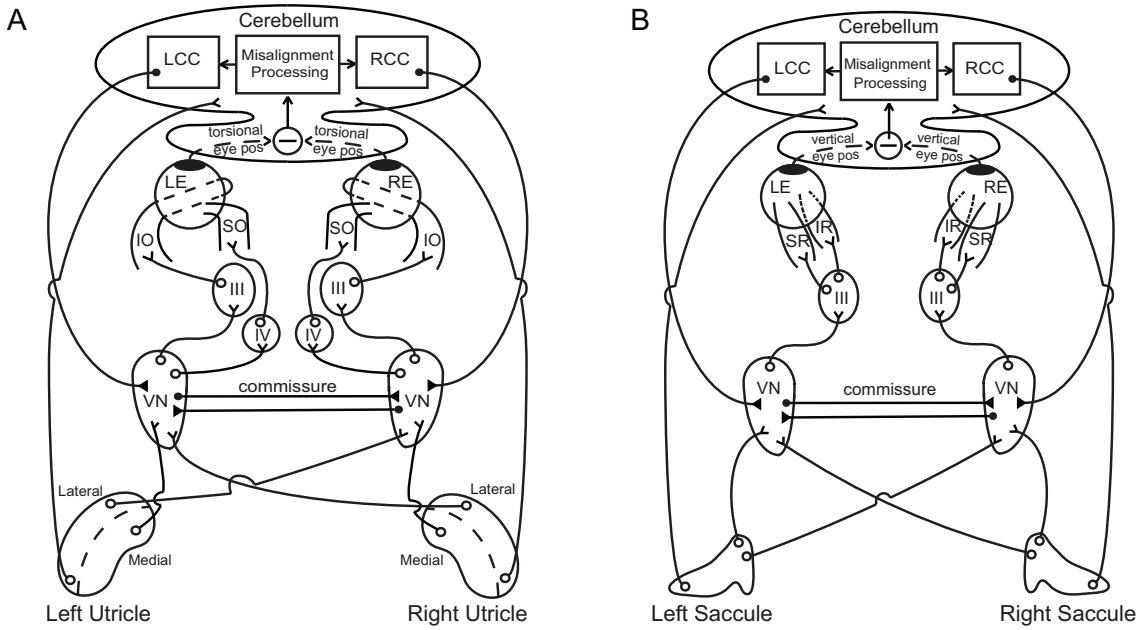

Figure 4.7 Otolith-ocular pathways facilitating binocular torsional (A) and vertical (B) eye positioning alignment. Primary afferents synapse in the vestibular nuclei (VN), which send projections to various oculomotor nuclei (III and IV) to control contraction of the appropriate eye muscles (SO, IO, SR, IR). Differences in left and right ocular positioning are computed in the cerebellum, which modulate the left and right compensation centers (LCC and RCC) to minimize ocular misalignments. Inhibitory compensation signals are fed back from the cerebellum to the VN. Commissural connections between the VN improve the sensitivity of otolith-mediated reflexes. Direct projections between the end organs and the cerebellum facilitate an immediate transmission of the current GIA to the structure responsible for determining compensatory parameters. Excitatory pathways are indicated by open circles, and inhibitory pathways are indicated by filled circles.

Shared between the utricular-ocular and saccular-ocular pathways are the commissural connections and cerebellar circuitry. Inhibitory commissural connections between the vestibular nuclei amplify any asymmetries between the left and right sides, which has been suggested to improve the sensitivity and resolution of otolith-mediated processes (Uchino et al. 1999; Karmali 2007). Direct projections from the end organs to the ipsilateral cerebellar nodulus and uvula are well established (Precht and Llinas 1969; Korte and Mugnaini 1979; Carleton and Carpenter 1984; Kevetter and Perachio 1986;

Barmack et al. 1993; Purcell and Perachio 2001), and it has been estimated that as many as 70% of primary vestibular afferents synapse in the cerebellum (Goldberg et al. 2012b). This feature enables the current g-level g to be a direct parameter in the central compensation functions. Secondary, bilateral projections from the VN to the cerebellum are also well established (Kotchabhakdi and Walberg 1978; Thunnissen et al. 1989; Barmack et al. 1992). Although there is considerable convergence of all vestibular primary afferents in the VN and in the cerebellum, distinct central vestibular areas have been shown to be more prominently influenced by utricular versus saccular signals. For example, in the VN, utricular afferents project more rostrally, while saccular afferents project more caudally; saccular afferents also project to the ventral y group (Newlands et al. 2002; Newlands et al. 2003; Highstein and Holstein 2006). This distinction likely facilitates slightly different compensatory parameters for utricular-ocular versus saccular-ocular control.

The cerebellum determines left-right ocular asymmetries through visual disparity cues and proprioceptive feedback from the eye muscles (Fuchs and Kornhuber 1969; Baker et al. 1972; Donaldson and Hawthorne 1979; Zee et al. 1981), in conjunction with information from primary and secondary afferent projections. The resulting perception dictates the central compensation model parameters of $R(g)$ and $L(g)$ (Marr 1969; Albus 1971; Ito 1972), likely computed in the flocculus and paraflocculus, which has been linked to the generation and plasticity of compensatory eye movements (Goldberg et al. 2012a). The central compensation functions are then fed back to the VN through direct, bilateral projections of cerebellar Purkinje cells (Batton et al. 1977; Noda et al. 1990). This vestibular-cerebellar-vestibular pathway provides a parallel inhibitory side loop that

can modulate the gain of the direct vestibulo-ocular pathways (Broussard and Kassardjian 2004; Goldberg et al. 2012a).

4.4 Discussion

The motivation behind developing the model presented here was to enhance our understanding of the otolith-ocular system, specifically in regards to eye positioning misalignments driven by static changes in otolith signaling. Examining these eye movements under exposure to novel g-levels allowed us to explore their pure, reflexive nature that is typically masked by central compensation. In essence, studying these systems in non-1g environments brought forth 1g-tuned performance characteristics that cannot be easily measured in 1g directly.

It is highly unlikely that the consistent VAN and TAN results obtained during parabolic-flight testing in all six subjects (with their small error bars and good repeatability early versus late inflight) would have arisen by accident. Thus, we believe that they represent some underlying neurophysiological mechanism that is modulated by g-level. As such, this model serves to explore one probable means by which changes in utricular and saccular signaling give rise to binocular positioning misalignments. The relatively small, but significant, magnitude of these misalignments was unlikely to induce functional visual decrements (although we did not explicitly test this, but can infer this to be the case from previous ground-based studies (Houtman et al. 1977; Guyton 1988)). However, their representation of underlying otolith asymmetries, previously linked to motion sickness susceptibility (von Baumgarten and Thümler 1979; Diamond and Markham 1991), render such seemingly small responses highly relevant for spaceflight operational

research. Applying modeling techniques to further our understanding of the fundamental neural connectivity, which may facilitate links to specific behavioral patterns, has important implications for countermeasure development to maximize crewmember safety and overall mission success.

In this chapter, we propose a simple model of the form $a + bg^{\varepsilon}$ that can appropriately transform binocular positioning data so that compensation for an inherent otolith asymmetry can be achieved in different g-levels. It is reasonable to expect the model parameters that compensate for torsional and vertical binocular positioning misalignments to vary slightly, in accordance with the different functional roles of the utricle and saccule and their corresponding dominant projections to particular divisions of the vestibular nuclei (Suzuki et al. 1969; Fluur 1970; Fluur and Mellstrom 1970b; Fluur and Mellstrom 1970a; Uchino et al. 1996; Isu et al. 2000; Newlands et al. 2002; Newlands et al. 2003; Goto et al. 2004; Highstein and Holstein 2006). Furthermore, the saccule is heavily tuned for postural control, including head-on-trunk stabilization and trunk-limb coordination (Wilson et al. 1977; Colebatch et al. 1994; Mhoon et al. 1997; Sato et al. 1997; Newlands et al. 2003). Why the saccular compensation requires a larger-than-linear amount of compensation (which can be accomplished in the model by a non-zero value of b or $\varepsilon > 1$) may be related to the simultaneous requirement of the saccule to compensate for postural deficiencies.

We presume that computation of the model parameters takes place in the cerebellum, which, in turn, feeds the necessary compensation functions back to the VN to modify oculomotor responses. However, it is also possible that some (or all) of this transformation takes place in the VN: the cerebellum sends the appropriate error signal (i.e., the

difference in left and right ocular alignment) to the VN that guides plasticity primarily within the VN (Miles and Lisberger 1981). This so-called brainstem hypothesis may better facilitate distinct utricular and saccular compensations, as less convergence between vestibular afferents of different origins (i.e., utricular versus saccular) is seen in the VN than in the cerebellum.

The mathematical transformations described in the central compensation functions of the proposed model (additive and multiplicative (gain) operations, nonlinear amplifications) are routinely observed in single neurons and within larger neural networks in both the brainstem and in the cerebellum (Chadderton et al. 2004; Silver 2010; Hildebrandt et al. 2011). Furthermore, it is possible that nonlinear amplifications of the GIA are performed by the primary afferents themselves, especially for g-levels near-zero and substantially greater than one, as evidenced by the sigmoidal force-response functions observed in squirrel monkey primary afferent recordings (Fernandez and Goldberg 1976b); as such, the ε parameter may be sent into the cerebellum directly.

We assume that the model parameters a, b, c, d, ε, and μ are fixed for a given individual and will vary across individuals depending on each person's inherent otolith asymmetry. One method for estimating these parameters is to perform the following experiment:

1. Expose an individual to a variety of g-levels (e.g., g_1, g_2, g_3, ..., g_n) and measure the amount of vertical and torsional ocular misalignment in each g-level (i.e., $I_1, I_2, I_3, ..., I_n$). Ensure that testing is performed fast enough within a given g-level such that no substantial adaptation occurs.

2. Perform a least squares fit on the data points $\{(g_1, I_1), (g_2, I_2), \ldots (g_n, I_n)\}$ by finding the a, b, and ε that minimize

$$\sum_{i=1}^{n} (I(g_i) - I_i)^2 = \sum_{i=1}^{n} (a + b{g_i}^{\varepsilon} - g_i(a + b) - I_i)^2$$

using numerical analyses.

The proposed model, with the parameters chosen appropriately, is consistent with the von Baumgarten and Thümler model. As is evident, the choice of $b = 0$ in the proposed model yields both the von Baumgarten and Thümler model of Figure 4.1 and $I(g) = a(1 - g)$ of equation (6). However, the choice of $\varepsilon = 1$ in the proposed model also yields $I(g) = a(1 - g)$. In other words, the results of von Baumgarten and Thümler could also have been obtained had they assumed that the compensation center on the (right) side of the weaker afferent signal supplies $R(g) = a + bg$, rather than $R(g) = a$. This indicates that the proposed model is in fact much closer to the von Baumgarten and Thümler model than may be seen at first glance, and may be considered a more detailed refinement of their model.

One important aspect not accounted for in the proposed model or in the von Baumgarten and Thümler model is any dependency of these otolith compensations on time; the models assume that their respective parameters are constants that are independent of time. In reality, this is likely not the case. We know from spaceflight literature that astronauts adapt their responses over various timescales to optimize performance in the novel g-levels (Michel et al. 1976; von Baumgarten 1986; Baroni et al. 2001; Williams et al. 2009). Furthermore, parabolic-flight research has demonstrated that repeated exposure to alternating g-levels also leads to adaptive responses over time

(Graybiel and Lackner 1983; Oman et al. 1996; Karmali 2007). However, the proposed model does correctly predict that once adaptation to a novel g-level is achieved (following exposure to some error signal over some unspecified period of time), re-adaptation to the original g-level elicits responses in the opposite direction. Hence, these models are accurate for predicting performance during baseline conditions (e.g., 1g), immediately following a change in g-level, and following complete compensation in the new g-level. While they can also be used to describe incomplete compensation (i.e., performance in the middle of the adaptive process), they cannot specify how long (temporally) it has taken to achieve the current amount of compensation. As no systematic adaptive responses were captured in our VAN and TAN parabolic-flight data (described more fully in Chapter 3), it was not possible to incorporate timing information into these models. However, future experiments that measure such responses over periods of time that are long enough to capture the time course of adaptation, (e.g., across multiple, consecutive parabolic flights) would facilitate the addition of such parameters to the currently proposed model.

Chapter 5

Vestibulo-Ocular Nulling quantifies perceived retinal slip

5.1 Introduction

5.1.1 Overview

The vestibulo-ocular reflex (VOR) facilitates gaze stability during head motion. As the head rotates and translates in space, the VOR generates compensatory eye movements so that the visual scene remains clear and stable on the retina. The ability to read signs while walking down the street or study flight-control instruments when flying through turbulent weather is mediated by an accurate VOR.

On Earth, pitch and roll head rotations (in the upright orientation) stimulate both the semicircular canals (SCCs) and the otolith organs: the SCCs transduce head velocity, while the otoliths transduce the magnitude and direction of the gravity vector. Thus, compensatory eye movements are dictated by concomitant SCC and otolith signals for pitch and roll head movements. Pure yaw rotations, on the other hand, do not alter the orientation of the head with respect to gravity, and so the direction in which gravity acts on the otolith organs is maintained during yaw movements (Berthoz et al. 1986); the corresponding compensatory eye responses stem from SCC input only (Tomko et al. 1988).

Furthermore, while horizontal eye movements elicited by horizontal vestibular and optokinetic stimuli are left-right symmetric, there exists an up-down asymmetry in vertical eye movements in response to vertical vestibular and optokinetic stimuli, the magnitude of which is enhanced by the presence of peripheral visual stimuli (Matsuo et al. 1979; Darlot et al. 1981; Matsuo and Cohen 1984; Van den Berg and Collewijn 1988; Murasugi and Howard 1989; Demer 1992; Ogino et al. 1996). In particular, the time constants for post-rotational or post-stimulus decay of upward slow-phase eye velocity (SPV) are longer than the time constants for downward SPV, indicating that stored neural activity related to SPV makes less of a contribution during upward than downward nystagmus (Darlot et al. 1981; Matsuo and Cohen 1984). This may be the case because (1) a larger portion of the vertical visual field lies below the horizon when the head is oriented in its typical upright position; hence, a larger number of downward fast phases may be necessary to reset the eye because there is typically a larger downward than upward range of motion, (2) downward head movements are assisted by gravity, while upward movements are opposed by it; therefore, asymmetrical neural control signals, which may be shared with the eyes, must be sent to the appropriate neck muscles to control the head, and (3) downward eye movements generated in response to optic flow during forward motion are suppressed (Guedry and Benson 1970); so the fact that upward SPV is greater than downward SPV may be the consequence of a reflex that evolved to assist with gaze stability during locomotion (Clément and Reschke 2008a). The asymmetry in vertical optokinetic nystagmus is eliminated when the otoliths are ablated, or when the head is reoriented into the upside-down position (Igarashi et al. 1979; Clément and Lathan 1991).

Given this clear interaction between the canals and otolith organs, dependent on gravity, it has therefore been hypothesized that during spaceflight, pitch (and roll) head movements may elicit miscalibrated eye responses due to gravity-dependent changes in the otolith-modulated component of the VOR. One would expect to observe an initial decrease in pitch VOR gain upon exposure to a hypo-g environment (e.g., in 0g) where the otolith contribution is lacking, and an initial increase in gain in a hyper-g environment (e.g., during takeoff, landing, and other g-level transitions) or immediately upon Earth-return where a larger otolith contribution exists. Additionally, one might expect to see a reversal in the up-down asymmetry of pitch VOR gain, attributable to the offloading of the constant 1g bias (presumably of saccular origin) in 0g (Clarke et al. 2000). Such gain changes could lead to gaze instability, oscillopsia, and disorientation, which would have detrimental consequences on piloting and other manual control tasks that require crew-members to turn their heads to view instruments and control panels. These maladapted reflexes could also lead to eyestrain, headache, and fatigue.

Unfortunately, the ability to evaluate changes in gaze stability inflight or immediately postflight has been extremely limited thus far, due to the lack of a portable technology to accurately perform such measures. Therefore, the purpose of the experiments in this chapter is to consider a new approach for rapidly and reliably capturing changes in vestibulo-ocular function during exposure to novel g-levels. An innovative assessment technique to evaluate the VOR without measuring eye movements is developed, which incorporates the same hand-held tablet platform described in the previous chapters. Importantly, our assessment technique attempts to bridge part of the gap between traditional measures of pure motor responses (e.g., VOR gain and phase) and subjective measures of

functional performance by employing a perceptual nulling task that quantifies how stable a target must actually be in order to be perceived as stationary in space. Laboratory experiments compare results from this nulling task to measures of VOR gain. Parabolic-flight experiments explore the viability of such an assessment technique in an operational environment and look for evidence of gravity-dependent changes in the VOR.

5.1.2 Dynamic otolith-modulation may improve VOR performance

Pitching head movements in novel g-levels are well known for inducing discomfort. They are the most provocative head-motion stimuli during parabolic flight (Lackner and Graybiel 1986), and astronauts have reported hypersensitivity to such motions in-flight and upon Earth-return (Thornton et al. 1987b; Oman et al. 1990; Black et al. 1999). Several investigators have measured the pitch VOR gain during and immediately following spaceflight, with limited success, but the results are not yet conclusive. Watt and colleagues did not observe any significant changes in the pitch VOR gain (relative to pre-flight tests) in two astronauts inflight (Watt et al. 1985). Berthoz and colleagues also did not see significant changes in gain in two different astronauts inflight (Berthoz et al. 1986), although this data was not collected until mission days five and seven (MD5, MD7), which is well beyond the time in which most astronauts become adapted to the orbital environment (Homick et al. 1987; Davis et al. 1988). However, Berthoz et al. did find significant phase leads inflight, and also increased gains upon Earth-return. The increased pitch VOR gain observed postflight suggests that adaptation to 0g may have resulted in an increase in the SCC contribution to the pitch VOR to ensure fully compensatory ocular responses inflight; hence, the additional otolith contribution immediately upon Earth-return resulted in the overall gain increase.

Viéville and colleagues found pitch VOR gain to be reduced early inflight in two crewmembers during active head movements at 0.2Hz (Viéville et al. 1986). These astronauts also experienced a reversal in the pitch VOR up-down gain asymmetry. Clarke and colleagues found a similar reversal in gain asymmetry in two different astronauts (Clarke et al. 2000). As expected, investigators have not detected any significant inflight or postflight difference in the yaw VOR (Thornton et al. 1985; Watt et al. 1985; Benson and Vieville 1986; Berthoz et al. 1986; Cohen et al. 1992).

One reason for the discrepancies among the various studies in inflight pitch VOR gain results may be due to experimental design. The study by Watt and colleagues employed a purely subjective assessment technique in which the astronaut looked at a target, covered the eyes and rapidly rotated the head 10-15° while attempting to maintain target fixation, removed the cover from the eyes, and then determined whether or not he perceived his eyes to still be on target (Watt et al. 1985). The fact that head movements were small, the target was 1.5m away, and the potential for re-fixation saccades as soon as the cover was removed, may have resulted in gaze-shifts that were undetected by the crewmember himself (e.g., due to the rapid, reflexive nature of such saccades). This may have been more accurately evaluated by a second crewmember observing the subject's eye movements directly. Furthermore, even if crewmembers had perceived changes in gaze direction, it is unclear how this could have been quantified to compute VOR gain values. Inflight assessments by other investigators were typically performed in the dark to remembered targets in order to prevent visual cues from masking underlying vestibular responses. However, the ability to recall such imaginary targets in the dark may be difficult when the gravitational reference that is typically available for generating an internal

representation of the surrounding environment on Earth is missing in space (Clément and Reschke 2008a). A third reason for the discrepancies may be that different astronauts adopt different neural strategies to account for differential otolith signaling, such as an increased reliance on visual or proprioceptive cues (Clément et al. 1999b).

On Earth, there is considerable evidence that angular rotation in the presence of dynamic otolith stimulation can lead to improved VOR performance. For example, Clément and colleagues found that pitch VOR gain in the upright orientation (otolith-modulating component) was more compensatory than pitch VOR gain while lying onside (lack of otolith-modulation component) during passive rotations at 0.8Hz (Clément et al. 1999a). Brettler and colleagues found that when rats were rotated such that only their SCCs were stimulated (upright yaw and nose-up roll), VOR gain was accurate above 0.2Hz, but was reduced and subject to substantial phase leads at lower frequencies (Brettler et al. 2000). Rotations that incorporated a changing gravity stimulus (nose-up yaw, onside yaw, and upright roll), on the other hand, elicited fully compensatory VOR gain and phase down to 0.02Hz. Furthermore, when the rats were inverted and then rotated in roll, anti-compensatory phase leads were present across all frequencies. Analogous results have been observed in rabbits (Barmack 1981; Van der Steen and Collewijn 1984) and cats (Rude and Baker 1988; Tomko et al. 1988).

Yakushin and colleagues demonstrated in monkeys that the orientation of the head relative to gravity during pitch VOR adaptation was a critical context for maintaining the adapted gain (Yakushin et al. 2000). When pitch VOR gain was adapted in the upright position, gain changes were symmetrical when animals were tested on their left and right sides. However, when pitch VOR gain was adapted onside, gain changes were

always larger when the animals were tested on that same side. The investigators concluded that pitch VOR gain changes are stored in the context of the head orientation in which the adaptation took place. Angelaki and colleagues have demonstrated that the otoliths have a strong modulatory effect on the angular VOR, especially during low-frequency motion (Angelaki et al. 1995).

It should be noted that two studies have shown no differences in upright versus onside pitch VOR in humans in 1g (Baloh and Demer 1991; Tweed et al. 1994). However, Baloh and Demer (1991) did observe asymmetries in upright versus onside and upward versus downward gain values in individual subjects, but these differences were not significant across the *pooled* average of all subjects. Additionally, Tweed and colleagues (1994) only tested at 0.3Hz, a frequency within the normal operating range of the semicircular canals; other investigators have found asymmetries to be more robust at lower frequencies where SCC signals are less reliable.

On the other hand, it is possible that while some subjects may not express different pitch VOR gain values in the upright versus onside positions on Earth, they may show deficient gains during spaceflight. On Earth, the gravity vector does not rotate relative to the head during onside pitch. However, it is nonetheless present, which may serve as a context cue to the CNS to not expect an otolith-moduling component during head movements in this orientation. In space, this 1g reference is no longer available, and so the CNS may still expect an otolith-modulating component during head pitch (Shelhamer and Zee 2003).

5.1.3 Traditional approaches to quantify the VOR

The primary approach for quantifying the VOR is to simultaneously record eye and head movements and then compare differences in their amplitudes and timings (see Chapter 1.3.1). Head-mounted video-oculography (VOG) devices offer the best portability for eye movement recordings, but their delicate and expensive equipment requires headgear that must be connected (non-wirelessly) to a high-powered laptop and computationally expensive processing algorithms. Furthermore, frequent occlusion of the pupil by the eyelids limits the range of vertical eye movements that can be accurately tracked by most VOG software. This was precisely the issue in our laboratory experiments described below: although pitch head movements were more relevant for our scientific goals, our new vestibulo-ocular assessment technique needed to be validated using yaw head movements due to the limited vertical tracking capabilities of our VOG system. An important strength of our assessment technique is that it provides equally reliable results during both yaw and pitch head motion.

Recording eye movements provides a direct, objective measure of the oculomotor response to a given head movement. However, this motor output does not incorporate any cognitive or perceptual factors (i.e., a sensory component) that may also aid in gaze stability. The dynamic visual acuity (DVA) test was developed to evaluate the ability to read during head motion without recording eye movements (Longridge and Mallinson 1984; Longridge and Mallinson 1987; Herdman et al. 1998). It is presumed to be a functional correlate of VOR gain (Benson and Barnes 1978; Longridge and Mallinson 1984). In the DVA test, head movements faster than a specified velocity trigger the presentation of an optotype (e.g., the letter “E” or “C”), and subjects are tasked with reporting its ori-

entation (i.e., up, down, left, or right). Correct responses lead to the generation of progressively smaller optotypes, until the individual can no longer accurately distinguish the letter's direction. At the end of the test, a dynamic visual acuity score is given, which relates the ability to see clearly with the head moving (dynamic visual acuity) relative to the ability to see clearly with the head still (static visual acuity). The DVA test can reliably distinguish among healthy individuals and patients with vestibular deficits (Herdman et al. 1998; Herdman 2003; Herdman 2007). However, one downside to the DVA test is that it can be time consuming (e.g., greater than 10min to test multiple head-movement directions using the version currently employed in our Johns Hopkins clinic). A second downside is that it is not an ideal test for adaptation experiments, as performing the test itself is an adapting (or de-adapting) stimulus. For example, in our experiment described below, telescopic lenses are employed to adapt the gain of the VOR. Throughout adaptation, VOR gain was probed in the dark to prevent washout. DVA probes could not be employed because the repetitive head movements while viewing the stationary optotypes would have either washed out adaptation if performed with the lenses off or augmented adaptation if performed with the lenses on. One of the advantages of our perceptual nulling task is that it does not elicit washout.

5.2 Objectives

The VOR assessment techniques described above are not ideal for evaluating the vestibulo-ocular system during spaceflight operations, where minimal equipment and rapid tests are necessary. As such, the experiments in this chapter were designed to:

6. Develop a technology to evaluate vestibulo-ocular function using portable hardware and simple tests.
7. Use this technology to compare measures of vestibulo-ocular function to traditional measures of VOR gain.
8. Quantify changes in vestibulo-ocular function during the altered g-levels of parabolic flight.

5.3 Materials and methods

5.3.1 VON design

When the head turns, if the eyes do not move appropriately to stabilize retinal images, the visual scene will undergo illusory motion proportional to the amount by which the eye movement is deficient in compensating for head motion. As such, an individual with a miscalibrated VOR will incorrectly perceive a stationary target as moving (oscillopsia). If this person can report the *amount* of illusory motion that he perceives for a given head movement, then a surrogate measure of vestibulo-ocular function can be obtained. This concept underlies the foundation of our Vestibulo-Ocular Nulling (VON) test.

In VON, head movement data is used to control the position of a visual target through a variable motion-gain in real-time (Figure 5.1). The subject adjusts the motion-gain until the target appears fixed-in-space during head movements. Thus, this VON motion-gain setting reflects the extent with which the target must be moved (either more or

less) relative to head motion so that the target appears visually stationary. This provides an objective measure of oscillopsia without recording eye movements.

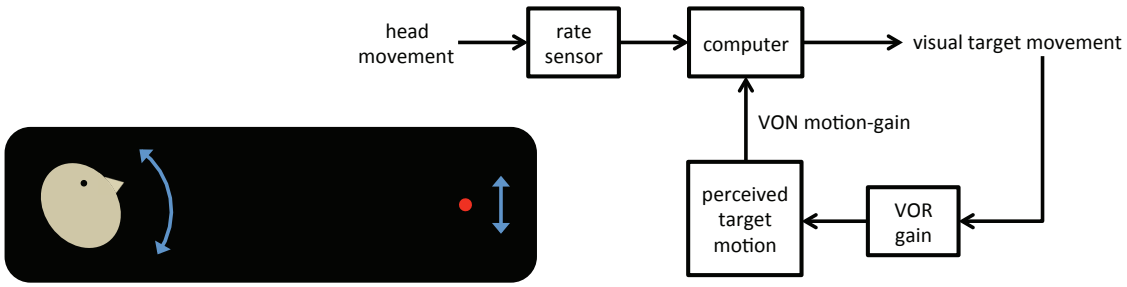

Figure 5.1 The Vestibulo-Ocular Nulling task. Head movement data controls the position of a visual target through a variable motion-gain in real-time. The subject moves his head (e.g., up and down) and adjusts the value of the motion-gain until the target appears fixed-in-space.

By definition, a VON motion-gain value of 1.0 means that the target is physically fixed-in-space. In other words, when VON motion-gain is set to 1.0, the target does not move on the VON display regardless of how the head moves. This is analogous to an individual with a perfectly compensatory VOR: when viewing a stationary target while moving the head (in any direction at any speed), the target does not appear to move—it remains fixed-in-space. In contrast, a VON motion-gain value of 0.0 means that the target moves in perfect synchrony with the head. This is equivalent to a VOR cancellation task, in which the target moves in the same direction and at the same speed as the head. If the VON motion-gain is set to a value less than 1.0 (e.g., VON motion-gain = 0.5), then, to a healthy individual with a perfectly compensatory VOR, the VON target will appear to move *in the same direction* as the head. Thus, when this person performs the VON task, he will need to *increase* the VON motion-gain (to a value of 1.0) in order to perceive the target as stationary during head motion. Alternatively, if the VON motion-gain is initially set to a value greater than 1.0 (e.g., VON motion-gain = 1.5), then, to this healthy individual, the VON target will appear to move *in the opposite direction* of the

head, and he will have to *decrease* the VON motion-gain (to a value of 1.0) in order to perceive the target as stationary during head motion. Novice subjects being trained on VON are taught these strategies. Although the VON task itself is highly intuitive for most people, engraining these concepts early enables subjects to perform the individual trials rapidly, as it "automates" the task so that subjects do not need to think about which direction the motion-gain should be adjusted based on how they perceive the target to be moving relative to their head motion. Of course simple trial and error can also be used.

In general, VON testing can be performed using angular or linear head movements, to evaluate the angular and linear VORs respectively, that are generated actively or passively. Additionally, subjects can sit or stand while doing the test. The experiments in this dissertation involve active, angular head movements while seated, although preliminary data from standing VON tests have been collected during parabolic flight and are discussed briefly in Chapter 7. VON testing with linear (translational) head movements requires knowledge of the subject-to-target distance to compute the appropriate compensatory gain values.

Several versions of VON hardware have been implemented over the years. As technology has improved (namely, hand-held AMOLED tablet computers and wireless motion sensors have become readily available), the portability of VON has significantly increased. The tablet-based version described in this section is the newest VON platform and represents the final hardware iteration. Small, proof-of-concept experiments have validated the use of this version of the hardware in the laboratory, and parabolic-flight testing with the tablet is scheduled as of this writing. For the laboratory and parabolic-flight experiments described in Sections 5.3.2 and 5.3.3, two earlier versions of the VON

hardware were employed. The laboratory experiment implemented a back-projected laser as the VON target, while the parabolic-flight experiment employed a head-mounted display (HMD) to project the VON target.

The newest set of VON hardware incorporates the same AMOLED tablet computer and wireless kinematic motion sensors described in a previous chapter (there are no specialized eyeglasses for this test) (Chapter 3.3.1). This particular tablet enables all testing to be performed in complete darkness (with the incorporation of a dark room or black shroud). Like the VAN and TAN tests described in Chapter 3, this is critical for ensuring that background visual cues do not influence VON motion-gain values. The goal of VON is to adjust the motion-gain until the target appears to be fixed-in-space during head motion, not fixed relative to a known stationary object, for example. As such, if the subject can see the border of the display, it is easily recognized that a "perfect" VON motion-gain is achieved by simply centering the target in the center of the display. Therefore, testing without extraneous visual cues is important.

At the beginning of a test session, one motion sensor is secured to the subject's head via an elastic strap. Additional reference sensors can be incorporated as needed (e.g., fixed to the trunk to examine deviations in postural sway during standing VON tests or on the floor of the aircraft to record g-level during parabolic-flight testing). The tablet is fixed relative to the subject's head: it is either held out in front, or mounted on a desk or wall. When the app is started, the VON home screen appears (Figure 5.2). The subject selects the appropriate motion sensor attached to his head, as well as any additional reference motion sensors (e.g., fixed to the trunk to record relative body sway or to the floor of the aircraft to record g-level), and in which direction the head movements will be

made (e.g., pitch or yaw). When the *open file* button is pressed, two new files (a *small file* and a *large file*) are created for storing the test results. During testing, the tablet's timestamp, current motion-gain value, trial number, and kinematic data from the tablet's onboard accelerometer and external wireless motion sensors are exported to the data files in real-time. The *small file* records a row of data each time the motion-gain is incrementally adjusted (in steps of 0.01 gain units), while the *large file* records a row of data every 10ms. The *large file* is necessary when capturing simultaneous body sway or changes in g-level, while the *small file* is typically sufficient when the subject is seated in a stationary environment. The file names are automatically generated based on the current date and timestamp (to prevent accidental overwriting). The subject presses the *new trial* button to begin the test block.

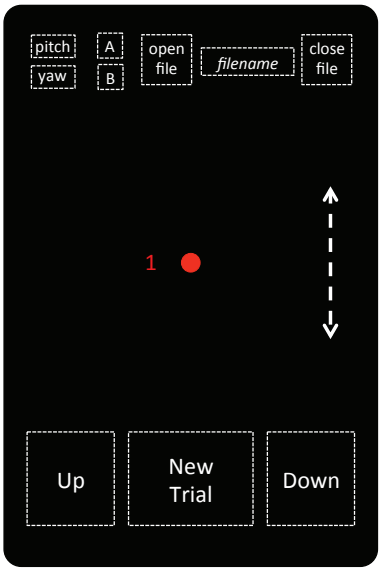

Figure 5.2 VON home screen. At the beginning of each test block the subject selects the direction of head movement (*pitch* or *yaw*), head motion sensor (*A* or *B*), and opens a new recording file (*open file*), which displays the filename. At the start of each trial, the program randomly selects an initial VON motion-gain, and the subject adjusts this value until the target appears fixed-in-space during head movements; this is accomplished by dragging the line using an invisible slider button (indicated by the dashed white double-arrow) or repeatedly pressing the up and down buttons on the bottom of the screen (areas outlined by the dashed-white boxes). During the actual testing, the white text is invisible and subjects use tactile feedback to interface with the program. The number of completed trials is displayed next to the target and moves with the target according to the current motion-gain value. At the end of the test block, the subject presses the upper right-hand corner of the screen to close the file.

Once the *new trial* button is pressed, the VON target (small red dot) is presented in the center of the screen, with the current trial number beside it. All other visual cues, including the test settings along the top of the screen and button labels on the bottom, are

eliminated, although the functions and vibrotactile feedback for the buttons that adjust the motion gain, reset the next trial, and close the current file remain active. The program randomly selects an initial motion-gain value between 1.1 and 1.5 or 0.5 and 0.9; the goal is for the program to select values that require the subject to adjust the value of the motion-gain, but not by so much that unnecessary time is wasted fine-tuning each trial. When the head moves, the target moves in accordance with the specified motion-gain. The subject adjusts this motion-gain, by either dragging an invisible slider located on the side of the screen or using the *up* and *down* buttons located near the bottom of the screen, until he perceives the target to be fixed-in-space during head movements. If there exists a range of motion-gains for which the target appears fixed-in-space, the subject is instructed to find the middle of that range. The trial counter moves with the VON target to prevent any stationary visual reference points. The final motion-gain value provides a measure of perceptual deficiency in the VOR. Once the trial is completed, the subject presses the (invisible) *new trial* button in the bottom center of the screen to generate the next trial. Once the desired number of trials has been completed, the subject closes the file using the *close file* button in the upper right-hand corner of the screen. Pressing the *close file* button illuminates the home screen once again.

If the subject has a perfectly compensatory VOR, then the subject should select VON motion-gain values equal to 1.0. Values above or below 1.0 describe the amount of deficiency in the vestibulo-ocular system. For example, suppose an individual has a known VOR gain of 0.5. This means his eyes only compensate for half of his head motion. So for example, when this person pitches his head up, his eyes will move down, but only by half as much. Suppose that he performs the VON test and that the initial motion-

gain is set to 1.0. At the start of the test when he is staring at the stationary VON target (before moving his head), the target is in the center of his fovea. When he pitches his head up, the target will appear to move down because his eyes are not rotating far enough to compensate for his head movement, and so the target will now appear in the lower half of his visual field instead of centered on the fovea. In order for him to perceive the target as fixed-in-space when he pitches his head, he must adjust the VON motion-gain so that the target moves in the same direction as the head (as viewed by an outside observer). This is accomplished by selecting a VON motion-gain less than 1.0.

In contrast, suppose another individual has a known VOR gain of 2.0 and the initial VON motion-gain is set to 1.0. When this person pitches his head up, the eyes move down, but by twice as much. Hence, from his perspective, the VON target will appear to move up because his eyes are rotating too far (i.e., the target will now appear in the upper half of the visual field instead of centered on the fovea). In order for him to perceive the target as fixed-in-space when he pitches his head, he must adjust the VON motion-gain so that the target moves in the opposite direction as the head (as viewed by an outside observer), which is achieved by selecting a VON motion-gain greater than 1.0. These concepts underlie the results for the adaptation experiment described in Section 5.4.

5.3.2 VON motion-gain versus VOR gain experiment

We were interested in how our perceptual measure of vestibulo-ocular function (VON motion-gain) compares to a traditional, physiologic measure of the vestibulo-ocular system (VOR gain), and so VON motion-gain and VOR gain were measured during adaptation to a pair of telescopic lenses. At the time of this experiment, the AMOLED tablet had not yet been acquired, and so an earlier version of the VON hard-

ware was employed, which incorporated a laptop computer, mirror galvanometer, back-projected laser (VON visual target), USB-powered data acquisition board (DAQ), USB-powered rate sensor (fixed to the subject via a custom-mold dental biteboard), and motion-gain dial (potentiometer). In this setup, the VON program controlled the motion of the projected laser through the galvanometer and DAQ based on the current setting of the motion-gain dial controlled by the subject.

In this experiment, twelve healthy subjects (Table 2.1) wore x0.5 minifying lenses for 20min, during which they performed active, yaw-plane, sinusoidal head rotations, as described in Chapter 2.5.1. The adaptation procedure was divided into four 5min blocks. During these blocks, subjects focused on a stationary target 1.5m away in a completely lit room. VON motion-gain and VOR gain were probed in between each adaptation block in the dark without the lenses. During the VON tests, the laser VON target was the only visible cue seen by the subject, and it was projected 1.5m in front of the subject. VOR gain testing was performed in complete darkness with subjects imagining a stationary VON target. At the beginning of each VOR gain test, subjects fixated this stationary VON target for several seconds, which was extinguished just prior to the start of the head movements. At the end of the adaptation period, a 5min washout session was implemented, in which subjects performed the same active, sinusoidal head movements in the light without the lenses. Following this washout, VON motion-gain and VOR gain were measured one final time in the dark. During each test probe, five VON trials were performed and twenty cycles of VOR gain data were collected.

Nine of the twelve test subjects (everyone except subjects A, H, and J) were completely naïve to the objectives of the experiment and the details as to how the minifying

lenses would alter the visual scene. These nine subjects had also never performed the VON task before. All subjects were trained on the VON task and completed twenty practice trials prior to the start of the experiment to reduce training effects. Furthermore, because it was anticipated that some subjects might have difficulty remembering the location of an imaginary target during VOR gain testing, subjects practiced making the twenty cycles of head movements while fixating an imaginary target three times.

Prior to the start of this experiment, initial pilot studies using this version of the VON hardware were performed during baseline testing only (no adaptation). These results demonstrated that healthy subjects could successfully null the VON target during head motion; VON motion-gain values were consistently close to approximately 1.0, as expected from healthy individuals. Based on this limited result, we hypothesized the following results would be obtained during the adaptation experiment:

1. Changes in VOR gain during lens-adaptation would match results observed by other investigators. Since VON motion-gain also represents a measure of gaze stability, we expected VON motion-gain values to portray a similar adaptive trend.
2. Because VON motion-gain also incorporates a perceptual aspect of vestibulo-ocular performance (as opposed to a pure motor reflex), VON motion-gain values may be more compensatory than VOR gain because subjects can employ other mechanisms of gaze stability, such as sensory fusion, to augment their VON performance. However, the subjective nature of such responses may result in motion-gain values that are more variable than VOR gain values.

After this main experiment was completed and the results were analyzed (Section 5.4.1), a smaller follow-on adaptation experiment was conducted in three of these subjects. The purpose of this subsequent experiment was to determine (1) if a flashing target may be a more viable stimulus than an imaginary remembered target during VOR gain measures, and (2) whether we could more explicitly define which aspect of vestibulo-ocular function the VON motion-gain quantifies. In this experiment, which occurred several months after the primary adaptation experiment, subjects adapted to the x0.5 minifying lenses during one 10min block using the same active, yaw-plane, sinusoidal head movements. Ten trials of VON motion-gain were collected prior to adaptation and five trials of VON motion-gain were collected after adaptation. Several additional pre- and post-adaptation VOR gain measures were collected: (1) in complete darkness to a remembered target (as during the main adaptation experiment), (2) with a flashing target (the stationary VON target was illuminated for 20ms every 2s), and (3) with a fixation target (the stationary VON target remained illuminated during the VOR gain tests). Furthermore, simultaneous eye and head movements were recorded during VON testing; once subjects selected their desired VON motion-gain, ten additional cycles of VOR gain data were collected while subjects viewed the VON target. To minimize washout following adaptation, the order of the post-adaptation tests were completed as follows: (1) VOR gain test while imagining a remembered target, (2) VON motion-gain test plus an additional 10 cycles of VOR gain data once the motion-gain value was set, (3) VOR gain test while viewing the flashing target, and (4) VOR gain test while viewing the steady target. For this experiment, we hypothesized the following:

1. The flashing target would provide a reference frame to which subjects could more consistently perform the VOR gain tests.
2. The fixation target would drive rapid washout of the adaptation.
3. Measures of VOR gain once VON motion-gain was set would generate VOR gain values that matched the VON motion-gain values.

5.3.3 Parabolic-flight experiment

Vestibulo-Ocular Nulling was also performed in the alternating g-levels of parabolic flight to validate the VON concept in an operational environment and to investigate the role of dynamic otolith stimulation in the angular VOR. For this experiment, all VON testing was carried out in the pitch plane, as pitching head movements stimulate both the SCCs and otolith organs in anything other than 0g. Five subjects, including three naïve fliers and two experienced fliers (Table 2.1), each flew one forty-parabola flight, which consisted of forty 0g parabolas (alternating with 1.8g pullout maneuvers). The VON tests were part of a larger battery of neurovestibular experiments, and so only six of the forty parabolas (either parabolas #1–6 or #16–21) were dedicated to VON testing for each subject. Testing was performed in both the 0g and 1.8g phases of flight. As in our other parabolic-flight experiments, subjects did not take any anti-motion sickness medication (Chapter 3.3.3).

The parabolic-flight version of the VON hardware in this case included the laptop computer, motion-gain dial, and head-mounted rate sensor from the laboratory experiment described above, but incorporated a head-mounted display (HMD) instead of the galvanometer and back-projected laser. The HMD (Virtual I/O iGlasses) consisted of two small LCD screens (co-located with each eye) onto which the VON target was dis-

played, which facilitated stereoscopic viewing at a convergence distance fixed at 1m. The advantage of the HMD was that it blocked all external vision without the need to enclose subjects under a black shroud. However, the backlight from the LCD screens provided a visible "rectangle" that moved with the head. This made VON training more challenging, as investigators needed to ensure that subjects were not using this rectangle as a reference for setting the motion-gain. But because the backlight moved with the head, subjects could not simply adjust the motion-gain so that the VON target remained fixed in the center of the screen, for example (this would be equivalent to a VON cancellation task (motion-gain equal to 0.0)). With sufficient practice, subjects developed their own strategies to ignore the backlight and adjust the motion-gain such that they perceived the VON target as fixed-in-space. Furthermore, during postflight data analysis, we considered the relative differences in the VON motion-gains selected during the 0g and 1.8g phases of flight and those selected in 1g, as opposed to the raw values of VON motion-gain in the three different g-levels. Preflight training, in which subjects completed approximately fifty VON trials, was performed in all subjects several days before each subject's respective flight. Training was refreshed on flight mornings, and ten trials of baseline 1g data were collected approximately one hour prior to takeoff.

Because this was the first time VON was being tested in the parabolic-flight environment, a primary objective was to consider the operational feasibility of performing such a test under altered gravity conditions. One main concern was whether or not naïve, unmedicated subjects could handle performing continuous pitching head movements in-flight, as such motions are known to be the most provocative type of head movement in parabolic flight (Lackner and Graybiel 1986). As such, we did not enforce strict head

movement criteria (e.g., specific head velocities paced by a metronome), as is typically done in the laboratory. Instead, subjects were trained preflight to move their head in a methodical, sinusoidal manner at approximately 0.5–0.75Hz. During inflight testing, if subjects could no longer perform the head movements at approximately the same velocities used during baseline training, they were asked to pause their testing until they felt well enough to resume the appropriate head movements. For some subjects, this resulted in a much smaller number of completed trials.

During inflight testing, subjects were loosely strapped to the floor of the aircraft and allowed to float several inches above the floor during the 0g portions of the parabolas (Figure 5.3). Subjects were instructed to perform as many successive VON trials as possible throughout the 0g and 1.8g phases of flight; trials were separated by g-level during postflight data analysis. If at any point subjects began to experience mild motion sickness symptoms, including hot or cold sweats or stomach awareness, head movements were stopped immediately, and subjects paused to rest.

Based on laboratory VON testing, past flight experience, and literature surrounding changes in the VOR during exposure to altered g-levels, the following hypotheses were made preflight:

1. Subject with no prior parabolic-flight experience would demonstrate reduced VON motion-gains in the 0g phases of flight and elevated motion-gains in the 1.8g phases of flight.
2. Subjects with prior parabolic-flight experience may show smaller g-level dependencies (if any) due to either context-specific adaptation or rapid re-adaptation to the 0g and 1.8g environments.

3. The repetitive pitching head movements required during VON may render the test undoable for some subjects due to motion sickness.

Figure 5.3 Subject performing VON in 0g. An older version of the VON hardware, which incorporates a head-mounted display and VON motion-gain dial, is s employed.

5.4 Results

5.4.1 VON quantifies perceived retinal slip

VOR gain and VON motion-gain results from the x0.5 minifying lens adaptation experiment are displayed in Figure 5.4 for all twelve subjects. VOR gain data were collected in complete darkness while subjects imagined a stationary target at 1.5m. VON motion-gain data were collected while viewing the laser VON target in an otherwise dark room. Both VOR gain and VON motion-gain tests were performed without the minifying lenses.

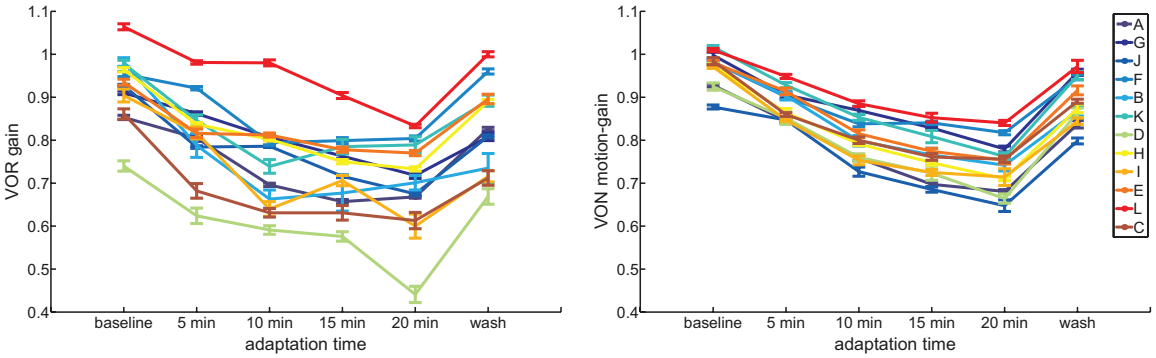

Figure 5.4 VOR gain and VON motion-gain results during adaptation to x0.5 minifying lenses. Baseline data was collected prior to donning of the lenses, probe tests were performed after 5, 10, 15, and 20min of adaptation, and wash data was collected after the 5min washout. Error bars represent 1SE.

When a healthy individual first dons x0.5 minifying lenses, head motion elicits compensatory eye movements equal in amplitude and opposite in direction (i.e., VOR gain values are initially equal to 1.0). Complete adaptation to such lenses means that stationary objects remain on a fixed location on the retina during head motion. To achieve this, eye movements must be adaptively adjusted so that they only move half as much (still in the opposite direction) for a given head movement, (i.e., VOR gain values equal to 0.5). Therefore, as adaptation to the lenses progresses, VOR gain values should decrease from 1.0 toward 0.5. Both the VOR gain data and VON motion-gain data displayed in Figure 5.4 follow this expected adaptation trend. However, two interesting results are readily observed. First, the baseline VOR gain values for most subjects were significantly different from 1.0, even though none of these subjects experience oscillopsia in everyday life. The exact values varied considerably across individuals, with all but one subject's baseline gain being less than 1.0. Baseline VON motion-gain values, on the other hand, were generally much closer to 1.0, although they were low in three subjects (A, J, and D). Second, the VOR gain adaptation curves for some subjects do not follow smooth, monotonic decrements from one probe to the next. In some instances, relatively

little adaptation was achieved (as measured by the difference in consecutive VOR gain values), while in other cases, substantial adaptation was achieved. The VON motion-gain adaptation curves were much more systematic, with regular decrements in motion-gain values as adaptation progressed.

The small baseline VOR gain values and variable VOR gain adaptation traces are likely related to the fact that VOR gain was measured in complete darkness with subjects imagining a stationary target. Measuring VOR gain in the absence of visual stimuli generally results in gain values less than 1.0 (Collewijn et al. 1983; Fetter et al. 1995; Das et al. 2000). This is because other mechanisms, including visual tracking, motor preprogramming, prediction, and mental set (i.e., the chosen imagined percept), interact synergistically to optimize compensatory eye movements in everyday experiences (Barr et al. 1976; Baloh et al. 1984; Weissman et al. 1989; Moller et al. 1990a; Moller et al. 1990b; Demer 1995; Paige et al. 1998; Matta and Enticott 2004). For example, Collewijn and colleagues (1983) measured VOR gain values of 0.92, on average among healthy individuals, during active head movements to remembered targets in the dark. Fetter and colleagues (1995) noted even smaller gains (although their testing was performed passively), and also that inter-subject variability was large. If subjects are distracted, fatigued, daydreaming, or their eyes begin to close, VOR gain values are variable and low (Weissman et al. 1989; Matta and Enticott 2004). All of the VOR gain values measured in our experiment were influenced by the subjects' relative abilities to accurately recall the location of the stationary target during head movements. Many of our subjects commented that knowing "where to look" during the VOR gain tests was difficult. This was especially true of the nine naïve individuals, who had not previously participated in VOR experi-

ments that required visualizing an imaginary target in the dark while moving the head. We attempted to alleviate at least some of this challenge by having subjects practice this task prior to the start of the experiment to help them develop an appropriate strategy.

Several weeks after the adaptation experiment was completed, additional baseline VOR gain testing was performed on subject D, the individual with the lowest baseline VOR gain value (0.74). Because his baseline gain was much lower than that of the other subjects, we wanted to explore how consistent his perception of a remembered target was and how much his VOR gain could be biased by this percept. Baseline VOR gain was measured under four conditions: (1) while imagining a stationary target (exactly as performed during the adaptation experiment), (2) while imagining a stationary target but being simultaneously distracted by mental arithmetic, (3) while imagining a target that moved with the head (VOR cancellation task), and (4) once more while imagining a stationary target (as during the adaptation experiment). His VOR gain values were (1) 0.80, (2) 0.61, (3) 0.48, and (4) 0.78. Hence, these results demonstrated that although subject D's perception of a stationary target in the dark was not truly stationary (VOR gain = 0.74, 0.80, and 0.78), his mental percept of this was relatively consistent across repeated trials, which were separated by multiple weeks or interspersed with additional tests of varying mental percepts. Since his VOR gain values were consistently lower than those of the other subjects, it is reasonable that his VON motion-gain values would also be reduced, which can be seen in Figure 5.4.

The low baseline VOR gain values for subjects A and J are expected, due to the fact that these individuals routinely wear eyeglasses that correct for myopia (nearsightedness). Such corrective spectacles alter the amount of visually-perceived rotation relative

to actual head rotation (Cannon et al. 1985). This is due to a prismatic effect (rotational magnification) of viewing objects through a line of sight not directed through the principal axis of the lens. The magnitude of this effect can be approximated by

$$M = \frac{40}{40 - D}$$

where D is the lens power measured in diopters and M is the magnification power (i.e., the amount of eye rotation that occurs when two targets separated by a given amount are alternately viewed) (Rubin 1974). Eyeglasses that correct for myopia incorporate lenses with negative dioptric powers, and thus magnification powers less than 1.0. So for example, the magnification power associated with a -4D prescription is approximately 0.91, which means that a VOR gain of 0.91 is required for retinal stability during head motion. Subjects A and J wear -4D and -7D prescriptions, which correspond precisely to their baseline VOR gain values of 0.92 and 0.85, respectively. We presume that this is why their baseline VON motion-gain values are also on the lower end of the spectrum.

The other principal result in the VOR gain adaptation data is that some subjects varied in the amount of adaptation from one adaptation block to the next, as measured by the relative differences in consecutive VOR gain probes. In other words, the change in VOR gain from one probe to the next did not follow smooth, monotonic decrements, especially in comparison to the much more consistent VON adaptation data. We can quantify this by fitting exponential functions to the VOR gain and VON motion-gain adaptation data and then comparing the residual sum of squares (RSS). To do this, we performed a linear regression analysis on the logarithm of the raw VOR gain and VON motion-gain data, and then computed the sum of squares of the resulting residuals. The results of this regression analysis and RSS values are displayed in Table 5.1. For eight of

the twelve subjects (A, G, J, D, H, I, E, and L), a linear fit of the logged VOR gain data was acceptable ($r^2 > 0.79$, $p < 0.05$ for these eight subjects). The four subjects whose data were more poorly fit by the linear regression (F, B, K, and C; $0.55 < r^2 < 0.75$, $p > 0.05$) were the individuals who expressed either little-to-no change or an occasional increase in their raw VOR gain values from one probe to the next. On the other hand, the logged VON motion-gain data could be accurately represented by a linear function for all twelve subjects ($r^2 > 0.86$ and $p < 0.05$ for all subjects). The RSS for the fitted VOR gain data ($\mu = 0.012$, $\sigma = 0.011$) was significantly larger than the RSS for the fitted VON motion-gain data ($\bar{x} = 0.003$, $s = 0.002$) (paired t-test, $p < 0.01$, effect size = 0.69). This indicates that the VON motion-gain data followed more systematic changes in gain across consecutive probes, and that these changes could be approximated by an exponential decay.

Table 5.1 Statistics for VOR gain and VON motion-gain adaptation data (r^2: correlation coefficient, p: p-value, RSS: residual sum of squares).

	VOR gain			VON motion-gain		
subject	r^2	p	RSS	r^2	p	RSS
A	0.87	0.021	0.0071	0.96	0.003	0.0025
G	1.00	0.000	0.0000	0.98	0.002	0.0008
J	0.91	0.012	0.0051	0.96	0.004	0.0030
F	0.75	0.058	0.0079	0.86	0.024	0.0032
B	0.65	0.100	0.0370	0.94	0.006	0.0032
K	0.55	0.151	0.0207	0.99	0.001	0.0007
D	0.89	0.016	0.0152	0.99	0.001	0.0008
H	0.91	0.011	0.0040	0.97	0.003	0.0020
I	0.81	0.037	0.0217	0.89	0.017	0.0076
E	0.79	0.044	0.0051	0.95	0.004	0.0024
L	0.94	0.006	0.0019	0.95	0.005	0.0013
C	0.74	0.062	0.0203	0.88	0.018	0.0056

While there are several possible explanations for the larger probe-to-probe variability in the VOR gain data, we believe that the primary reason was, once again, the inability to consistently recall an imagined target across the different VOR gain probe tests, as described above. The three non-naïve subjects (A, H, and J) had each performed multiple VOR adaptation experiments in the past, and they appeared to have less difficulty fixating an imaginary target than the naïve subjects. They had three of the least variable adaptation curves (small RSS values), indicating that they may have been better able to consistently fixate the imagined target. Additionally, there is evidence that the ability to maintain a spatial reference frame becomes harder as adaptation progresses, which is described below in Section 5.5.1. This may have resulted in different perceptions of a fixed imaginary target further along in the adaptation process, which would have led to the more variable responses that are especially prevalent in the later test probes (e.g., after 15 or 20min of adaptation).

Another reason for the varying VOR gain adaptation curves may be fatigue during the adaptation blocks or probe tests (e.g., idly disregarding the moving visual scene without attempting to stabilize the images during adaptation or not actively fixating the imagined target during the probes). However, we believe this effect was likely minimal since all subjects were highly motivated individuals and the investigators were adamant about reminding them to stay alert throughout the experiment. Fatigue or negligence during adaptation is highly unlikely because a similar erratic behavior was not observed in the VON motion-gain. Lastly, since subjects were asked to make active head movements, and thus were in control of their own adaptation stimulus, it is possible that they were exposed to varying amounts of adaptive stimulation during the different adaptation

blocks depending on how much or how fast they moved their head. However, this is not likely to be a large contributor either, as subjects were paced by a metronome, practiced the head movements prior to the start of the experiment, and the investigators continually provided feedback regarding speed and amplitude during the training and adaptation blocks.

In five subjects, the sizes of the error bars for the individual VON motion-gain probes were considerably smaller than the sizes of the error bars for the corresponding VOR gain probes (paired t-test, $p < 0.05$). This was initially surprising, as we had anticipated that perceptual responses might be more variable than simple ocular reflexes. However, in light of the discussion above, this was likely due to the fact that during VON, subjects controlled a visible target. This finding is consistent with other studies, which have demonstrated that the errors bars associated with VOR gain are significantly smaller when an actual fixation target, rather than an imagined one, is present (Baloh et al. 1984; Demer 1992).

The VON motion-gain values were more compensatory than VOR gain values, as evidenced by their values being closer to 1.0 (Figure 5.4). This indicates that subjects likely employed other compensatory strategies (besides retinal slip) to determine when the VON target was stable (e.g., sensory mechanisms, catch-up saccades, etc.). Others have found similar results. For instance, Demer and Amjadi measured retinal slip during dynamic visual acuity testing when healthy individuals were exposed to varying telescopic spectacles (Demer and Amjadi 1993). They showed that the visual system can tolerate up to 2°/s of retinal slip before functional decrements in dynamic visual acuity occur. Grunfeld and colleagues examined adaptation to oscillopsia in bilateral labyrinthine-

defective patients and found that adaptation was related to both the patient's personal attitude regarding the recovery process and the development of an increased tolerance to movement of images on the retina during self-motion (Grunfeld et al. 2000). Thus, the CNS can augment pure motor responses with sensory adjustments to elicit compensatory behaviors and percepts. This synergistic augmentation between sensory and motor components is often referred to as *sensory-motor fusion*. Sensory-motor fusion is a common theme among other oculomotor systems. For example, while binocular positioning alignment is primarily driven by compensatory vergence movements (motor), the sensory component optimizes the alignment (Panum 1858; von Tschermak-Seysenegg 1942; Perlmutter and Kertesz 1978). Finally, it is plausible that subjects recruited other compensatory motor responses, such as catch-up saccades, to aid in VON. Because eye movements were not measured during VON testing, this could not be directly verified, but others have demonstrated that catch-up saccades are employed during adaptation to left-right reversing prisms (Melvill Jones et al. 1988). Furthermore, catch-up saccades are the primary mechanism by which vestibular hypofunction patients maintain fixation on a visual target (Halmagyi et al. 1990; Tian et al. 2000; Weber et al. 2008).

On average, subjects required between five and ten sinusoidal head cycles to complete each VON trial. This is equivalent to approximately 8-15s per trial, as the head movements were paced by a metronome. Although some subjects claimed that performing the nulling task was more difficult later in adaptation, there was no significant difference in the length of time to complete a trial early (after 5min) versus late (after 20min) in adaptation (paired t-test, $p > 0.05$). Further reasoning behind this is discussed in Section 5.5.1. Thus, completing five VON trials during a given probe took less than two

minutes, including short breaks between trials. This can be contrasted with the time to complete one VOR gain probe. It took approximately three minutes to start the recording software, don the goggles and adjust them for comfort, and center the camera on the subject's eye. Eye calibration took one minute. We requested twenty cycles of head movements, with several seconds of stationary data on either side, which equates to approximately thirty seconds of data, as paced by the metronome. Hence, one round of VOR gain testing took approximately five minutes. The intuitive nature of VON and the simplicity of the hardware enabled VON testing to be faster than VOR gain testing.

In the smaller follow-on experiment, we investigated the role of three different visual targets (imagined, flashing, and fixation) on VOR gain before and after 10min of adaptation to the x0.5 minifying lenses. Results from our three subjects are displayed in Table 5.2. The pre-adaptation tests using imaginary targets were fairly consistent with baseline VOR gain results obtained in the main adaptation experiment (Figure 5.4). Pre-adaptation tests using flashing and fixed targets were generally compensatory. After adaptation, VOR gain values were the smallest when subjects imagined a stationary target, as expected from the results of the main adaptation experiment and other studies that compared VOR gain in the dark with and without fixation targets. Post-adaptation VOR gain values to fixed targets were largest, which is also expected, as this stationary reference provided a de-adapting stimulus. The gain values for the flashing target are slightly larger than those associated with an imagined target and much smaller than those associated with a fixed target, and these differences are significant ($p < 0.05$ in both cases). Unfortunately, we cannot definitively state whether the VOR gain values associated with the flashing target provided more or less accurate representations of the adaptation be-

cause there are two possible reasons why these gains might be larger than those observed under the imagined-target condition: (1) the flashing target provided a stable reference frame that improved compensatory eye responses, or (2) the target elicited washout. Because the flashing target was only illuminated for 20ms, it is unlikely that it generated a substantial amount of washout. However, it would have been better if the flashing had been triggered by head motion (e.g., when the head changes direction at zero velocity), as opposed to randomly every 2s, to further reduce the chance of adverse washout. Future experiments that incorporate longer adaptation exposures with multiple VOR gain probes that employ a flashing target would determine whether providing a flashing target enables more systematic VOR gain responses from one probe to the next.

Table 5.2 VOR gain (mean ± SE) measured with different visual stimuli (imagined, flashing, and fixation targets) before and after 10min of adaptation to x0.5 minifying lenses.

test	target	H	I	C
pre	imagined	0.99 ± 0.01	1.01 ± 0.00	0.92 ± 0.01
	flashing	0.99 ± 0.01	1.00 ± 0.01	0.78 ± 0.03
	fixation	0.98 ± 0.00	1.01 ± 0.01	0.98 ± 0.01
post	imagined	0.79 ± 0.01	0.72 ± 0.01	0.82 ± 0.02
	flashing	0.83 ± 0.01	0.76 ± 0.02	0.86 ± 0.02
	fixation	0.94 ± 0.01	0.98 ± 0.03	0.91 ± 0.01

In this smaller experiment, we were also interested in what specific aspect of vestibulo-ocular function is quantified by VON motion-gain, and so we recorded simultaneous eye and head movements once the VON motion-gain was set. The paired differences in VON motion-gain and VOR gain pre- and post-adaptation are plotted for the three subjects in Figure 5.5. In all cases (pre- and post-adaptation) and for all subjects, these differences are close to zero. Since VOR gain is a measure of retinal slip, *VON motion-gain quantifies perceived retinal slip*. The "perceptual" aspect of VON motion-gain encom-

passes the sensory and non-retinal-slip motor (e.g., catch-up saccades) components that, together with retinal slip, generate an individual's perception of gaze stability.

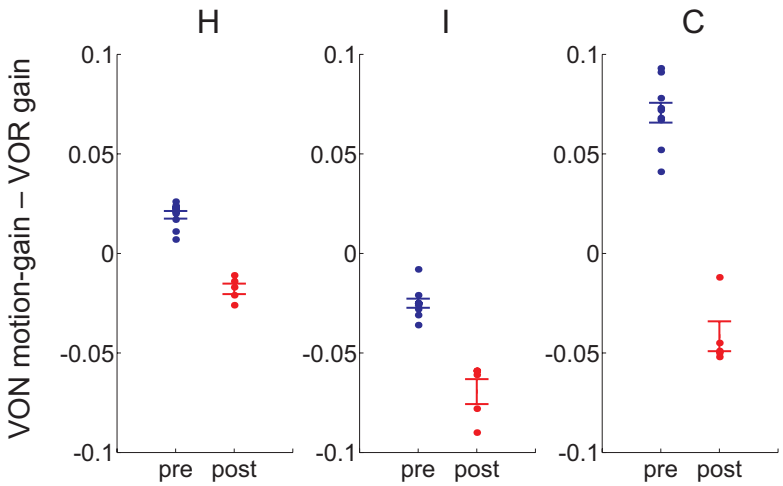

Figure 5.5 Difference in VON motion-gain and VOR gain once subjects set the VON motion-gain. Dots represent paired differences. Error bars are 1SE and centered on the mean of these paired differences.

5.4.2 VON motion-gain is modulated by g-level

VON data were collected in five healthy subjects during the alternating g-levels of parabolic flight (Table 2.1) to evaluate the operational capacity of the VON assessment test and to further explore how the VOR modulates with static otolith signaling. For each subject, pitch-plane VON tests were performed either during parabolas #1-6 (early in-flight) or during parabolas #16-21 (mid-flight). Naïve fliers who had not previously flown in parabolic flight (subjects O, P, and Q) were tested during parabolas #1-6, and experienced fliers (subjects M (1400 parabolas) and R (6400 parabolas)) were tested during parabolas #16-21.

During the dedicated VON parabolas, subjects completed as many VON trials as possible. Synchronized accelerometer data from a reference sensor attached to the floor of the aircraft enabled separation of the individual trials by g-level in the postflight analy-

sis. Within the six-parabola test block, subjects were able to perform 5-10 trials during the 0g phases and 6-13 trials during the 1.8g phases. The primary complaint from all subjects (naïve and experienced) was that the continuous head movements during both the 0g and 1.8g phases of flight were extremely challenging due to the increased propensity for motion sickness. Only subjects O and M did not experience any adverse symptoms during their respective flights, although subject M is a highly experienced flier and had recently flown one week of parabolic flights four months prior to this flight, and subject O took short breaks between each VON trial. Subject R, who had the most parabolic-flight experience of all the subjects but had not flown in two years, experienced nausea at the end of his flight. Subject Q experienced symptoms within his first several parabolas, and was unable to confidently perform a sufficient number of VON trials to be included in the final dataset (although it should be noted that his one 0g and two 1.8g trials did follow a similar trend to the other naïve test subjects). Since the completion of these flights, alternative types of head motion have been considered, which may help mitigate some of the adverse symptoms induced by the continuous sinusoidal movements employed here. These are described further in Section 5.5.2.

In terms of general operational reliability, the hardware and software performed well. However, the hardware was not ideal from the standpoint of portability. The head-mounted display was heavy, especially during the 1.8g pullouts, and the long cables connecting the HMD and motion-gain dial to the laptop were frequently tangled and snagged during the 0g phases of flight. Because the HMD occluded external vision (subjects were essentially blind to the outside world during testing), multiple operators were required to run the VON program from the laptop (mounted to the floor of the aircraft) and monitor

the subjects. Self-administration of the VON test using the HMD would not have been feasible. Future flights will incorporate the VON tablet platform (described in Section 5.3.1), which will be much more amenable to the parabolic-flight environment.

The raw VON motion-gain results are displayed in the left graph of Figure 5.6. One readily observed feature is the large gain values for all subjects in 1g. This is an unfortunate artifact due to the backlight of the LCD screen inside the HMD, which provided a visible rectangular border that moved with the head. Hence, for a healthy individual on Earth, properly adjusting the motion-gain so that the VON target appeared fixed-in-space during head motion necessarily meant that the target must move relative to this visible rectangle. Because this can cause initial confusion, subjects underwent significant preflight training (completing at least fifty training trials) to overcome this distraction. By the end of the training, they had each developed their own consistent strategy for what fixed-in-space meant for them while viewing the target in the HMD. This training took place several days prior to the subjects' respective flights, and so training was briefly refreshed on flight mornings prior to baseline 1g data collection.

Therefore, it is perhaps best to consider the relative relationships between the baseline 1g results and the inflight results, namely the difference between the data observed in 0g and the data observed in 1g, and the difference between the data observed in 1.8g and the data observed in 1g. We can center these differences at a VON motion-gain of 1.0 in 1g for better comparison with the VOR gain results observed by others during spaceflight and during upright versus onside testing on Earth. These results are displayed in the graph on the right of Figure 5.6. If we assume that subjects were able to maintain a consistent strategy for how to "ignore" the visible LCD screen in all g-levels, which is

reasonable given the extensive training and verbal confirmation from the subjects, we can disregard its potential effects by considering relative differences.

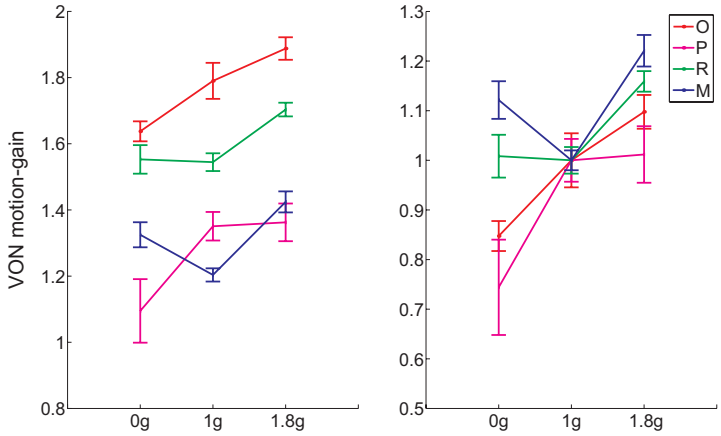

Figure 5.6 Pitch-plane VON motion-gain results from four subjects during parabolic flight. (Left) Raw data. (Right) Relative differences between novel-g and 1g centered at a VON motion-gain of 1.0 in 1g. Error bars are 1SE.

Subjects O, P, and R demonstrated a significant difference in VON motion-gain values between the 0g and 1.8g phases of parabolic flight (paired t-tests, $p < 0.05$ for these subjects). Specifically, VON motion-gain was reduced in hypo-g and elevated in hyper-g, supporting the notion that the pitch VOR is modulated by dynamic otolith input: the lack of otolith signaling in 0g renders smaller gain values, while the increased otolith signaling in 1.8g renders larger gain values. The 0g and 1.8g data from subject M follow this general trend, although the difference was not statistically significant ($p = 0.12$).

The gain differences for subjects O, P, and R are relatively consistent with the gain differences measured by others during spaceflight missions. For example, Viéville and colleagues (1986) noted a significant decrease in pitch VOR gain, on the order of 20% relative to preflight values, on the first day of flight (FD1). Berthoz and colleagues (1986) observed VOR gain to be increased by 10-30% the day after landing (R+1), relative to two, four, and six days after landing (R+2,4,6). Our subjects expressed larger gain

differences than what has been observed on Earth during upright versus onside pitch (Barmack 1981; Tomko et al. 1988; Clément et al. 1999a; Brettler et al. 2000), but this may be expected since the prevalent 1g force on Earth may serve as a context cue to the CNS to not expect an otolith-modulation during onside pitch (Shelhamer and Zee 2003).

Previous studies have indicated that past parabolic-flight experience may enable rapid re-adaptation of sensorimotor reflexes due to savings or context-specific adaptation (Lackner and Graybiel 1982; Shelhamer et al. 2002). Two of our subjects (M and R) had flown many parabolas prior to these flights, which may be reflected in the fact that they demonstrated the two smallest differences in pitch VON motion-gain out of our four subjects. The smallest difference came from subject M, who had most recently flown four months prior to this flight.

In summary, the results from this parabolic-flight experiment were promising for VON as a potential assessment of vestibulo-ocular function in an operational setting. Data was only collected in four individuals, and so the g-level dependences observed thus far should be considered cautiously. However, improvements in the VON hardware and potential changes in the nature of the head movements to make the test less provocative will provide a suitable platform for future flight experiments.

5.5 Discussion

Precise visual fixation requires that the gain of VOR must be set such that retinal slip is minimal. However, while a normally functioning VOR is necessary, it is not sufficient for optimum gaze-stability during head movement (Demer 1995). The Vestibulo-Ocular Nulling task provides a reliable measure of perceived retinal slip without record-

ing eye movements. By quantifying the perceptual deficiency in the VOR, we are able to define a 'real-world' performance metric that may have more functional utility than VOR gain alone.

The overarching objective of the experiments in this chapter was to explore the ability of our Vestibulo-Ocular Nulling technique to accurately portray vestibulo-ocular function quickly and with minimal equipment. The newest VON apparatus employs a hand-held tablet computer and small wireless motion sensors, and formal parabolic-flight experiments with this technology are planned. However, the earlier versions of VON, which incorporated a back-projected laser and head-mounted display, were sufficient for validating the VON concept and provided valuable information regarding vestibulo-ocular function during short-term adaptation to a visual-vestibular disruption and during exposure to novel gravity environments. In practice, VON has been primarily implemented using active, angular head movements (pitch and yaw), primarily because of their relevance to spaceflight research. However, this test could also be employed passively or with linear head motion. Furthermore, larger visual scenes could be employed, especially in a laboratory environment, to evaluate the vestibulo-ocular system in the presence of more realistic visual stimuli, and also to make the test amenable for evaluation of the roll VOR.

5.5.1 VON provides a reliable means for quantifying visual-vestibular adaptation

The goal of the lens-adaptation experiment was to compare the difference in a pure motor response, namely VOR gain, to our new perceptual VON motion-gain. The primary outcome was that VON motion-gain was closer to 1.0 than VOR gain, which was

likely a result of the ability to employ sensory compensation to augment the VOR gain. Furthermore, VON motion-gain was highly consistent, both within a given subject during multiple test probes and across subjects. Our VOR gain results showed less systematic behaviors than VON motion-gain results due to the challenges of testing the VOR in the dark with an imaginary target; however, our VOR gain results were nonetheless highly consistent with what others have shown (Gonshor and Melvill Jones 1976; Miles and Eighmy 1980; Cannon et al. 1985).

It is important to recognize that although the VON target is visible during VON testing, performing VON is not, in and of itself, a de-adapting stimulus during an adaptation experiment because the subject controls how the target moves relative to the head motion. For example, suppose a test subject is presented with a VON target whose motion-gain is initially set to 1.0, but this individual has already been down-adapted to a VOR gain of 0.8. As soon as this subject initiates a head movement, he will realize that the target appears to move, and would therefore begin to adjust the VON motion-gain (down to approximately 0.8). Thus, as long as subjects perform the VON test correctly (i.e., they do not execute repeated head-movements under a VON motion-gain setting in which they clearly perceive the target to be moving during head motion), VON does not washout adaptation. This is an important advantage of VON over other assessment techniques, such as VOR gain measures while viewing a stationary target or DVA testing.

Vestibulo-ocular function incorporates both sensory and motor components. The motor component can be quantified by measuring VOR gain (simultaneous recordings of eye and head movements). The sensory component can be quantified by performing VON and subtracting the resulting motion-gain from VOR gain. However, it is likely

that there is a range of sensory inputs that facilitate adequate gaze stability. This is analogous to Panum's fusional area for binocular alignment, as discussed in Chapter 3. We observed this during the main adaptation experiment when subjects reported during some of their VON probes that there existed a small range of motion-gain values in which they could perceive the target to be fixed-in-space during head motion. To quantify this vestibulo-ocular sensory fusion range explicitly, we could perform an experiment similar to the *always above* and *always below* VAN and TAN tests in Chapter 3. Initial VON motion-gains could be programmed to be *always too large* or *always too small*, and subjects would be tasked with incrementally changing the motion-gain in one direction only (i.e., down for the *always too large* test and up for the *always too small* test) until they just perceive the VON target to be fixed-in-space during head motion. Furthermore, these additional probes could be completed during an adaption experiment to examine whether this sensory range changes during adaptation.

Another interesting anecdotal report from several subjects was that executing the VON tests became more difficult as adaptation progressed. One subject (J) described it as follows: "I would reach a point [during the later VON probes] in which the VON motion-gain setting was as good as I could get it. I perceived that the target was still moving slightly when I moved my head, but I couldn't get rid of this motion by adjusting the motion-gain dial. If I turned the [motion-gain] dial up slightly, the target appeared to move more, but if I turned the dial down, the target immediately started moving in the other direction. Often, I would see the direction of the target movement reverse as I got closer to the point where my head changed directions. It was the strangest thing. As soon as I washed out, this effect was gone." Several subjects described similar experiences. Alt-

hough the nulling task was apparently more difficult later in adaptation, it is interesting that this did not manifest in a systematic increase in the amount of time (or number of head movements) required to complete the VON trails. However, this is probably because subjects recognized quickly that this effect did not "go away" with additional head movements or fine-tuning of the motion-gain, and so it is likely that subjects simply performed the test as best as they could, and moved on to the next trial. This effect may be visible in the VON error bars, as a systematic increase in the mean of the standard error was observed across all subjects. At baseline, $\mu_{SE} = 0.0051 \pm 0.0019$, after 5min of adaptation, $\mu_{SE} = 0.0071 \pm 0.0030$, and after 20min of adaptation, $\mu_{SE} = 0.0091 \pm 0.0046$. However, these differences were only significant when comparing the size of the error bars at baseline and after 5min or at baseline and after 20min (F-test, $p < 0.05$). This effect may also be mirrored in the VOR gain data, as some subjects demonstrated less consistent gain changes during the later test probes (e.g., after 15 or 20min of adaptation).

An interesting, and likely related, result was observed when we attempted to perform a different experiment in which VON was tested while wearing various telescopic spectacles (x0.5, x2) in the un-adapted state. The goal of this experiment was to simply validate the VON concept by demonstrating that VON motion-gains change in a predictable manner when various telescopic lenses are worn. However, as soon as VON was attempted while wearing a pair of lenses (of any magnification power), the nulling task was simply not feasible. In fact, four different test subjects reported more exaggerated versions of subject J's comments above. While it was possible to reduce the apparent motion of the VON target by adjusting the motion-gain, the motion could never be eliminated. It would be interesting to examine whether the nulling task becomes easier once

subjects become more adapted to the lenses. This would be a nice alternative finding to what was observed above: as subjects became more adapted to the lenses, and were tested without the lenses on, VON became more difficult.

Our current hypothesis regarding why VON became more difficult during the later test probes is that subjects may have experienced a loss in spatial referencing during adaptation. In VON, subjects are asked to null apparent visual motion. However, as adaptation progresses, what they perceive as "stationary" is actually moving. Furthermore, none of the subjects achieved complete adaptation during the four adaptation blocks, and so gaze stability was disrupted throughout the duration of the experiment. Hence, it is not unlikely that during the adaptation process, the ability to accurately localize a target's position or velocity, especially in the absence of other sensory cues, is lost. A similar effect is seen in astronauts following spaceflight. As vestibular processes are re-adapting to Earth's gravity, crewmembers' perceptions of self-motion in the absence of visual cues is grossly exaggerated and tilted relative to preflight perceptions (Clément et al. 1995). We can test this hypothesis by employing an additional perceptual test that specifically examines the ability to maintain an accurate spatial reference frame during adaptation, such as a saccade-to-remembered-targets test or a point-to-remembered-targets test.

5.5.2 Parabolic-flight experiments mandate VON portability and provide evidence for otolith-modulation of the pitch VOR

The parabolic-flight experiments were valuable for confirming the need for portable VON hardware. The bulky head-mounted display and long connecting cables were cumbersome in the parabolic-flight environment. The current tablet-based platform will provide a much simpler apparatus that will also facilitate self-assessment, without the

heavy reliance on operators or other trained personnel. Furthermore, incorporating AMOLED technology will eliminate extraneous visual cues that make the test more challenging to complete and confound the numerical results.

Nonetheless, the parabolic-flight results obtained with the head-mounted display demonstrated that pitch VON is modulated by dynamic otolith input in at least some individuals. Future testing with a larger sample size, improved hardware, and a separation of upward versus downward head movements will enable us to better characterize the extent, or possibly lack-thereof, of this otolith-modulation. Our nulling task incorporates a perceptual component, which allows us to quantify an additional aspect of gaze stability that is not normally captured in traditional VOR gain measures alone. This is important because dynamic visual acuity, a functional correlate of the VOR, has been shown to be reduced postflight (Peters et al. 2011). Hence, the ability to quickly quantify changes in the vestibulo-ocular system with simple, portable technology may facilitate preflight or inflight countermeasure development to mitigate such decrements in gaze stability.

While the results obtained with the head-mounted display were not ideal due to the moving visible background, they are consistent with a previous VON experiment performed in the laboratory, which was subject to a similar artifact. The VON hardware employed in this experiment was the first VON platform, and it incorporated an LCD laptop computer to display the VON target. Thus, learning to "ignore" the laptop screen's backlight during VON required significant pre-experiment training. With this platform, we performed a small pilot experiment in which four subjects executed pitch-plane VON while wearing 1.5, 2, 3.25, 4, and 6D spectacles. Two test blocks were completed for each pair of spectacles: one in which the initial VON motion-gains were *always too*

large, and one in which the initial motion-gains were *always too small*; these thresholds were based on the VON motion-gain values necessary to null the target motion for the current lens optics. During the *always too large* tests, subjects were only allowed to lower the motion-gain, while during the *always too small* tests, subjects were only allowed to increase the motion-gain. The results from this experiment, averaged over the four subjects, are displayed in Figure 5.7.

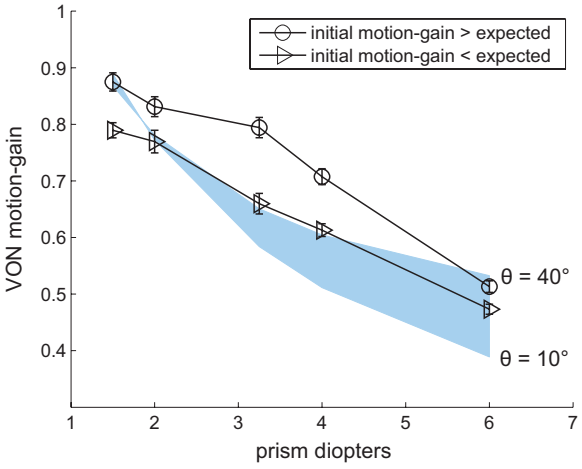

Figure 5.7 Pitch-plane VON results averaged over four subjects wearing various prisms. Initial motion-gain values were such that subjects only adjusted in one direction (up or down). Differences in results between these two tests represent the amount of perceptual fusion. Blue shading represents expected motion-gain values based on lens optics and amplitude (θ) of head movement.

The blue-shaded region represents the expected VON motion-gain values based on the lens optics and head-movement amplitude (head velocity and excursion were not strictly controlled in this experiment). The vertical gap between the *always too large* and *always too small* results represents the range of perceptual fusion. These results show a general trend that follows the expected trajectory based on the lens optics, although there is an apparent offset in the results from the theoretical motion-gain values most likely due to the strategy employed by the subjects to ignore the visual background. However, relative differences can be considered, as was done with our parabolic-flight results. Together, this pilot study and the parabolic-flight results demonstrate that even in the presence

of extraneous visual cues, naïve subjects can successfully perform VON, with sufficient training.

One of the main outcomes from the parabolic-flight experiment was the realization of how challenging it is for a given individual to make continuous pitching head movements in novel gravity environments. Although the uncomfortable nature of such motions is described in the literature, it was unknown precisely how much and at what speed these head movements would be tolerable for individuals who do not routinely experience motion sickness on Earth. In general, symptoms were minimized when subjects took frequent breaks, especially at the immediate onset of symptoms, even if it was in the middle of a trial. For example, subject O made 2-3 cycles of head movements and then paused for several seconds before performing another 2-3 cycles; he was our only naïve test subject who did not experience nausea later in flight.

Because of this, we have considered alternative ways to perform VON that would be less provocative in future flights. One viable option may be to work in the position domain instead of the velocity domain. In a position-based VON test, the subject would make a single rapid head movement in one direction and then adjust the motion-gain based on whether the VON target appeared to "jump" in the same direction as the head or in the opposite direction. Hence, instead of making continuous, sinusoidal head movements with continual adjustments to the VON motion-gain, subjects would perform single head movements with breaks in between to adjust the motion-gain. Providing subjects with the time to think about which way the target moves relative to the head may result in less trial-and-error, and therefore fewer head movements for a given trial. This technique can be considered a more objective, quantifiable version of the one employed

by Watt and colleagues (1985) during spaceflight, and we plan to test this procedure in upcoming flights using the tablet-based VON platform.

Chapter 6

Strength of baseline inter-trial correlations forecast adaptive capacity in the VOR

6.1 Introduction

6.1.1 Overview

Meaningful interactions with the environment require complex integration of sensory inputs coupled with highly coordinated motor outputs. The inherent plasticity in the sensorimotor system provides a remarkably adaptable motor-control system that facilitates compensation for movement errors that arise from both internal (e.g., pathological) and external (e.g., environmental) perturbations. The body readily modifies behavior in response to extreme challenges, such as vestibular lesions or the changing gravity levels associated with spaceflight, as well as sporadic demands that occur during everyday life, such as donning a new pair of reading glasses or fatigue during exercise. Furthermore, even an accurate, highly-functioning sensorimotor system continues to actively fine-tune motor responses to better optimize performance (Whitacre and Bender 2010). Hence, the adaptive capabilities of the sensorimotor system enable superior performance under a wide variety of circumstances.

While healthy persons generally show favorable adaptation following the miscalibration of a sensorimotor process, individual differences exist: some people adapt faster

or more fully than others. Vestibular patients recovering from unilateral labrynthectomies require varying amounts of rehabilitation therapy, and some take longer to recover than others (Norre and Beckers 1989; Cass et al. 1996). Astronauts enduring the same flight-motion profiles respond differently to changes in g-level (Wood et al. 2011). One of the biggest challenges of space motion sickness is the large variability in symptoms, and corresponding functional decrements, from one crewmember to the next (Davis et al. 1988; Locke 2003). This renders preflight-adaptation training and countermeasure development difficult. From an operational perspective, it would be highly advantageous to know ahead of time which crewmembers may have more difficulty adjusting to novel g-levels. Currently, the best predictor of adaptive performance during spaceflight is previous flight experience (Davis et al. 1988; Clément and Reschke 2008b; Wood et al. 2011). In other words, what astronauts experience during their first mission is likely what they will experience on subsequent missions. (Although in terms of motion sickness susceptibility, this is not strictly the case: some astronauts improve slightly on their second flight, while others actually fare worse (Davis et al. 1988)). However, many crewmembers fly only once, and with the advent of longer-duration missions beyond low-Earth orbit, this will most certainly be the case. Hence, it would be beneficial to be able to forecast adaptation ability in first-time astronauts without having to expose them to the 0g environment first. This type of knowledge could guide individualized pre-flight training or in-flight countermeasures, as well as assignment of specific roles on the crew. Therefore, the primary objective of this chapter is to look for baseline performance metrics that correlate with adaptive capabilities.

6.1.2 Inherent variability may predict performance

Variability is an inherent feature of all biological systems, and can be described as normal fluctuations in motor performance across multiple repetitions of a given task (Stergiou et al. 2006). Traditionally, this "noise" has been deemed a random process, of little functional use (Glass and Mackey 1988). However, recent investigations across a variety of different physiological systems suggest that this variability may represent a deliberate, actively-regulated process that can facilitate both flexibility and adaptability (Conrad 1986; West 2013).

Two studies to-date have demonstrated that variability in baseline performance is strongly correlated with motor adaptation (Wong and Shelhamer 2014; Wu et al. 2014). Although the definitions of variability described by these authors represent significantly different system properties, as described below, the idea that a parameter that has been traditionally dismissed as "inconvenient" or even "erroneous" might forecast adaptive performance is both intriguing and unexpected.

The study by Wu and colleagues (2014) examined adaptation of arm-movement trajectories during a reaching task by means of reward-based learning. In this experiment, subjects performed repeated reaching movements between two targets with (during training) and without (at baseline) error feedback (reward). Their performance metric was quantified by deviations between the ideal trajectory and the actual one. The primary finding was that individuals who expressed larger variability, defined by the standard deviation in the performance metric during the baseline trials, exhibited higher learning rates during the training period. This suggests that general motor variability during arm-reaching movements may be predictive of motor adaptation in this system. One way to

reconcile this potentially surprising finding is to consider variability as an exploratory process, by which new motor patterns can be tested. Motor programs that generate both stable (persistent) and flexible (variable) behavioral outputs allow the system to maintain a sufficient level of performance while simultaneously searching for better options to prevent the system from becoming "stuck" in local minima (Smith et al. 2002; Davids et al. 2003).

6.1.3 Baseline inter-trial correlations forecast adaptation in the saccadic system

Recent work in our laboratory has demonstrated that baseline *inter-trial correlations* provide information that may be predictive of adaptive capabilities. By inter-trial correlations, we mean correlations in the trial-to-trial fluctuations that transpire as a consequence of correcting for previous performance errors over multiple time scales. The *strength* of inter-trial correlations effectively describes how much of the past influences the present. These variations in performance from one trial to the next are distinct from the gross system variability described in the Wu et al. (2014) study, which instead describes the *net* variability about a central mean; inter-trial correlations explicitly describe the temporal ordering of the individual trials within the time series.

In the study by Wong and Shelhamer (2014), it was discovered that the strength of inter-trial correlations of successive saccade amplitudes performed during a baseline predictive-saccade task correlate strongly with rate of learning in a saccade-adaptation task. In the predictive-saccade task, healthy subjects made alternating saccades between two fixed targets that were horizontally separated by 10°, which promoted anticipation ("prediction") of the subsequent target's location and timing before it was visually ac-

quired. Subjects performed 300 of these predictive-saccades at baseline (prior to adaptation), and the temporal fluctuations associated with these time series were quantified by various techniques developed for the analysis of fractal scaling. One parameter used to describe the strength of inter-trial correlations was β, defined as the negative slope of the power spectrum of the sequence of predictive-saccade amplitudes when plotted on log-log axes. The details of β are described further in Section 6.2.2, but, briefly, β describes the rate of decay of inter-trial correlations. Larger β values represent stronger inter-trial correlations across longer timescales ("long-term correlations"), while smaller β values resemble weaker inter-trial correlations. A value of zero represents uncorrelated trials, or white noise. Following the predictive-saccade task, saccade amplitude gain was adapted over 300 trials using the conventional double-step paradigm. In this paradigm, saccades are made between two alternating targets, but while the saccades are in process, the target is surreptitiously "jumped" to a new position, thereby inducing error-correction mechanisms by which the gain-state is modified. The rate of adaptation was quantified by the slope of a linear regression fit through the adaptation trials.

The primary conclusion from this experiment was that subjects who exhibited stronger long-term correlations in their baseline predictive-saccade task were the fastest adapters; those who exhibited weaker long-term correlations adapted slower (Figure 6.1). Long-term correlations reflect low frequency activity, which implies a relationship among trials that persists over long timescales (i.e., a long-memory process). Hence, these results indicate that subjects who made more use of prior error information (from previous saccades) to generate their next saccade were better able to quickly adapt saccade-amplitude gain.

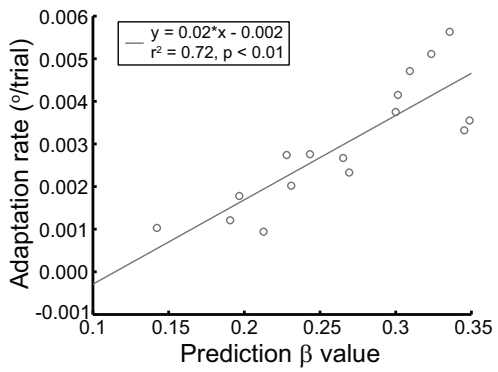

Figure 6.1 Correlation between rate of saccade adaptation and β derived from baseline predictive-saccades. From Figure 3 of *Wong, AL and Shelhamer, M (2014). Similarities in error processing establish a link between saccade prediction at baseline and adaptation performance. J Neurophysiol [Epub ahead of print]*.

This finding is highly significant, as it is one of the first experiments to successfully correlate baseline performance with adaptive capabilities in a sensorimotor system. The existence of such a relationship, especially if it can be demonstrated in other motor processes, has important ramifications for the both the clinical and the spaceflight communities. For example, the observed results in the saccadic system may be useful in the design of individualized rehabilitation protocols for patients with oculomotor disorders.

6.2 Objectives

The primary objective of the following experiment was to consider inter-trial correlations in baseline VOR gain data to determine whether they could forecast adaptation in the vestibulo-ocular system. Based on the results in the saccadic system, we hypothesized that the strength of inter-trial correlations, namely, the use of prior performance information to modulate current and future behavior, would correlate with adaptive capacity in the VOR.

6.3 Materials and methods

6.3.1 Experimental procedures

In this experiment, twelve healthy subjects performed a series of 420 baseline head-impulses followed by 20min of VOR gain adaptation while wearing x0.5 minifying lenses (Table 2.1). The details of the adaptation are described in full in Chapters 2.5.1 and 5.3.2. *Adaptation extent* was defined as the difference between the baseline and 20min VOR gain probes, which we will now refer to as the pre-adaptation and post-adaptation VOR gain tests, respectively, to avoid confusion between the baseline VOR gain probe from Chapter 5 and the baseline head-impulse VOR gain block in this chapter.

Prior to these 20min of adaptation, subjects performed 7min of active, yaw-plane, head-impulses, paced with a metronome at 60bpm (one head-impulse per second, 420 total head-impulses), while viewing a stationary laser target projected 1.5m away in an otherwise dark room. During these head-impulses, subjects moved their heads rapidly across the midline through an angle of approximately 30° (approximately 300°/s peak velocity and 5000°/s^2 peak acceleration, on average). The goal of these head-impulses was to provide a large baseline dataset from which fundamental properties of the vestibulo-ocular system could be examined for comparison with the adaptation data. One baseline VOR gain value was calculated for each head-impulse, as described in Chapter 2.5.2, thereby rendering 420 baseline head-impulse VOR gain values for each subject. Two subjects (C and L) were eliminated from this experiment due to excessive blinking during the baseline head-impulse test (see Section 6.3.2).

6.3.2 Quantifying inter-trial correlations

Spectral analysis was employed to examine the baseline head-impulse VOR gain data, and inter-trial correlations were the primary parameter of interest. These trial-to-trial fluctuations can be quantified by examining the auto-correlation function (ACF, typically denoted as $R_{xx}(\tau)$). The ACF describes the linear cross-correlation between the signal and a time-shifted version of itself. For a stationary process X_t (a signal whose mean μ and variance σ^2 are time-independent), the ACF is defined mathematically as

$$R_{xx}(\tau) = \frac{\mathrm{E}[(X_t - \mu)(X_{t+\tau} - \mu)]}{\sigma^2}$$

where E is the expected value operator and τ is the time lag. For well-behaved processes (e.g., those in which the ACF can be defined), $-1 < R_{xx}(\tau) < 1$, with 1 indicating perfect correlation and −1 indicating perfect anti-correlation. Subtracting the mean and dividing by the variance normalizes the ACF such that $R_{xx}(\tau = 0) = 1$ (a signal is perfectly correlated with an exact (non-time-shifted) version of itself).

The decay of the ACF provides meaningful information regarding the strength of inter-trial correlations, namely, how rapidly information from past trials is "forgotten." For a completely uncorrelated white noise process, $R_{xx}(\tau = 0) = 1$ and $R_{xx}(\tau \neq 0) = 0$, meaning that there is no correlation among any trials, as expected from a process without memory (Figure 6.2 Upper-left). Thus, a no-memory process has no inter-trial correlations. On the other hand, for integrated white noise, where each subsequent trial can be thought of as the sum of all previous trials, $R_{xx}(\tau) = 1$ for all τ, as the process has infinite memory (Figure 6.2 Upper-right). An infinite-memory process has infinite inter-trial correlations. Between a no-memory process and an infinite-memory process is a continuum of different memory processes. Informally, we can consider processes as "longer-

memory" when their ACF decay more gradually, which is indicative of longer-term correlations, and "shorter-memory" when their ACF decay more rapidly, which is indicative of shorter-term correlations[4] (Figure 6.2 Upper-middle).

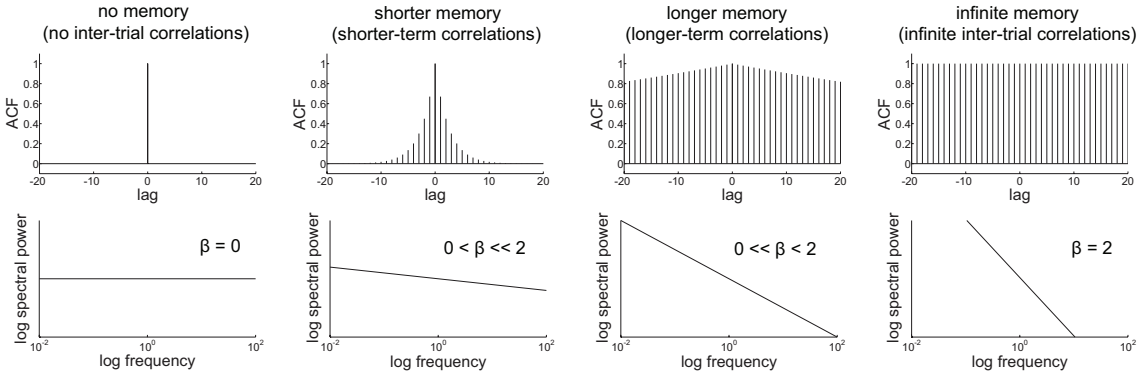

Figure 6.2 Autocorrelation functions (ACF), power spectra, and β values for various processes.

Longer-term correlations reflect low-frequency activity, which is more easily measured in the frequency domain. Therefore, we use the power spectrum to describe these inter-trial correlations. The power spectrum (or power spectral density PSD, typically denoted as $S_{xx}(f)$) is the frequency domain equivalent of the ACF, and it represents how much power is accounted for by each frequency bin in the time series. The power spectrum is computed by taking the Fourier transform of the ACF. Both the ACF and power spectrum provide useful information about periodicities (repeated patterns) within the time signal: how trials are temporally correlated, indicated by the magnitude of the ACF at various lags, suggest dominant frequencies in the power spectrum. The decay of

[4] In the mathematical community, the phase "long-term correlations" is indicative of a *fractal process*, namely, a process whose ACF decays as a power law. Based on the results of several fractal-analysis techniques, our VOR-gain data do not appear to be fractal in structure. Therefore, we use the phrase "longer-term correlations" to denote those VOR datasets that exhibit relatively larger proportions of lower-frequency activity. Similarly, we use the phrase "shorter-term correlations" in reference to time series that exhibit relatively smaller proportions of lower-frequency activity. In contrast, the baseline predictive-saccade data observed by Wong and Shelhamer (2014) are likely fractal, and hence we use the term "long-term correlations" in describing these data.

the ACF is related to the decay in the power spectrum. Longer-memory processes (i.e., those that exhibit stronger longer-term correlations) have ACFs that decay gradually and power spectrums that contain a larger ratio of low frequency, relative to high frequency, information. In contrast, shorter-memory processes (i.e., those that exhibit weaker longer-term correlations) have ACFs that decay faster and power spectrums that contain a larger ratio of high frequency, relative to low frequency, information.

The decay of the power spectrum yields a straight line on a log-log frequency plot. We quantify this line by the parameter β, where β is defined as the negative slope of the power spectrum when plotted on log-log axes. Hence, β is a measure of the strength of inter-trial correlations. Larger (positive) β values represent more relative power in the lower-frequency portion of the power spectrum, and are thus indicative of longer inter-trial correlations (Figure 6.2 Lower-right). Smaller (positive) β values represent more relative power in the higher-frequency portion of the power spectrum, and are thus indicative of shorter inter-trial correlations (Figure 6.2 Lower-left)[5]. A β value equal to zero represents no inter-trial correlations (uncorrelated white noise).

There are several important mathematical properties that a time signal must have so that the results obtained from spectral analyses are statistically reliable. The first is stationarity. This means, informally, that the statistics of the underlying distribution (in particular, the mean and variance) do not change over time. Although a rigorous mathematical test of stationarity was not performed, it is reasonably assumed. Subjects continually viewed a fixed target during the head-impulses, thereby centering the mean of the

[5] Negative β values are still indicative of shorter-term inter-trial correlations. They represent more relative power in the high-frequency portion of the power spectrum in comparison to a white-noise process, and are hence indicative of time series that tend to fluctuate about the mean more often than chance. This implies that inter-trial correlations will be negative (anti-correlated) for small lags in the ACF.

VOR gain around 1.0, and the total time of the baseline test was limited to seven minutes to minimize unfavorable effects such as fatigue or boredom, which may have otherwise resulted in shifts in the mean or larger variances during the later portion of the test.

Additionally, the discrete time series cannot contain "breaks," meaning that individual data points cannot be eliminated from within the time signal. Doing so would disrupt the temporal correlations. Therefore, all baseline head-impulse gain data were included, with the exception of blinks that occurred at the time of peak head velocity (when the VOR gain was measured) because no reliable eye-movement information was available. Importantly, this requires the inclusion of those trials that may appear to be outliers. To minimize blinks during peak head velocities, subjects were instructed to blink, when necessary, at the end of a head movement during the momentary "pauses" between the head-impulses. However, for some individuals, blinking during a fast head rotation can be a reflexive response that is difficult to suppress, and this was the case for two of the subjects (C and L). Because the number of blinks during peak head rotation exceeded 11% of their total trials, which was also considerably larger than the proportion of blinks for the other ten subjects, these individuals were eliminated from the subject pool. The remaining ten subjects blinked in less than 3.6% of the total number of trials. Of these ten subjects, the largest number of blinks was 15. So for our ten subjects, we removed only the trials containing blinks, and then truncated the baseline head-impulse gain datasets at a total of 405 trials.

The final mathematical requirement is that the underlying distribution must be reasonably well behaved. This means that the statistical moments, namely skewness (asymmetry about the mean) and kurtosis ("peakedness" (width-of-peak) about the

mean), must be reasonably bounded. Large skew asymmetries or excess kurtosis can occur when outliers are present in the time series, which was the case for all ten of our subjects. Therefore, data containing such outliers must be mathematically transformed so that this statistical challenge, namely the effect of these outliers, is eliminated prior to Fourier analysis. However, simply removing the outliers is not an appropriate solution, as this destroys temporal correlations. Our method for resolving this is described below in Section 6.4.2, and involves replacing the baseline head-impulse gain data with an appropriate *surrogate* dataset.

A surrogate dataset is simply a dataset that embodies some hypothesis about the data that it is representing but randomizes other properties. Surrogates are typically computer-generated, and so many surrogate datasets can be produced from a single hypothesis, which enables empirical statistical bounds (i.e., error bars) to be placed on that hypothesis. Throughout this chapter, several surrogate data-analysis methods are employed to (1) replace outliers in the baseline head-impulse VOR gain data, and (2) to test the probability that the observed β values did not arise by chance.

6.4 Results

6.4.1 VOR gain adaptation varied across subjects

The mean pre- and post-adaptation VOR gain values for each subject are displayed in Figure 6.3. VOR gain adaptation extent was defined as the difference between these two values. All subjects demonstrated significant adaptation following the 20min

adaptation period (mean gain adaptation extent ± s.d., 0.225 ± 0.057), but the precise amount was variable across subjects.

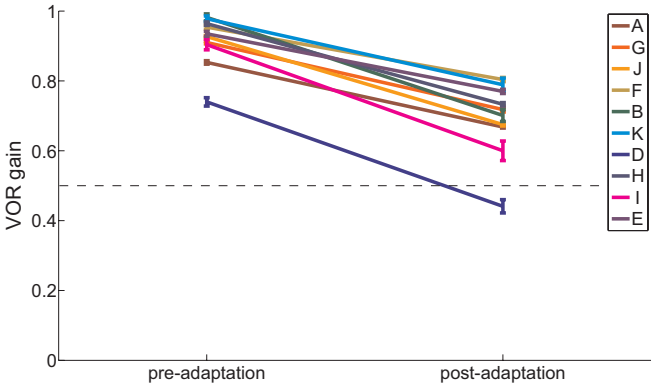

Figure 6.3 Pre- and post-VOR gain adaptation results.

6.4.2 Baseline VOR gain data were subject to outliers

All subjects demonstrated baseline head-impulse VOR gain values whose means were approximately equal to 1.0, but variable from trial to trial. The baseline gain data from one representative subject is displayed in the left graph of Figure 6.4. From this graph, it is readily observed that some of the head-impulses resulted in VOR gain values that were considerably different from 1.0 (i.e., outliers) (Figure 6.4 Center). This was seen in all subject's baseline head-impulse data, and is consistent with the literature surrounding the nature of VOR head-impulses in healthy individuals (Black et al. 2005; Jorns-Haderli et al. 2007). However, the presence of such outliers resulted in excess kurtosis, and sometimes skew-asymmetries, in the underlying distributions, which are not amenable to spectral analysis. To deal with this statistical complication, each subject's raw baseline VOR gain data was replaced with rank-ordered Gaussian random variables (GRVs). This transformation yielded a surrogate dataset that was appropriate for Fourier analysis. These rank-ordered GRV surrogates were created in the following manner: 405 Gaussian random variables were computer-generated and then rank-ordered based on the

amplitude rank-order of the raw head-impulse gain data (Figure 6.4 Right). This process was repeated 100 times to generate 100 rank-ordered GRV surrogate datasets per subject. Note that while the outliers have been, effectively, "reigned in" through this transformation, their outlier "status" has not been changed. In other words, the trials that were farthest from the mean in the raw VOR gain data (i.e., the outliers) are the same trials that are farthest from the mean in the surrogate data. This is demonstrated by the arrows in the center and left graphs in Figure 6.4.

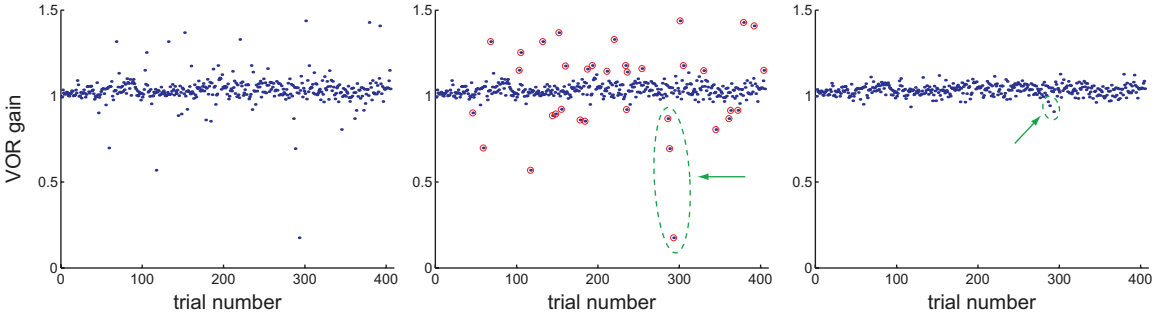

Figure 6.4 Baseline head-impulse VOR gain data from one representative subject. (Left) Raw VOR gain data. (Center) Outliers circled. (Right) Sample rank-ordered GRV surrogate dataset. Green arrows demonstrate how the position of outliers in the raw data (center) is preserved in the surrogate data (right).

For the purpose of subsequent analyses, the baseline gain values that were designated as outliers were determined by those data points that precipitated excess kurtosis in the underlying distribution. These data points were selected as follows. The mean and kurtosis of the raw gain values were computed. For all subjects, the kurtosis was larger than 3.0, due to the presence of the outliers. The value of 3.0 is the kurtosis observed in a normal distribution, which was our criterion for designating outliers. The gain data were then sorted based on their distance from the mean, and the data point farthest from the mean was removed. The mean and kurtosis were recomputed, and the kurtosis was checked against the value of 3.0. If the kurtosis was larger than 3.0, the next farthest data

point from the mean was removed. This process was repeated until enough outliers were eliminated, one at a time, to render the kurtosis just less than 3.0. As a final verification, the skewness was computed. For all subjects, once the outliers were removed, the skewness of the remaining data was bounded between -0.2 and +0.2, indicating that the underlying distribution was approximately symmetric. Thus, those data points that were removed during this kurtosis-trimming procedure were the data points designated as outliers. For our ten subjects, the baseline gain data contained 8-40 outliers (2-10% of the total number of baseline trials).

These outliers were the data points whose amplitudes differed the most between the rank-ordered GRV surrogates and the original data, as the rank-ordered GRV transformation effectively "reigns them in" (Figure 6.4 Right). So in this regard, our mathematical transformation of the raw data had the largest effect on the outliers. To verify that the rank-ordered GRV surrogates were still an accurate representation of each subject's trial-to-trial performance, which is required for our β values to be credible, the trials on either side of the outliers were further examined.

There are two general theories regarding the nature of outliers. The most common perception is that outliers are simply noise, namely, that they are extraneous events that occur sporadically with no specific purpose. On the one hand, others have posited that outliers are intentional, exploratory processes whose existence is used to modify subsequent behavior (Conrad 1986; Stergiou and Decker 2011). If the outliers in our baseline gain data were exploratory, then the rank-ordered GRV transformation (i.e., the "reigning in") may mask important information regarding trial-to-trial performance. Therefore, we tested the null hypothesis (H_0) that there is no difference in VOR gain be-

tween the trial just before and the trial just after an outlier, against the alternative (H_A) that there is a difference in VOR gain between the trial just before and the trial just after an outlier. If our outliers were indeed exploratory, then we would expect to see performance changes in the trials immediately following the outliers, as subjects adjusted their actions based on the results of the outliers. However, if the outliers were simply noise, then we would expect no difference in the gain values before and after an outlier occurred (i.e., no behavioral modifications as a result of the outliers). A linear, mixed-effects, repeated-measures model, which treated pre- and post-outlier VOR gain values as a fixed variable, test subjects as a random variable, and allowed separate intercepts for each subject, showed no significant difference between the pre- and post-outlier trials ($p < 0.01$). It was therefore concluded that the outliers were simply random, occasional occurrences that did not systematically alter behavior, and so our rank-ordered GRV transformation was not masking or eliminating any substantial motor learning as a result of the outliers.

The ACF and power spectrum were computed for each subject's surrogate datasets. A linear regression analysis was applied to the power spectrum (plotted on log-log axes), and β was derived from the negative slope of this linear fit. One rank-ordered GRV surrogate dataset and its corresponding ACF and power spectrum from a representative subject are displayed in Figure 6.5.

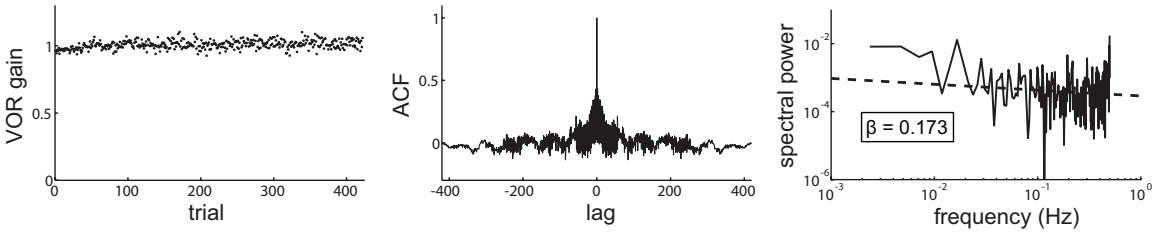

Figure 6.5 Rank-ordered GRV surrogate dataset (Left) and corresponding auto-correlation function (Center) and power spectrum (Right) from one representative subject.

6.4.3 Baseline inter-trial correlations forecast adaptation in the VOR

VOR gain adaptation extent was highly correlated with the β values derived from the baseline rank-ordered GRV surrogates (Figure 6.6, $r^2 = 0.72$, $p < 0.01$). More specifically, the larger the β value (the stronger the inter-trial correlations), the weaker the adaptive capacity (the smaller the VOR adaptation extent) of the individual. This strong linear trend suggests that the strength of the inter-trial correlations in successive baseline VOR gain values (i.e., the temporal structure, quantified by β) forecasts adaptive capacity in the VOR.

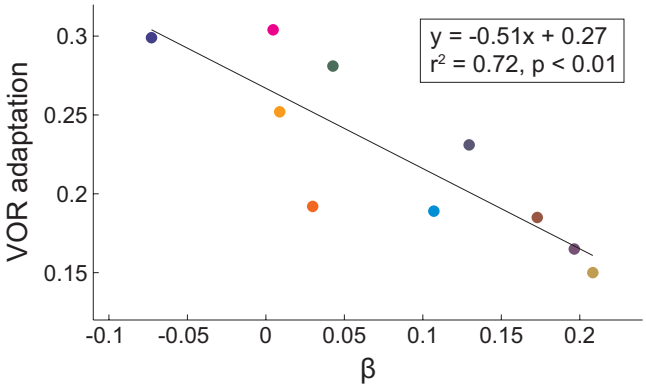

Figure 6.6 Correlation between VOR adaptation extent and β, where β is derived from the rank-ordered GRV surrogates of baseline head-impulse VOR gain values.

Statistically, it is possible that this correlation simply occurred by chance. This could happen, for example, if the baseline VOR gain values were just random values drawn from some underlying distribution. Therefore, to test the possibility that the correlation did not arise by chance, we employed another surrogate data-analysis technique in which time-shuffled surrogates of the rank-ordered GRV surrogates were generated by randomly shuffling the order of the rank-ordered GRV data values. Such a time-shuffling destroys the temporal correlations, but preserves the underlying distribution. Hence, these new shuffled-surrogates maintain all of the properties of the original baseline data, except for the trial-to-trial time-ordering of the individual gain values. We then re-

computed the correlation plot using these time-shuffled surrogates. If inter-trial correlations are a significant driving force behind the original correlation depicted in Figure 6.6, then randomly scrambling the temporal structure should result in β values close to zero (analogous to uncorrelated white noise) and no relation between this altered β and adaptation. This is in fact what happens (Figure 6.7).

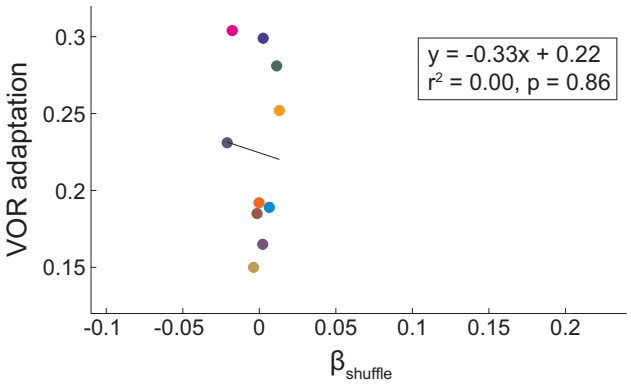

Figure 6.7 Correlation between VOR adaptation extent and $\beta_{shuffle}$, where $\beta_{shuffle}$ is derived from time-shuffled surrogates of the rank-ordered GRV surrogates.

This finding suggests that trial-to-trial fluctuations in baseline VOR gain data may reflect the ability of the VOR to adapt to novel perturbations. Others have posited that simpler measures of general variability may be related to adaptive capabilities (Wu et al. 2014). To that end, we also examined whether standard statistical parameters of the baseline VOR gain data, namely mean, standard deviation, skewness, and kurtosis, were correlated with adaptation extent. No such correlation was found (Figure 6.8, $r^2 < 0.12$, $p > 0.32$). This validates our hypothesis that it is not the overall system variability (i.e., standard deviation), but fluctuations in the trial-to-trial time-ordering of the successive gain values (i.e., temporal structure) that is related to the adaptation performance.

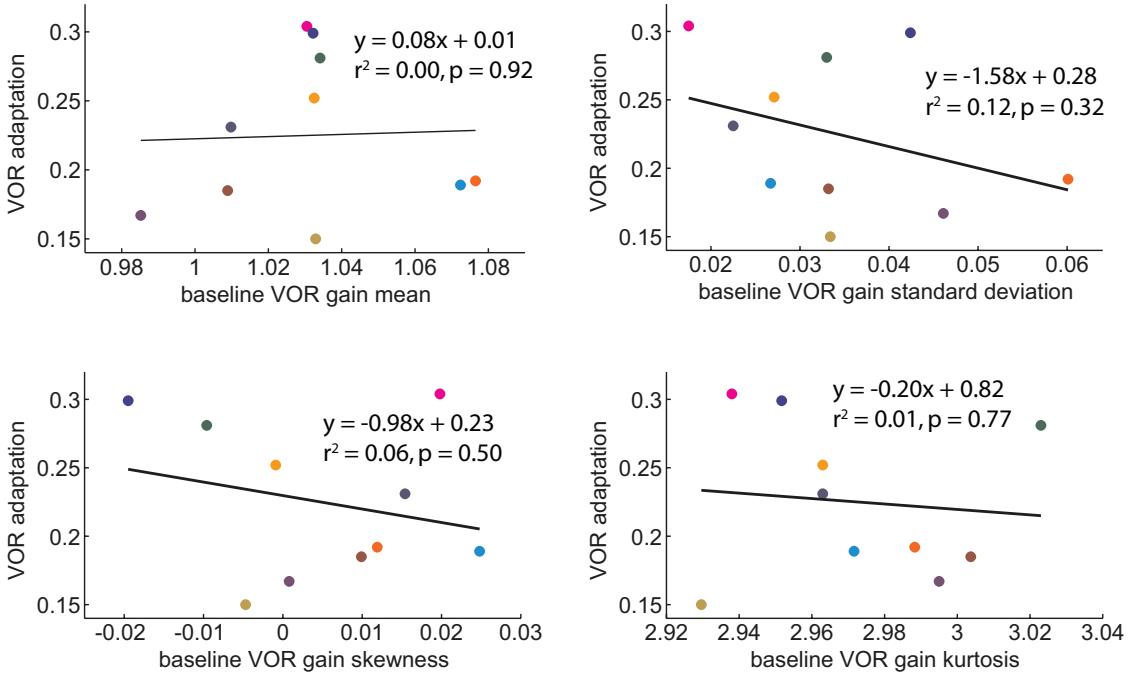

Figure 6.8 Correlation between VOR adaptation extent and standard statistical parameters. No correlation is observed between VOR adaptation extent and the mean, standard deviation, skewness, or kurtosis of the baseline rank-ordered GRV surrogates.

6.5 Discussion

Trial-to-trial variations around a mean are often designated as the "noise" of the system. Here, we describe a process by which these variations are not simply random, sporadic occurrences. Our results instead suggest that such temporal fluctuations may reflect an active, intentional motor-learning mechanism that can be related to the adaptive capabilities of the system.

In this experiment, we found that the strength of inter-trial correlations of baseline VOR gain amplitudes, quantified by β, was highly correlated with adaptation to a novel visual-vestibular perturbation. Subjects whose baseline VOR gain data demonstrated relatively longer-memory behaviors (i.e., power spectra exhibiting relatively larger ratios of

lower-frequency to higher-frequency content) were the individuals who adapted the least, while subjects who demonstrated shorter-memory behaviors (i.e., power spectra exhibiting relatively smaller ratios of lower-frequency to higher-frequency content) adapted the most. In fact, the β values associated with subjects who adapted most were near zero, which indicated that their baseline VOR gain data exhibited little-to-no inter-trial correlations (analogous to an uncorrelated white noise process). Notably, the parameter that strongly correlated with adaptation was a property of the time series that preserved the temporal order in which the individual trials occurred, not net variability (e.g., the standard deviation of the baseline VOR gain values).

In this experiment, adaptation extent was derived from the baseline and 20min VOR gain probes described in Chapter 5. It should be noted that there was no correlation between β and the earlier adaptation probes tested 5, 10, and 15min into the adaptation. One reason for this may be because the adaptation was closer to being complete after 20min than during the earlier gain probes, and hence the probe at 20min is a more accurate reflection of adaptation capability. Recall that the 20min of adaptation data were fit with exponentials to examine the consistency in gain changes from one probe to the next (see Chapter 5.4.1). For the subjects whose data was better characterized by these exponentials, the 20min VOR gain probe fell much closer to (if not directly on top of) the asymptotes of these curves, whereas earlier probes were located on either the more linear or the transitional regions. Thus, following 20min, VOR gain had reached a more "stable" phase in the adaptation process for most subjects.

This idea may also be related to why β correlated with VOR-adaptation *extent* in this experiment, but saccade-adaptation *rate* in the experiment by Wong and Shelhamer

(2014). In our VOR experiment, the adaptation data were more accurately represented by exponential fits, rather than linear fits (readily observed in Figure 5.4), whereas in the saccade experiment, the adaptation data were more accurately portrayed through linear fits. In general, motor adaptation tends to follow an exponential trend, but the initial stages of adaptation are often approximated as linear. Hence, the differing metrics that correlated with β in these two experiments (i.e., extent versus rate) may be understood in light of the two different adaptation stimuli employed in these experiments. During the adaptation portion of the VOR experiment, subjects made sinusoidal head movements paced at 0.75Hz for 20min (equivalent to 900 complete cycles). This, coupled with the short latency of the VOR, meant that retinal-slip information could be used continuously and immediately to update the gain-state of the VOR. In contrast, only 300 adaptation saccades were performed during the saccade-adaptation experiment. Because saccades cannot be modified inflight, subjects effectively had only 300 "chances" to modify their gain-state. Thus, when considering where these systems ended up on the overall adaptation trajectory at the conclusion of the adaptation period, it is not surprising that VOR adaptation had progressed further (i.e., onto the asymptotic "tail" of the adaptation curve) than saccade adaptation (i.e., still on the initial linear portion of the adaptation curve). While this argument may lead to the presumption that a linear fit applied through an earlier portion of the VOR gain adaptation data (to compute a VOR gain-adaptation *rate*) should then necessarily correlate with β, it must be remembered that while saccade adaptation was recorded for all 300 adaptation trials, VOR gain was only probed once every five minutes. Hence, applying such a linear fit is not possible with this dataset.

Finally, no correlation between β and any of the VON motion-gain probes was observed. However, in light of the discussion in Chapter 5, this is to be expected, since VOR gain and VON motion-gain measure different aspects of the vestibulo-ocular system: VOR gain quantifies motor compensation for retinal slip, while VON motion-gain quantifies motor plus sensory retinal slip. Since β was derived from a series of baseline VOR gain values, we would expect it to relate to VOR gain behavior and not necessarily VON motion-gain behavior. Perhaps if 420 baseline VON trials had been employed, we would have found a similar correlation with vestibulo-ocular adaptation quantified by VON motion-gain.

6.5.1 Strong correlation is maintained using raw baseline data

It is interesting to note that the correlation between the VOR adaptation data and β_{raw} derived from the raw baseline VOR gain data is even stronger than the correlation observed using the rank-ordered GRV surrogates (Figure 6.9 Left, $r^2 = 0.84$, $p < 0.01$). Furthermore, no correlation exists between VOR adaptation data and $\beta_{raw,shuffle}$ derived from time-shuffled versions of the raw baseline VOR gain data, as all $\beta_{raw,shuffle}$ values collapse to zero (Figure 6.9 Right, $r^2 = 0.07$, $p = 0.47$). Although there are some statistical considerations when computing β_{raw} from the raw data, which warranted the use of rank-ordered GRV surrogates in the first place, it is nonetheless encouraging to find that the trend is maintained when the data generated explicitly by the subjects is employed.

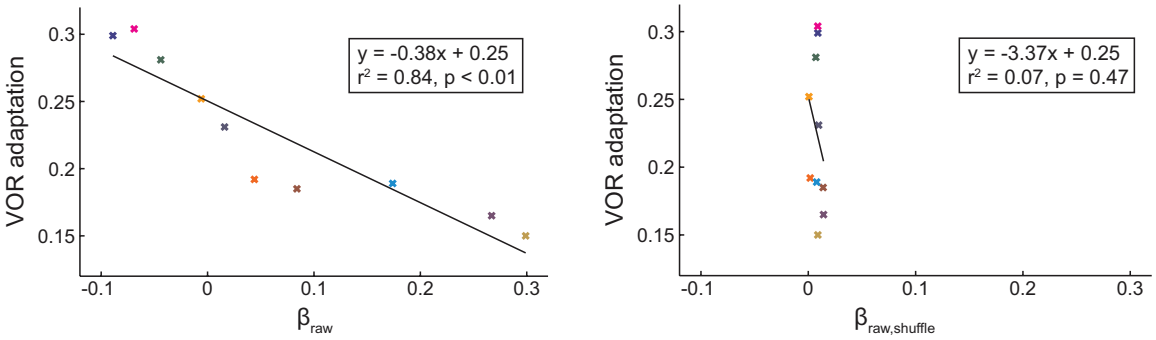

Figure 6.9 Correlations between VOR adaptation extent and β derived from raw baseline VOR gain data. (Left) VOR adaptation extent strongly correlates with β_{raw}. (Right) No correlation is observed between VOR adaptation extent and $\beta_{raw,shuffle}$ derived from time-shuffled surrogates of the raw baseline VOR gain data.

However, the maintenance of (and perhaps slight improvement in) this correlation in the presence of the outliers may lend to the suspicion that it is the outliers themselves that drive the correlation, since the outliers are the data point that are modified most by the rank-ordered GRV transformation. This hypothesis was tested through another set of surrogates in which the outliers maintain their original positions, while the non-outliers are randomly shuffled in time. If the outliers are the predominant factor, then the correlation result should be maintained, even as the temporal correlations within the majority of the data (i.e., the non-outliers) are disrupted. No such correlation is observed when these surrogates are generated from either the raw data or the rank-ordered GRV surrogates ($r^2 < 0.15$, $p > 0.3$), and hence, it is highly unlikely that our correlation is derived solely as a result of the outliers.

6.5.2 The VOR and saccadic systems work in synergy

The short latency of the VOR (on the order of several milliseconds) enables retinal slip information to be used almost immediately (Collewijn and Smeets 2000) to correct for errors. Furthermore, if the CNS detects that the VOR is miscalibrated, eye velocity can be modulated during the movement since retinal-slip error is available in real

time. In our experimental protocol, subjects were given continuous visual feedback during the baseline head-impulses (they were viewing a point target), and thus the VOR was able to perform online corrections quickly, should retinal slip occur. Because this online feedback is immediately available and is the most relevant, up-to-date measure of the accuracy of the VOR, it is unnecessary – and possibly prohibitory – for the brain to store and use error information from previous trials to adjust the next trial.

This is in contrast to the results observed in the saccadic system, where larger adaptive capacities (in terms of rate of adaptation) were associated with stronger long-term correlations. Saccades are ballistic in nature. They are rapid eye movements, whose duration lasts less than the response time of the visual system (approximately 100ms) (Gellman et al. 1990). As such, visual feedback cannot be used to modify the saccade once it has been initiated (Leigh and Zee 2006c). If an error in the saccade trajectory is made, it is not until at least one saccade later that behavior can be modified. Therefore, the only way by which error corrections can occur in the saccadic system is on a trial-by-trial basis. So it is both necessary and desirable to retain previous performance information to modify behavior. This may in fact be why predictive-saccades exhibit ACF's that decay more slowly (specifically, as a power law (Wong and Shelhamer 2014)) than the ACFs associated with VOR data.

Taken together, these results may reflect the synergistic behavior of the phylogenetically "old" vestibulo-ocular system and the relatively "new" saccadic system in mediating gaze stability. The VOR operates promptly and automatically in response to head motion, providing smooth, continuous gaze control. Saccades enable quick, voluntary shifts in the line of sight. Hence, where one system is bounded, the other is enhanced.

These systems can operate simultaneously, such as to facilitate gaze-shifts during head motion ("gaze-saccades," (Laurutis and Robinson 1986)). Or alternatively, when one system is lacking (e.g., due to pathology), the other can supplement. For example, it is well known that during both adaptation to novel visual-vestibular perturbations and compensation for vestibular lesions, for example, saccades are typically recruited to augment the deficient VOR (Bloomberg et al. 1991; Tian et al. 2000; Schubert et al. 2006).

In light of these two experiments on saccades and the VOR, one might posit that an individual's propensity to retain, as opposed to rapidly forget, information might be a more global characteristic of that individual's sensorimotor processing (a "sensorimotor phenotype"). In other words, if an individual exhibits strong inter-trial correlations in one sensorimotor system, is it necessarily the case that he also expresses strong inter-trial correlations in other systems? Such a finding would mean that characterizing baseline performance in one system would not only lead to predictions regarding adaptive capacities in that system, but also predictions about adaptive performance in other systems. This would certainly be an impressive revelation.

In consideration of this, we compared the β values and adaptation performance across the six subjects who happened to participate in both the saccade and VOR experiments. Unfortunately, there was no systematic trend between β and adaptation performance across the two experiments (Figure 6.10). The β values derived from the baseline saccade data were not the same β values derived from the baseline VOR gain data, and those subjects who were high-performing adapters in one experiment, were not necessarily low-performing adapters in the other experiment.

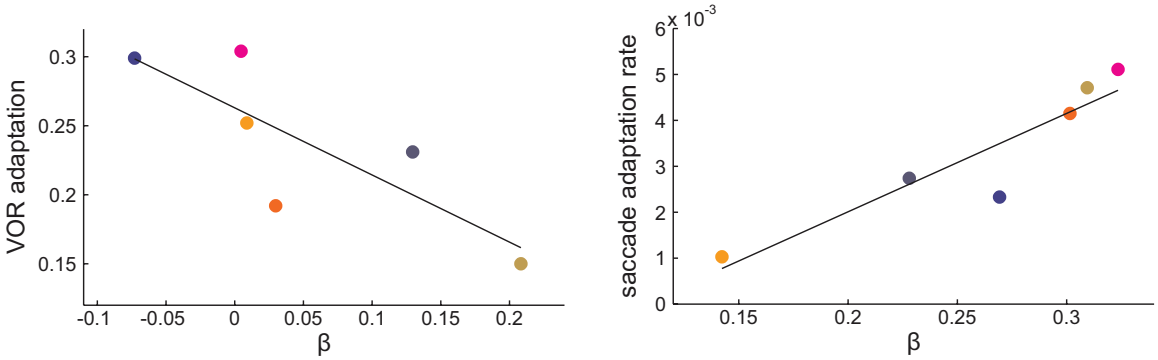

Figure 6.10 Comparisons across the saccade and VOR experiments in six subjects. Six subjects participated in both the VOR and saccade experiments. (Left) VOR adaptation extent versus β derived from the baseline rank-ordered GRV surrogates. (Right) Saccade adaptation rate (measured in °/trial) versus β derived from the baseline predictive-saccades. β was not conserved across the experiments. Subjects who were high-performing adapters in one experiment were not necessarily low-performing adapters in the other experiment.

However, this result does not negate the concept that β may be a more global sensorimotor predictor. In fact, such a presumption at this point would be premature, as we have only considered β in two oculomotor systems to-date. It may have an important predictive role in posture or locomotion, for example. Since many parameters of the locomotor system can be modified "inflight" (e.g., stride length and timing) perhaps the β values derived from VOR gain data will correlate with some aspect of performance during walking. Future experiments are needed to assess such cross-system possibilities.

Chapter 7

Conclusions

7.1 Summary

In this dissertation we describe the design, development, and implementation of three innovative approaches for quantifying binocular positioning misalignments and the vestibulo-ocular reflex: Vertical Alignment Nulling (VAN), Torsional Alignment Nulling (TAN), and Vestibulo-Ocular Nulling (VON). Notably, these techniques do not require traditional eye-movement recordings, eliminating the need for invasive and delicate equipment, time-consuming calibration procedures, and computationally expensive processing algorithms. Rather they emphasize functional attributes of the oculomotor system to maximize the transfer of test results to real-world performance metrics. The tests themselves are simple and intuitive, thereby enabling them to be performed rapidly, on the order of several seconds per trial. The associated portable hardware (a hand-held, tablet-based platform) and efficient assessment capabilities make this technology an ideal tool for scientists and clinicians who require rapid evaluation of oculomotor function with minimal equipment.

Otolith asymmetries manifest as vertical and torsional binocular positioning misalignments. In Chapter 3, we evaluate the functional consequences of such misalignments through Vertical and Torsional Alignment Nulling (VAN and TAN). In these tests, the

subject wears red-blue eyeglasses (one lens is red, the other is blue) and views one red and one blue line on a tablet computer; this provides different visual information to each eye. The subject aligns the red and blue lines, initially offset vertically from one another during VAN or rotated relative to one another in TAN, until he perceives a single continuous line. The amount of vertical or rotational offset in the final line positions provides a surrogate measure of vertical and torsional binocular misalignments, respectively. Through laboratory experiments, we demonstrated that VAN and TAN accurately portray visual disparities induced by optical prisms of known prismatic power. By offsetting the initial line positions *always above* or *always below* the expected final positions, we were able to explore the relative contributions of perceptual fusion to a primarily motor-driven response.

VAN and TAN testing in the parabolic-flight environment revealed that variability in preflight torsional misalignments strongly correlates with motion sickness susceptibility, and that binocular positioning is gravity-dependent. Although the motion sickness correlation has only been verified in three subjects to-date, it is possible that a baseline measure of torsional disconjugacy might be predictive of motion sickness susceptibility in altered gravity levels. Additionally, we found that both vertical and torsional binocular positioning misalignments increase upon exposure to novel g-levels, which provides evidence for a 1g-tuned central compensation mechanism that accounts for individual, innate asymmetries between the left and right otolith systems. This compensation appears to become miscalibrated in the 0g and 1.8g phases of parabolic flight, based on the rendered increased misalignments. Furthermore, we observed that the direction of torsional misalignment reverses when transitioning from 1g to 0g versus from 1g to 1.8g, which is

compatible with the otolith-asymmetry central-compensation model proposed by von Baumgarten and Thümler and is consistent with the results of other investigators (von Baumgarten and Thümler 1979; Diamond and Markham 1991). In contrast, the direction of vertical misalignment is maintained in both 0g and 1.8g. To that end, we developed a bilateral control systems model in Chapter 4 that could successfully portray both the increased binocular misalignments and gravity-dependent changes in direction observed inflight. Specifically, our model is a more general version of the one proposed by von Baumgarten and Thümler (1979), and it incorporates a nonlinear gravity-dependent component that provides the appropriate flexibility. The model is robust to small changes in the model parameters, and it can be mapped to plausible neuroanatomical structures.

In Chapter 5, we described the Vestibulo-Ocular Nulling (VON) task as a means to evaluate the vestibulo-ocular reflex. In VON, head motion controls the position of a visual target through a variable motion-gain in real-time. Subjects adjust this motion-gain until the target appears fixed-in-space with head movements. By measuring the amount of illusory motion experienced for a given head movement, we can obtain a surrogate measure of VOR gain. Comparisons between VON motion-gain and VOR gain during adaptation to a visual-vestibular perturbation demonstrated that VON motion-gain provides a rapid, reliable measure of perceived retinal slip that is more consistent than conventional VOR gain. By employing a technique that quantifies the perceptual deficiency in the VOR, we were able to define a real-world performance metric that may have more utility than VOR gain alone.

On Earth, ocular responses to pitching head movements are driven by both the semicircular canals (angular rotation of the head) and the otolith organs (tilt with respect

to gravity). We explored how the pitch VOR is regulated by changes in static otolith signaling by measuring VON motion-gain in the alternating g-levels of parabolic flight. We found that VON motion-gain modulates with g-level in first-time flier, providing evidence for an otolith-modulating component of the angular VOR.

In Chapter 6, we investigated how individual adaptive capabilities in the vestibulo-ocular system might be predicted from baseline measures alone, without exposure to an adaptive stimulus. We quantified the inter-trial correlations in baseline VOR gain, namely the trial-to-trial fluctuations that transpire as a consequence of correcting for previous performance errors over multiple time scales, and demonstrated a strong linear trend between the strength of these inter-trial correlations and VOR gain adaptation. Specifically, subjects who exhibited weaker inter-trial correlations adapted the most. This is in contrast to results observed in the saccadic eye-movement system, where subjects who demonstrate stronger inter-trial correlations adapted faster (Wong and Shelhamer 2014). These opposing outcomes can be ascribed to differences regarding how incoming error information is processed by each system. The short latency of the VOR provides an (almost) immediate measure of the accuracy of the system, thereby rendering the use of past information unnecessary. On the other hand, saccades cannot be modified inflight, and so the only way in which error information can be processed in this system is by recalling the performance from previous saccades.

7.2 Implications

The three perceptual nulling tasks developed in this dissertation provide a means for rapidly and unobtrusively quantifying the vestibular control of eye movements. The-

se innovative approaches provide important performance-based complements to traditional physiological assessments, which may better enable the transfer of test results to real-world applications. Importantly, while much of work described in the preceding chapters is directed towards spaceflight operations and research, these findings are equally applicable and significant for the clinical community. For example, VAN and TAN are potentially viable tools for diagnosing unilateral vestibular lesions: knowledge of the directions of perceptual misalignments can be ascribed to specific ocular muscles and their corresponding oculomotor pathways. Additionally, VON may provide a more efficient and patient-tolerable means of assessing gaze instabilities.

The inclusion of parabolic-flight testing in our protocols enabled us to explore the underlying neurophysiological processes governing otolith-ocular control by providing a unique environment that unmasked inherent vestibular properties, which might otherwise go undetected due to 1g-tuned compensatory control mechanisms. The development of a physiologically plausible model to account for such properties (e.g., innate otolith asymmetries) allows us to not only characterize the behavior of the otolith-ocular system, but also propose a means by which the underlying pathways might be organized to produce such results. Understanding this neural circuitry may enable us to pair changes in specific anatomical structures to changes in behavior, which has important implications for the development of interventions. These could include countermeasures to facilitate adaptation to novel g-levels or rehabilitation protocols to facilitate terrestrial compensation for pathology.

One of the highlights of the sensorimotor system is its remarkable ability to adapt to novel situations. However, significant variability in adaptive capabilities (e.g., in

terms of its extent and rate) exists across individuals, thereby rendering the development of appropriate rehabilitation protocols for patients or preflight countermeasures for astronauts difficult. Hence, in this dissertation, we explored the possibility of various baseline metrics, inherent within the individual, in forecasting adaptation without exposure to an adaptive stimulus. The findings to-date suggest that various measures of variability may provide such predictive parameters. We discovered that net variability in baseline measures of torsional misalignments correlated strongly with motion sickness; this is related to the adaptability of the neurovestibular system to novel gravitational environments. We also found that temporal fluctuations (trial-to-trial variability) in baseline VOR gain correlated strongly with VOR gain adaptation. Such findings are highly significant, as they may facilitate the design of *individualized* interventions.

The technological developments described in this dissertation were principally designed for sensorimotor assessment in the spaceflight environment, which necessitated tests that were simple, intuitive, efficient, and could be self-administered, as well as hardware that was portable and computationally inexpensive. However, our tablet-based platform has applications beyond spaceflight operations, including bedside clinical testing, remote field-testing, or any application limited by time constraints, resources, technical personnel, or clinical expertise. Furthermore, the open-access nature of mobile app development software makes this device amenable for integration with other physiological monitoring devices, including, for example, those used to measure autonomic and cardiovascular function. Integrating medical monitoring across multiple physiologic systems provides two important advantages. First, it saves valuable time and resources. This is particularly important for the spaceflight community, with the prospect of even

longer and more remote missions to Mars and beyond, where we will no longer have the luxury to study individual systems in isolation. Second, it allows us to investigate performance in a more holistic manner (e.g., how a person's sensorimotor system adapts on a *global* scale to restore function following disturbance), as opposed to the pervasive tendency to analyze responses in isolation, which limits our understanding of the overall functional capacity of the individual.

7.3 Future work

7.3.1 Technological enhancements

The work in this dissertation has demonstrated that VAN, TAN, and VON can provide meaningful measures of vestibulo-oculomotor function. There are several general design improvements that may further increase the efficiency and effectiveness of these three tests. First, it would be valuable to incorporate simple analyses directly into the mobile apps, so that a novice subject or technician could obtain immediate results at the end of the test. For example, a *print results* option, appearing automatically after a file is closed, might display a graph of the raw data and its associated mean and standard deviation. The ability to automatically upload results to an online server would enable remote access and subsequent analysis of the data by a medical examiner or research professional (e.g., home-based testing). Incorporating a wireless joystick or keypad would enable the tablet to be placed at a farther distance, and so comparisons in performance under near and far viewing conditions could be explored. A lanyard between the subject's neck and the tablet would better control subject-to-screen distance, which is partic-

ularly important in VAN. Finally, a portable shroud would eliminate the need for testing in a dark room or building a light-proof "tent" around the subject when testing is performed outside the laboratory; this could be as simple as a piece of black cloth fixed to a pair of goggles and the central portion of the tablet, leaving the upper and bottom portions free for the fingers to make use of the tactile-feedback, target-control buttons.

There are many adjunct tests to VAN, TAN, and VON that would be simple to implement on the tablet and highly effective for clinical and spaceflight research. Notably, a Horizontal Alignment Nulling (HAN) test would provide a means to quantify horizontal vergence. This will enable us to better characterize the variability in vertical and torsional misalignments across subjects. Such a test is particularly interesting for future parabolic-flight experiments because anecdotal reports from previous fliers indicate that vergence may vary systematically with g-level.

Furthermore, it will likely save time if VAN and TAN are combined into a single two-dimensional test, in which the moving line is offset both vertically and rotationally; the subject would adjust both the vertical position and torsional orientation during each trial. Alternatively, a single three-dimensional test could be implemented by displaying red and blue crosshairs instead of horizontal lines; the subject would overlay the center of the crosshairs to quantify vertical misalignment and horizontal vergence angle and rotate them on top of one another to quantify torsional misalignment. Doing so may lead to new findings that better capture the coupled nature of binocular positioning.

One potential limitation in the current implementation of VAN and TAN is that the program displays the next trial as soon as the previous trial is complete. Novice subjects who undergo incomplete or improper instruction may therefore adjust the moving

line according to how large of a "jump" they perceive when the next trial is displayed, instead the moving line's relative position to the stationary line. One way to minimize this possibility is to momentarily blank the screen between each trial.

In Chapter 5, we described an alternative approach for VON testing during parabolic flight to minimize the adverse symptoms brought out by continuous, sinusoidal head movements. In this version, single head-movement "steps" would be performed, with momentary breaks in between for the subject to adjust the motion-gain based on the direction in which he perceived the target to move during the head movement. No programmatic changes are required for this test, only a difference in instruction to the subjects as to how they should move their heads.

Two additional oculomotor assessment tests can be easily incorporated that would complement VAN, TAN, and VON and provide a complete oculomotor assessment package. A subjective visual vertical (SVV) test could be incorporated, which would provide a portable platform to quantify unilateral utricular asymmetries. This could be accomplished by displaying a single vertical line (without the use of the red and blue filters) that the subject rotates until he perceives it to be aligned with gravity. Employing the onboard accelerometer would enable the tablet to be precisely aligned with gravity as a reference. Additionally, an alternative measure of gaze-stability is the dynamic visual acuity (DVA) test, described in Chapter 5.1.3. A variation on this test could be incorporated into the VON test in which an optotype, instead of a dot, is displayed as the VON target. Subjects would then be tasked with (1) nulling the target motion (a measure of perceived retinal slip), and (2) correctly identifying the optotype (a measure of dynamic visual acuity).

Aside from these numerous oculomotor assessment tests, the tablet-based platform is a solid foundation for a completely portable sensorimotor assessment battery. Additional wireless motion sensors (already employed by VAN, TAN, and VON) placed on the head, trunk, and limbs would facilitate measures of coordinated body movements during standing balance and locomotion. Because these sensors are small (watch-sized) and unobtrusive, such tests can be performed in natural environments under natural movements. This provides significant advantages over the traditional posture platforms, gait mats, and treadmills routinely employed in the clinic, including an improvement in overall simplicity and the potential for better transfer of results to real-world settings. Such techniques are currently being implemented as part of our Sensorimotor Assessment and Rehabilitation Apparatus (SARA) project.

7.3.2 Follow-on experiments

The results obtained from the various experiments outlined in Chapters 3 through 6 lend themselves to several important follow-on experiments to enhance our understanding of vestibulo-oculomotor control and adaptation to novel perturbations. First, measurements of three-dimensional, binocular eye movements during VAN and TAN testing will enable the investigation of the relative contributions of the motor (eye movement) and sensory (motor minus nulling results) components to the perception of binocular positioning alignment. Performing such measures during adaptation to a novel perturbation, such as a prismatic correction or prolonged centrifugation, will demonstrate how the relative relationship between the motor and sensory contributions might change as oculomotor reflexes are adjusted. This is the VAN and TAN analogy to the VON motion-gain versus VOR gain experiment demonstrated in Chapter 5.

Second, correlating parabolic-flight motion-sickness susceptibility and baseline TAN testing in a larger population of naïve parabolic-flight subjects (regardless of whether they perform TAN inflight) would provide more substantial support for (or against) the hypothesis that large variability in torsional binocular positioning in 1g may be predictive of motion sickness susceptibility in novel g-levels. Additional VAN and TAN testing in the parabolic environment, in which subjects are tested across multiple consecutive flights, may enable the incorporation of a temporal component into the central compensation model proposed in Chapter 4. This could provide valuable knowledge regarding how neurophysiological pathways are reorganized during adaptation. The addition of a preflight, 1g supine test would allow us to correlate the magnitude of ocular positioning misalignments in altered gravity levels with a common terrestrial experience. Further modeling work should also incorporate cross-striolar inhibition.

Third, a similar VON motion-gain adaptation experiment could be performed (without measuring eye movements) in which subjects adjust the motion-gain in one direction only. This would be the VON motion-gain equivalent to the VAN and TAN *always above* and *always below* tests described in Chapter 3, with an additional adaptation component. This would allow us to characterize how much perceptual fusion facilitates gaze stability, and how this capacity changes during exposure to a particular disruption.

Fourth, the discovery that the strength of inter-trial correlations in baseline measures strongly correlates with adaptive capabilities in two different oculomotor systems begs the question as to whether or not similar correlations can be found in other sensorimotor systems. Importantly, the results obtained in the saccadic and vestibulo-ocular systems are complementary, in that in one system, strong inter-trial correlations represent

favorable adaptive capabilities, whereas in the other system, strong inter-trial correlations are unfavorable. Hence, if strong trends between baseline inter-trial correlations and adaptation are observed in other physiological systems, the results will likely be paralleled in one of the oculomotor systems. This renders a potential connection between this new physiological system and either the saccadic or vestibulo-ocular system, which may lead to the possibility that a single predictor (derived in one system) may have more widespread predictive capabilities across multiple systems.

In conclusion, the experiments described in this dissertation have enhanced our understanding of the behavioral performance and adaptability of vestibulo-oculomotor control. The ability to evaluate binocular positioning misalignments and the vestibulo-ocular reflex rapidly with portable equipment provides a technology with applications beyond spaceflight operations. The modeling and predictability work provides a viable foundation for individualized training protocols and countermeasure development.

References

Abeele S, Bock O (2001) Mechanisms for sensorimotor adaptation to rotated visual input. Exp Brain Res 139:248-253

Adrian ED (1943) Discharges from vestibular receptors in the cat. J Physiol 101:389-407

Ahn SC, Lee CY, Kim DW, Lee MH (2000) Short-term vestibular responses to repeated rotations. J Vestib Res 10:17-23

Albus JS (1971) A theory of cerebellar function. Math Bio Sci 10:25-61

Allison RS, Howard IP, Fang X (2000) Depth selectivity of vertical fusional mechanisms. Vision Res 40:2985-2998

Anderson JH, Blanks RH, Precht W (1978) Response characteristics of semicircular canal and otolith systems in cat. I. Dynamic responses of primary vestibular fibers. Exp Brain Res 32:491-507

Angelaki DE, Hess BJ, Suzuki JI (1995) Differential processing of semicircular canal signals in the vestibulo-ocular reflex. J Neurosci 15:7201-7216

Angelaki DE, McHenry MQ, Dickman JD, Newlands SD, Hess BJ (1999) Computation of inertial motion: neural strategies to resolve ambiguous otolith information. J Neurosci 19:316-327

Anken RH, Kappel T, Rahmann H (1998) Morphometry of fish inner ear otoliths after development at 3g hypergravity. Acta Otolaryngol 118:534-539

Baarsma EA, Collewijn H (1975) Eye movements due to linear accelerations in the rabbit. J Physiol 245:227-249

Bacal K, Billica RD, Bishop S (2003) Neurovestibular symptoms following space flight. J Vestib Res 13:93-102

Bagian JP (1991) First intramuscular administration in the U.S. Space Program. J Clin Pharmacol 31:920

Bagolini B (1976) Sensorio-motorial anomalies in strabismus: (anomalous movements). Doc Ophthalmol 41:23-41

Bahill AT, Stark L (1975) Overlapping saccades and glissades are produced by fatigue in the saccadic eye movement system. Exp Neurol 48:95-106

Baker R, Precht W, Llinas R (1972) Mossy and climbing fiber projections of extraocular muscle afferents to the cerebellum. Brain Res 38:440-445

Baloh RW, Demer JL (1991) Gravity and the vertical vestibulo-ocular reflex. Exp Brain Res 83:427-433

Baloh RW, Enrietto J, Jacobson KM, Lin A (2001) Age-related changes in vestibular function: a longitudinal study. Ann N Y Acad Sci 942:210-219

Baloh RW, Henn V, Jager J (1982) Habituation of the human vestibulo-ocular reflex with low-frequency harmonic acceleration. Am J Otolaryngol 3:235-241

Baloh RW, Lyerly K, Yee RD, Honrubia V (1984) Voluntary control of the human vestibulo-ocular reflex. Acta Otolaryngol 97:1-6

Barmack NH (1981) A comparison of the horizontal and vertical vestibulo-ocular reflexes of the rabbit. J Physiol 314:547-564

Barmack NH, Baughman RW, Eckenstein FP, Shojaku H (1992) Secondary vestibular cholinergic projection to the cerebellum of rabbit and rat as revealed by choline

acetyltransferase immunohistochemistry, retrograde and orthograde tracers. J Comp Neurol 317:250-270
Barmack NH, Baughman RW, Errico P, Shojaku H (1993) Vestibular primary afferent projection to the cerebellum of the rabbit. J Comp Neurol 327:521-534
Baroni G, Pedrocchi A, Ferrigno G, Massion J, Pedotti A (2001) Motor coordination in weightless conditions revealed by long-term microgravity adaptation. Acta Astronaut 49:199-213
Barr CC, Schultheis LW, Robinson DA (1976) Voluntary, non-visual control of the human vestibulo-ocular reflex. Acta Otolaryngol 81:365-375
Bartl K, Schneider E, Glasauer S (2005) Dependence of the torsional vestibulo-ocular reflex on the direction of gravity. Ann N Y Acad Sci 1039:455-458
Batton RR, 3rd, Jayaraman A, Ruggiero D, Carpenter MB (1977) Fastigial efferent projections in the monkey: an autoradiographic study. J Comp Neurol 174:281-305
Beaton KH, Pierson K, McDermott C, Shelhamer M, Zee DS, Schubert MC (2014) Vestibulo-ocular nulling: quantifying perceived retinal slip without recording eye movements. In: Association for Research in Otolaryngology, San Diego, CA
Bello S, Paige GD, Highstein SM (1991) The squirrel monkey vestibulo-ocular reflex and adaptive plasticity in yaw, pitch, and roll. Exp Brain Res 87:57-66
Benson AJ, Barnes GR (1978) Vision during angular oscillation: the dynamic interaction of visual and vestibular mechanisms. Aviat Space Environ Med 49:340-345
Benson AJ, Vieville T (1986) European vestibular experiments on the Spacelab-1 mission: 6. Yaw axis vestibulo-ocular reflex. Exp Brain Res 64:279-283
Bergamin O, Straumann D (2001) Three-dimensional binocular kinematics of torsional vestibular nystagmus during convergence on head-fixed targets in humans. J Neurophysiol 86:113-122
Berthoz A, Brandt T, Dichgans J, Probst T, Bruzek W, Vieville T (1986) European vestibular experiments on the Spacelab-1 mission: 5. Contribution of the otoliths to the vertical vestibulo-ocular reflex. Exp Brain Res 64:272-278
Blaber E, Marcal H, Burns BP (2010) Bioastronautics: the influence of microgravity on astronaut health. Astrobiology 10:463-473
Black FO, Paloski WH, Doxey-Gasway DD, Reschke MF (1995) Vestibular plasticity following orbital spaceflight: recovery from postflight postural instability. Acta Otolaryngol (Supp) 2:450-454
Black FO, Paloski WH, Reschke MF, Igarashi M, Guedry FE, Anderson DJ (1999) Disruption of postural readaptation by inertial stimuli following space flight. J Vestib Res 9:369-378
Black RA, Halmagyi GM, Thurtell MJ, Todd MJ, Curthoys IS (2005) The active head-impulse test in unilateral peripheral vestibulopathy. Arch Neurol 62:290-293
Bloomberg J, Melvill Jones G, Segal B (1991) Adaptive modification of vestibularly perceived rotation. Exp Brain Res 84:47-56
Bloomberg JJ, Mulavara AP (2003) Changes in walking strategies after spaceflight. IEEE Eng Med Biol Mag 22:58-62
Bloomberg JJ, Peters BT, Smith SL, Huebner WP, Reschke MF (1997) Locomotor head-trunk coordination strategies following space flight. J Vestib Res 7:161-177

Bracchi F, Gualierotti T, Morabito A, Rocca E (1975) Multiday recordings from the primary neurons of the statoreceptors of the labyrinth of the bull frog. The effect of an extended period of "weightlessness" on the rate of firing at rest and in response to stimulation by brief periods of centrifugation (OFO-A orbiting experiment). Acta Otolaryngol (Supp) 334:1-27

Brettler SC, Rude SA, Quinn KJ, Killian JE, Schweitzer EC, Baker JF (2000) The effect of gravity on the horizontal and vertical vestibulo-ocular reflex in the rat. Exp Brain Res 132:434-444.

Bronstein AM, Gresty MA (1988) Short latency compensatory eye movement responses to transient linear head acceleration: a specific function of the otolith-ocular reflex. Exp Brain Res 71:406-410

Broussard DM, Kassardjian CD (2004) Learning in a simple motor system. Learn Mem 11:127-136

Burian HM (1939) Fusional movements: role of peripheral retinal stimuli. Arch Opthalmol 21:486-491

Cannon SC, Leigh RJ, Zee DS, Abel LA (1985) The effect of the rotational magnification of corrective spectacles on the quantitative evaluation of the VOR. Acta Otolaryngol 100:81-88

Carey JP, Della Santina CC (2005) Principles of applied vestibular physiology. In: Cummings CW (ed) Cummings Otolaryngology–Head & Neck Surgery. Mosby, Philadelphia, pp 3115-3159

Carleton SC, Carpenter MB (1984) Distribution of primary vestibular fibers in the brainstem and cerebellum of the monkey. Brain Res 294:281-298

Cass SP, Borellofrance D, Furman JM (1996) Functional outcome of vestibular rehabilitation in patients with abnormal sensory-organization testing. Am J Otol 17:581-594

Chadderton P, Margrie TW, Hausser M (2004) Integration of quanta in cerebellar granule cells during sensory processing. Nature 428:856-860

Cheung BS, Money KE, Howard IP, et al. (1992) Human ocular torsion during parabolic flights: an analysis with scleral search coil. Exp Brain Res 90:180-188

Clarke AH, Engelhorn A (1998) Unilateral testing of utricular function. Exp Brain Res 121:457-464

Clarke AH, Engelhorn A, Hamann C, Schonfeld U (1999) Measuring the otolith-ocular response by means of unilateral radial acceleration. Ann N Y Acad Sci 871:387-391

Clarke AH, Grigull J, Mueller R, Scherer H (2000) The three-dimensional vestibulo-ocular reflex during prolonged microgravity. Exp Brain Res 134:322-334

Clarke AH, Schonfeld U, Helling K (2003) Unilateral examination of utricle and saccule function. J Vestib Res 13:215-225

Clarke AH, Teiwes W, Scherer H (1993) Evaluation of the torsional VOR in weightlessness. J Vestib Res 3:207-218

Clément G, Darlot C, Petropoulos A, Berthoz A (1995) Eye movements and motion perception induced by off-vertical axis rotation (OVAR) at small angles of tilt after spaceflight. Acta Otolaryngol 115:603-609

Clément G, Lathan CE (1991) Effects of static tilt about the roll axis on horizontal and vertical optokinetic nystagmus and optokinetic after-nystagmus in humans. Exp Brain Res 84:335-341
Clément G, Reschke MF (2008a) Compensatory eye movements. In: Neuroscience in Space. Springer, New York, pp 163-188
Clément G, Reschke MF (2008b) Neuroscience in space. Springer, New York
Clément G, Wood SJ, Lathan CE, Peterka RJ, Reschke MF (1999a) Effects of body orientation and rotation axis on pitch visual-vestibular interaction. J Vestib Res 9:1-11
Clément G, Wood SJ, Reschke MF, Berthoz A, Igarashi M (1999b) Yaw and pitch visual-vestibular interaction in weightlessness. J Vestib Res 9:207-220
Cohen B, Kozlovskaya I, Raphan T, et al. (1992) Vestibuloocular reflex of rhesus monkeys after spaceflight. J Appl Physiol 73:121S-131S
Cohen B, Maruta J, Raphan T (2001) Orientation of the eyes to gravitoinertial acceleration. Ann N Y Acad Sci 942:241-258
Cohen HS (2003) Update on the status of rehabilitative countermeasures to ameliorate the effects of long-duration exposure to microgravity on vestibular and sensorimotor function. J Vestib Res 13:405-409
Colebatch JG, Halmagyi GM, Skuse NF (1994) Myogenic potentials generated by a click-evoked vestibulocollic reflex. J Neurol Neurosurg Psychiatry 57:190-197
Collewijn H, Ferman L, Van den Berg AV (1988) The behavior of human gaze in three dimensions. Ann N Y Acad Sci 545:105-127
Collewijn H, Martins AJ, Steinman RM (1983) Compensatory eye movements during active and passive head movements: fast adaptation to changes in visual magnification. J Physiol 340:259-286
Collewijn H, Smeets JB (2000) Early components of the human vestibulo-ocular response to head rotation: latency and gain. J Neurophysiol 84:376-389
Collewijn H, Van der Steen J, Ferman L, Jansen TC (1985) Human ocular counterroll: assessment of static and dynamic properties from electromagnetic scleral coil recordings. Exp Brain Res 59:185-196
Conrad M (1986) What is the use of chaos? In: Holden AV (ed) Chaos. Princeton University Press, Princeton, pp 3-14
Cornell ED, Macdougall HG, Predebon J, Curthoys IS (2003) Errors of binocular fixation are common in normal subjects during natural conditions. Optom Vis Sci 80:764-771
Correia MJ (1998) Neuronal plasticity: adaptation and readaptation to the environment of space. Brain Res Brain Res Rev 28:61-65
Crawford JD, Vilis T (1991) Axes of eye rotation and Listing's law during rotations of the head. J Neurophysiol 65:407-423
Crone RA, Everhard-Hard Y (1975) Optically induced eye torsion. I. Fusion cyclovergence. Graefes Arch Clin Exp Ophthalmol 195:231-239
Cullen KE (2004) Sensory signals during active versus passive movement. Curr Opin Neurobiol 14:698-706
Cullen KE, Roy JE (2004) Signal processing in the vestibular system during active versus passive head movements. J Neurophysiol 91:1919-1933

Dai M, McGarvie LA, Kozlovskaya I, Raphan T, Cohen B (1994) Effects of spaceflight on ocular counterrolling and the spatial orientation of the vestibular system. Exp Brain Res 102:45-56

Darlot C, Lopez-Barneo J, Tracey D (1981) Asymmetries of vertical vestibular nystagmus in the cat. Exp Brain Res 41:420-426

Das VE, Yaniglos S, Leigh RJ (2000) The influence of light on modulation of the human vestibulo-ocular reflex. J Vestib Res 10:51-55

Davids K, Glazier P, Araujo D, Bartlett R (2003) Movement systems as dynamical systems: the functional role of variability and its implications for sports medicine. Sports Med 33:245-260

Davis JR, Jennings RT, Beck BG (1993a) Comparison of treatment strategies for space motion sickness. Acta Astronaut 29:587-591

Davis JR, Jennings RT, Beck BG, Bagian JP (1993b) Treatment efficacy of intramuscular promethazine for space motion sickness. Aviat Space Environ Med. 64:230-233.

Davis JR, Vanderploeg JM, Santy PA, Jennings RT, Stewart DF (1988) Space motion sickness during 24 flights of the space shuttle. Aviat Space Environ Med 59:1185-1189

Della Santina CC, Potyagaylo V, Migliaccio AA, Minor LB, Carey JP (2005) Orientation of human semicircular canals measured by three-dimensional multiplanar CT reconstruction. J Assoc Res Otolaryngol 6:191-206

Demer JL (1992) Mechanisms of human vertical visual-vestibular interaction. J Neurophysiol 68:2128-2146

Demer JL (1995) Evaluation of vestibular and visual oculomotor function. Otolaryngol Head Neck Surg 112:16-35

Demer JL, Amjadi F (1993) Dynamic visual acuity of normal subjects during vertical optotype and head motion. Invest Ophthalmol Vis Sci 34:1894-1906

Demer JL, Porter FI, Goldberg J, Jenkins HA, Schmidt K (1989) Adaptation to telescopic spectacles: vestibulo-ocular reflex plasticity. Invest Ophthalmol Vis Sci 30:159-170

Denise P, Etard O, Zupan L, Darlot C (1996) Motion sickness during off-vertical axis rotation: prediction by a model of sensory interactions and correlation with other forms of motion sickness. Neurosci Lett 203:183-186

Diamond SG, Markham CH (1991) Prediction of space motion sickness susceptibility by disconjugate eye torsion in parabolic flight. Aviat Space Environ Med 62:201-205.

Diamond SG, Markham CH (1992a) Ocular torsion as a test of the asymmetry hypothesis of space motion sickness. Acta Astronaut 27:11-17.

Diamond SG, Markham CH (1992b) Validating the hypothesis of otolith asymmetry as a cause of space motion sickness. Ann Ny Acad Sci 656:725-731

Diamond SG, Markham CH (1998) The effect of space missions on gravity-responsive torsional eye movements. J Vestib Res 8:217-231

Diamond SG, Markham CH, Money KE (1990) Instability of ocular torsion in zero gravity: possible implications for space motion sickness. Aviat Space Environ Med 61:899-905

Diamond SG, Markham CH, Simpson NE, Curthoys IS (1979) Binocular counterrolling in humans during dynamic rotation. Acta Otolaryngol 87:490-498

Donaldson IM, Hawthorne ME (1979) Coding of visual information by units in the cat cerebellar vermis. Exp Brain Res 34:27-48
Einstein A (1908) Über das Relativitätsprinzip und die aus demselben gezogenen Folgerungen. Jahrb Radioakt 4:411-462
Fender D, Julesz B (1967) Extension of Panum's fusional area in binocularly stabilized vision. J Opt Soc Am 57:819-830
Fernandez C, Goldberg JM (1971) Physiology of peripheral neurons innervating semicircular canals of the squirrel monkey. II. Response to sinusoidal stimulation and dynamics of peripheral vestibular system. J Neurophysiol 34:661-675
Fernandez C, Goldberg JM (1976a) Physiology of peripheral neurons innervating otolith organs of the squirrel monkey. I. Response to static tilts and to long-duration centrifugal force. J Neurophysiol 39:970-984
Fernandez C, Goldberg JM (1976b) Physiology of peripheral neurons innervating otolith organs of the squirrel monkey. II. Directional selectivity and force-response relations. J Neurophysiol 39:985-995
Fetter M, Misslisch H, Sievering D, Tweed D (1995) Effects of full-field visual input on the three-dimensional properties of the human vestibuloocular reflex. J Vestib Res 5:201-209
Flook JP, McGonigle BO (1977) Serial adaptation to conflicting prismatic rearrangement effects in monkey and man. Perception 6:15-29
Fluur E (1970) The interaction between the utricle and the saccule. Acta Otolaryngol 69:17-24
Fluur E, Mellstrom A (1970a) Saccular stimulation and oculomotor reactions. Laryngoscope 80:1713-1721
Fluur E, Mellstrom A (1970b) Utricular stimulation and oculomotor reactions. Laryngoscope 80:1701-1712
Fuchs AF, Kornhuber HH (1969) Extraocular muscle afferents to the cerebellum of the cat. J Physiol 200:713-722
Gauthier GM, Robinson DA (1975) Adaptation of the human vestibuloocular reflex to magnifying lenses. Brain Res 92:331-335
Gellman RS, Carl JR, Miles FA (1990) Short latency ocular-following responses in man. Vis Neurosci 5:107-122
Gerrits NM, Epema AH, van Linge A, Dalm E (1989) The primary vestibulocerebellar projection in the rabbit: absence of primary afferents in the flocculus. Neurosci Lett 105:27-33
Glass L, Mackey MC (1988) From Clocks to Chaos: The Rhythms of Life. Princeton University Press
Goldberg JM, Wilson VJ, Cullen KE (2012a) The cerebellum and the vestibular system. In: The vestibular system: A sixth sense. Oxford University Press, New York, pp 364-405
Goldberg JM, Wilson VJ, Cullen KE (2012b) Neuroanatomy of central vestibular pathways. In: The Vestibular System: A Sixth Sense. Oxford University Press, New York, pp 137-190
Goldberg JM, Wilson VJ, Cullen KE (2012c) The vestibular system in everyday life. In: The vestibular system: A sixth sense. Oxford University Press, New York, pp 3-20

Gonshor A, Melvill Jones G (1976) Extreme vestibulo-ocular adaptation induced by prolonged optical reversal of vision. J Physiol 256:381-414
Goto F, Meng H, Bai R, Sato H, Imagawa M, Sasaki M, Uchino Y (2004) Eye movements evoked by selective saccular nerve stimulation in cats. Auris Nasus Larynx 31:220-225
Graybiel A, Lackner JR (1983) Motion sickness: acquisition and retention of adaptation effects compared in three motion environments. Aviat Space Environ Med 54:307-311
Graybiel A, Miller EF, Homick JL (1977) Experiment M131. Human vestibular function. In: Johnston RS, Dietlein LF (eds) Biomedical Results from Skylab. NASA, Washington, D.C., pp 74-103
Graybiel A, Wood CD, Miller EF, Cramer DB (1968) Diagnostic criteria for grading the severity of acute motion sickness. Aerosp Med 39:453-455
Grunfeld EA, Morland AB, Bronstein AM, Gresty MA (2000) Adaptation to oscillopsia: a psychophysical and questionnaire investigation. Brain 123 (Pt 2):277-290
Guedry FE (1974) Psychophysics of vestibular sensation. In: Kornhuber HH (ed) Handbook of Sensory Physiology. Springer Verlag, Berlin, pp 3-154
Guedry FE, Benson AJ (1970) Tracking performance during sinusoidal stimulation of the vertical and horizontal semicircular canals. In: Recent Advances in Aerospace Medicine. Springer, pp 276-288
Guyton DL (1988) Ocular torsion: sensorimotor principles. Graefes Arch Clin Exp Ophthalmol 226:241-245
Hall CD, Heusel-Gillig L, Tusa RJ, Herdman SJ (2010) Efficacy of gaze stability exercises in older adults with dizziness. J Neurol Phys Ther 34:64-69
Halmagyi GM, Curthoys IS, Cremer PD, Henderson CJ, Todd MJ, Staples MJ, D'Cruz DM (1990) The human horizontal vestibulo-ocular reflex in response to high-acceleration stimulation before and after unilateral vestibular neurectomy. Exp Brain Res 81:479-490
Han YH, Kumar AN, Reschke MF, Somers JT, Dell'Osso LF, Leigh RJ (2005) Vestibular and non-vestibular contributions to eye movements that compensate for head rotations during viewing of near targets. Exp Brain Res 165:294-304
Hara N, Steffen H, Roberts DC, Zee DS (1998) Effect of horizontal vergence on the motor and sensory components of vertical fusion. Invest Ophthalmol Vis Sci 39:2268-2276
Harlow HF (1949) The formation of learning sets. Psychol Rev 56:51-65
Harm DL, Parker DE (1994) Preflight adaptation training for spatial orientation and space motion sickness. J Clin Pharmacol 34:618-627
Helling K, Hausmann S, Clarke AH, Scherer H (2003) Experimentally induced motion sickness in fish: possible role of the otolith organs. Acta Otolaryngol 123:488-492
Herdman SJ (2000) Vestibular Rehabilitation. F.A. Davis Company, Philadelphia
Herdman SJ, Hall, C. D., Schubert, M. C., Das, V. E., Tusa, R. J. (2007) Recovery of dynamic visual acuity in bilateral vestibular hypofunction. Arch Otolaryngol Head Neck Surg 133:383-389
Herdman SJ, Schubert, M. C., Das, V. E., Tusa, R. J. (2003) Recovery of dynamic visual acuity in unilateral vestibular hypofunction. Arch Otolaryngol Head Neck Surg 129:819-824

Herdman SJ, Tusa RJ, Blatt P, Suzuki A, Venuto PJ, Roberts DC (1998) Computerized dynamic visual acuity test in the assessment of vestibular deficits. Am J Otol 19:790-796

Highstein SM, Holstein GR (2006) The anatomy of the vestibular nuclei. Prog Brain Res 151:157-203

Hikosaka O, Maeda M (1973) Cervical effects on abducens motoneurons and their interaction with vestibulo-ocular reflex. Exp Brain Res 18:512-530

Hilbig R, Anken RH, Sonntag G, Hohne S, Henneberg J, Kretschmer N, Rahmann H (2002) Effects of altered gravity on the swimming behaviour of fish. Adv Space Res 30:835-841

Hildebrandt KJ, Benda J, Hennig RM (2011) Multiple arithmetic operations in a single neuron: the recruitment of adaptation processes in the cricket auditory pathway depends on sensory context. J Neurosci 31:14142-14150

Hoagland H (1930) The Weber-Fechner law and the all-or-none theory. J Gen Psychol 3:351-373

Hoffman RA, Brookler KH (1978) Underrated neurotologic symptoms. Laryngoscope 88:1127-1138

Homick JL, Reschke MF, Vanderploeg JM (1987) Prediction of susceptibility to space motion sickness. In: Graham MD, Kemink JL (eds) The Vestibular System: Neurophysiologic and Clinical Research. Raven Press, New York, pp 39-49

Houtman WA, Roze JH, Scheper W (1977) Vertical motor fusion. Doc Ophthalmol 44:179-185

Houtman WA, Roze JH, Scheper W (1981) Vertical vergence movements. Doc Ophthalmol 51:199-207

Howard IP, Allison RS, Zacher JE (1997) The dynamics of vertical vergence. Exp Brain Res 116:153-159

Igarashi M, Takahashi M, Kubo T, Levy JK, Homick JL (1979) Effect of macular ablation on vertical optokinetic nystagmus in the squirrel monkey. ORL J Otorhinolaryngol Relat Spec 40:312-318

Ijiri K (1995) How the four fish astronauts were selected. In: Ijiri K (ed) The First Vertebrate Mating in Space—A Fish Story. Ricut, Tokyo, pp 39-50

Istl-Lenz Y, Hyden, D., Schwarz, D. W. (1985) Response of the human vestibulo-ocular reflex following long-term 2x magnified visual input. Exp Brain Res 57:448-455

Isu N, Graf W, Sato H, Kushiro K, Zakir M, Imagawa M, Uchino Y (2000) Sacculo-ocular reflex connectivity in cats. Exp Brain Res 131:262-268

Ito M (1972) Neural design of the cerebellar motor control system. Brain Res 40:81-84

Jell RM, Stockwell CW, Turnipseed GT, Guedry FE (1988) The influence of active versus passive head oscillation, and mental set on the human vestibulo-ocular reflex. Aviat Space Environ Med 59:1061-1065

Johnston JL, Sharpe JA (1994) The initial vestibulo-ocular reflex and its visual enhancement and cancellation in humans. Exp Brain Res 99:302-308

Jorns-Haderli M, Straumann D, Palla A (2007) Accuracy of the bedside head impulse test in detecting vestibular hypofunction. J Neurol Neurosurg Psychiatry 78:1113-1118

Karmali F (2007) Vertical eye misalignments during pitch rotation and vertical translation: evidence for bilateral asymmetries and plasticity in the otolith-ocular

reflex. In: Biomedical Engineering, vol PhD. Johns Hopkins University, Baltimore, MD
Karmali F, Ramat S, Shelhamer M (2006) Vertical skew due to changes in gravitoinertial force: a possible consequence of otolith asymmetry. J Vestib Res 16:117-125
Karmali F, Shelhamer M (2008) The dynamics of parabolic flight: flight characteristics and passenger percepts. Acta Astronaut 63:594-602
Kertesz AE (1981) Effect of stimulus size on fusion and vergence. J Opt Soc Am 71:289-293
Kertesz AE, Jones RW (1970) Human cyclofusional response. Vision Res 10:891-896
Kertesz AE, Sullivan MJ (1978) The effect of stimulus size on human cyclofusional response. Vision Res 18:567-571
Kevetter GA, Perachio AA (1986) Distribution of vestibular afferents that innervate the sacculus and posterior canal in the gerbil. J Comp Neurol 254:410-424
Kluzik J, Diedrichsen J, Shadmehr R, Bastian AJ (2008) Reach adaptation: what determines whether we learn an internal model of the tool or adapt the model of our arm? J Neurophysiol 100:1455-1464
Kompanejetz S (1925) On compensatory eye movements in deaf-mutes. Acta Otolaryngol 7:323-334
Kondrachuk AV (2003) Qualitative model of otolith-ocular asymmetry in vertical eccentric rotation experiments. Hear Res 178:59-69
Kornilova L, Iakovleva I, Tarasov I, Gorgiladze G (1983) Vestibular dysfunction in cosmonauts during adaptation to zero-g and readaptation to 1 g. In: (International Union of Physiological Sciences, Commission on Gravitational Physiology, Annual Meeting, 5 th, Moscow, USSR, July 26-29, 1983) Physiologist, Supplement(ISSN 0031-9376), vol 26
Korte GE, Mugnaini E (1979) The cerebellar projection of the vestibular nerve in the cat. J Comp Neurol 184:265-277
Kotchabhakdi N, Walberg F (1978) Cerebellar afferent projections from the vestibular nuclei in the cat: an experimental study with the method of retrograde axonal transport of horseradish peroxidase. Exp Brain Res 31:591-604
Krakauer JW (2009) Motor learning and consolidation: the case of visuomotor rotation. In: Sternad D (ed) Advances in Experimental Medicine and Biology. Springer, pp 405-421
Kramer P, Shelhamer M, Zee DS (1998) Short-term vestibulo-ocular adaptation: influence of context. Otolaryngol Head Neck Surg 119:60-64
Lackner JR, Dizio P (2006) Space motion sickness. Exp Brain Res 175:377-399
Lackner JR, Graybiel A (1982) Rapid perceptual adaptation to high gravitoinertial force levels: evidence for context-specific adaptation. Aviat Space Environ Med 53:766-769
Lackner JR, Graybiel A (1986) Head movements in non-terrestrial force environments elicit motion sickness: implications for the etiology of space motion sickness. Aviat Space Environ Med 57:443-448
Lackner JR, Graybiel A, Johnson WH, Money KE (1987) Asymmetric otolith function and increased susceptibility to motion sickness during exposure to variations in gravitoinertial acceleration level. Aviat Space Environ Med 58:652-657

Lancaster WB (1939) Detecting, measuring, plotting and interpreting ocular deviations. Arch Opthalmol 22:867-880
Laurutis VP, Robinson DA (1986) The vestibulo-ocular reflex during human saccadic eye movements. J Physiol 373:209-233
Leigh RJ, Zee DS (2006a) Diagnosis of peripheral ocular motor palsies and strabismus. In: Gilman S (ed) The Neurology of Eye Movements, 4th edn. Oxford University Press, New York, pp 385-474
Leigh RJ, Zee DS (2006b) Methods available for measuring eye movements. In: Gilman S (ed) The Neurology of Eye Movements, 4th edn. Oxford University Press, New York, pp 722-725
Leigh RJ, Zee DS (2006c) The saccadic system. In: Gilman S (ed) The Neurology of Eye Movements, 4th edn. Oxford University Press, New York, pp 108-187
Leigh RJ, Zee DS (2006d) Vergence eye movements. In: Gilman S (ed) The Neurology of Eye Movements, 4th edn. Oxford University Press, New York, pp 343-382
Lisberger SG, Miles FA, Optican LM (1983) Frequency-selective adaptation: evidence for channels in the vestibulo-ocular reflex? J Neurosci 3:1234-1244
Locke J (2003) Space motion sickness symptomatology: 20 years' experience of NASA's space shuttle program. Aviat Space Environ Med 74:101
Loe PR, Tomko DL, Werner G (1973) The neural signal of angular head position in primary afferent vestibular nerve axons. J Physiol 230:29-50
Longridge NS, Mallinson AI (1984) A discussion of the dynamic illegible "E" test: a new method of screening for aminoglycoside vestibulotoxicity. Otolaryngol Head Neck Surg 92:671-677
Longridge NS, Mallinson AI (1987) The dynamic illegible E-test. A technique for assessing the vestibulo-ocular reflex. Acta Otolaryngol 103:273-279
Lowenstein O, Sand A (1940) The mechanism of the semicircular canal. A study of the responses of single-fibre preparations to angular accelerations and to rotation at constant speed. Proc R Soc Lond [Biol] 129:256-275
Maklad A, Fritzsch B (2003) Partial segregation of posterior crista and saccular fibers to the nodulus and uvula of the cerebellum in mice, and its development. Brain Res Dev Brain Res 140:223-236
Markham CH, Diamond SG (1992) Further evidence to support disconjugate eye torsion as a predictor of space motion sickness. Aviat Space Environ Med 63:118-121
Markham CH, Diamond SG (1993) A predictive test for space motion sickness. J Vestib Res 3:289-295
Markham CH, Diamond SG, Stoller DF (2000) Parabolic flight reveals independent binocular control of otolith- induced eye torsion. Arch Ital Biol 138:73-86
Marr D (1969) A theory of cerebellar cortex. J Physiol 202:437-470
Martin TA, Keating JG, Goodkin HP, Bastian AJ, Thach WT (1996) Throwing while looking through prisms 2. Specificity and storage of multiple gaze-throw calibrations. Brain 119:1199-1211
Matsuo V, Cohen B (1984) Vertical optokinetic nystagmus and vestibular nystagmus in the monkey: up-down asymmetry and effects of gravity. Exp Brain Res 53:197-216
Matsuo V, Cohen B, Raphan T, de Jong V, Henn V (1979) Asymmetric velocity storage for upward and downward nystagmus. Brain Res 176:159-164

Matta FV, Enticott JC (2004) The effects of state of alertness on the vestibulo-ocular reflex in normal subjects using the vestibular rotational chair. J Vestib Res 14:387-391
Maxwell JS, Schor CM (1996) Adaptation of vertical eye alignment in relation to head tilt. Vision Res 36:1195-1205
Maxwell JS, Schor CM (1999) Adaptation of torsional eye alignment in relation to head roll. Vision Res 39:4192-4199
Maxwell JS, Schor CM (2006) The coordination of binocular eye movements: vertical and torsional alignment. Vision Res 46:3537-3548
Mayne R (1974) A systems concept of the vestibular organs. In: Kornhuber HH (ed) Handbook of Sensory Physiology. Springer Verlag, Berlin Heidelberg New York, pp 493-580
Melvill Jones G, Berthoz A, Segal B (1984) Adaptive modification of the vestibulo-ocular reflex by mental effort in darkness. Exp Brain Res 56:149-153
Melvill Jones G, Guitton D, Berthoz A (1988) Changing patterns of eye-head coordination during 6 h of optically reversed vision. Exp Brain Res 69:531-544
Merfeld DM (2003) Rotation otolith tilt-translation reinterpretation (ROTTR) hypothesis: a new hypothesis to explain neurovestibular spaceflight adaptation. J Vestib Res 13:309-320
Merfeld DM, Park S, Gianna-Poulin C, Black FO, Wood SJ (2005) Vestibular perception and action employ qualitatively different mechanisms. I. Frequency response of VOR and perceptual responses during translation and tilt. J Neurophysiol 94:186-198
Merfeld DM, Zupan L, Peterka RJ (1999) Humans use internal models to estimate gravity and linear acceleration. Nature 398:615-618
Mhoon EE, Bernstein LP, Towle VL (1997) Saccular influence on the otolith-spinal reflex and posture during sudden falls of the cat. Am J Otol 18:86-92
Michel EL, Johnston RS, Dietlein LF (1976) Biomedical results of the Skylab Program. Life Sci Space Res 14:3-18
Migliaccio AA, Della Santina CC, Carey JP, Minor LB, Zee DS (2006) The effect of binocular eye position and head rotation plane on the human torsional vestibuloocular reflex. Vision Res 46:2475-2486
Miles FA, Eighmy BB (1980) Long-term adaptive changes in primate vestibuloocular reflex. I. Behavioral observations. J Neurophysiol 43:1406-1425
Miles FA, Lisberger SG (1981) Plasticity in the vestibulo-ocular reflex: a new hypothesis. Annu Rev Neurosci 4:273-299
Misslisch H, Tweed D, Hess BJ (2001) Stereopsis outweighs gravity in the control of the eyes. J Neurosci 21:RC126
Moller C, Odkvist LM, White V, Cyr D (1990a) The plasticity of compensatory eye movements in rotatory tests. I. The effect of alertness and eye closure. Acta Otolaryngol 109:15-24
Moller C, White V, Odkvist LM (1990b) Plasticity of compensatory eye movements in rotatory tests. II. The effect of voluntary, visual, imaginary, auditory and proprioceptive mechanisms. Acta Otolaryngol 109:168-178
Moore B (1981) Principal component analysis in linear systems: Controllability, observability, and model reduction. IEEE Trans Autom Control 26:17-32

Mulavara AP, Cohen HS, Bloomberg JJ (2009) Critical features of training that facilitate adaptive generalization of over ground locomotion. Gait Posture 29:242-248

Mullane M (2006) Riding Rockets: The Outrageous Tales of a Space Shuttle Astronaut. Scribner, New York

Murasugi CM, Howard IP (1989) Up-down asymmetry in human vertical optokinetic nystagmus and afternystagmus: contributions of the central and peripheral retinae. Exp Brain Res 77:183-192

NASA (2009) Research and technology development to support crew health and performance in space exploration missions: NASA research announcement NNJ09ZSA002N. In: National Aeronautics and Space Administration, Johnson Space Center: Exploration Systems Mission Directorate - Human Research Program, Houston

Nelson JI (1975) Globality and stereoscopic fusion in binocular vision. J Theor Biol 49:1-88

Newlands SD, Purcell IM, Kevetter GA, Perachio AA (2002) Central projections of the utricular nerve in the gerbil. J Comp Neurol 452:11-23

Newlands SD, Vrabec JT, Purcell IM, Stewart CM, Zimmerman BE, Perachio AA (2003) Central projections of the saccular and utricular nerves in macaques. J Comp Neurol 466:31-47

Noda H, Sugita S, Ikeda Y (1990) Afferent and efferent connections of the oculomotor region of the fastigial nucleus in the macaque monkey. J Comp Neurol 302:330-348

Nooij SAE, Vanspauwen R, Bos JE, Wuyts FL (2011) A re-investigation of the role of utricular asymmetries in space motion sickness. J Vestibul Res-Equil 21:141-151

Norre ME, Beckers A (1989) Vestibular habituation training: exercise treatment for vertigo based upon the habituation effect. Otolaryngol Head Neck Surg 101:14-19

Ogino S, Kato I, Sakuma A, Takahashi K, Takeyama I (1996) Vertical optokinetic nystagmus in normal individuals. Acta Otolaryngol (Supp) 522:38-42

Ogle KN (1964) Binocular Vision. Hafner, New York

Ogle KN, Prangen AD (1953) Observations on vertical divergences and hyperphorias. AMA Arch Ophthalmol 49:313-334

Oman CM (1982) A heuristic mathematical model for the dynamics of sensory conflict and motion sickness. Acta Otolaryngol (Supp) 392:1-44

Oman CM, Lichtenberg BK, Money KE (1990) Space motion sickness monitoring experiment: Spacelab 1. In: Crampton GH (ed) Motion and Space Sickness. CRC Press, Boca Raton, FL, pp 217-246

Oman CM, Pouliot CF, Natapoff A (1996) Horizontal angular VOR changes in orbital and parabolic flight: human neurovestibular studies on SLS-2. J Appl Physiol 81:69-81

Paige GD (1992) Senescence of human visual-vestibular interactions. 1. Vestibulo-ocular reflex and adaptive plasticity with aging. J Vestib Res 2:133-151

Paige GD, Telford L, Seidman SH, Barnes GR (1998) Human vestibuloocular reflex and its interactions with vision and fixation distance during linear and angular head movement. J Neurophysiol 80:2391-2404

Paige GD, Tomko DL (1991a) Eye movement responses to linear head motion in the squirrel monkey. I. Basic characteristics. J Neurophysiol 65:1170-1182

Paige GD, Tomko DL (1991b) Eye movement responses to linear head motion in the squirrel monkey. II. Visual-vestibular interactions and kinematic considerations. J Neurophysiol 65:1183-1196

Paloski WH, Reschke MF, Black FO, Doxey DD, Harm DL (1992) Recovery of postural equilibrium control following spaceflight. Ann NY Acad Sci 656:747-754

Panum PL (1858) Physiologische Untersuchungen über das Sehen mit zwei Augen. Schwer

Parker DE (2003) Spatial perception changes associated with space flight: implications for adaptation to altered inertial environments. J Vestib Res 13:331-343

Parker DE, Reschke MF, Arrott AP, Homick JL, Lichtenberg BK (1985) Otolith tilt-translation reinterpretation following prolonged weightlessness: implications for preflight training. Aviat Space Environ Med 56:601-606

Perlmutter AL, Kertesz AE (1978) Measurement of human vertical fusional response. Vision Res 18:219-223

Peterka RJ (1992) Response characteristics of the human torsional vestibuloocular reflex. Ann NY Acad Sci 656:877-879

Peters BT, Miller CA, Brady RA, Richards JT, Mulavara AP, Bloomberg JJ (2011) Dynamic visual acuity during walking after long-duration spaceflight. Aviat Space Environ Med 82:463-466

Precht W, Llinas R (1969) Functional organization of the vestibular afferents to the cerebellar cortex of frog and cat. Exp Brain Res 9:30-52

Purcell IM, Perachio AA (2001) Peripheral patterns of terminal innervation of vestibular primary afferent neurons projecting to the vestibulocerebellum in the gerbil. J Comp Neurol 433:48-61

Putcha L, Berens KL, Marshburn TH, Ortega HJ, Billica RD (1999) Pharmaceutical use by U.S. astronauts on space shuttle missions. Aviat Space Environ Med 70:705-708

Pyykko I, Schalen L, Matsuoka I (1985) Transdermally administered scopolamine vs. dimenhydrinate. II. Effect on different types of nystagmus. Acta Otolaryngol 99:597-604

Reason JT, Brand JJ (1975) Motion Sickness. Academic Press, London

Reschke MF, Bloomberg JJ, Harm DL, Paloski WH (1994) Space flight and neurovestibular adaptation. J Clin Pharmacol 34:609-617

Reschke MF, Bloomberg JJ, Harm DL, Paloski WH, Layne C, McDonald V (1998) Posture, locomotion, spatial orientation, and motion sickness as a function of space flight. Brain Res Rev 28:102-117

Reschke MF, Fisher EA, Kofman IS, Cerisano JM, Harm DL, Bloomberg JJ (2011) Walk on floor eyes closed test: a unique test of spaceflight induced ataxia. In: Space Forum 2011 - Dedicated to the 50th Anniversary of the First Man in Space, Moscow, Russia

Reschke MF, Kornilova LN, Harm DL, Bloomberg JJ, Paloski WH (1996) Neurosensory and sensory-motor function. In: Leach Huntoon CS, Antipov VV, Grigoriev AI (eds) Space Biology and Medicine, pp 135-193

Riley BB, Moorman SJ (2000) Development of utricular otoliths, but not saccular otoliths, is necessary for vestibular function and survival in zebrafish. J Neurobiol 43:329-337

Roberts DC, Shelhamer M, Wong A (2008) A new "wireless" search-coil system. Proceedings of the Eye Tracking Research and Applications Symposium (Etra 2008):197-204

Robinson DA (1963) A method of measuring eye movement using a scleral search coil in a magnetic field. IEEE Trans Biomed Electron BME-10:137-145

Robinson DA (1975) Oculomotor control signals. In: Bach-y-Rita P, Lennerstrand G (eds) Basic Mechanisms of Ocular Motility and Their Clinical Implications. Pergamon Press, Oxford, pp 337-374

Roller CA, Cohen HS, Kimball KT, Bloomberg JJ (2001) Variable practice with lenses improves visuo-motor plasticity. Brain Res Cogn Brain Res 12:341-352

Rubin ML (1974) Optics for Clinicians. Triad Scientific Publishers, Gainsville

Rude SA, Baker JF (1988) Dynamic otolith stimulation improves the low frequency horizontal vestibulo-ocular reflex. Exp Brain Res 73:357-363

Sakaguchi M, Taguchi K, Sato K, Akahira T, Netsu K, Katsuno S, Ishiyama T (1997) Vestibulo-ocular reflex and visual vestibulo-ocular reflex during sinusoidal rotation in children. Acta Otolaryngol (Supp) 528:70-73

Sato H, Imagawa M, Isu N, Uchino Y (1997) Properties of saccular nerve-activated vestibulospinal neurons in cats. Exp Brain Res 116:381-388

Schaefer KP, Meyer DL (1974) Compensation of vestibular lesions. In: Kornhuber HH (ed) Handbook of Sensory Physiology. Springer, New York, pp 463-490

Scherer H, Helling K, Hausmann S, Clarke AH (1997) On the origin of interindividual susceptibility to motion sickness. Acta Otolaryngol 117:149-153

Schmidt RA (1975) A schema theory of discrete motor skill learning. Psychol Rev 82:225-260

Schubert MC, Della Santina CC, Shelhamer M (2008) Incremental angular vestibulo-ocular reflex adaptation to active head rotation. Exp Brain Res 191:435-446

Schubert MC, Migliaccio AA, Santina CCD (2006) Modification of compensatory saccades after aVOR gain recovery. J Vestibul Res-Equil 16:285-291

Schwarz U, Miles FA (1991) Ocular responses to translation and their dependence on viewing distance. I. Motion of the observer. J Neurophysiol 66:851-864

Seidler RD (2004) Multiple motor learning experiences enhance motor adaptability. J Cogn Neurosci 16:65-73

Seidler RD (2007) Aging affects motor learning but not savings at transfer of learning. Learn Mem 14:17-21

Seidman SH, Telford L, Paige GD (1998) Tilt perception during dynamic linear acceleration. Exp Brain Res 119:307-314

Sharma K, Abdul-Rahim AS (1992) Vertical fusion amplitude in normal adults. Am J Ophthalmol 114:636-637

Shelhamer M, Beaton KH (2009, unpublished raw data) Color and neck vibration serve as secondary augment cues to enhance context-specific adaptation of saccade gain.

Shelhamer M, Beaton KH (2012) Pre-flight sensorimotor adaptation protocols for suborbital flight. J Vestib Res 22:139-144

Shelhamer M, Clendaniel RA (2002a) Context-specific adaptation of saccade gain. Exp Brain Res 146:441-450

Shelhamer M, Clendaniel RA (2002b) Sensory, motor, and combined contexts for context-specific adaptation of saccade gain in humans. Neurosci Lett 332:200-204
Shelhamer M, Clendaniel RA, Roberts DC (2002) Context-specific adaptation of saccade gain in parabolic flight. J Vestib Res 12:211-221
Shelhamer M, Robinson DA, Tan HS (1992) Context-specific adaptation of the gain of the vestibulo-ocular reflex in humans. J Vestib Res 2:89-96
Shelhamer M, Zee DS (2003) Context-specific adaptation and its significance for neurovestibular problems of space flight. J Vestib Res 13:345-362
Shojaku H, Watanabe Y, Ito M, Mizukoshi K, Yajima K, Sekiguchi C (1993) Effect of transdermally administered scopolamine on the vestibular system in humans. Acta Otolaryngol (Supp) 504:41-45
Shumway-Cook A, Horak FB (1990) Rehabilitation strategies for patients with vestibular deficits. Neurol Clin 8:441-457
Si X, Angelaki DE, Dickman JD (1997) Response properties of pigeon otolith afferents to linear acceleration. Exp Brain Res 117:242-250
Silver RA (2010) Neuronal arithmetic. Nat Rev Neurosci 11:474-489
Smith T, Husbands P, Layzell P, O'Shea M (2002) Fitness landscapes and evolvability. Evol Comput 10:1-34
Spoor F, Wood B, Zonneveld F (1994) Implications of early hominid labyrinthine morphology for evolution of human bipedal locomotion. Nature 369:645-648
Steinhausen W (1933) Über die beobachtung der cupula in den bogengängsampullen des labyrinthes bei des lebenden hechts. Archiv für die Gesante Physiologie des Meschen und der Tierre 232:500-512
Stergiou N, Decker LM (2011) Human movement variability, nonlinear dynamics, and pathology: is there a connection? Hum Mov Sci 30:869-888
Stergiou N, Harbourne R, Cavanaugh J (2006) Optimal movement variability: a new theoretical perspective for neurologic physical therapy. J Neurol Phys Ther 30:120-129
Suzuki JI, Tokumasu K, Goto K (1969) Eye movements from single utricular nerve stimulation in the cat. Acta Otolaryngol 68:350-362
Szentagothai J (1950) The elementary vestibulo-ocular reflex arc. J Neurophysiol 13:395-407
Teleford L, Seidman SH, Paige GD (1997) Dynamics of squirrel monkey linear vestibuloocular reflex and interactions with fixation distance. J Neurophysiol 78:1775-1790
Thornton WE, Biggers WP, Thomas WG, Pool SL, Thagard NE (1985) Electronystagmography and audio potentials in space flight. Laryngoscope 95:924-932
Thornton WE, Moore TP, Pool SL (1987a) Space motion sickness: characterization and etiology. In: Bungo M, Bagian T, Bowman M, Levitan B (eds) Results of the Life Sciences DSOs Conducted Aboard the Space Shuttle 1981-1986. NASA Space Biomedical Research Institute, Houston, TX, pp 159-170
Thornton WE, Moore TP, Pool SL, Vanderploeg JM (1987b) Clinical characterization and etiology of space motion sickness. Aviat Space Environ Med 58:A1-8
Thunnissen IE, Epema AH, Gerrits NM (1989) Secondary vestibulocerebellar mossy fiber projection to the caudal vermis in the rabbit. J Comp Neurol 290:262-277

Tian J, Crane BT, Demer JL (2000) Vestibular catch-up saccades in labyrinthine deficiency. Exp Brain Res 131:448-457
Tomko DL, Wall CD, Robinson FR, Staab JP (1988) Influence of gravity on cat vertical vestibulo-ocular reflex. Exp Brain Res 69:307-314
Tomlinson RD, Saunders GE, Schwarz DW (1980) Analysis of human vestibulo-ocular reflex during active head movements. Acta Otolaryngol 90:184-190
Tweed D, Sievering D, Misslisch H, Fetter M, Zee DS, Koenig E (1994) Rotational kinematics of the human vestibuloocular reflex. I. Gain matrices. J Neurophysiol 72:2467-2479
Uchino Y, Sasaki M, Sato H, Imagawa M, Suwa H, Isu N (1996) Utriculoocular reflex arc of the cat. J Neurophysiol 76:1896-1903
Uchino Y, Sato H, Kushiro K, et al. (1999) Cross-striolar and commissural inhibition in the otolith system. Ann N Y Acad Sci 871:162-172
Van den Berg AV, Collewijn H (1988) Directional asymmetries of human optokinetic nystagmus. Exp Brain Res 70:597-604
Van der Steen J, Collewijn H (1984) Ocular stability in the horizontal, frontal and sagittal planes in the rabbit. Exp Brain Res 56:263-274
Viéville T, Clément G, Lestienne F, Berthoz A (1986) Adaptive modifications of the optokinetic vestibulo-ocular reflexes in microgravity. In: Keller EL, Zee DS (eds) Adaptive Processes in Visual and Oculomotor Systems. Pergamon Press, New York, pp 111-120
Viirre E, Tweed D, Milner K, Vilis T (1986) A reexamination of the gain of the vestibuloocular reflex. J Neurophysiol 56:439-450
Vogel H, Kass JR (1986) European vestibular experiments on the Spacelab-1 mission: 7. Ocular counterrolling measurements pre- and post-flight. Exp Brain Res 64:284-290
von Baumgarten RJ (1986) European vestibular experiments on the Spacelab-1 mission: 1. Overview. Exp Brain Res 64:239-246
von Baumgarten RJ, Baldrighi G, Shillinger GL, Jr. (1972) Vestibular behavior of fish during diminished G-force and weightlessness. Aerosp Med 43:626-632
von Baumgarten RJ, Thümler R (1979) A model for vestibular function in altered gravitational states. Life Sci Space Res 17:161-170
von Bechterew W (1909) Die Funktion der Nervenzentren. Jena: Gustav Fischer
von Tschermak-Seysenegg A (1942) Einführung in die physiologische optik. Springer-Verlag, Berlin
Voogd J, Gerrits NM, Ruigrok TJ (1996) Organization of the vestibulocerebellum. Ann N Y Acad Sci 781:553-579
Waterston JA, Barnes GR (1992) Visual-vestibular interaction during head-free pursuit of pseudorandom target motion in man. J Vestib Res 2:71-88
Watt DG, Money KE, Bondar RL, Thirsk RB, Garneau M, Scully-Power P (1985) Canadian medical experiments on Shuttle flight 41-G. Can Aeronaut Space J. 31:215-226.
Weber KP, Aw ST, Todd MJ, McGarvie LA, Curthoys IS, Halmagyi GM (2008) Head impulse test in unilateral vestibular loss: vestibulo-ocular reflex and catch-up saccades. Neurology 70:454-463

Weissman BM, DiScenna AO, Ekelman BL, Leigh RJ (1989) Effect of eyelid closure and vocalization upon the vestibulo-ocular reflex during rotational testing. Ann Otol Rhinol Laryngol 98:548-550
Welch RB, Bridgeman B, Anand S, Browman KE (1993) Alternating prism exposure causes dual adaptation and generalization to a novel displacement. Percept Psychophys 54:195-204
West BJ (2013) Fractal Physiology and Chaos in Medicine. World Scientific
Wetzig J (1983) Untersuchungen uber das Schwimmverhalten einseitig entstateter Fische unter kurzzeitiger Ein- wirkung von Scherelosigkeit. In, vol PhD. University of Mainz, Mainz, Germany
Wetzig J, Reiser M, Martin E, Bregenzer N, von Baumgarten RJ (1990) Unilateral centrifugation of the otoliths as a new method to determine bilateral asymmetries of the otolith apparatus in man. Acta Astronaut 21:519-525
Whitacre J, Bender A (2010) Degeneracy: a design principle for achieving robustness and evolvability. J Theor Biol 263:143-153
White RJ (1998) Weightlessness and the human body. Sci Am 279:58-63
Williams DR (2003) The biomedical challenges of space flight. Annu Rev Med 54:245-256
Williams DR, Kuipers A, Mukai C, Thirsk R (2009) Acclimation during space flight: effects on human physiology. Can Med Assoc J 180:1317-1323
Wilson VJ, Gacek RR, Maeda M, Uchino Y (1977) Saccular and utricular input to cat neck motoneurons. J Neurophysiol 40:63-73
Wilson VJ, Melvill Jones G (1979) Mammalian Vestibular Physiology. Plenum Press, New York
Winkelman JE (1951) Peripheral fusion. AMA Arch Ophthalmol 45:425-430
Wong AL, Shelhamer M (2014) Similarities in error processing establish a link between saccade prediction at baseline and adaptation performance. J Neurophysiol
Wood SJ (2002) Human otolith-ocular reflexes during off-vertical axis rotation: Effect of frequency on tilt-translation ambiguity and motion sickness. Neurosci Lett 323:41-44
Wood SJ, Loehr JA, Guilliams ME (2011) Sensorimotor reconditioning during and after spaceflight. NeuroRehabilitation 29:185-195
Wood SJ, Reschke MF, Sarmiento LA, Clément G (2007) Tilt and translation motion perception during off-vertical axis rotation. Exp Brain Res 182:365-377
Wu HG, Miyamoto YR, Gonzalez Castro LN, Olveczky BP, Smith MA (2014) Temporal structure of motor variability is dynamically regulated and predicts motor learning ability. Nat Neurosci 17:312-321
Wuyts FL, Hoppenbrouwers M, Pauwels G, Van de Heyning PH (2003) Utricular sensitivity and preponderance assessed by the unilateral centrifugation test. J Vestib Res 13:227-234
Yakushin SB, Raphan T, Cohen B (2000) Context-specific adaptation of the vertical vestibuloocular reflex with regard to gravity. J Neurophysiol 84:3067-3071
Yamamoto H, Arai M (1975) Study on vertical and cyclofusional amplitude in human. Jpn Rev Clin Ophthalmol 69:1382-1384
Yegorov A, Samarin G (1970) Possible change in the paired operation of the vestibular apparatus during weightlessness. Kosm Biol Aviakosm Med 4:85-86

Young LR (1974) Perceptions of the body in space: mechanisms. In: Darian-Smith I (ed) Handbook of Physiology - The Nervous System. American Physiological Society, Bethseda, MD, pp 1023-1066

Young LR, Oman CM, Watt DG, Money KE, Lichtenberg BK (1984) Spatial orientation in weightlessness and readaptation to earth's gravity. Science 225:205-208

Young LR, Oman CM, Watt DG, Money KE, Lichtenberg BK, Kenyon RV, Arrott AP (1986) M.I.T./Canadian vestibular experiments on the Spacelab-1 mission: 1. Sensory adaptation to weightlessness and readaptation to one-g: an overview. Exp Brain Res 64:291-298

Young LR, Sinha P (1998) Spaceflight influences on ocular counterrolling and other neurovestibular reactions. Otolaryngol Head Neck Surg 118:S31-34.

Zee DS, Yamazaki A, Butler PH, Gucer G (1981) Effects of ablation of flocculus and paraflocculus of eye movements in primate. J Neurophysiol 46:878-899

Curriculum Vita

Kara Huffman Beaton March 2014
Born: December 13, 1981
Evanston, Illinois

Educational History

Ph.D.	March 2014	Biomedical Engineering Johns Hopkins School of Medicine Mentor: Mark Shelhamer, Sc.D.
S.M.	June 2006	Aeronautics and Astronautics Massachusetts Institute of Technology Mentor: Raymond J. Sedwick, Ph.D.
B.S.	May 2004	Aerospace Engineering University of Illinois
Minor	May 2004	Mathematics University of Illinois

Professional Experience

Teaching assistant	Spring 2012	BME Systems and Controls
Teaching assistant	Fall 2011	BME Modeling and Design
Research Engineer	2007-2008	NASA Johnson Space Center Neuroscience Laboratory, Houston, TX
Research Engineer	2006-2007	Naval Aerospace Medical Research Laboratory, Pensacola FL
Research Assistant	2004-2006	MIT Aeronautics and Astronautics Space Systems Laboratory, Cambridge MA

Scholarships/Fellowships

2010-2012	Training Program in Hearing and Balance, JHU Biomedical Engineering Fellowship, NIH T32 DC000023
2008-2010	Neuroengineering Training Initiative, JHU Biomedical Engineering Fellowship, NIH T32 EB003383
2004-2006	Research Assistantship, MIT Aeronautics and Astronautics
2000-2004	Women in Engineering Distinguished Scholars and Calvin B. Niccols College of Engineering Scholarships, U of I (tuition support)

Honors

2014	The National Space Biomedical Research Institute Dr. David Watson Graduate Student Fellow Best Scientific Poster (monetary award)
2011	JHU Graduate Student Association Travel Award

2004	U of I Aerospace Engineering H.S. Stillwell Memorial Award (most outstanding scholastic achievement)
2003 (inducted)	Phi Kappa Phi (Academic Honor Society), member
2002 (inducted)	Sigma Gamma Tau (Aerospace Engineering Honor Society), member
2002 (inducted)	Tau Beta Pi (Engineering Honor Society), member
2001-2004	U of I Edmund J. James Scholar
2000-2004	U of I Chancellor's Scholar and enrolled in campus honors program

Publications

Shelhamer M, **Beaton KH** (2012) Preflight sensorimotor adaptation protocols for suborbital flight. J Vestib Res 22(2):139-144

Shelhamer M, **Beaton KH** (2010) Mission to Mars: training and maintenance of sensorimotor responses; considerations based on context-specific adaptation. J Cosmology 12:3817-3824

Posters and Presentations

Beaton KH, Pierson K, McDermott C, Shelhamer M, Zee DS, Schubert MC (2014) Vestibulo-ocular nulling: quantifying perceived retinal slip without recording eye movements. 37th Meeting for the Association of Research in Otolaryngology, San Diego CA, February 2014 (poster)

Beaton KH, Wong AL, Shelhamer M (2014) Predicting sensorimotor adaptive capacities from inter-trial correlations in baseline measures. NASA Human Research Program Investigator's Workshop, Galveston TX, February 2014 (poster)

Beaton KH, Schubert MC, Shelhamer M (2013) Novel techniques for rapid assessment of oculomotor function. 43rd Annual Meeting of the Society for Neuroscience, Washington D.C., November 2013 (poster)

Beaton KH, Schubert MC, Shelhamer M (2013) Symptom free in zero-g? A portable technology for rapid, multi-system assessment and the potential for predicting in-flight performance. Next Generation Suborbital Researchers Conference, Broomfield CO, June 2013 (poster)

Beaton KH. Follow the noise: forecasting adaptive capabilities from baseline metrics. Johns Hopkins University Center for Hearing and Balance, May 2013 (invited talk)

Beaton KH, Shelhamer M (2013) Influence of postural demand on adaptation of the vestibulo-ocular reflex. NASA Human Research Program Investigator's Workshop, Galveston TX, February 2013 (poster)

Beaton KH, Holly JE, Clément GR, Wood SJ (2011) Translational vestibulo-ocular reflex motion perception during interaural linear acceleration: comparison of different motion paradigms. 41th Annual Meeting of the Society for Neuroscience, Washington DC, November 2011 (poster)

Beaton KH, Wong AL, Schubert MC, Shelhamer M (2011) Covariance in the vestibulo-ocular reflex, postural balance, and locomotion during adaptation to 2.5X magnifying lenses. Space Forum Dedicated to the 50th Anniversary of Human Spaceflight, Moscow Russia, October 2011 (invited talk)

Beaton KH, Shelhamer M (2011) Design considerations for postflight sensorimotor testing and rehabilitation. 18th International Academy of Astronautics Humans in Space Symposium, Houston TX, April 2011 (poster)

Beaton KH, Shelhamer M (2011) Gravity dependence on the pitch vestibulo-ocular reflex. 8th Symposium on the Role of the Vestibular Organs in Space Exploration, Houston TX, April 2011 (invited talk)

Beaton KH, Shelhamer M (2011) Sensorimotor assessment for suborbital passengers: a recommended protocol. Next Generation Suborbital Researchers Conference, Orlando FL, February 2011 (poster)

Beaton KH, Wong AL, Shelhamer M (2010) Doing the right thing when the right thing varies with the setting: context-specific adaptation of sensorimotor responses. 40th Annual Meeting of the Society for Neuroscience, San Diego CA, November 2010 (invited talk)

Beaton KH. Assessing vestibulo-ocular function without measuring eye movements. Johns Hopkins University Center for Hearing and Balance, October 2010 (invited talk)

Beaton KH, Ying HS, Roberts DC, Shelhamer M (2010) Assessing vestibulo-ocular function without measuring eye movements. XXVI Bárány Society Meeting, Reykjavik, Iceland, August 2010 (invited talk)

Beaton KH, Holly JE, Clément GR, Wood SJ (2009) Effects of frequency and motion paradigm on perception of tilt and translation during periodic linear acceleration. 32nd Meeting for the Association of Research in Otolaryngology, Baltimore MD, February 2009 (poster)

Beaton KH, Holly JE, Clément GR, Wood SJ (2008) Effects of frequency and tilt angle during off-vertical axis rotation on human motion perception. XXV Bárány Society Meeting, Kyoto, Japan, April 2008 (invited talk)

Beaton KH, McGrath BJ, McGrath EA, Rupert AH (2007) Using spatial disorientation training to create a normative database for screening dynamic visual and vestibular abnormalities in military aviation. Proceedings, 77th Annual Scientific Meeting of the Aerospace Medical Association, New Orleans LA. Aviation Space and Environmental Medicine, 78 (3), 295-296 (invited talk)

Beaton KH, McGrath BJ, Rupert AH (2006) Military tactile applications using tactile situational awareness system (TSAS): lessons learned. 51st Annual Meeting of the Human Factors and Ergonomics Society, San Francisco CA, September 2006 (invited talk)

Huffman KM, Sedwick RJ (2006) Designing star trackers to meet micro-satellite requirements. American Institute for Aeronautics and Astronautics SpaceOps Conference, Rome, Italy, June 2006 (poster)